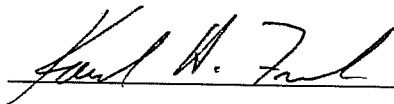



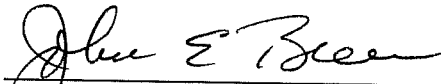
**Development of Design Procedures for
Steel Girder Bolted Splices**

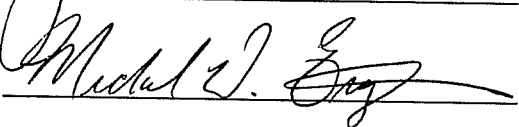
Approved by
Dissertation Committee:











**Development of Design Procedures for
Steel Girder Bolted Splices**

by

Firas Sheikh Ibrahim, B.S., M.S.

Dissertation

Presented to the Faculty of the Graduate School of
The University of Texas at Austin
in partial fulfillment
of the requirements
for the Degree of

Doctor of Philosophy

The University of Texas at Austin

December, 1995

Development of Design Procedures for

Steel Girder Bolted Splices

Publication No. _____

Firas Sheikh Ibrahim, Ph.D.

The University of Texas at Austin, 1995

Supervisor: Karl H. Frank

The results of 32 full-scale tests of steel girder bolted splices are presented. Simple design procedures for the splices of symmetric, unsymmetric, and composite girders are developed. The design procedures were based on the non-linear analysis of the web bolts and were verified by the 32 full-scale specimen tests. The procedures include the effect of the difference in the flange forces on the web splice for unsymmetric girders. The design procedures cover the cases of slip-critical splices and the bearing-type splices. It is found that, when the flanges are adequate to carry the applied moment, the web bolts need only to be designed for the applied shear at an eccentricity calculated as the distance from the centroid of the bolts to the centerline of the splice. It is also found that, when the flanges are not adequate to carry the applied moment, the web bolts need to be designed for the previous applied shear along with the moment in excess of the flanges' capacity. Further, the analysis of eccentrically loaded bolted connections is reviewed. It is found that, the elastic analysis of the bolts appears to be adequate and there is no need to perform nonlinear analysis of the bolts.

2.5.1. Description of the testing programs.....	54
2.5.2. Results and discussion.....	56
2.6. SUMMARY.....	72
2.7. CONCLUSIONS.....	73
CHAPTER 3.....	74
3. MATERIAL TESTING.....	74
3.1 INTRODUCTION.....	74
3.2 TENSILE COUPON TESTS.....	74
3.3 BOLT SLIP AND SHEAR TESTS.....	77
3.3.1 Test Set-Up.....	78
3.3.2 Single-shear tests for individual bolts in compression splices.....	79
3.3.3 Double slip and shear tests for individual bolts in tension splices.....	83
3.3.4 The effect of preload on the shear strength of an individual bolt.....	91
3.3.5 The effect of hole making procedure on the shear strength of an individual bolt.....	93
3.3.6 The effect of material loading history on the shear strength of an individual bolt.....	97
3.3.7 Comparison between the shear strength of 3/4 in. A325 bolts tested in compression and in tension splices.....	99
3.3.8 Summary and conclusions of bolt shear tests.....	100
CHAPTER 4.....	101
4. LARGE-SCALE EXPERIMENTAL PROGRAM FOR STEEL GIRDER BOLTED SPLICES.....	101
4.1. INTRODUCTION.....	101
4.2. TEST SET-UP.....	101
4.3. DETAILS OF THE STEEL GIRDER SPLICE TESTS.....	107
4.4. TEST PROCEDURES OF GIRDER SPLICES.....	114
4.5. THE FABRICATION, INSTRUMENTATION, LOADING, AND BEHAVIOR OF A TYPICAL UNSYMMETRIC SPLICE WITH INADEQUATE FLANGES.....	114

4.6. TEST RESULTS OF GIRDER SPLICES	121
4.7. DISCUSSION OF TEST RESULTS	124
4.7.1. Web Splices	124
4.7.1.1. The Behavior and analysis of web splices up to Slip.....	124
4.7.1.2. The Behavior and analysis of web splices after Slip	128
4.7.1.3. The effect of the hole size of the web bolts on the strength of web splices.....	136
4.7.1.4. Summary and conclusions of web splice tests.....	138
4.7.2. Web-Flange Splices	139
4.7.2.1. The Behavior of W-F splices up to Slip.....	139
4.7.2.1.1. Adequate moment slip resistance of the flanges:.....	140
4.7.2.1.2. Inadequate moment slip resistance of the flanges:	141
4.7.2.2. The Behavior of W-F splices after Slip	143
4.7.2.2.1. Adequate small flange:.....	143
4.7.2.2.2. Inadequate small flange:	144
4.7.2.2.3. Inadequate flanges:	144
4.7.2.3. The effect of the shear in the flanges on the strength of w-f splices with adequate flanges	153
4.7.2.3.1. The Plastic Model for predicting the flanges shear in symmetric w-f splices with adequate flanges, $M \leq M_f$	153
4.7.2.3.2. Comparison between the Plastic Model for predicting the flanges shear and test results	161
4.7.2.4. The theoretical distribution of forces for unsymmetric w-f splices at the service level (Slip).....	163
4.7.2.4.1. Adequate slip moment resistance of the flanges:.....	163
4.7.2.4.2. Inadequate slip moment resistance of the flanges:	163
4.7.2.5. The theoretical distribution of forces for unsymmetric w-f splices at the ultimate level (maximum load)	167
4.7.2.5.1. Adequate small flange, $M < M_f$	167
4.7.2.5.2. Adequate big flange and inadequate small flange, $M_f < M < M_F$	168
4.7.2.5.3. Inadequate flanges, $M > M_F$	170

4.7.2.6. Comparison between the theoretical and experimental loads at both the service (slip) and the ultimate level (maximum load)	171
4.7.2.7. The effect of the moment shear interaction on the strength of w-f splice plates	185
4.7.2.8. The effect of the web bolts preload on the strength of w-f splices	190
4.7.2.9. Summary and conclusions of web-flange splice tests	191
CHAPTER 5	194
5. DESIGN PROCEDURES FOR STEEL GIRDER BOLTED SPLICES	194
5.1. INTRODUCTION	194
5.2. DESIGN PROCEDURES	195
5.2.1. The distribution of design forces between the flange and web splices	195
5.2.1.1. The distribution of forces at the service level (Slip)	196
5.2.1.1.1. Adequate moment resistance of the flanges:	196
5.2.1.1.2. Inadequate moment resistance of the flanges:	197
5.2.1.2. The distribution of forces at the ultimate level (maximum load)	199
5.2.1.2.1. Adequate small flange:	200
5.2.1.2.2. Adequate big flange and inadequate small flange	202
5.2.1.2.3. Inadequate flanges:	203
5.2.2. Splice Design	204
5.2.2.1. The design of flange splice plates	204
5.2.2.2. The design of web splice plates	206
5.2.2.3. The design of flange bolts	208
5.2.2.4. The design of web bolts	209
CHAPTER 6	211
6. COMPOSITE GIRDER BOLTED SPLICE DESIGN EXAMPLES	211
6.1. DESIGN EXAMPLE 1, SPLICE IN A NEGATIVE MOMENT REGION	211

6.1.1. Design Forces	212
6.1.1.1. Required Slip Resistance	212
6.1.1.2. Required strength of the member	213
6.1.1.3. AASHTO Design Forces.....	213
6.1.2. Splice Design.....	215
6.1.2.1. The design of flange bolts.....	215
6.1.2.2. The design of web bolts	216
6.1.2.3. The design of flange splice plates	217
6.1.2.4. The design of web splice plates.....	221
6.2. DESIGN EXAMPLE 2, SPLICE IN A POSITIVE MOMENT REGION	224
6.2.1. Design Forces	225
6.2.1.1. Required Slip Resistance	225
6.2.1.2. Required strength of the member	225
6.2.1.3. AASHTO Design Forces.....	226
6.2.2. Splice Design.....	229
6.2.2.1. The design of flange bolts.....	229
6.2.2.2. The design of web bolts	230
6.2.2.3. The design of flange splice plates:	232
6.2.2.4. The design of web splice plates.....	235
6.3. DESIGN EXAMPLE 3, SPLICE IN A POSITIVE MOMENT REGION	238
6.3.1. Design Forces	239
6.3.1.1. Required Slip Resistance	239
6.3.1.2. Required strength of the member	239
6.3.1.3. AASHTO Design Forces.....	240
6.3.2. Splice Design.....	242
6.3.2.1. The design of flange bolts.....	242
6.3.2.2. The design of web bolts	243
6.3.2.3. The design of flange splice plates	244
6.3.2.4. The design of web splice plates.....	246

CHAPTER 7	249
7. SUMMARY AND CONCLUSIONS	249
REFERENCES	254
VITA	256

List of Tables

TABLE 2-1 DETAILS OF THE BOLTED SPECIMENS USED IN THE COMPARISON	56
TABLE 2-2 COMPARISON BETWEEN THE NONLINEAR C, ELASTIC C, AND TEST RESULTS OF FULL-SIZE SPECIMENS	57
TABLE 2-3 COMPARISON BETWEEN THE NONLINEAR C, ELASTIC C, AND TEST RESULTS OF WEB SPLICES	58
TABLE 2-4 COMPARISON BETWEEN THE THEORETICAL LOAD LEVEL IN EACH BOLT USING THE NONLINEAR AND THE ELASTIC METHODS FOR SPECIMENS B2 & B3	66
TABLE 2-5 THE % DIFFERENCE BETWEEN THE THEORETICAL LOAD LEVEL IN EACH BOLT USING THE NONLINEAR AND THE ELASTIC METHODS FOR SPECIMENS B2 & B3	66
TABLE 2-6 COMPARISON BETWEEN THE THEORETICAL SHEAR CONTRIBUTION OF EACH BOLT USING THE NONLINEAR AND THE ELASTIC METHODS FOR SPECIMENS B2 & B3	69
TABLE 2-7 COMPARISON BETWEEN THE THEORETICAL MOMENT CONTRIBUTION OF EACH BOLT USING THE NONLINEAR AND THE ELASTIC METHODS FOR SPECIMENS B2 & B3	69
TABLE 3-1 ACTUAL VERSUS NOMINAL DIMENSIONS OF WEB SPLICE PLATES	75
TABLE 3-2 ACTUAL VERSUS NOMINAL DIMENSIONS OF FLANGE SPLICE PLATES	75
TABLE 3-3 TENSILE COUPON AVERAGE RESULTS FOR THE SPLICE PLATE MATERIAL	76
TABLE 3-4 TENSILE COUPON AVERAGE RESULTS FOR THE GIRDER MATERIAL	76
TABLE 3-5 ACTUAL VERSUS NOMINAL DIAMETERS OF WEB BOLTS	77
TABLE 3-6 THE RESULTS OF COMPRESSION SINGLE-SHEAR TESTS ON A325 5/8" BOLTS	80
TABLE 3-7 THE RESULTS OF SINGLE-SHEAR COMPRESSION TESTS OF A325 3/4" BOLTS	82
TABLE 3-8 THE ESTIMATED DOUBLE SHEAR CAPACITY OF A325 3/4" BOLTS TESTED IN COMPRESSION SPLICES	83
TABLE 3-9 THE RESULTS OF TENSION DOUBLE-SHEAR TESTS ON HAND-TIGHT 3/4" A325 BOLTS WITH 3/8" OUTER PLATES (THREADS ARE INCLUDED IN ONE SHEAR PLANE)	88
TABLE 3-10 THE RESULTS OF TENSION DOUBLE-SHEAR TESTS ON PRETENSIONED 3/4" A325 BOLTS WITH 3/8" OUTER PLATES (THREADS ARE INCLUDED IN ONE SHEAR PLANE)	89
TABLE 3-11 THE RESULTS OF TENSION DOUBLE SLIP AND SHEAR TESTS ON PRETENSIONED 3/4 A325 BOLTS WITH 3/16" OUTER PLATES (THREADS ARE EXCLUDED FROM BOTH SHEAR PLANES)	90
TABLE 3-12 THE EFFECT OF PRELOAD ON THE SHEAR STRENGTH OF BOLTS	92

TABLE 3-13 THE EFFECT OF THE HOLE MAKING PROCEDURE ON THE SHEAR STRENGTH OF BOLTS	93
TABLE 3-14 THE HARDNESS OF WEB SPLICE PLATE AND GIRDER MATERIAL AROUND PUNCHED HOLES ..	94
TABLE 3-15 THE HARDNESS OF THE WEB SPLICE PLATE AND GIRDER MATERIAL AROUND DRILLED HOLES	96
TABLE 3-16 THE EFFECT OF MATERIAL LOADING HISTORY ON THE SHEAR STRENGTH OF HAND-TIGHT BOLTS.....	98
TABLE 3-17 THE SHEAR STRENGTH OF HAND-TIGHT 3/4 IN. A325 BOLTS TESTED IN COMPRESSION AND IN TENSION SPLICES	99
TABLE 4-1 GEOMETRICAL DETAILS OF THE 24 IN. BEAM SPLICES	108
TABLE 4-2 GEOMETRICAL DETAILS OF THE 40 IN. BEAM WEB SPLICES	108
TABLE 4-3 GEOMETRICAL DETAILS OF THE 40 IN. BEAM WEB-FLANGE SPLICES.....	109
TABLE 4-4 DISTRIBUTION OF THE BOLTS FOR THE 24 IN. BEAM SPLICES	109
TABLE 4-5 DISTRIBUTION OF THE BOLTS FOR THE 40 IN. BEAM WEB SPLICES	110
TABLE 4-6 DISTRIBUTION OF THE BOLTS FOR THE 40 IN. BEAM WEB-FLANGE SPLICES.....	111
TABLE 4-7 SLIP AND SHEAR RESISTANCE OF AN INDIVIDUAL WEB BOLT OF THE TESTED SPLICES	112
TABLE 4-8 SELF WEIGHT FORCES AT THE CENTERLINE OF THE 40 IN. BEAM SPLICES.....	113
TABLE 4-9 TEST RESULTS OF GIRDER WEB SPLICES	122
TABLE 4-10 TEST RESULTS OF WEB-FLANGE SYMMETRIC SPLICES	123
TABLE 4-11 TEST RESULTS OF WEB-FLANGE UNSYMMETRIC GIRDER SPLICES	123
TABLE 4-12 THE THEORETICAL SLIP LOADS USING BOTH ELASTIC AND PLASTIC ANALYSES OF THE WEB BOLTS	125
TABLE 4-13 COMPARISON BETWEEN THE THEORETICAL LOAD LEVEL IN EACH BOLT USING THE ELASTIC, NONLINEAR, AND EMPIRICAL NONLINEAR METHODS FOR SPECIMEN 11 (PRETENSIONED WEB BOLTS).....	133
TABLE 4-14 COMPARISON BETWEEN THE THEORETICAL LOAD LEVEL IN EACH BOLT USING THE ELASTIC, NONLINEAR, AND EMPIRICAL NONLINEAR METHODS FOR SPECIMEN 30 (HAND-TIGHT WEB BOLTS).....	134
TABLE 4-15 THE LINEAR, NONLINEAR, AND TEST RESULTS OF WEB SPLICES	136
TABLE 4-16 THE THEORETICAL PLASTIC MODEL VERSUS TEST RESULTS FOR THE 24 IN. BEAM SPLICES	162
TABLE 4-17 TEST RESULTS OF SYMMETRIC W-F SPLICES AT SERVICE LOAD.....	172
TABLE 4-18 TEST RESULTS OF UNSYMMETRIC W-F SPLICES AT SERVICE LOAD	172

TABLE 4-19 TEST RESULTS OF SYMMETRIC W-F GIRDER SPLICES AT MAXIMUM LOAD	173
TABLE 4-20 TEST RESULTS OF UNSYMMETRIC W-F GIRDER SPLICES AT MAXIMUM LOAD	174
TABLE 4-21 THE TESTED MOMENT TO FLANGES MOMENT CAPACITY FOR THE 24 IN. BEAM SPLICES.....	182
TABLE 4-22 THE TESTED MOMENT TO FLANGES MOMENT CAPACITY FOR THE 40 IN. BEAM SPLICES.....	183

List of Figures

FIGURE 1-1 TYPICAL WEB-FLANGE BOLTED SPLICE.....	1
FIGURE 1-2 TYPICAL HIGH STRENGTH BOLT.....	3
FIGURE 1-3 THE LOAD TRANSFER IN A SLIP CRITICAL CONNECTION.....	4
FIGURE 1-4 THE TRANSFER OF SHEARING LOAD THROUGH BEARING AND SHEARING STRESSES IN A BEARING-TYPE CONNECTION.....	5
FIGURE 1-5 BOLT SHEAR FAILURE.....	5
FIGURE 1-6 BOLT IN SINGLE AND IN DOUBLE SHEAR.....	6
FIGURE 1-7 THE LOAD VERSUS BEARING DEFORMATION FOR A HIGH STRENGTH SINGLE BOLT SUBJECTED TO SHEAR IN A BEARING-TYPE CONNECTION WITH NO HOLE CLEARANCE.....	7
FIGURE 1-8 THE LOAD VERSUS BEARING DEFORMATION FOR A HIGH STRENGTH SINGLE BOLT SUBJECTED TO SHEAR IN A BEARING-TYPE CONNECTION WITH HOLE CLEARANCE.....	8
FIGURE 1-9 TYPICAL BEARING DEFORMATION AT THE EDGE OF THE HOLE.....	9
FIGURE 1-10 TYPICAL CONCENTRICALLY LOADED CONNECTIONS.....	11
FIGURE 1-11 PLATE FAILURE BY FRACTURING OF THE NET SECTION.....	15
FIGURE 1-12 TYPICAL BLOCK SHEAR FAILURE IN A TENSION CONNECTION.....	17
FIGURE 1-13 TYPICAL BEARING DEFORMATION FAILURE IN TENSION CONNECTIONS.....	18
FIGURE 1-14 TYPICAL TEAR OUT FAILURE OF AN EDGE BOLT.....	18
FIGURE 1-15 AN ECCENTRICALLY LOADED GROUP OF BOLTS.....	20
FIGURE 1-16 TYPICAL BLOCK SHEAR RUPTURE IN A BOLTED WEB CONNECTION.....	23
FIGURE 1-17 A PROBABLE DISTRIBUTION OF THE SHEAR AND MOMENT BETWEEN THE WEB AND FLANGE SPLICES.....	25
FIGURE 1-18 THE FORCE DISTRIBUTION IN W-F SPLICES SUGGESTED BY THE 2ND. EDITION OF THE LRFD MANUAL.....	26
FIGURE 1-19 THE AASHTO FORCE DISTRIBUTION IN W-F SPLICES.....	27
FIGURE 1-20 THE FORCE DISTRIBUTION IN W-F SPLICES RECOMMENDED BY SALMON AND JOHNSON.....	28
FIGURE 1-21 THE DESIGN FORCES ON THE WEB AND FLANGE SPLICES RECOMMENDED BY KULAK, FISHER, AND STRUIK.....	30
FIGURE 2-1 TYPICAL EXAMPLES OF ECCENTRICALLY LOADED GROUP OF BOLTS.....	34

FIGURE 2-2 THE EMPIRICAL NONLINEAR LOAD-DEFORMATION RESPONSE OF AN INDIVIDUAL HIGH STRENGTH BOLT USED IN THE ULTIMATE STRENGTH METHOD.....	39
FIGURE 2-3 THE INSTANTANEOUS CENTER OF ROTATION OF THE GROUP OF BOLTS	40
FIGURE 2-4 THE PIECE-WISE LINEAR BOLT RESPONSE MODEL	43
FIGURE 2-5 THE ELASTIC CENTER OF ROTATION METHOD	48
FIGURE 2-6 COMPARISON BETWEEN THE DISPLACEMENT COMPONENT OF THE BOLTS FOR THE TRADITIONAL VECTOR METHOD AND THE DISPLACEMENT OF THE BOLTS FOR THE ELASTIC CENTER OF ROTATION.....	54
FIGURE 2-7 C COEFFICIENT VERSUS E/D RATIO FOR SPECIMEN B1.....	59
FIGURE 2-8 C COEFFICIENT VERSUS E/D RATIO FOR SPECIMENS B4 AND B5.....	60
FIGURE 2-9 C COEFFICIENT VERSUS E/D RATIO FOR SPECIMEN B6 & B7.....	60
FIGURE 2-10 C COEFFICIENT VERSUS E/D RATIO FOR SPECIMEN B8	61
FIGURE 2-11 THE % DIFFERENCE BETWEEN THE NONLINEAR AND ELASTIC ANALYSIS.....	65
FIGURE 2-12 THE % DIFFERENCE BETWEEN THE NONLINEAR AND ELASTIC ANALYSIS.....	65
FIGURE 2-13 THE BOLT NUMBERING USED IN TABLE 2-5 FOR SPECIMENS B2 & 3	67
FIGURE 2-14 THE ELASTIC AND NONLINEAR LEVEL OF LOAD IN EACH BOLT OF SPECIMENS B2 AND B3 AS A FUNCTION OF E/D	67
FIGURE 2-15 THE ELASTIC AND NONLINEAR NORMALIZED SHEAR CONTRIBUTION OF EACH BOLT OF SPECIMENS B2 AND B3 AS A FUNCTION OF E/D	70
FIGURE 2-16 THE ELASTIC AND NONLINEAR NORMALIZED MOMENT CONTRIBUTION OF EACH BOLT OF SPECIMENS B2 AND B3 AS A FUNCTION OF E/D	70
FIGURE 3-1 TEST SET-UP FOR SINGLE BOLT IN COMPRESSION SINGLE-SHEAR SPLICE	78
FIGURE 3-2 TEST SET-UP FOR SINGLE BOLT IN TENSION DOUBLE SLIP AND SHEAR SPLICE.....	79
FIGURE 3-3 LOAD VERSUS BEARING DEFORMATION OF AN INDIVIDUAL 3/4 IN. A325 HIGH STRENGTH BOLT IN A SINGLE SHEAR COMPRESSION SPLICE WITH RIGID PLATES	81
FIGURE 3-4 TYPICAL TEST BOLT BEFORE FAILURE, TESTED IN A TENSION SPLICE	84
FIGURE 3-5 TYPICAL TEST BOLT AFTER FAILURE, TESTED IN A TENSION SPLICE	85
FIGURE 3-6 LOAD VERSUS JOINT DEFORMATION FOR 3/4" A325 BOLTS TESTED IN DOUBLE SHEAR TENSION SPLICES	87
FIGURE 3-7 THE LOAD VERSUS JOINT DEFORMATION FOR AN INDIVIDUAL 3/4 IN. A325 PRETENSIONED AND HAND-TIGHT BOLT IN DOUBLE SHEAR TENSION SPLICES	92

FIGURE 3-8 THE HARDNESS TEST SPECIMEN	95
FIGURE 3-9 THE EFFECT OF HOLE MAKING PROCEDURE ON THE HARDNESS OF THE PLATE	95
FIGURE 3-10 THE LOAD VERSUS JOINT DEFORMATION FOR AN INDIVIDUAL 3/4 IN. A325 BOLT IN DOUBLE SHEAR NEW AND REUSED TENSION SPLICES	98
FIGURE 4-1 THE 24 IN. BEAM TEST SET-UP.....	103
FIGURE 4-2 THE 40 IN. BEAM TEST SET-UP.....	104
FIGURE 4-3 A PHOTOGRAPH OF THE 40 IN. BEAM TEST-UP	106
FIGURE 4-4 THE GEOMETRICAL DETAILS AND THE DISTRIBUTION OF BOLTS OF THE TESTED SPLICES.....	107
FIGURE 4-5 THE INSTRUMENTATION OF A TYPICAL SPLICE	116
FIGURE 4-6 THE PERMANENT DEFORMATION OF THE GIRDER AT THE END OF THE FIRST CYCLE (CHANNEL 2).....	116
FIGURE 4-7 THE THEORETICAL VERSUS ACTUAL SLIP LOAD OF THE WEB SPLICE OF SPLICE 10 (CHANNEL 5).....	117
FIGURE 4-8 THE LOAD VERSUS RELATIVE HORIZONTAL GIRDER DEFLECTION AT THE SPLICE LOCATION OF SPLICE 10 (CHANNEL 9).....	118
FIGURE 4-9 THE LOAD VERSUS VERTICAL DEFLECTION AT THE SPLICE LOCATION OF SPLICE 10 (CHANNEL 2).....	119
FIGURE 4-10 THE LOAD VERSUS NORMALIZED STRAIN IN THE SMALL AND BIG FLANGE OF SPLICE 10 (CHANNELS 10 & 11).....	120
FIGURE 4-11 THE SLIP BEHAVIOR OF ECCENTRICALLY LOADED GROUP OF BOLTS UP TO SLIP.....	126
FIGURE 4-12 THE LOAD VERSUS VERTICAL DEFLECTION (CHANNEL 2) AT THE SPLICE LOCATION UP TO SLIP FOR SPECIMEN 11.....	126
FIGURE 4-13 THE LOAD VERSUS VERTICAL DEFLECTION (CHANNEL 2) AT THE SPLICE LOCATION UP TO SLIP FOR SPECIMEN 12.....	127
FIGURE 4-14 THE LOAD VERSUS VERTICAL DEFLECTION (CHANNEL 2) AT THE SPLICE LOCATION UP TO SLIP FOR SPECIMEN 13.....	127
FIGURE 4-15 THE LOAD VERSUS VERTICAL DEFLECTION (CHANNEL 2) AT THE SPLICE LOCATION UP TO SLIP FOR SPECIMEN 31 (SHORT SLOTTED HOLES).....	128
FIGURE 4-16 THE LOAD VERSUS JOINT DEFORMATION FOR DOUBLE SHEAR TENSION SPLICE WITH ONE BOLT FOR DIFFERENT BEARING TO SHEAR RATIOS	130

FIGURE 4-17 THE LOAD DEFLECTION BEHAVIOR OF TYPICAL WEB SPLICE WITH PRETENSIONED BOLTS (SPLICE 11)	131
FIGURE 4-18 THE NUMBERING OF THE WEB BOLTS FOR SPECIMEN 11	132
FIGURE 4-19 THE NUMBERING OF THE WEB BOLTS FOR SPECIMEN 30	132
FIGURE 4-20 THE EFFECT OF SIZE OF THE WEB HOLES ON THE STRENGTH AND DEFORMATION OF WEB SPLICES.....	137
FIGURE 4-21. THE SLIP BEHAVIOR OF A BOLTED SPLICE WITH ADEQUATE SLIP MOMENT RESISTANCE OF THE FLANGES.....	141
FIGURE 4-22. THE SLIP BEHAVIOR OF A BOLTED SPLICE WITH INADEQUATE SLIP MOMENT RESISTANCE OF THE FLANGES.....	142
FIGURE 4-23 TYPICAL FAILED UNSYMMETRIC W-F SPLICE WITH ADEQUATE SMALL FLANGE	145
FIGURE 4-24 THE FAILED WEB SPLICE OF A TYPICAL UNSYMMETRIC W-F SPLICE WITH ADEQUATE SMALL FLANGE.....	146
FIGURE 4-25 TYPICAL FAILED UNSYMMETRIC W-F SPLICE WITH INADEQUATE SMALL FLANGE AND ADEQUATE BIG FLANGE.....	147
FIGURE 4-26 THE BIG FLANGE SPLICE OF A TYPICAL FAILED UNSYMMETRIC W-F SPLICE WITH INADEQUATE SMALL FLANGE AND ADEQUATE BIG FLANGE	148
FIGURE 4-27 THE SMALL FLANGE SPLICE OF A TYPICAL FAILED UNSYMMETRIC W-F SPLICE WITH INADEQUATE SMALL FLANGE AND ADEQUATE BIG FLANGE	149
FIGURE 4-28 TYPICAL FAILED UNSYMMETRIC W-F SPLICE WITH INADEQUATE FLANGES	150
FIGURE 4-29 THE BIG FLANGE SPLICE OF A TYPICAL FAILED UNSYMMETRIC W-F SPLICE WITH INADEQUATE FLANGES.....	151
FIGURE 4-30 THE SMALL FLANGE SPLICE OF A TYPICAL FAILED UNSYMMETRIC W-F SPLICE WITH INADEQUATE FLANGES.....	152
FIGURE 4-31 THE FAILURE MODE FOR A W-F BOLTED SPLICE WITH ADEQUATE FLANGES.....	154
FIGURE 4-32 THE PLASTIC MODEL FOR PREDICTING THE SHEAR STRENGTH OF W-F SPLICES INCLUDING THE SHEAR CARRIED BY THE FLANGES WITH EQUAL SHEAR GAPS	154
FIGURE 4-33 THE IDEALIZED STRESS DISTRIBUTION IN BOTH THE SMALL AND BIG FLANGE PLATES DUE TO BOTH AXIAL LOAD AND BENDING MOMENT IF THE FLANGES.....	156
FIGURE 4-34 THE PLASTIC MODEL FOR PREDICTING THE SHEAR STRENGTH OF W-F SPLICES INCLUDING THE SHEAR CARRIED BY THE FLANGES WITH UNEQUAL SHEAR GAPS	161
FIGURE 4-35. THE SLIP DESIGN FORCES FOR AN UNSYMMETRIC BOLTED SPLICE.....	166

FIGURE 4-36 THE FORCE DISTRIBUTION BETWEEN THE WEB AND FLANGE SPLICES FOR THE CASE OF ADEQUATE FLANGES	167
FIGURE 4-37 THE FORCE DISTRIBUTION BETWEEN THE WEB AND FLANGE SPLICES FOR THE CASE OF INADEQUATE SMALL FLANGE AND ADEQUATE BIG FLANGE	169
FIGURE 4-38 THE FORCE DISTRIBUTION BETWEEN THE WEB AND FLANGE SPLICES FOR THE CASE OF INADEQUATE FLANGES.....	170
FIGURE 4-39 THE LOAD VERSUS VERTICAL DEFLECTION (CHANNEL 2) AT THE SPLICE FOR SPLICE 1 (SYMMETRIC ADEQUATE FLANGES).....	174
FIGURE 4-40 THE LOAD VERSUS VERTICAL DEFLECTION (CHANNEL 2) AT THE SPLICE FOR SPLICE 2 (SYMMETRIC ADEQUATE FLANGES).....	175
FIGURE 4-41 THE LOAD VERSUS VERTICAL DEFLECTION (CHANNEL 2) AT THE SPLICE FOR SPLICE 3 (SYMMETRIC ADEQUATE FLANGES).....	175
FIGURE 4-42 THE LOAD VERSUS VERTICAL DEFLECTION (CHANNEL 2) AT THE SPLICE FOR SPLICE 4 (SYMMETRIC ADEQUATE FLANGES).....	176
FIGURE 4-43 THE LOAD VERSUS VERTICAL DEFLECTION (CHANNEL 2) AT THE SPLICE FOR SPLICE 6 (SYMMETRIC INADEQUATE FLANGES).....	176
FIGURE 4-44 THE LOAD VERSUS VERTICAL DEFLECTION (CHANNEL 2) AT THE SPLICE FOR SPLICE 16 (SYMMETRIC ADEQUATE FLANGES).....	177
FIGURE 4-45 THE LOAD VERSUS VERTICAL DEFLECTION (CHANNEL 2) AT THE SPLICE FOR SPLICE 18 (SYMMETRIC ADEQUATE FLANGES AT SERVICE LOAD & INADEQUATE FLANGES AT MAXIMUM LOAD; $M=M_p$, $V=V_p$).....	177
FIGURE 4-46 THE LOAD VERSUS VERTICAL DEFLECTION (CHANNEL 2) AT THE SPLICE FOR SPLICE 18 (SYMMETRIC ADEQUATE FLANGES AT SERVICE LOAD & INADEQUATE FLANGES AT MAXIMUM LOAD; $M=M_p$, $V=V_p$).....	178
FIGURE 4-47 THE LOAD VERSUS VERTICAL DEFLECTION (CHANNEL 2) AT THE SPLICE FOR SPLICE 7 (UNSYMMETRIC INADEQUATE SMALL FLANGE)	178
FIGURE 4-48 THE LOAD VERSUS VERTICAL DEFLECTION (CHANNEL 2) AT THE SPLICE FOR SPLICE 8 (UNSYMMETRIC INADEQUATE SMALL FLANGE)	179
FIGURE 4-49 THE LOAD VERSUS VERTICAL DEFLECTION (CHANNEL 2) AT THE SPLICE FOR SPLICE 9 (UNSYMMETRIC INADEQUATE FLANGES)	179
FIGURE 4-50 THE LOAD VERSUS VERTICAL DEFLECTION (CHANNEL 2) AT THE SPLICE FOR SPLICE 10 (UNSYMMETRIC INADEQUATE FLANGES)	180

FIGURE 4-51 THE LOAD VERSUS VERTICAL DEFLECTION (CHANNEL 2) AT THE SPLICE FOR SPLICE 15 (UNSYMMETRIC ADEQUATE FLANGES AT SERVICE LOAD & INADEQUATE SMALL FLANGE AT MAXIMUM LOAD).....	180
FIGURE 4-52 THE LOAD VERSUS VERTICAL DEFLECTION (CHANNEL 2) AT THE SPLICE FOR SPLICE 17 (UNSYMMETRIC ADEQUATE FLANGES).....	181
FIGURE 4-53 THE LOAD VERSUS VERTICAL DEFLECTION (CHANNEL 2) AT THE SPLICE FOR SPLICE 19 (UNSYMMETRIC INADEQUATE FLANGES WITH HAND-TIGHT WEB BOLTS)	181
FIGURE 4-54 TYPICAL FAILED SYMMETRIC W-F SPLICE WITH INADEQUATE FLANGES, $M=M_p$, $V=V_p$, SPLICE 18.....	186
FIGURE 4-55 TYPICAL FAILED SYMMETRIC W-F SPLICE WITH INADEQUATE FLANGES, $M=M_p$, $V=V_p$, SPLICE 20.....	187
FIGURE 4-56 THE TOP FLANGE OF A TYPICAL FAILED SYMMETRIC W-F SPLICE WITH INADEQUATE FLANGES, $M=M_p$, $V=V_p$, SPLICE 18.....	188
FIGURE 4-57 THE BOTTOM FLANGE OF A TYPICAL FAILED SYMMETRIC W-F SPLICE WITH INADEQUATE FLANGES, $M=M_p$, $V=V_p$, SPLICE 18.....	189
FIGURE 4-58 THE EFFECT OF PRELOAD IN THE WEB BOLTS ON THE STRENGTH AND DEFORMATION OF WEB-FLANGE SPLICES	190
FIGURE 6-1 THE STEEL GIRDER OF EXAMPLE 1	212
FIGURE 6-2 SPLICE DETAILS OF EXAMPLE 1	222
FIGURE 6-3 LONGITUDINAL VIEW OF THE SPLICE OF EXAMPLE 1.....	223
FIGURE 6-4 THE COMPOSITE GIRDER OF EXAMPLE 2.....	224
FIGURE 6-5 SPLICE DETAILS OF EXAMPLE 2	236
FIGURE 6-6 LONGITUDINAL VIEW OF THE SPLICE OF EXAMPLE 2.....	237
FIGURE 6-7 THE COMPOSITE GIRDER OF EXAMPLE 3	238
FIGURE 6-8 SPLICE DETAILS OF EXAMPLE 3	247
FIGURE 6-9 LONGITUDINAL VIEW OF THE SPLICE OF EXAMPLE 3	248

Chapter 1

1. Introduction

Rolled beams or plate girders might be spliced for a variety of reasons, such as:

1. the required full length may not be available from the mill
2. the designer may desire a change in the cross section of the beam
3. the fabricator might find it economical to splice the beam at certain locations to reduce shipping lengths or lifting loads

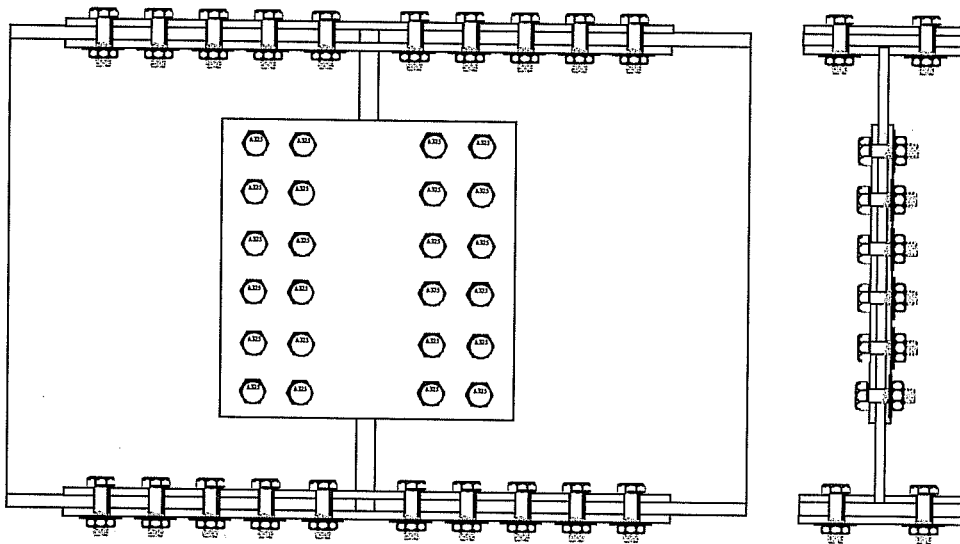


Figure 1-1 Typical web-flange bolted splice

Flange splices are single or double steel plates lapped across the joint and bolted to the flanges on each side of the joint. Double flange splice plates are used to utilize the double shear capacity of the bolts which reduces the number of bolts and shortens the length of the flange splice. Web splices are usually double steel

plates to stiffen the web out of plane and to utilize the double shear capacity of the bolts which reduces the number of bolts. The web plates are lapped across the joint and bolted to the webs on each side of the joint. When both the flanges and the web are spliced, the splice is called web-flange splice (w-f splice). Figure 1-1 shows a typical bolted web-flange splice.

1.1. Background

The behavior of an individual bolt must be thoroughly understood before the behavior of a bolted splice can be understood. Moreover, the behavior of the individual splice component of a bolted web-flange splice must be thoroughly understood before the behavior of a bolted web-flange splice can be understood. Therefore, section 1.1.1 will first introduce the behavior of an individual high strength bolt subjected to an applied shear. Then, section 1.1.2 will introduce the behavior of bolted connections subjected to concentric and eccentric shear.

1.1.1. The behavior and capacity of an individual high-strength bolt subjected to shear

The following discussion applies to a high strength bolt subjected to a force perpendicular to its axis, a shearing force. Figure 1-2 shows a typical high strength bolt.

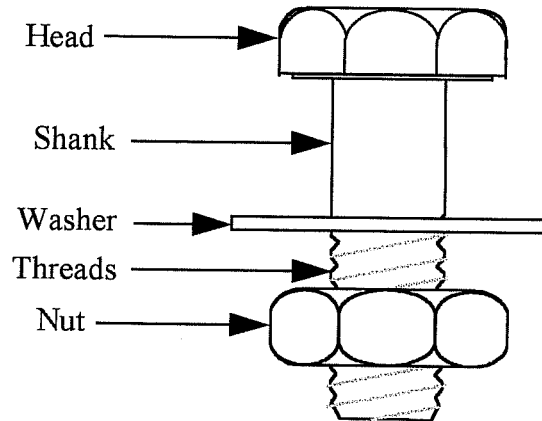


Figure 1-2 Typical high strength bolt

A high strength bolt can transfer the load between the connected plates through one of two methods:

1. Frictional resistance between the connected plates:

When a high strength bolt is tightened fully, a clamping force (T) will be produced. The clamping force prevents any relative movement between the connected plates by utilizing the friction between the plates. The clamping force is a function of the level of tightening of the bolt. The frictional resistance is a function of the clamping force T and the coefficient of friction, μ , of the faying surfaces of the connected plates and is equal to μT . When the load, P , transferred through the connection exceeds the frictional resistance μT , the connected plates slip. The connections that depend on transferring the load through friction are

called slip-resistant or slip-critical connections. They are usually used when any relative movement of the connected plates or misalignment of the connected members can not be tolerated. Consequently, at the service level in a bridge, the load transferred should be always less than the frictional resistance of the connected plates. Figure 1-3 depicts the load transfer in a slip-critical connection.

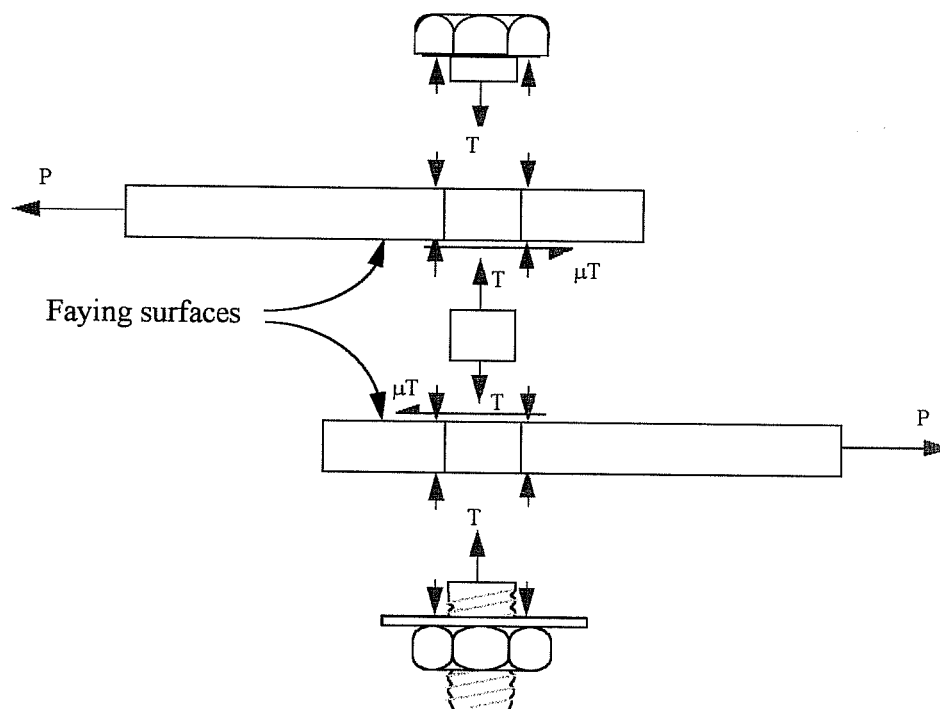


Figure 1-3 The load transfer in a slip critical connection

2. Shear / Bearing strength:

When the applied load exceeds the frictional resistance of the connected plates, the connected plates move in opposite directions and the bolt comes into contact with the connected plates and transfers the load through bearing and shearing stresses. The contact area between the bolt and the connected plates is called the bearing area. The stress in the vicinity of the bolt-plate contact area is called the bearing

stress. The distribution of the bearing stresses is unknown. However, for ductile materials (such as structural steel), a uniform stress distribution can be assumed. Thus, the bearing stress can be approximated as the load transferred by the bolt divided by both the thickness of the plate and the bolt diameter. The bearing stresses on the bolt cause a shearing force on the bolt as shown in Figure 1-4. The connections that depend on transferring the load through bearing and shearing stresses are called bearing-type connections. Figure 1-4 depicts the transfer of shearing load through bearing and shearing stresses in a bearing-type connection.

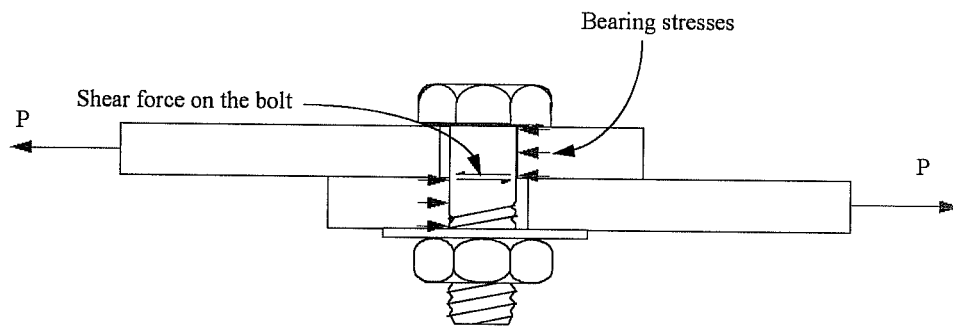


Figure 1-4 The transfer of shearing load through bearing and shearing stresses in a bearing-type connection

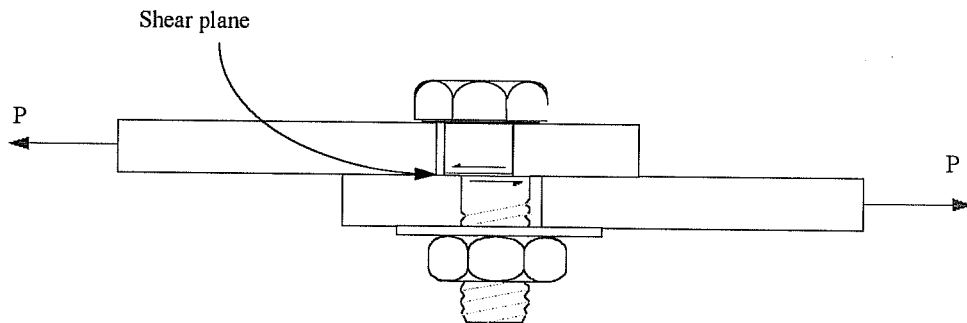


Figure 1-5 Bolt shear failure

The bearing-type connection fails when either the bolts shear as shown in Figure 1-5, or when the plate fails. Failure of the plate will be discussed later in this Chapter.

In a typical flange connection, the shear may act through one or two shearing planes and the connection is called single shear or double shear connection, respectively. The shear plane by definition is the plane between the connected plates that are moving in opposite directions. Figure 1-6 shows a bolt in single and in double shear.

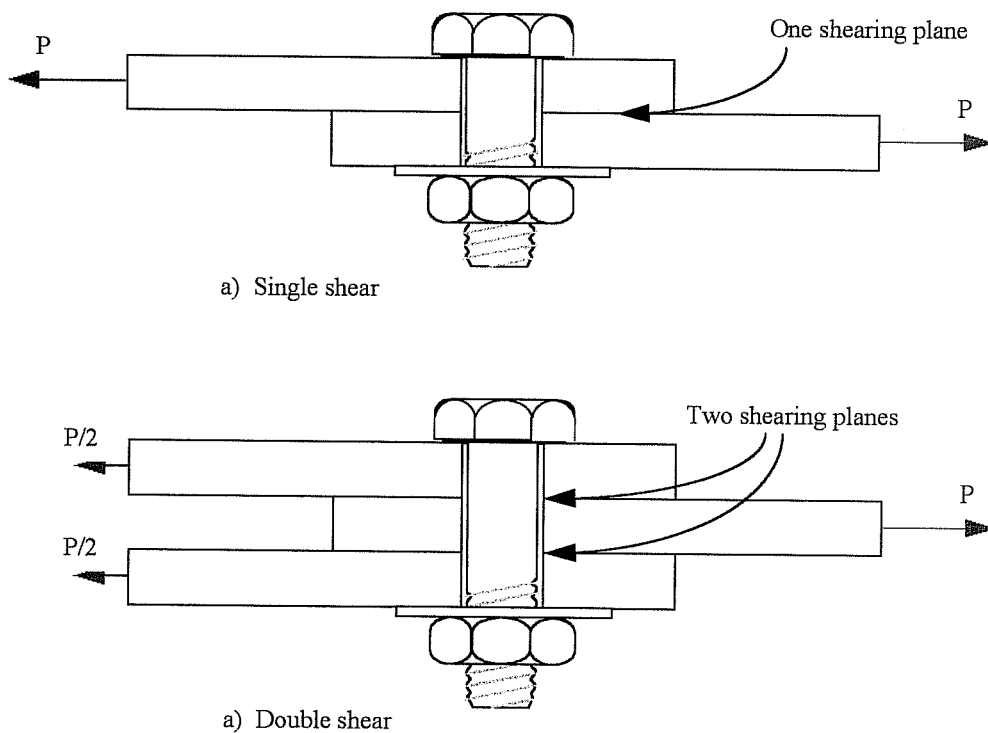


Figure 1-6 Bolt in single and in double shear

The load versus bearing deformation for a high strength single bolt subjected to shear in a bearing-type connection is shown in Figure 1-7. Initially, the bolt behaves elastically provided that the hole diameter of the connected plates matches exactly the bolt diameter or that the bolt is initially in contact with the connected plates. When the load increases and the shear stress in the bolt or the bearing stress in the plate exceeds the elastic limit, the connection behaves inelastically and its stiffness decreases until either shearing of the bolt or failure of the plate occurs.

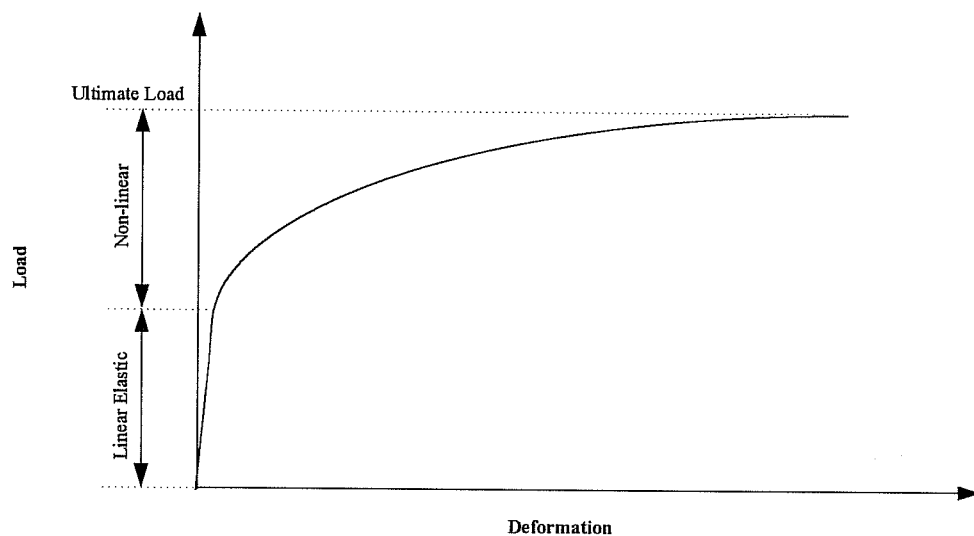


Figure 1-7 The load versus bearing deformation for a high strength single bolt subjected to shear in a bearing-type connection with no hole clearance

The holes in the connected plates are larger than the bolt diameter for ease of assembly. Therefore, a more practical load-deformation response of an individual tightened high strength bolt is shown in Figure 1-8. Initially, the bolt does not carry any shear load and the load is transferred completely through the

frictional resistance of the faying surfaces of the connected plates. When the load exceeds the frictional resistance, the plates slip and the bolt comes into bearing with the connected plates. As the load increases, the load is transferred partially through friction and partially through bearing stresses. When the stress in either the bolt (shear stress) or in the plate (bearing stress) exceeds the elastic limit, the connection behaves inelastically and the stiffness of the connection decreases until either shearing of the bolt or failure of the plate occurs.

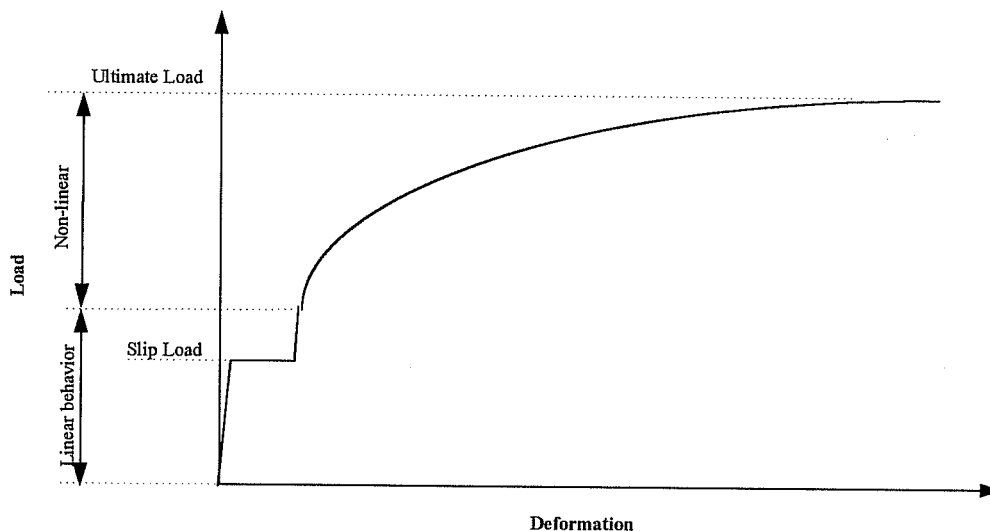


Figure 1-8 The load versus bearing deformation for a high strength single bolt subjected to shear in a bearing-type connection with hole clearance

At failure of the connection, the maximum bearing deformation is a function of the plate thickness and strength as well as the bolt diameter and strength. For large bearing strength ($3F_u$), the bearing deformation can be excessive because the plate is subjected to a stress much larger than its tensile strength at the edge of the hole. When the hole deforms excessively the plate material becomes upset and piles

up around the hole in the area of plate-bolt contact. Figure 1-9 shows typical bearing deformation at the edge of the hole.

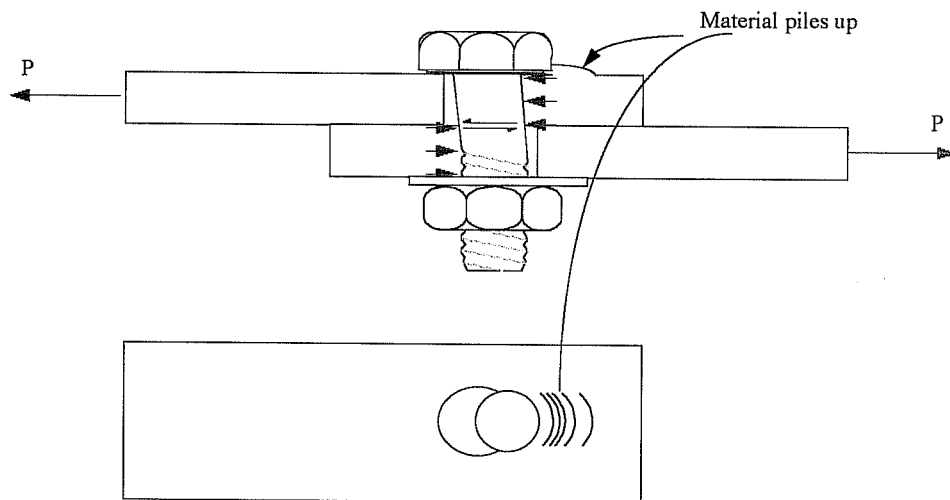


Figure 1-9 Typical bearing deformation at the edge of the hole

To limit the excessive bearing deformation, the RCSC¹ recommends limiting the bearing stress in the plate to 2.4 times its tensile strength ($2.4F_u$). If the deformation is not of concern of the designer, a value of 3.0 times the tensile strength of the plate ($3.0F_u$) can be used.

The shear capacity of high strength bolt is equal to the area of the bolt subjected to shear times the shear strength of the bolt material. The shear capacity of the bolt material was determined experimentally² to be about 62% to 68% of the tensile strength of the bolt when tested in a tension and compression splice, respectively. Thus, the single shear capacity of an individual high strength bolt can be conservatively determined from the following equation:

$$p = 0.6F_{ub} A_b \quad (1-1)$$

Where:

- p the single shear capacity of an individual high strength bolt
- 0.6 the approximate ratio of shear to tensile strength of the bolt material
- F_{ub} the ultimate strength of the bolt in tension
- A_b the cross sectional area of the bolt that lies in the shear plane. A_b is equal to the cross sectional area of the shank when the shank lies in the shear plane. Conversely, A_b is equal to the effective threads area of the bolt that equals to about 80%¹ of the shank area when the threads of the bolt lie in the shear plane

1.1.2. The behavior and strength of concentrically loaded bolted connections

A concentrically loaded connection is usually used to connect axially loaded members and can be bearing-type or slip critical. The load transferred through the connection acts at the center of gravity of bolts and along the longitudinal centroidal axis of the connected plates. Examples of such connections are shown in Figure 1-10. When the group of bolts are subjected to a single shear, the connection is called a single lap joint. On the other hand, when the bolts are subjected to a double shear, the connection is called a symmetric butt splice.

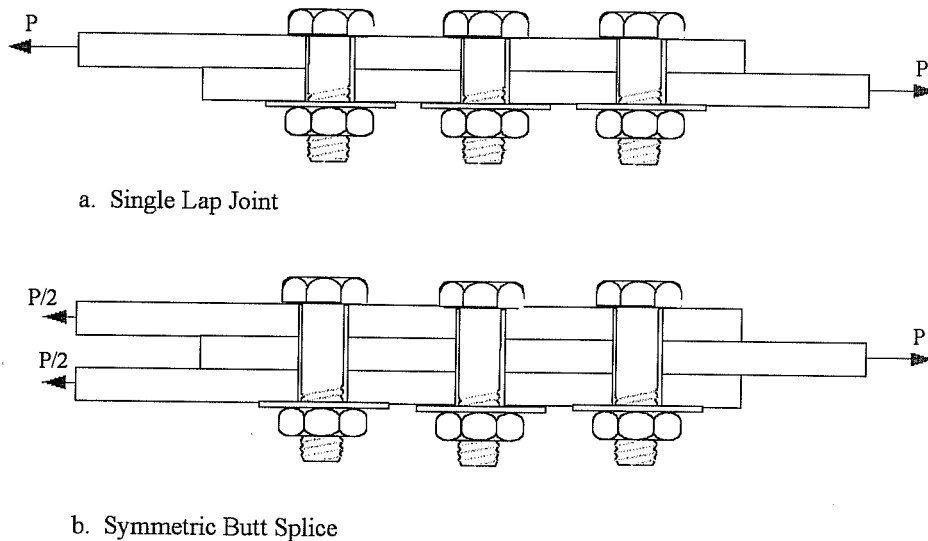


Figure 1-10 Typical concentrically loaded connections

1.1.2.1. Behavior and strength up to slip

Initially in a fully tightened concentrically loaded bolted connection, the load is transferred completely through friction at the first and last rows of bolts perpendicular to the applied load. Then, as load increases, the friction zones move successively toward the middle row of bolts. When the load exceeds the frictional resistance provided by all the bolts in the connection, a large relative displacement occurs. This large relative displacement is called the major slip. Theoretically, the magnitude of the major slip ranges from zero up to two hole clearances. The value of the major slip depends on the location of the bolts in their respective holes after the assembly process is completed.

Since a major slip will not occur until all bolts reach their individual slip resistance, the slip resistance of the connection is normally calculated as the sum of the slip loads of all individual bolts:

$$P_s = N_b N_s \mu T \quad (1-2)$$

Where:

- P_s the slip load of the connection
 N_b the number of bolts in the connection
 N_s the number of slip planes between the connected plates
 μ the coefficient of friction of the faying surfaces
 T the tension in the bolts

1.1.2.2. Behavior and strength after slip

After a major slip occurs, the first and last row of bolts come into bearing with the connected plates. As the load increases, the holes in the first and last rows deform and the bearing zone moves progressively toward the middle row and all the bolts come into bearing with the connected plates. At this stage, the load is transferred through friction and bearing stresses. When the stress in the bolts or in the connected plates exceeds the yield stress of bolts in shear or plates in bearing, the connection behaves inelastically. Finally, as the load increases, the stiffness of the connection decreases until the failure of either the bolts or the connected plates.

The followings are the modes of failure of the concentrically loaded bearing-type bolted connections:

1. Bolt shear failure

In this case, the shear capacity of the bolts in the connection is a function of the joint length². When all the bolts come into bearing with the connected plates, the first and last row of bolts carry most of the load due to the relatively large deformations of the plates at those locations. For long connections, the first and

last row of bolts will undergo large bearing deformation before the bolts in the middle of the connection develop their shear capacity. Thus, the first and last row of bolts will fail first and the shear capacity of the connection is smaller than the sum of the shear capacities of all the bolts. Conversely, the bolts in compact connections (where the connected length is short and there is only a few number of rows) will eventually be able to carry an equal amount of load due to the large deformation of the bolts and bearing deformation of the plate.

Since the shear capacity of the bolts in a concentrically loaded connection is a function of the joint length, the RCSC¹ recommends using a shear capacity equals to 80 % of the sum of the shear capacities of all bolts for connections shorter than 50 inches. On the other hand, the RCSC¹ recommends using a shear capacity equals to 64 % of the total shear capacity of the bolts for connections longer than 50 inches. Hence, for concentrically loaded connections, the shear capacity is equal to the following:

$$P_v = N_b N_s \phi p \quad (1-3)$$

where:

- P_v the shear capacity of the connection
- N_b the total number of bolts in the connection
- N_s the number of shear planes
- ϕ shear strength reduction factor due to the length of the connection
 - $\phi = 0.8$ for connections shorter than 50 inches
 - $\phi = 0.64$ for connections longer than 50 inches
- p the single shear capacity of one bolt

2. Plate failure by fracturing of the net section

If the stress at the net section of a concentrically loaded connection reaches the ultimate strength of the plate material, the plate fractures at the net section. as shown in Figure 1-11. Initially as the load is applied, the stress at the net section next to the hole is larger than the stress away from the hole due to the stress concentration factor. As the load increases, the stress at the edge of the hole increases linearly up to reaching the proportional limit of the plate material. After exceeding the yield stress at the edge of the hole, the distribution of stress across the net section depends on the ductility of the plate material. For ductile plate material, the stress at the edge of the hole remains at the yield level and the stress away from the edge of the hole increases up to reaching the yield stress of the plate material. At this time, the stress at the net section is uniform and equals to the yield stress. Materials made of high strength steel do not have a definite yield point nor a yield plateau. Therefore, the material at the edge of the hole might strain harden and might reach the ultimate strength of the material before the material away from the edge hole reaches its ultimate strength.

Since structural steel is ductile, the use of a uniform stress distribution at the net section should be sufficient for most cases. Therefore, the net section fracture strength of the connection can be calculated as follows:

$$P_n = A_n F_u \quad (1 - 4)$$

Where:

- P_n the net section fracture capacity of the critical plate
- A_n the net area of the critical plate = $t (B - N_r d_h)$

- t the thickness of the critical plate
 B the width of the critical plate
 N_r the number of holes across the width of the critical plate (number of rows)
 d_h the effective diameter of the hole = the diameter of the hole plus 1/16 in.
 F_u the tensile strength of the critical plate

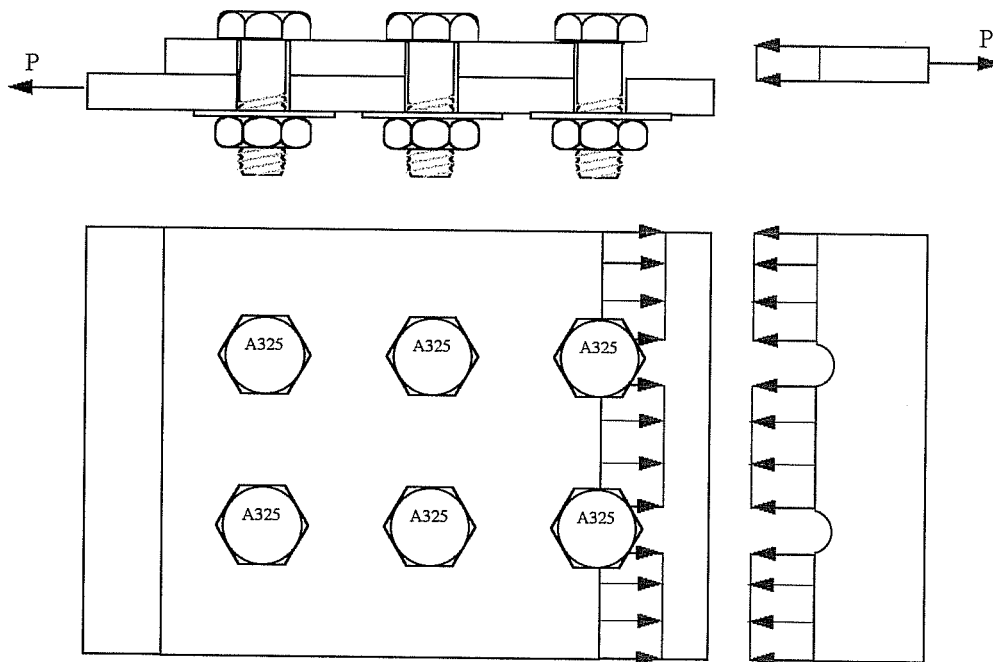


Figure 1-11 Plate failure by fracturing of the net section

3. Plate failure by block shear

A portion of the connection might tear out as shown in Figure 1-12. This failure is called a block shear failure. Block shear failure usually occurs in thin plates when the connected length is short. The block shear rupture is a

combination of fracture at the net section and yielding at the gross section of a perpendicular plane. For a large tensile area and a small shear area, the failure mode occurs by fracturing of the net tensile area and yielding of the gross shear area. For a small tensile area and a large shear area, the failure mode occurs by fracturing of the net shear area and yielding of the gross tensile area.

Thus, the tear out failure might occur in one of the two following modes:

When $0.6F_u A_{nv} > F_u A_{nt}$ the failure mode will be a combination of tension yield along edge b-c and shear fracture along edges a-b and c-d. The block shear capacity for this case can be calculated as follows:

$$P = 0.6F_u A_{nv} + F_y A_{gt} \quad (1-5)$$

When $F_u A_{nt} > 0.6F_u A_{nv}$ the failure mode will be a combination of tensile fracture along edge b-c and shear yield along edges a-b and c-d. The block shear capacity for this case can be calculated as follows:

$$P_{bs} = 0.6F_y A_{gv} + F_u A_{nt} \quad (1-6)$$

Where:

- P_{bs} the block shear capacity of the connected critical plate
- F_y the yield strength of the critical plate
- F_u the tensile strength of the critical plate
- 0.6 the ratio of shear to tensile strength of the plate material
- A_{gt} the gross area subjected to tension
- A_{nt} the net area subjected to tension

A_{nv} the net area subjected to shear
 A_{gv} the gross area subjected to shear.

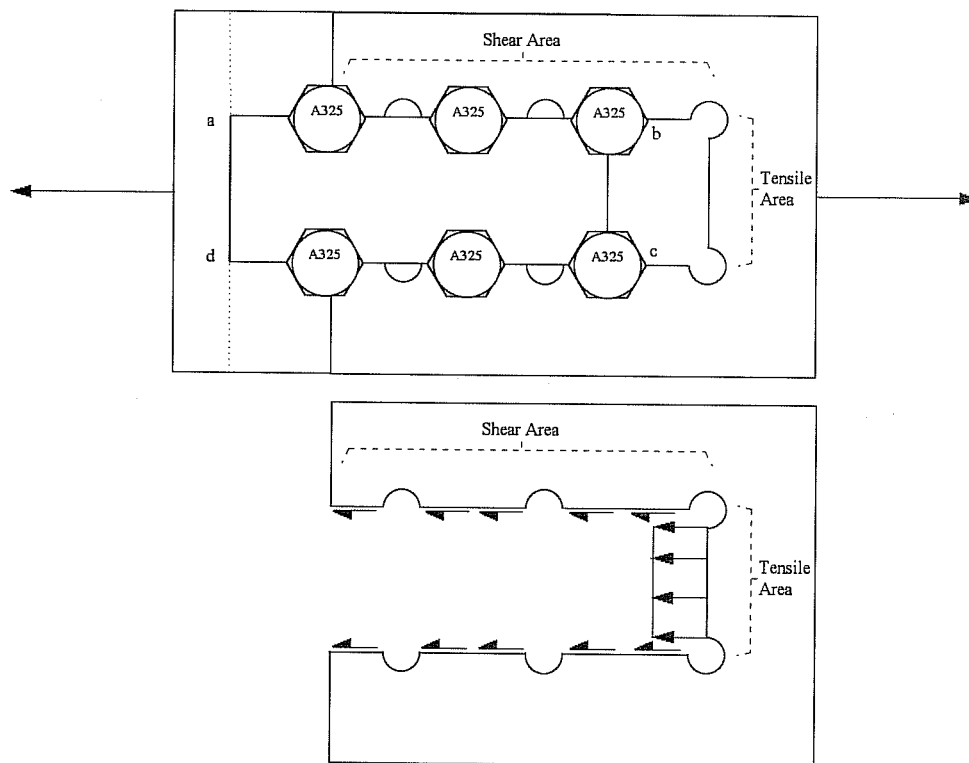


Figure 1-12 Typical block shear failure in a tension connection

4. Plate failure by excessive hole deformation

Another plate failure mode is the bearing failure of the plate. At the edge of the hole, the plate is subjected to a stress much larger than its tensile strength. Consequently, the hole deforms excessively and the plate material becomes upset and piles up around the hole in the area of plate-bolt contact. Figure 1-13 shows a bearing deformation failure. This failure can be prevented by limiting the bearing strength to 2.4 times the strength of the plate.

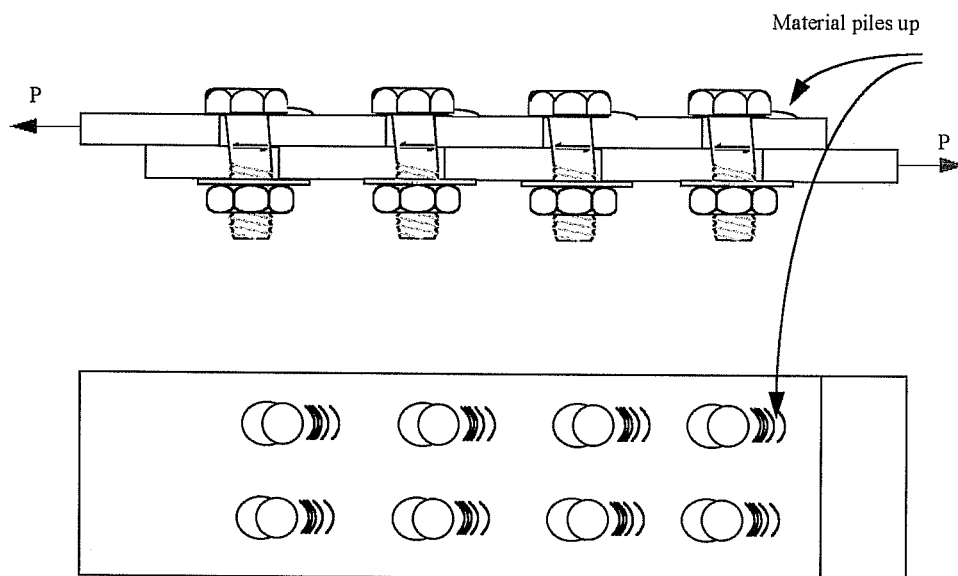


Figure 1-13 Typical bearing deformation failure in tension connections

5. Plate failure by tearing out of the edge bolt

Plate failure by tearing out of the edge bolt occurs when the edge bolt is too close to the edge of the plate. The plate shears along two inclined planes and a tear out failure occurs. Figure 1-14 shows a typical tear out failure of an edge bolt.

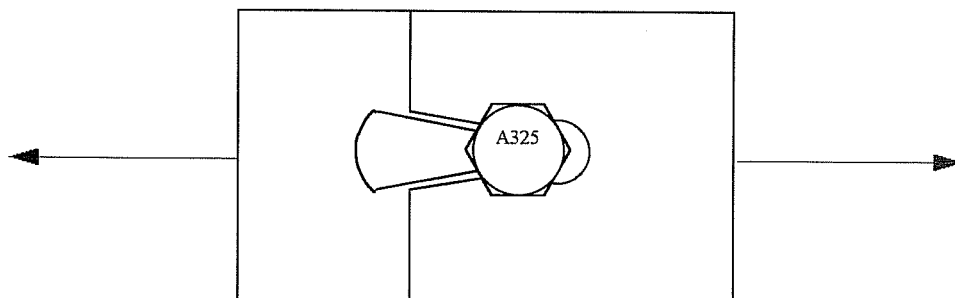


Figure 1-14 Typical tear out failure of an edge bolt

Since the tear out failure is associated with shearing of the plate along the inclined planes shown in Figure 1-14, the tear out capacity can be approximated by ignoring the inclination of the shearing planes:

$$P = 2t(L - 0.5d)(0.6F_u) \quad (1 - 7)$$

Where:

- 2 the number of shearing planes
- t the thickness of the critical plate
- L the distance from the plate edge to the center line of the edge bolt
- d the diameter of the bolt
- 0.6 the assumed shear to tensile strength of the connected plate material
- F_u the tensile strength of the plate

1.1.3. The behavior and capacity of bolted connections subjected to eccentric shear

If the shear does not act at the center of gravity of the connection bolts, the bolts will be subjected, at their centroid, to a twisting moment along with the applied shear. This twisting moment is equal to the shear times the shear eccentricity; where the eccentricity is the perpendicular distance from the center of gravity of the bolts to the shear line of action. The twisting moment tends to rotate the resultant force in each bolt away from the direction of the applied shear and, therefore, reduce the total shear capacity of the connection. Figure 1-15 shows an example of an eccentrically loaded group of bolts.

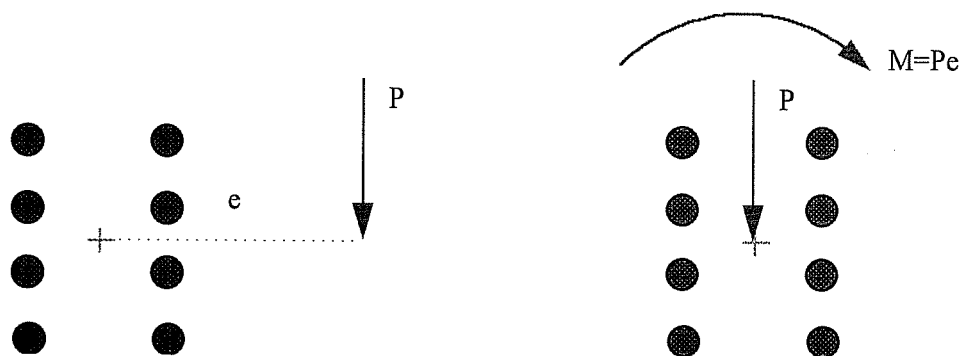


Figure 1-15 An eccentrically loaded group of bolts

Eccentrically loaded connections can be either slip-critical or bearing-type connections. Moreover, the bolts can be subjected to single or double shear. Initially, the load is transferred completely by the frictional resistance of the faying surfaces, provided that the bolts are fully pretensioned, and the bolt that lies the furthest from the center of rotation, usually called the critical bolt, carries the largest load. As the load increases the resultant force in each bolt increases. When all the bolts reach their individual slip loads (the assumption that a slip will not occur until all bolts reach their individual slip resistance will be examined later in Chapter 4), the connected plates slip and the critical bolt comes into bearing with the connected plates. Then, as the load increases the connection behaves elastically until the stress in either the bolt or the plates reaches the yield stress of the material. Any additional load beyond the yield load will cause the connection to behave inelastically. Then, the stiffness of the connection starts to decrease with any additional load. Finally, a failure occurs in either the bolts or the connected plates.

Eccentrically loaded connections can fail by either bolt shear failure or by plate failure:

1. Bolt shear failure

As mentioned earlier, the resultant in each bolt will not be parallel to the line of action of the applied shear due to the twisting moment caused by the eccentricity. Therefore, the total shear capacity will be less than the sum of the shear capacities of all bolts. The shear capacity of eccentrically loaded group of bolts is normally calculated as follows:

$$P = C N_s p \quad (1-8)$$

Where:

P is the total shear capacity of the connection

C is a coefficient that is equal to the eccentric shear capacity of the bolts divided by the shear capacity of one bolt. This coefficient can be calculated by either the traditional elastic vector method or by the nonlinear method of analysis³. These two methods will be reviewed and discussed later in Chapter 2 in detail

2. Plate failure

The plate of eccentrically loaded connection might fail in one of the following modes:

a) Bending Failure

This failure happens when the moment exceeds the moment capacity of the plate. The moment capacity of the plate is out of the scope of this dissertation and will not be discussed any further.

b) Shear Failure

This failure occurs when the applied shear exceeds the fracture capacity on the net section of the plate. However, in order for the plate to reach strain hardening, it has to undergo a very large deformation with respect to the deformation at first yield. Therefore, the applied shear should be limited to the shear yield capacity of the gross section of the plate. Thus, the shear capacity of the plate can be calculated as follows:

$$P = \text{minimum of } (0.6 A_g F_y, 0.6 A_n F_u) \quad (1-9)$$

Where:

- P is the shear capacity of the connection
- A_g is the gross area of the connected plate = $d_p t$
- d_p is the depth of the connected plate
- t is the thickness of the connected plate
- A_n is the net area of the connected plate = $[d_p - n d_h] t$
- n is the number of bolts in one vertical row
- d_h is the effective diameter of the hole = the diameter of the hole plus 1/16 in.
- F_y, F_u is the yield, ultimate stress of the connected plate, respectively.

c) Block Shear Rupture of the connected plates

This failure is a combination of shear and tension where the yield is reached on the gross section and the fracture strength is reached on the net section on a plane perpendicular to the first plane. Figure 1-16 shows a typical block shear rupture in a bolted web connection.

A portion of the connected might tear out as shown in Figure 1-12. This failure is called a block shear failure. Block shear failure usually occurs in thin plates when the connection length is short. The block shear rupture is not a fracture failure but a combination of fracture at the net section and yielding at the gross section of a perpendicular plane. For a large tensile area and a small shear area, the failure mode occurs by fracturing of the net tensile area and yielding of the gross shear area. For a small tensile area and a large shear area, the failure mode occurs by fracturing of the net shear area and yielding of the gross tensile area.

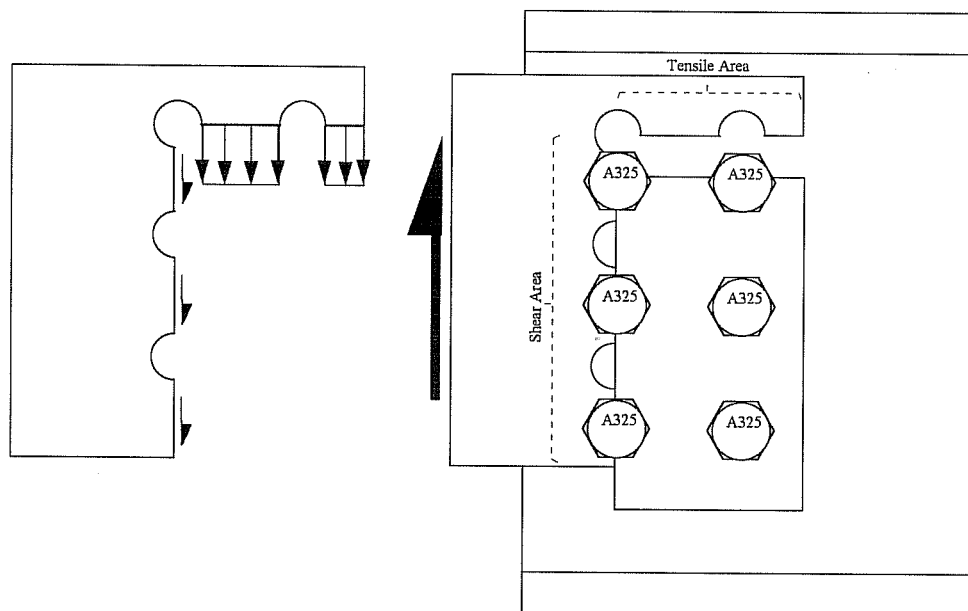


Figure 1-16 Typical block shear rupture in a bolted web connection

Thus, the tear out failure might occur in one of the two following modes:

When $0.6F_u A_{nv} > F_u A_{nt}$ the failure mode will be a combination of tension yield along the gross tensile area and shear fracture along net the shear area. The block shear capacity for this case can be calculated as follows:

$$P = 0.6F_u A_{nv} + F_y A_{gt} \quad (1-10)$$

- d) When $F_u A_{nt} > 0.6F_u A_{nv}$ the failure mode will be a combination of tensile fracture along the net tensile area and shear yield along the gross shear area. The block shear capacity for this case can be calculated as follows:

$$P = 0.6F_y A_{gv} + F_u A_{nt} \quad (1-11)$$

1.2. Problem Statement

The web-flange splice must transfer the shear and moment of the beam at the location of the splice. Unfortunately, the distribution of the shear and moment between the flange and web splices is unknown. Figure 1-17 shows a probable distribution of the shear and moment between the web and flange splices.

In general, the design of a web-flange splice involves answering four major questions:

1. Where should the splice be located?
2. What are the design forces for the splice?
3. What is the distribution of the design forces between the web and flange splices?
4. How should the bolts and the splice plates of the web and flange splices be designed?

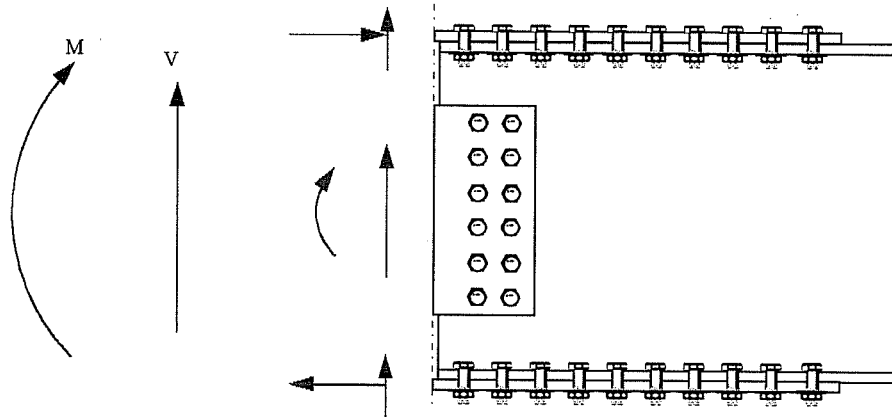


Figure 1-17 A probable distribution of the shear and moment between the web and flange splices

The LRFD³ manual enforces no limitation on the location of the splice. However, it requires beam or girder splices to develop the strength required by the actual forces at the point of the splice. Moreover, it recommends that designers specify some minimum strength requirements at the splice when the splice is located at the contraflexure point. This recommendation is due to the fact that the contraflexure point migrates as the applied load changes during the life time of the structure. Nevertheless, the LRFD gives no recommendation on the amount of this minimum strength requirement. Furthermore, the LRFD manual³ suggests designing the flange splice to carry the total applied moment and the web splice to carry the shear at an eccentricity calculated as the distance from the centroid of the web bolts to the centerline of the splice. Figure 1-18 shows the force distribution in w-f splices suggested by the 2nd. edition of the LRFD manual³.

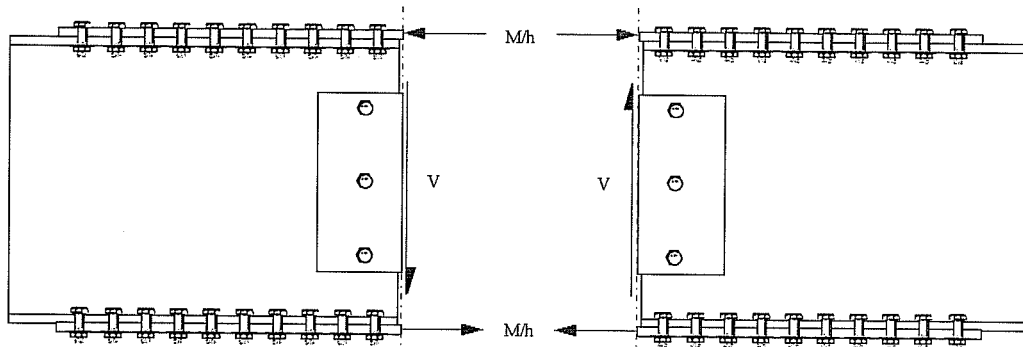


Figure 1-18 The force distribution in w-f splices suggested by the 2nd. edition of the LRFD manual

On the other hand, AASHTO⁴-10.18.2.5 prefers that splices in continuous spans be located at or near points of contraflexure. Moreover, AASHTO-10.18.1.1 requires that splices be designed for the average of the required strength at the point of splice and the strength of the member at that point but, in any event, not less than 75% of the strength of the member. AASHTO-10.18.2.1 requires that web splices be designed for the portion of the design moment resisted by the web, and for the moment due to eccentricity of the shear introduced by the splice connection. AASHTO-10.18.2.2 requires that flange splices be designed for the portion of the design moment not resisted by the web. Figure 1-19 shows the AASHTO force distribution in w-f splices (AASHTO-10.18.2.1 and 10.18.2.2).

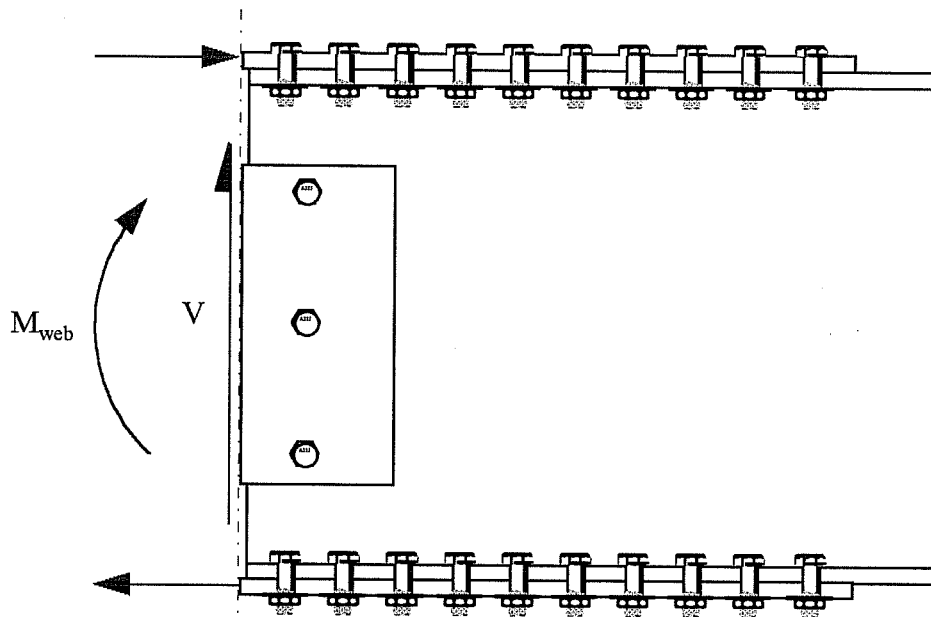


Figure 1-19 The AASHTO force distribution in w-f splices

Different researchers and authors recommend different design procedures. Salmon and Johnson⁵ recommend that, in high shear and moment locations, the web splice be designed for the portion of the design moment resisted by the web and for the moment due to eccentricity of the shear introduced by the splice geometry. Salmon and Johnson⁵ also recommend neglecting any eccentricity effect on the web when the splice is located at low shear and moment location. Figure 1-20 shows the force distribution in w-f splices recommended by Salmon and Johnson.

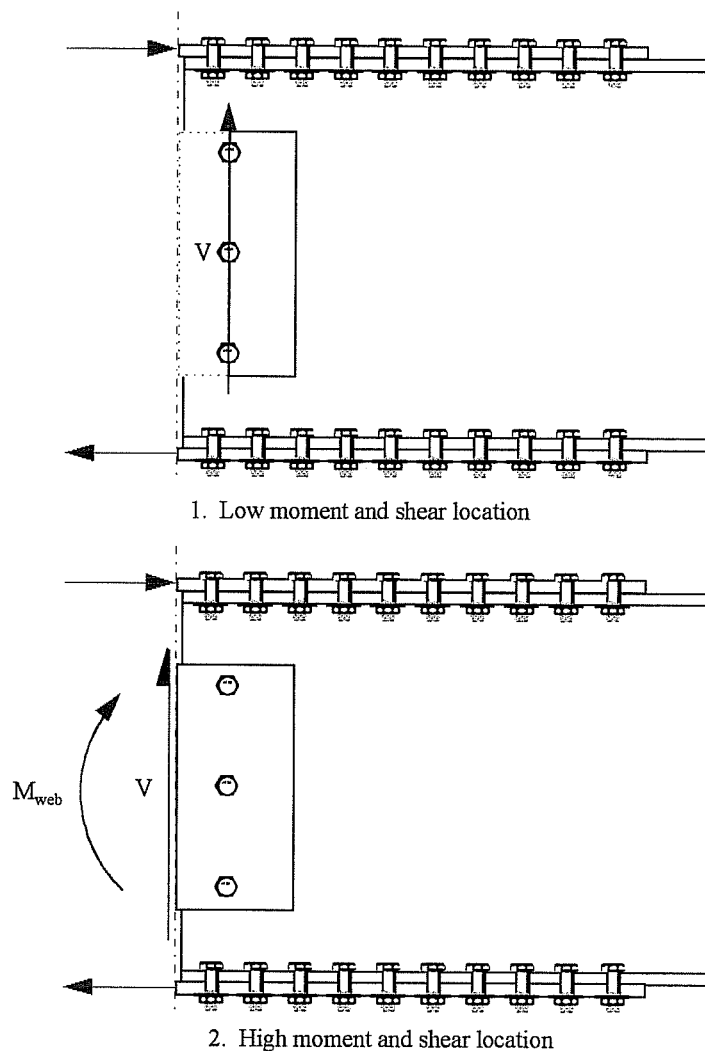


Figure 1-20 The force distribution in w-f splices recommended by Salmon and Johnson

Kulak, Fisher, and Struik² recommend designing the flange splice for the total design moment and designing the web splice for either:

1. A force, equal to the total shear, that satisfies the equilibrium equations as follows:

- a) The vertical resultant of the bolt forces should equal the total vertical shear
 - b) The summation of the external moment, the moment due to the axial load in the flanges, and the moment due to the resultant of the bolt forces about the instantaneous center of rotation of the web bolts equals to zero
2. An eccentric force that equals the total shear acting at an eccentricity calculated as the distance between the center of gravity of the opposite bolt groups to the center of gravity of the bolt group under consideration.

Figure 1-21 shows the design forces on the web and flange splices recommended by Kulak, Fisher, and Struik².

Kulak and Green⁶ recommend, based on an experimental program performed on web splices located at the inflection point, that bolt groups on each side of web splices located at the inflection point be designed for the total shear that acts at the centerline of the splice and for the moment caused by the eccentricity of the shear. This eccentricity is the distance from the centerline of the splice to the centroid of the web bolts.

Gaylord, Jr., Gaylord, and Stallmeyer⁷ follow a stress analysis approach instead of load approach; they first calculate the maximum bending stress in the web and add it vectorially to the average shear stress to get the resultant stress. Then, they assume the stress to be constant along the depth of the web. They multiply it by the web splice area along one vertical spacing to get the resultant

force on one horizontal row of bolts, then the bolts in this horizontal row must be able to carry the resultant load.

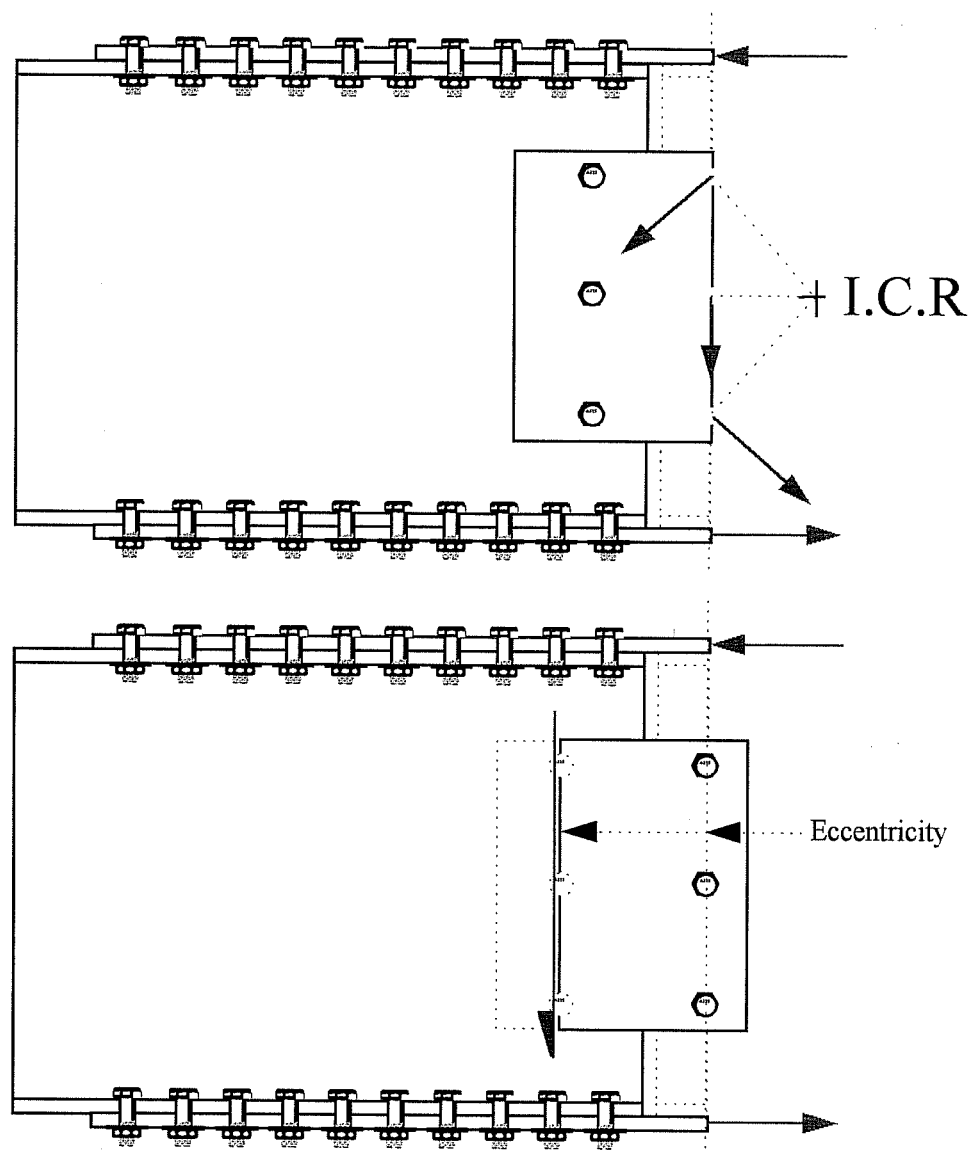


Figure 1-21 The design forces on the web and flange splices recommended by Kulak, Fisher, and Struik

As can be seen from the previous discussion, different design procedures are available for bolted web-flange splices. These different design procedures will result in a different number of bolts, especially for the web splice. Furthermore, testing programs have been limited to web splices, where only the webs were connected, located at the inflection point⁶, and to flange splices⁸, where only the flanges were connected, and for the latter, the flange splices were not tested to failure but they were used to explore the effect of holes in the flanges on the plastic moment capacity of beams. No testing program was performed on web-flange splices. Therefore, a testing program on web-flange splices and on web splices not located at the inflection point needs to be done.

1.3. Purpose

The purpose of this research was to investigate the behavior of web-flange bolted splices of symmetric and unsymmetric girders, determine the distribution of the applied forces between the web and flange splices, and finally determine the distribution of the web splice forces within the web bolts.

The research was oriented to answer the following questions for both the slip-critical and bearing-type bolted web-flange splices of steel bridges:

1. For symmetric splices

- Does the web splice need to be designed for moment when the flanges are adequate to carry the applied moment?
- If the web splice can be designed for shear only, can the bolts be designed as concentrically loaded connection neglecting any eccentricity effect on the shear capacity of the bolts.

- How can the bolts in the web splice be reasonably designed when the applied moment exceeds the moment capacity of the flanges?
2. For unsymmetric splices of steel or composite girders
- Does the web need to be designed for moment when the flanges of the steel girder or composite section have adequate capacity to carry the applied moment?
 - If the moment exceeds the moment capacity of the steel girder flanges but is still less than the moment that can be carried by both the beam flanges and the concrete slab, does the web need to be designed for moment ?
 - How can the web be reasonably designed when the design moment exceeds the moment that can be carried by the steel girder flanges and the concrete slab combined?

The purpose of this dissertation is to present the findings of the analytical and experimental research programs conducted on steel girder bolted splices, develop design procedures, and finally demonstrate the application of the design procedures by means of design examples.

1.4. Scope

In Chapter 2, the available analyses of eccentrically loaded bolted connections are reviewed and the proper method of analysis is recommended. In Chapter 3, the results of the splice material testing are presented and discussed. The effect of hole making, preload in the bolts, and material loading history on the shear strength of high strength bolts is determined. In Chapter 4, the results of 32 full-scale tests of steel girder bolted splices are presented and discussed. The distribution of moment and shear between the web and flange splices is determined and compared with test results. Chapter 5, presents simple design procedures for the splices of symmetric, unsymmetric, and composite girders. Chapter 6 presents three design examples using actual forces on composite bridge girders to demonstrate the application of the design procedures. Finally, Chapter 7, summarizes the results of this research and draws conclusions from the results of the testing program.

Chapter 2

2. Review of the analysis of eccentrically loaded group of bolts

2.1. Introduction

Eccentrically loaded group of bolts can be found in bolted web splices, bolted beam-column connections, and bolted brackets. Figure 2-1 shows typical examples of eccentrically loaded group of bolts.

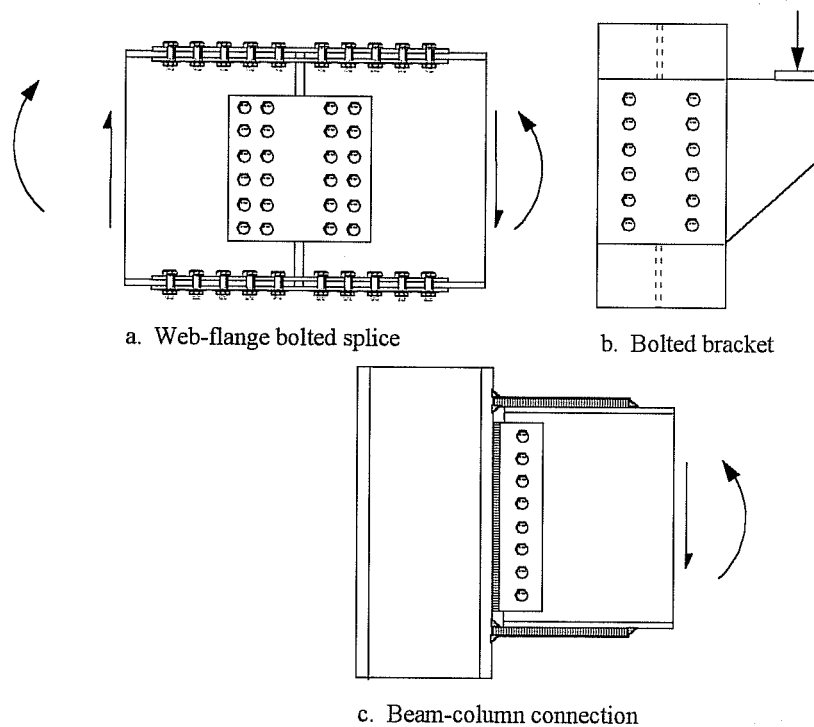


Figure 2-1 Typical examples of eccentrically loaded group of bolts

In this Chapter, the available analyses of eccentrically loaded group of bolts are reviewed. A linear elastic instantaneous center of rotation (EC) method of

analysis is developed. The theoretical results of the EC and of the present methods of analysis are compared with two previous testing programs. Finally, conclusions with regard to the proper method of analysis are made.

2.2. Historical background

The design forces for a bolted web splice are eccentric to the group of web bolts. Therefore, the splice is normally designed as an eccentrically loaded bolted connection. The main objective of the analysis of eccentrically loaded group of bolts is to determine the distribution of the design forces within the bolts and, hence, the capacity of the connection. However, the equilibrium equations are not sufficient to determine the distribution of the design forces within the bolts. Therefore, simplified assumptions need to be made to facilitate the analysis.

The analysis of an eccentrically loaded bolted connection was first solved by using the elastic vector method that can be found in many text books^{3, 4}. In this method, the shear and moment are transferred to the centroid of the bolts. Then, the analysis is broken down into two analyses; the analysis of the bolt forces due to the concentric applied shear, and the analysis of the bolt forces due to the moment applied at the centroid of the bolts. It is further assumed that the connected plates are infinitely rigid, the bolts are elastic, and all the bolts have the same cross sectional area. The concentric shear analysis is done by assuming that the shear is distributed equally among the bolts. Therefore, the force component that acts at any bolt due to shear is calculated by dividing the total shear by the total number of bolts. The analysis of the bolt forces due to the applied moment is done by assuming that the bolts rotate about their center of gravity. Moreover, it is assumed that the force in any bolt is proportional to its distance to the center of

rotation which coincides with the center of gravity of the bolts. The force component due to moment on a bolt is calculated as follows^{5,10}:

$$R = \frac{Md}{\sum d^2} \quad (2-1)$$

where:

M is the centroidal moment

d is the radial distance from the bolt to the center of gravity of the group of bolts

After performing the concentric shear and centroidal moment analyses, the force resultant in each bolt can be obtained by vectorially adding the force component due to the concentric shear to that due to the centroidal moment. The capacity of the connection is reached when the force on the critical bolt, the bolt that has the largest force resultant, reaches the bolt's design capacity. The elastic vector method is simple; however, it was reported to be unduly conservative¹⁰ when compared with test results. Therefore, several research programs were conducted on the eccentric shear problem of bolted and riveted joints to improve the predicted shear capacity of the joint.

In an effort to increase the predicted capacity of the riveted connections obtained using elastic analysis, Higgins¹⁰ developed two empirical formulas that reduced the actual eccentricity. The two empirical formulas are shown in the two following equations:

$$l_{\text{eff}} = l_{\text{act}} - \frac{1 + 2n}{4} \quad (2-2)$$

$$l_{\text{eff}} = l_{\text{act}} - \frac{1 + n}{2} \quad (2-3)$$

where:

- l_{eff} is the effective eccentricity
- l_{act} is the actual eccentricity
- n is the number of fasteners per gage line

Equations 2-2 and 2-3 are used for equally spaced fasteners on a single, and two or more gage lines, respectively. The reduced eccentricity was achieved by introducing a reduction term, the second term in each of Equations 2-2 and 2-3, to the actual eccentricity. This reduction term is a function of only the number of bolts in one gage line. Higgins¹⁰ reasons for making the reduction term a function of the number of bolts were as follows:

1. The effect of a given amount of eccentricity on the shear capacity of the connection should decrease as the number of bolts increases
2. As the number of bolts increases the capacity of the connections increases due to the effect of the frictional resistance of both the fasteners and the connected plates, and to the effect of the ductility of the bolts

The concept of a reduced eccentricity was then adopted in the 6th edition of the AISC (American Institute of Steel Construction) manual.

Due to the empirical nature of the reduced eccentricity concept, further studies were done to explore the use of plastic analysis on the bolts^{11, 13}. In the plastic analysis of the bolts, it is assumed that all the bolts reach their individual ultimate capacity at failure, as opposed to the elastic analysis which assumes that only the critical bolt reaches its design capacity at failure. In general, the plastic analysis requires iterative solution scheme to satisfy the equilibrium equations. To facilitate the plastic analysis and design of the bolts, Abolitz¹¹ developed interaction diagrams and formulas and was succeeded by Shermer¹³ who developed design tables that were based on the plastic analysis of the bolts. The idea of employing plastic analysis in eccentric bolted connections was questioned and criticized by Fisher and Kulak¹² and by Kulak¹⁴ for two reasons:

1. High strength bolts do not have a definite yield point and, therefore, are not suitable for plastic analysis
2. In addition to the static equilibrium, compatibility must be satisfied. The need of meeting compatibility can be illustrated by the case of concentrically loaded connections. For this case, the shear capacity is a function of the connection length and the shear capacity is less than the algebraic sum of the individual shear capacity of each bolt

Up to this point, the previous methods assumed either elastic or plastic behavior of the bolts. Sherwood, Crawford, and Kulak⁹ developed the ultimate strength method which took into account the nonlinear load-deformation response of an individual bolt. To account for the actual load-deformation response of the bolts, the empirical load-deformation formula, found by Wallaert and Fisher¹⁵, was employed in the analysis. This empirical formula is shown in Equation 2-4. Figure 2-2 shows the empirical nonlinear load-deformation response of an individual high strength bolt used in the ultimate strength method.

$$R = R_{ult} (1 - e^{-\mu\Delta})^\lambda \quad (2-4)$$

where:

R is the force in the bolt under consideration

R_{ult} is the ultimate strength of the bolt

e is the base of the natural logarithm (2.718)

μ, λ are materials-dependent regression coefficients, equal to 10 and 0.55 for A36 steel plates and 3/4" A325 high strength bolts

Δ is the bearing deformation of the bolt under consideration

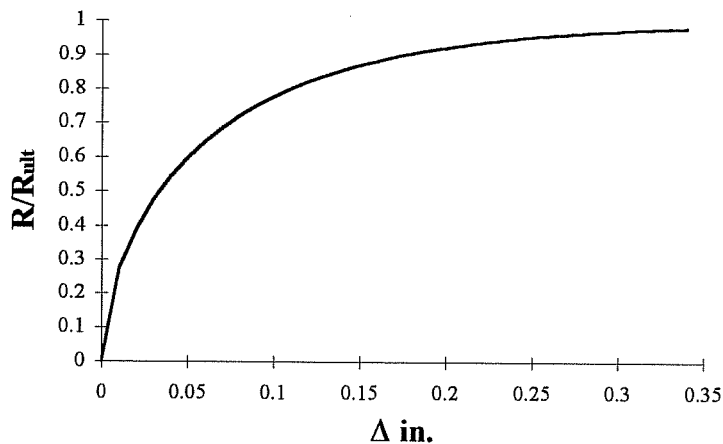


Figure 2-2 The empirical nonlinear load-deformation response of an individual high strength bolt used in the ultimate strength method

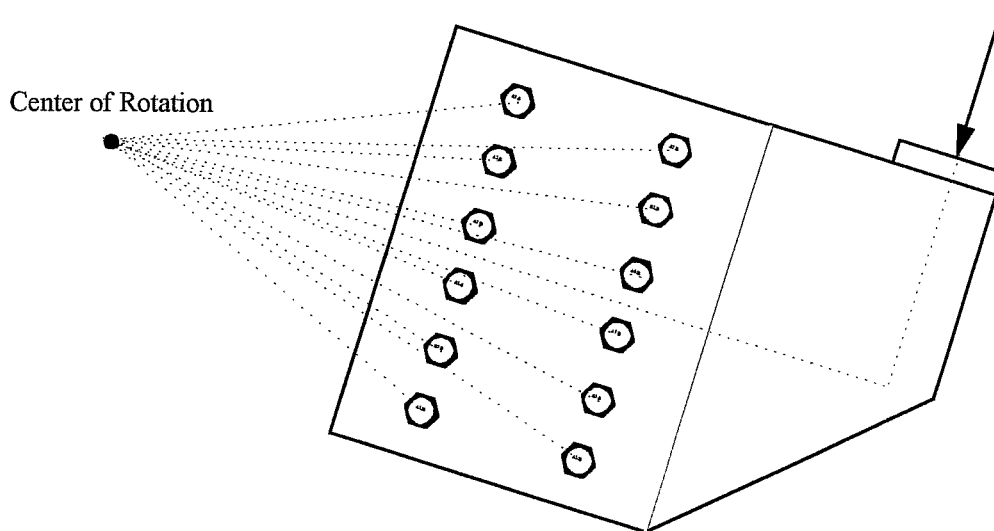


Figure 2-3 The instantaneous center of rotation of the group of bolts

In the ultimate strength method, a few assumptions were made:

1. The bolts rotate about an instantaneous center of rotation and not the center of gravity as shown in Figure 2-3
2. The connecting plates are infinitely rigid, therefore, the deformation of any bolt is proportional to its radial distance from the center of rotation
3. The connection fails when the bolt farthest from the center of rotation reaches its maximum deformation which can be obtained from testing of individual bolts

For a given configuration of bolts and for a given eccentricity, the steps involved in the nonlinear analysis are as follows:

1. Guess a location of the instantaneous center

2. At failure, the critical bolt reaches its maximum deformation Δ_{\max}
3. The deformation in any bolt can be calculated from equation 2-5

$$\Delta_i = \Delta_{\max} \frac{d_i}{d_{\max}} \quad (2-5)$$

where:

- Δ_i is the deformation of the bolt under consideration
- Δ_{\max} is the maximum deformation of the critical bolt at failure; equal to 0.34 inches for 3/4" A325 bolts and A36 steel plates
- d_i is the radial distance from the bolt under consideration to the center of rotation
- d_{\max} is the radial distance from the critical bolt to the center of rotation

4. After determining the deformation of all the bolts, the force in any bolt can be calculated from the empirical load-deformation equation (equation 2-4)
5. After determining the forces in all the bolts, the static equilibrium equations must be satisfied. If the equilibrium equations are not satisfied, a new location of the center of rotation is assumed, and steps 1 through 5 are repeated until the equilibrium of the internal and external forces is achieved

The nonlinear ultimate strength method was adopted in the 1st. and the 2nd. editions of the LRFD manual of steel construction.

In an effort to improve the efficiency of the ultimate strength method, more studies were done. Brandt¹⁶ proposed a rapid solution to improve the efficiency of

the ultimate strength method. In this solution, the elastic solution is chosen as a starting point for the iterative solution. The solution include the following steps:

1. Determine the elastic center of rotation. The elastic center of rotation is obtained by summing moments of the force components of the bolts due to the concentric applied shear, the force components of the bolts due to the centroidal moment, and the applied moment at the elastic center of rotation
2. Determine the elastic C coefficient ($C = \text{the theoretical eccentric shear capacity of the bolts} / \text{the shear capacity of one bolt}$)
3. Determine an approximate value for the ultimate strength C coefficient. To do this, the steps used in the ultimate strength method are used except for the fact that the elastic center is used instead of the ultimate center
4. Iterate to improve the approximate C coefficient. This is done by determining the unbalanced forces at the center of rotation and, thus, calculating the shift in the center of rotation to balance the unbalanced forces

The last step is repeated until a stable solution is obtained.

Marsh¹⁷ acknowledged the fact that Brandt's solution is less time consuming than the original ultimate strength method. However, he suggested modifying Brandt's solution for a faster solution as follows:

1. Use the elastic center of rotation as an acceptable approximate center of rotation
2. Assume that all the bolts reach their ultimate capacity at failure
3. Equilibrium check needs not to be performed

On the other hand, Iwankiw¹⁸ supported Brandt's solution. However, he suggested accepting the first approximate ultimate strength solution as a good estimate of the true ultimate solution since one cycle yields results within 10% of the true ultimate solution.

Also, Rutenberg¹⁹ in an effort to simplify the nonlinear analysis suggested a step-by-step method using a rigid plate-piece-wise linear bolt model. Figure 2-4 shows the piece-wise linear bolt response model.

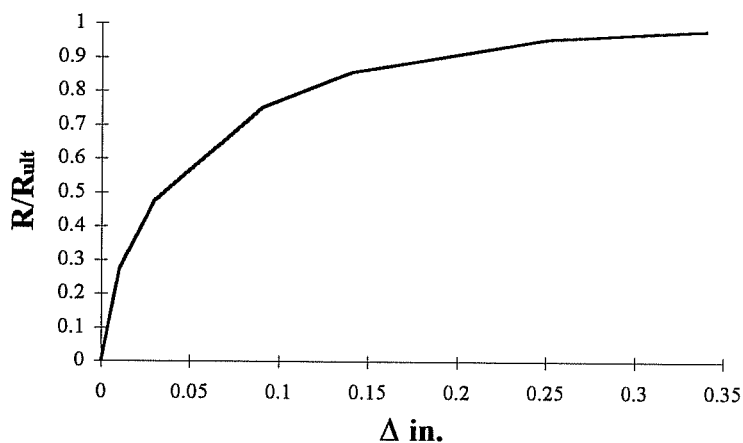


Figure 2-4 The piece-wise linear bolt response model

In Rutenberg's method, a series of incremental elastic analyses, all having simple explicit solutions replace the trial and error nonlinear analysis. Rutenberg's method is based on the following assumptions:

1. The bolts rotate about an incremental instantaneous center of rotation due to an incremental change in load

2. The incremental displacement in the bolt is perpendicular to its distance from the incremental center of rotation
3. Changes in load direction have negligible effects on the fastener response
4. The connected plates are infinitely rigid at all times
5. The load-deformation response of an individual fastener is piece-wise linear
6. The ultimate strength is reached when the critical fastener reaches its ultimate capacity

2.3. Discussion of previous work and the need for a further study

In general, there are three approaches to the analysis of the eccentrically loaded bolts:

1. Elastic analysis
2. Plastic analysis
3. Nonlinear analysis

In general, the elastic analysis is direct and simple; however, it was reported to be unduly conservative when compared with test results. If using a reduced eccentricity, the elastic analysis yields results that are closer to test values. However, the reduced eccentricity is empirical and may not be applicable to all geometries.

The plastic analysis is indirect and iterative. Further, it does not represent the actual behavior of eccentrically loaded bolted connections where only the critical bolt fails while the rest of the bolts are not fully loaded.

The nonlinear analysis suggested by Sherwood, Crawford, and Kulak⁹ is rational though unconservative. In the nonlinear analysis, the location of the instantaneous center is unknown and, therefore, a trial and error solution must be carried out. Consequently, the method is computer-dependent for connections with large number of bolts. In the solution suggested by Brandt to improve the efficiency of the nonlinear analysis, the analysis remains computer-dependent, time consuming, and unconservative. As far as the solution suggested by Marsh to improve the efficiency of the nonlinear analysis, the employment of plastic theory in the solution does not agree with the actual behavior of the eccentrically loaded bolted connections and is unconservative. The suggestion by Iwankiw to use only the first cycle of Brandt's solution is fast and direct. However, the solution remains unconservative. Further, knowing that the equilibrium equations are not satisfied, the accuracy of the solution is unknown. Finally, in the incremental elastic analysis done by Rutenburg, the number of steps depends directly on the number of fasteners. Therefore, for a large number of fasteners, the use of computers is essential to the solution.

In this research, it is felt that there is a need for further evaluation of the available analyses of the eccentrically loaded group of bolts to improve the predicted results and to shorten the computation time simultaneously.

2.4. The Elastic Center of Rotation Method

2.4.1. Introduction

The concept of the elastic center of rotation is not new. However, when used and derived by Brandt, the analysis was broken down into a concentric shear analysis and an applied centroidal moment analysis. Further, in the concentric shear analysis, the shear was distributed equally among the fasteners.

In the following method derived herein, the analysis is not broken into two analyses. Further, compatibility is enforced. Nevertheless, when enforcing the compatibility, a simplified linear load-deformation response of each individual bolt is assumed.

2.4.2. Assumptions

1. The load-deformation response of an individual bolt is linear
2. The group of bolts rotates about an instantaneous center of rotation which is different, in general, than the center of gravity of the bolts
3. The connected plates are infinitely rigid and, therefore, the deformation in any bolt is proportional to its distance from the elastic center of rotation
4. The connection fails when the critical bolt that lies the farthest from the instantaneous center of rotation reaches its maximum deformation
5. To simplify the analysis, the geometry of the connection is assumed symmetrical about the horizontal axis that passes through the centroid

Nomenclature:

e.c.r	is the elastic center of rotation
$\sum M_{e.c.r}$	is the summation of the external and internal moments about the elastic center of rotation
P	is the applied load
e	is the eccentricity of the applied load
r_o	is the distance between the centroid of the bolts and the elastic center of rotation
R_i	is the force resultant in the bolt under consideration
\overline{d}_i, d_i	is the radial distance of the bolt under consideration with respect to the elastic center of rotation, centroid of the bolts, respectively
\overline{X}_i, X_i	is the X coordinate of the bolt under consideration with respect to coordinate system that passes through the elastic center of rotation, centroid of the bolts, respectively
\overline{Y}_i, Y_i	is the Y coordinate of the bolt under consideration with respect to coordinate system that passes through the elastic center of rotation, centroid of the bolts, respectively
m, n	is the number of bolts in a horizontal, and in a vertical row, respectively
F_y	is the vertical component of the force resultant in the bolt under consideration
R_{ult}	is the ultimate capacity of an individual bolt
max	denotes the bolt that lies the farthest from the center of rotation; critical bolt

2.4.3. Mathematical Derivation

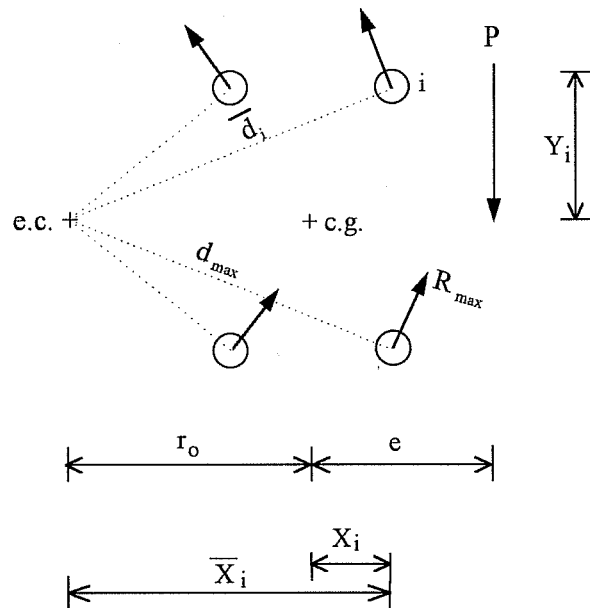


Figure 2-5 The elastic center of rotation method

At the center of rotation shown in Figure 2-5, the external moment should equilibrate the internal moment. Thus:

$$\sum M_{e.c.r} = 0 \Rightarrow P(e + r_o) = \sum R_i \bar{d}_i \quad (2-6)$$

where:

$$\bar{d}_i = \sqrt{Y_i^2 + \bar{X}_i^2} = \sqrt{Y_i^2 + (r_o + X_i)^2} \quad (2-7)$$

Also:

$$\bar{X}_i = (r_o + X_i) \quad (2-8)$$

By writing the vertical force equilibrium equation, we get:

$$\Sigma F_y = 0 \Rightarrow P = \Sigma \left(\frac{R_i \bar{X}_i}{d_i} \right) \quad (2-9)$$

from the assumption that the plates are infinitely rigid (elastic), and since the load-deformation response of an individual bolt is linear, one can write:

$$\frac{R_i}{d_i} = \frac{R_{ult}}{d_{max}} \quad (2-10)$$

from equations 2-6, 2-8, and 2-9

$$\Sigma \left[R_i \left(\frac{r_o + X_i}{d_i} \right) \right] (e + r_o) = \Sigma (R_i \bar{d}_i) \quad (2-11)$$

by substituting equation 2-10 into equation 2-11

$$\left[\frac{R_{ult}}{d_{max}} \Sigma (r_o + X_i) \right] (e + r_o) = \frac{R_{ult}}{d_{max}} \Sigma \bar{d}_i^2 \quad (2-12)$$

equation 2-12 can be rewritten as:

$$\Sigma \overline{d_i^2} = (e + r_o) \Sigma (r_o + X_i) \quad (2-13)$$

substitute equation 2-7 in 2-13:

$$\Sigma (Y_i^2 + \overline{X_i^2}) = (e + r_o) \Sigma (r_o + X_i) \quad (2-14)$$

from equation 2-14 and equation 2-8:

$$\Sigma (Y_i^2 + (r_o + X_i)^2) = (e + r_o) \Sigma (r_o + X_i) \quad (2-15)$$

By expanding the terms on the left side of equation 2-15, one gets:

$$\Sigma (Y_i^2 + (X_i^2 + 2X_i r_o + r_o^2)) = (e + r_o) \Sigma (r_o + X_i) \quad (2-16)$$

By expanding the terms of equation 2-16, one gets:

$$2r_o \Sigma X_i + mnr_o^2 + \Sigma (X_i^2 + Y_i^2) = mner_o + mnr_o^2 + e \Sigma X_i + r_o \Sigma X_i \quad (2-17)$$

To determine the location of the elastic center of rotation, equation 2-17 can be rearranged as follows:

$$r_o = \frac{\Sigma d_i^2 - e \Sigma X_i}{mne - \Sigma X_i} \quad (2-18)$$

By substituting equation 2-8 and equation 2-10 into equation 2-9, one gets:

$$P = \frac{R_{ult}}{d_{max}} \sum (r_o + X_i) = \frac{R_{ult}}{d_{max}} (mnr_o + \sum X_i) \quad (2-19)$$

Equation 2-19 yields a C value of:

$$C = \frac{P}{R_{ult}} = \frac{mnr_o + \sum X_i}{\sqrt{(r_o + X_{max})^2 + Y_{max}^2}} \quad (2-20)$$

Equation 2-20 determines the normalized shear capacity of the eccentrically loaded group of bolts. If the group of bolts is symmetric about the vertical axis that passes through its centroid, equation 2-18 can be simplified to the following:

$$r_o = \frac{\sum (X_i^2 + Y_i^2)}{mne} = \frac{\sum d_i^2}{mne} \quad (2-21)$$

Equation 2-21 shows that the location of the elastic instantaneous center of rotation is a function of the eccentricity and the bolts geometry with respect to the center of gravity. The level of applied load, shear and moment, does not affect the location of the center of rotation.

To determine the C coefficient for eccentrically loaded group of bolts which is symmetric about the vertical axis that passes through its centroid, substitute equation 2-21 in equation 2-20:

$$C = \frac{1}{\sqrt{\frac{1}{mn} + \frac{2 \sum X_{\max} e}{\sum d_i^2} + mn \left(\frac{ed_{\max}}{\sum d_i^2} \right)^2}} \quad (2-22)$$

Equation 2-22 determines the C coefficient which represents the effective number of bolts that resist the eccentric shear. The difference between the actual number of bolts and the C coefficient represents the number of bolts lost due to the effect of the eccentricity.

2.4.4. Comments and Observations on the elastic center of rotation

It is interesting to note that the location of the elastic center derived by Brandt and the C coefficient obtained from traditional elastic vector method are identical to those obtained from the elastic instantaneous center method. The only difference is that the force in the critical bolt is limited to the allowed load on the bolt when using the traditional elastic vector method, whereas, the critical bolt is permitted to reach its ultimate capacity when using the elastic center of rotation method. To explain the equality of the results obtained from both methods, the translation of the bolts in both methods will be compared herein.

The elastic instantaneous center method is based on a rotation about the instantaneous center which produces a translation perpendicular to the radius of rotation of each bolt. This inclined translation of each bolt can be broken down into a horizontal and a vertical translation. On the other hand, the elastic vector method is based on a vertical translation of all the bolts and on a rotation about center of gravity of the bolts which produces a translation perpendicular to the

radius of rotation of each bolt. Figure 2-6 shows a comparison between the translation of the bolts obtained from the elastic center of rotation method and those obtained using the elastic vector method

The elastic center of rotation method yields equal vertical translations of all the bolts. To examine the equality of the vertical translation of all the bolts obtained from the elastic center of rotation method, let us consider the case of zero eccentricity where the resultant in each bolt is vertical. Since all bolts rotate about a center of rotation and since the translation of each bolt is perpendicular to the center of rotation, the center of rotation will be located at a horizontal infinity. Also, since the deformation of any bolt is proportional to its distance from the center of rotation which is located at a horizontal infinity, the deformation of all the bolts will be identical. The equality of the vertical translation of all the bolts in the elastic center of rotation method results in equal vertical forces of the bolts, the same as the concentric shear problem results when using the elastic vector method.

On the other hand, the radial component of translation (with respect to the center of gravity) of all the bolts obtained from the elastic center method will also be identical to the radial translation obtained using the elastic vector method. This can be explained by considering the special case of infinite eccentricity or zero shear (pure moment). For this case, the center of rotation will coincide with the center of gravity and, therefore, the elastic center method yields the same bolt deformation and forces as those of the elastic vector method.

Since both the elastic vector method and the elastic instantaneous center method yield identical results, both methods will be referred to as the elastic method.

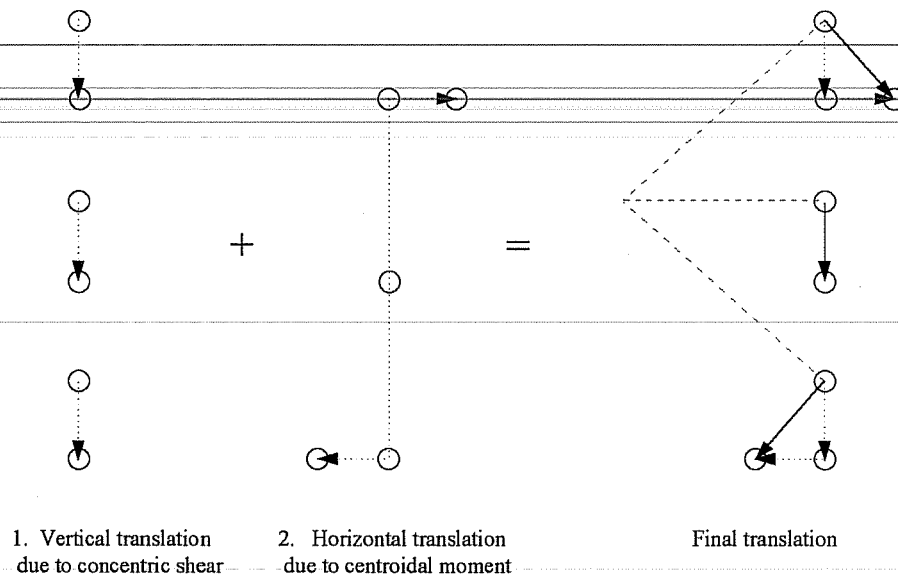


Figure 2-6 Comparison between the displacement component of the bolts for the traditional vector method and the displacement of the bolts for the elastic center of rotation

2.5. Comparison between the elastic, nonlinear method, and previous test results

2.5.1. Description of the testing programs

The results of two testing programs^{6, 9} performed on eccentrically loaded bolted connections are compared with those obtained from the elastic and the nonlinear methods of analyses. Further, the difference between the two methods of analyses is examined.

The first testing program was performed by Sherwood, Crawford, and Kulak⁹ on eccentrically loaded bolted clip angles. The second testing program was performed by Green and Kulak⁶ on bolted web splices located at the inflection point. For both testing programs the double shear capacity of one bolt was obtained from double shear splice tests. Compression and tension splices were used in the first and second testing programs, respectively, to determine the shear capacity of the bolts in the connection. The use of tension splices in the second testing program was done after the observation that the shear capacity of bolts loaded in tension splices is 10% lower than that of bolts loaded in compression splices⁶. The bolts used in the first testing program were from the same production lot, while, those used in the second program were from two different lots. The average double shear capacity of one bolt was 74 kips for the first program⁹. For the second testing program, the average double shear capacity of one bolt was 74.9 kips and 77.3 kips for bolts obtained from the first and second lots, respectively⁶. For the latter program, specimens C1 through C4 were manufactured using bolts from the first lot, whereas, specimen C5 was manufactured using bolts from the second lot. The bolts in the first testing program were pretensioned and the bolts in the second program were snug. The holes in both testing programs were the same size as the bolts (no hole clearance). The number of bolts used, the horizontal pitch, the vertical pitch, and the eccentricity of the applied load used in both testing programs are shown in Table 2-1.

Table 2-1 Details of the bolted specimens used in the comparison

Program	Specimen	m	n	b	D	e
1	B1	1	5	2.5	-	8
1	B2	1	5	3	-	10
1	B3	1	5	3	-	12
1	B4	1	6	3	-	13
1	B5	1	6	3	-	15
1	B6	2	4	3	2.5	12
1	B7	2	4	3	2.5	15
1	B8	2	5	2.5	2.5	15
2	C1	1	2	4.125	-	1.25
2	C2	1	2	3.125	-	1.25
2	C3	1	2	8.625	-	2.0
2	C4	1	3	3.500	-	2.0
2	C5	2	2	4.750	2.375	2.0

where:

m, n the number of bolts in a horizontal and a vertical row, respectively

D, b the horizontal and vertical spacing, in inches, of the bolts, respectively

e the eccentricity, in inches, of the applied load

2.5.2. Results and discussion

In the following discussion and for both testing programs, the test C values were obtained by dividing the test loads by the average double shear capacity of one bolt. The elastic C values were obtained by the elastic center of rotation method, equation 2-22.

The results of the nonlinear analysis in the first testing program were based on the published load-deformation relation of one bolt as shown in equation 2-23:

$$R = R_{ult} \left(1 - e^{-10\Delta}\right)^{0.55} \quad (2-23)$$

However, since the load-deformation response of the bolts used in the second testing program was not given, the nonlinear C values were obtained by dividing the loads predicted using the empirical nonlinear instantaneous center method given in Reference 6 by the average double shear capacity of the corresponding bolts. The test, nonlinear, and elastic C values of the first and second programs are shown in Table 2-2 and Table 2-3, respectively.

Table 2-2 Comparison between the nonlinear C, elastic C, and test results of full-size specimens

Specimen	e / d	n × m	C	C	Error _n	C	Error _e	Error _n - Error _e
			Test	Nonlinear	%	Elastic	%	%
B1	0.80	5	1.52	1.72	+13.2	1.49	-2.0	15.2
B2	0.83	5	1.55	1.65	+6.5	1.44	-7.1	13.6
B3	1.00	5	1.28	1.40	+9.4	1.21	-5.5	14.9
B4	0.87	6	1.70	1.85	+8.8	1.56	-8.2	17.0
B5	1.00	6	1.49	1.62	+8.7	1.36	-8.7	17.4
B6	1.33	8	1.78	1.98	+11.2	1.69	-5.1	16.3
B7	1.67	8	1.43	1.62	+13.3	1.38	-3.5	16.8
B8	1.50	10	1.80	2.07	+15.0	1.72	-4.4	19.4

Table 2-3 Comparison between the nonlinear C, elastic C, and test results of web splices

Specimen	e / d	n × m	C	C	Error _n	C	Error _e	Error _n - Error _e
			Test	Nonlinear	%	Elastic	%	%
C1	0.30	2	1.65	1.68	+1.8	1.70	+3.0	-1.2
C2	0.40	2	1.55	1.56	+0.6	1.56	+0.6	0.0
C3	0.23	2	1.71	1.82	+6.3	1.81	+5.8	0.5
C4	0.29	3	2.35	2.49	+3.4	2.28	-3.0	6.4
C5	0.42	4	2.32	2.40	+3.3	2.13	-8.2	11.5

where:

- e/d the ratio of the eccentricity to the depth of the bolted region; the bolted region is the distance from the centroid of the top bolt to the centroid of the bottom bolt
- C_{test} the test ultimate load normalized with respect to the ultimate capacity of one bolt, P_{test}/R_{ult}
- C_{nonlinear} the theoretical nonlinear ultimate load normalized with respect to the ultimate capacity of one bolt, $P_{nonlinear}/R_{ult}$
- C_{elastic} the theoretical elastic ultimate load normalized with respect to the ultimate capacity of one bolt, $P_{elastic}/R_{ult}$
- Error the error of the theoretical predicted ultimate load with respect to the test ultimate load. A positive error represents an unconservative error, whereas, a negative error represents a conservative error

Also, the normalized eccentric shear capacities of the specimens, with respect to the concentric shear capacities, used in the first testing program were plotted as a function of the e/d ratio as shown in Figure 2-7 through Figure 2-10. This was done to determine how the two methods compare to each other over a wider range than the range tested, and to determine how the two methods compare with test results. Figure 2-7 through Figure 2-10 show that test results lie between the elastic and the nonlinear solution.

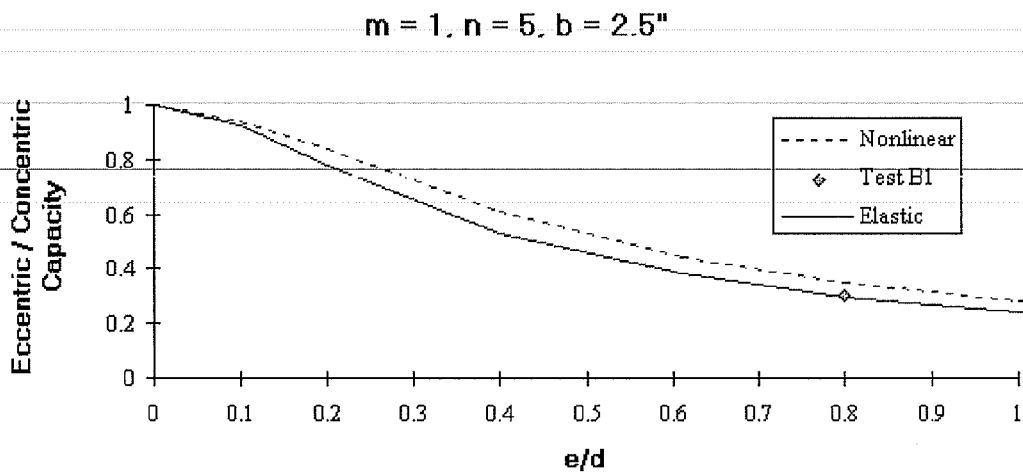


Figure 2-7 C coefficient versus e/d ratio for specimen B1

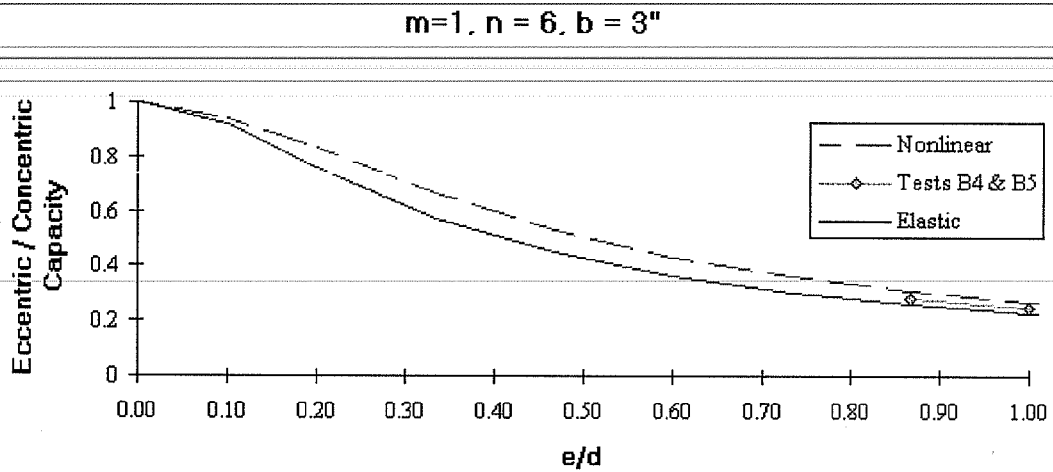


Figure 2-8 C coefficient versus e/d ratio for specimens B4 and B5

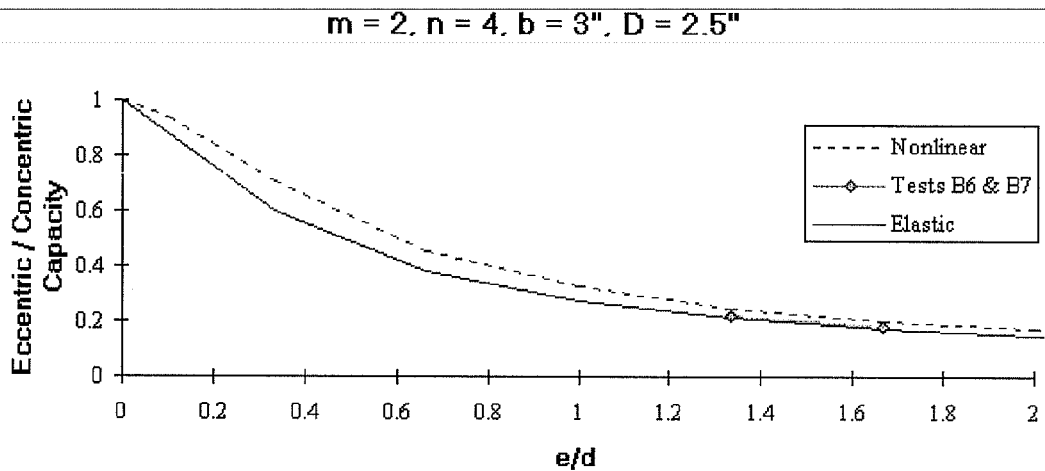


Figure 2-9 C coefficient versus e/d ratio for specimen B6 & B7

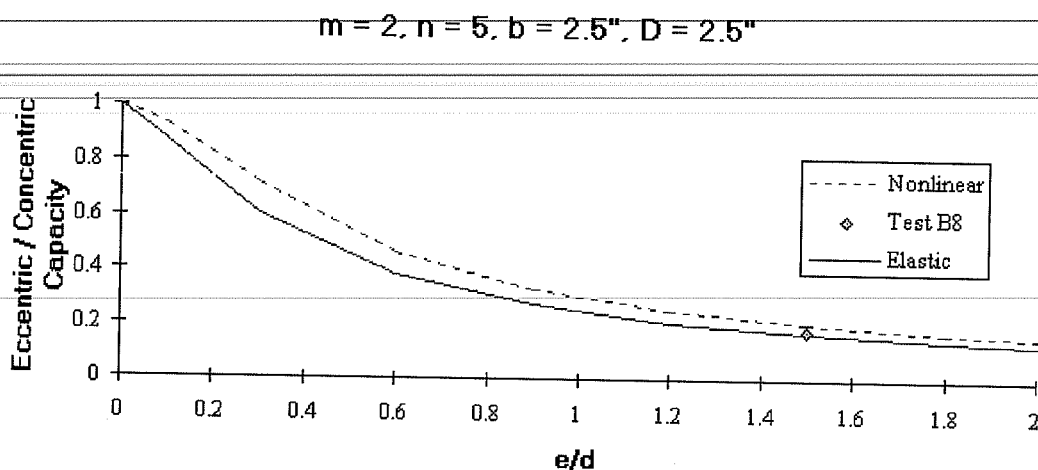


Figure 2-10 C coefficient versus e/d ratio for specimen B8

Table 2-2 and Table 2-3 show that the elastic analysis predicted the actual capacities with an error that ranged from -2.0% to -8.7% and +5.8% to -8.2% for the first and second testing program, respectively. The average absolute error for the elastic method was 5.6% and 4.1% for the first and second testing program, respectively. On the other hand, the nonlinear analysis predicted the actual capacities with an error that ranged from +6.5% to +15.0% and +0.6% to +6.3% for the first and second testing program, respectively. The average absolute error for the nonlinear method was 10.8% and 3.1% for the first and second testing program, respectively. Therefore, it can be concluded that for bolts placed in holes with no hole clearance both methods of analyses yield results that are reasonably accurate. However, the nonlinear analysis is unconservative, whereas, the elastic analysis is conservative, except for the case of two bolts (specimens C1, C2, and C3) where both analyses yielded identical unconservative results.

Theoretically, for the case of two bolts, both the nonlinear and the elastic analysis should yield identical C values and center of rotations since according to both methods both bolts reach their ultimate capacities simultaneously at failure. The identical results can be noted in Table 2-3 for specimens C1 through C3 that had only two bolts. However, there is a small difference in the experimental C values due to the empirical nonlinear load-deformation equation (Equation 2-23) of an individual bolt. By substituting the value of the maximum deformation (0.34 in.) assumed in the ultimate strength method in Equation 2-23, a bolt force of $0.982R_{ult}$ is obtained. As far as the unconservativeness of the predicted capacity for the case of two bolts, it is thought herein that when the connection undergoes excessive rotation at failure, the applied load becomes inclined with respect to the original geometry of the bolts. This inclination of the applied force causes the center of rotation to move away from the rotated axis of symmetry of the bolts and, thus, making the problem unsymmetrical.

For both testing programs, the average elastic error was almost constant; 5.6 %, 4.1 %. Therefore, the elastic method yields consistent results regardless of the test parameters and the test setup. On the other hand, the average nonlinear error changed from 10.8 % in the first testing program to 3.1 % in the second testing program. This change in the nonlinear error was maybe due to the different procedure used in obtaining the individual bolt shear capacity and to the change in test parameters. For the second testing program, the shear capacity of an individual bolt was obtained using a tension splice as opposed to compression splice for the first program. Test results have shown that tension splices yield lower shear capacity of individual bolts than compression splices. Thus, the use of the tension splices in assessing the shear capacity of individual bolts may have contributed in

lowering the unconservativeness of the nonlinear analysis. Further, the total number of bolts ranged from 5 to 10 in the first testing program, whereas, the total number of bolts in the second testing program was roughly one half of that of the first program (ranged from 2 to 4). Also, the e/d ratio ranged from 0.8 to 1.67 in the first testing program, whereas, the e/d ratio in the second testing program ranged from only 0.23 to 0.42 which is roughly one fourth of that of the first program. As will be shown herein, the number of bolts and e/d ratio affects the predicted strength of the connection.

In order to examine the effect of the number of bolts and the e/d ratio on the predicted shear capacity of the splices obtained using the elastic and the nonlinear analyses, specimens B1 through B8 of the first testing program have been chosen for further analysis since the load deformation equation of the bolts used is at hand. The experimental e/d ratios were 0.80 to 1.67. However, the ratios considered herein ranged from 0.1 to 10 in order to get a broader insight of the change in the predicted shear capacities for different number of bolts and e/d ratios. The nonlinear capacities were obtained by performing nonlinear analysis utilizing the published load-deformation equation (equation 2-23). The elastic capacities were obtained from elastic analysis utilizing equation 2-22. The percent difference between the results of both methods is calculated using the elastic results as the reference values. Figure 2-11 and Figure 2-12 represent the difference between the two analyses for different number of bolts and e/d ratios. Also, the test results are plotted on these Figures to show how well they agree with the results of elastic analysis.

Figure 2-11 and Figure 2-12 show that the difference between the results of the two analyses increases as the number of bolts increases. Also, the difference increases as the e/d ratio increases; however, it stabilizes for large e/d ratios.

In order to explain the effect of the number of bolts and the e/d ratio on the difference in the results obtained using the elastic and the nonlinear analyses, specimens B2 and B3 have been chosen for further examination. The experimental e/d ratios were 0.83 and 1.00 for specimens B2 and B3, respectively. However, the ratio considered in the following examination ranged from 0.1 to 10 in order to get a broader insight of the change in the force resultant on each bolt for different e/d ratios. The load level in each bolt (the force resultant in each bolt divided by the shear capacity of the bolt $\times 100$) and the C value of the connection using the nonlinear and elastic analyses are shown in Table 2-4. Also, the difference in the values of the load level in each bolt and in the C values of the connection presented in Table 2-4 are shown in Table 2-5. In calculating the difference between the two methods, the elastic values were used as the reference for the comparison. The bolt numbering used in Table 2-5 for specimens B2 & B3 is shown in Figure 2-13.

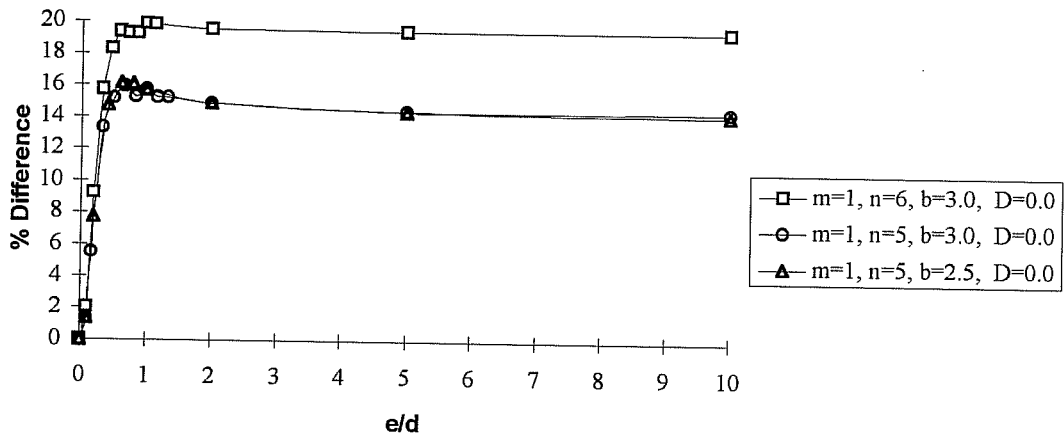


Figure 2-11 The % difference between the nonlinear and elastic analysis

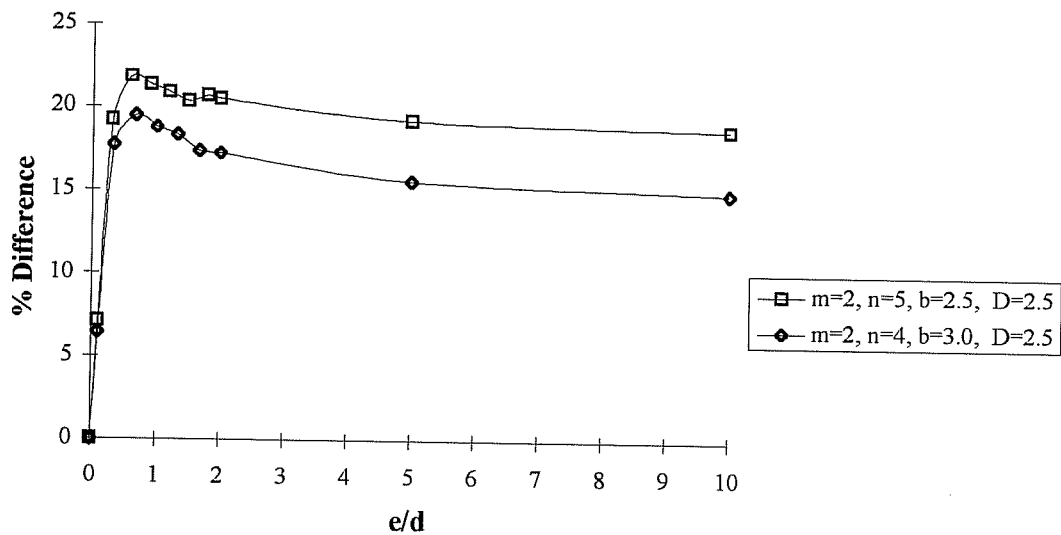


Figure 2-12 The % difference between the nonlinear and elastic analysis

Table 2-4 Comparison between the theoretical load level in each bolt using the nonlinear and the elastic methods for specimens B2 & B3

e/d	0.1	0.83	1	2	10	0.1	0.83	1	2	10
Bolt	% Load (Elastic)					% Load (Nonlinear)				
1	100	100	100	100	100	98.2	98.2	98.2	98.2	98.2
2	94.7	55.9	54.2	51.1	50.1	97.8	90.4	90.1	89.6	89.5
3	92.9	28.7	24.3	12.4	2.5	97.6	65.9	59.9	39.0	11.2
4	94.7	55.9	54.2	51.1	50.1	97.8	90.4	90.1	89.6	89.5
5	100	100	100	100	100	98.2	98.2	98.2	98.2	98.2
C	4.64	1.44	1.21	0.62	0.25	4.71	1.66	1.40	0.71	0.29

Table 2-5 The % difference between the theoretical load level in each bolt using the nonlinear and the elastic methods for specimens B2 & B3

e/d	0.1	0.83	1	2	10
Bolt	% Difference				
1	-1.8	-1.8	-1.8	-1.8	-1.8
2	+3.3	+61.7	66.2	+75.3	+78.6
3	+5.1	+130	+147	+215	+348
4	+3.3	+61.7	66.2	+75.3	+78.6
5	-1.8	-1.8	-1.8	-1.8	-1.8
C	+1.5	15.3	15.7	14.5	14.4

where:

% Difference is the difference between the nonlinear and the elastic load levels in the bolt under consideration, with respect to the elastic solution

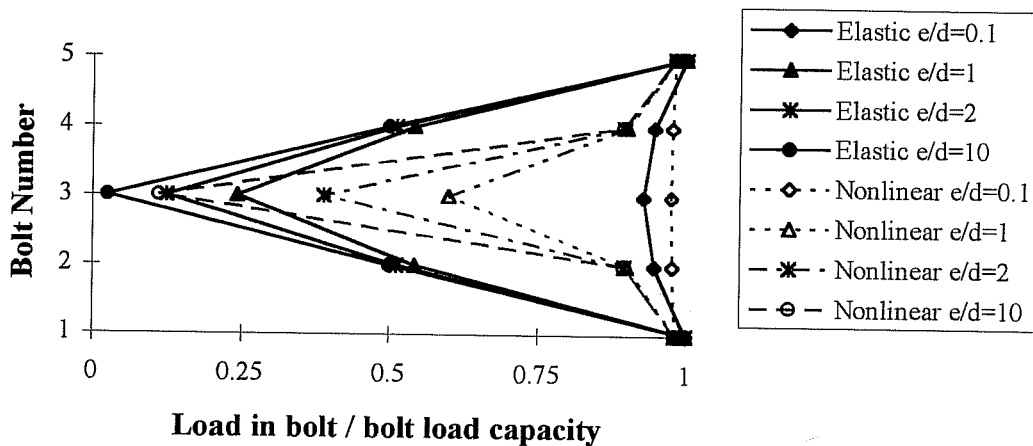


Figure 2-14 The elastic and nonlinear level of load in each bolt of specimens B2 and B3 as a function of e/d

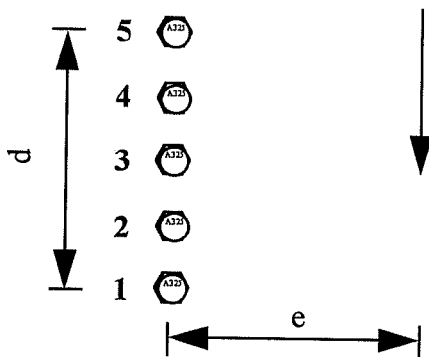


Figure 2-13 The bolt numbering used in Table 2-5 for specimens B2 & 3

Table 2-4, Table 2-5, and Figure 2-14 show that, for a small ratio of e/d (0.1 or smaller) both methods yield almost the same forces in the interior bolts (bolts 2, 3, and 4) and edge bolts (bolts 1 and 5). As the e/d ratio increases, the difference in the interior bolt forces increases significantly where the nonlinear analysis yields load level for the interior bolts that are larger than those obtained from the elastic analysis. Consequently, the range between both solutions gets larger as the number of interior bolts increases. Also, the rate of change of this difference increases the most for the bolts that are closer to the center of rotation. This can be seen by noting that the difference for bolt number 3 increased from +5.1 % to 348 % when e/d changed from 0.1 to 10, while, for bolt number 2, the difference increased from +3.3 % to +78.6 %. Since the center of rotation approaches the center of gravity as the ratio of e/d increases, more bolts will be closer to the center of rotation. Thus, the range between both solutions gets larger as the e/d ratio increases.

The previous discussion showed how the two methods assign different forces for the interior bolts. However, these forces do not have the same orientations when using the two methods of analyses. Therefore, it is felt herein that comparing the contribution of each bolt to the vertical shear capacity and to the moment capacity would give a more thorough understanding of the differences between the two methods. Table 2-6 and Table 2-7 show the contribution of each bolt to the shear and moment capacities according to the two different analyses.

Table 2-6 Comparison between the theoretical shear contribution of each bolt using the nonlinear and the elastic methods for specimens B2 & B3

e/d	0.1 to 10	0.1	0.83	1	2	10
Bolt	% Shear (Elastic)	% Shear (Nonlinear)				
1	20	19.3	11	10.3	8.1	3.8
2	20	20.4	19.2	18.3	14.6	7
3	20	20.8	39.6	42.7	54.7	78.4
4	20	20.4	19.2	18.3	14.6	7
5	20	19.3	11	10.3	8.1	3.8

Table 2-7 Comparison between the theoretical moment contribution of each bolt using the nonlinear and the elastic methods for specimens B2 & B3

e/d	0.1 to 10	0.1	0.83	1	2	10
Bolt	% Moment (Elastic)	% Moment (Nonlinear)				
1	40	40.1	34.7	34.6	34.4	34.3
2	10	10.6	15.2	15.4	15.6	15.6
3	0	0	0	0	0	0
4	10	10.6	15.2	15.4	15.6	15.6
5	40	40.1	34.7	34.6	34.4	34.3

To visualize the different contribution of moment and shear assumed by each method of analysis, Figure 2-15 and Figure 2-16 show these contributions as a function of the e/d ratio.

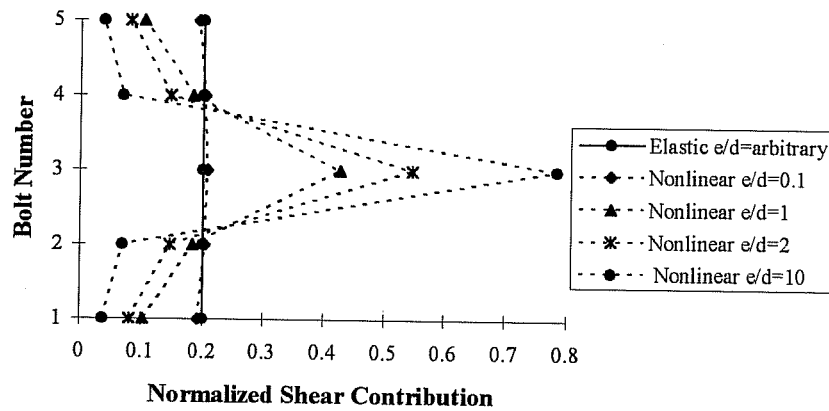


Figure 2-15 The elastic and nonlinear normalized shear contribution of each bolt of specimens B2 and B3 as a function of e/d

Table 2-6, Table 2-7, Figure 2-15, and Figure 2-16 show that, regardless of the e/d ratio, the bolt contribution to both moment and shear is always constant when using the elastic analysis. On the other hand, when using the nonlinear analysis, the bolt contribution to moment and shear varies as a function of the e/d

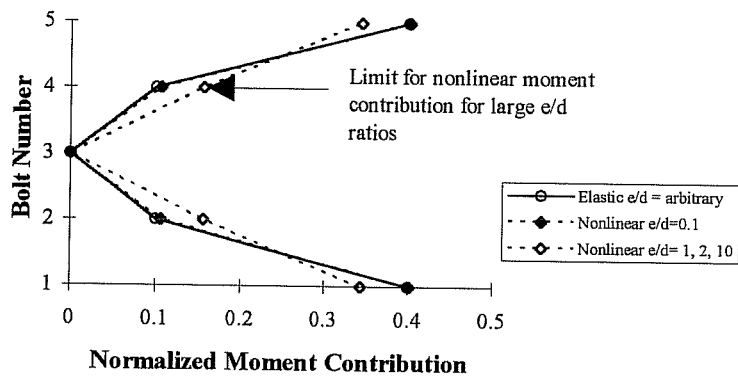


Figure 2-16 The elastic and nonlinear normalized moment contribution of each bolt of specimens B2 and B3 as a function of e/d

ratio. For a small ratio of e/d , 0.1 or less, both methods assign roughly the same amount of shear and moment. As the e/d ratio increases, the nonlinear analysis assigns less shear and moment to the edge bolts and more shear and moment to the interior bolts. This can be thought of as a redistribution, plastification, of the applied forces to the interior bolts. Consequently, the range between the elastic and nonlinear analyses will increase as either the number of bolts or the e/d ratio increases. However, and for large values of e/d , the moment distribution approaches a limit as shown in Figure 2-16. This limit explains the stability of the difference between the two method for large e/d ratios.

For connections without hole clearance and with three or more bolts, test results lie between the elastic solution and the nonlinear solution. Therefore, it can be concluded that the redistribution of moment and shear in the bolts is overestimated in the nonlinear analysis. Moreover, the elastic analysis appears to be adequate and close to test result. Nevertheless, it should be remembered that when performing the elastic analysis on the bolts, the critical bolt should be permitted to reach its ultimate capacity and should not be limited, as was done traditionally, to its allowed load. Accordingly, the misconception that the elastic analysis is unduly conservative is not due to the conservative nature of the elastic analysis but rather to limiting the critical bolt to its allowed load.

2.6. Summary

- For connections with three or more bolts placed in holes with no clearance, test results lie between the elastic and the nonlinear solutions
- The nonlinear analysis using the empirical load-deformation equation is unconservative
- The main difference between the two methods is the load assignment to the interior bolts. Since test results lie between the results of the two methods, it is expected that the elastic analysis underestimates the load to the interior bolts, while on the contrary, the empirical nonlinear analysis overestimates the loads in the interior bolts. Thus, the unconservativeness of the nonlinear analysis might be caused from overestimating the redistribution of forces to the interior bolts
- For connections with three or more bolts placed in holes with no clearance, the elastic analysis is conservative
- For the special case of connections with only two fully tensioned bolts, the elastic and the nonlinear analyses yield identical results since both bolts are assumed to reach their ultimate capacities at failure. Also, for the special case of connections with only two bolts, the elastic and the nonlinear analyses yield unconservative results due to the second order effects caused by the excessive rotation of the connection at failure. However, the magnitude of this unconservative error is negligible
- The range between the elastic and nonlinear solution gets larger as either the number of bolts or e/d ratio increases due to the difference in the forces in the interior bolts assigned by each method.

2.7. Conclusions

The following conclusions are based upon the tests available in the literature. For eccentrically loaded group of bolts placed in holes with no clearance:

- The range between the elastic and nonlinear solutions gets larger as either the number of bolts or e/d ratio increases. However, test results lie between both solutions
- A simple direct elastic analysis for eccentrically loaded group of bolts appears to be safe and adequate, provided that the critical bolt is permitted to reach its ultimate capacity

Since the e/d ratio examined in this Chapter was limited to 1.67, the analysis of eccentrically loaded group of bolts will be reexamined in Chapter 4 for the experimental e/d ratios up to 6.7. Also, when examining the difference of the load in each bolt between the nonlinear and elastic analysis, the elastic analysis was used as a reference for the comparison. Therefore, in Chapter 4, the load in each bolt due to the empirical nonlinear and due to the elastic analysis will be reexamined and compared with the nonlinear analysis using the measured load-deformation response of an individual bolt.

Chapter 3

3. Material Testing

3.1 Introduction

In this Chapter, the splice plates, beam material, and bolts used to manufacture the bolted beam splices were tested. The results of the tensile coupons of the splice plates and the web and flanges of the test beams are presented. The single shear capacity of an individual bolt tested in compression splices are presented. Also, the double slip and shear strength of an individual bolt tested in tension splices are presented and discussed.

Different preload in the web bolts, different hole making procedures, and material with different loading history (reused holes) were used in manufacturing the beam splices. Therefore, to properly estimate the capacity of the bolted beam splices, the effect of the preload in the bolts, hole making procedures, and material loading history on the shear strength of an individual bolt is examined.

3.2 Tensile coupon tests

Tensile coupon tests were done on the flanges and webs of the 24 and 40 in. beams, and on all the splice plates used. Table 3-1 and Table 3-2 show both the actual and the nominal dimensions of the splice plates. Table 3-1 and Table 3-2 show that the actual dimensions showed a 0.3 % to 7.5 % variations in the dimensions.

Table 3-1 Actual versus nominal dimensions of web splice plates

Plate #	Thickness in.		
	Actual	Nominal	Variation %
1	0.403	0.375	7.5
2	0.182	0.1875	2.7

Table 3-2 Actual versus nominal dimensions of flange splice plates

Plate #	Width in.			Thickness in.		
	Actual	Nominal	Variation %	Actual	Nominal	Variation %
3	8.072	8	0.9	0.495	0.5	1.0
4	10.03	10	0.3	0.503	0.5	0.6
5	7.508	7.5	0.8	0.246	0.25	1.4

All tensile coupons were machined to a width of approximately 1.5 inches. The 200 kip universal testing machine was used to test the tensile coupons. The x-y plotter was used to plot the load versus the axial deformation of the tensile coupon up to strain hardening. In the linear elastic range of the coupon's material, the rate of loading was approximately 0.1 inch per minute. After reaching the yield plateau, the rate of loading increased to 0.2 inch per minute. For all the coupons tested, three values for the static yield were recorded at several locations of the yield plateau and then were averaged to obtain the static yield. Each static yield load was recorded after shutting off the machine for about five minutes. Then, the load was increased monotonically until fracturing of the coupon. After fracturing of the coupon, the elongated length was measured and the percent elongation at fracture was calculated based on the original 8 inch gage length. The yield and ultimate stresses were obtained by averaging the values from the different coupons

tested. The average results, based on two coupons, of the tensile coupons are shown in Table 3-3 and Table 3-4. The yield stress of all the coupons was above the minimum specified by ASTM; 36 ksi and 50 ksi for A36 and A572 grade 50 steel, respectively. Also, the ultimate stress was above the minimum specified by ASTM; 58 ksi and 65 ksi for A36 and A572 grade 50 steel, respectively. All coupons failed in a ductile failure with total axial elongation that ranged from 24.6 to 30.6 %.

Table 3-3 Tensile coupon average results for the splice plate material

Plate #	Location	Thickness in.	Static Yield ksi	Dynamic Yield ksi	Dynamic Ultimate ksi	Elongation %
1	Web	0.403	40.7	42.6	65.6	26.8
2	Web	0.182	39.7	39.9	65.6	26.1
3	Flange	0.495	52.7	56.0	74.4	24.6
4	Flange	0.503	44.1	46.1	68.5	25.4
5	Flange	0.246	43.9	45.8	64.3	25.5

Table 3-4 Tensile coupon average results for the girder material

Section	Location	Static Yield ksi	Dynamic Yield ksi	Static Ultimate ksi	Dynamic Ultimate ksi	Percent Elongation %
W24x55	Flange	41.6	44.8	59.6	63.9	29.3
W24x55	Web	42.3	45.3	58.6	62.5	30.6
W40x167	Flange	51.8	53.3	-	75.0	27.3
W40x167	Web	51.2	54.2	-	74.6	24.6

3.3 Bolt slip and shear tests

All bolts were ASTM medium-carbon-steel A325 bolts. For the 24 in. beam splices, the web bolts were tested for shear in compression splices and were hand-tight; no preload. For the 40 in. beam splices, the load versus bearing deformation response of the bolts and actual material used in manufacturing the tested splices was needed for the non-linear analysis of the web bolts. Therefore, the bolts were tested in tension splices manufactured from the actual beams and splice plate material. Since some of the tested 40 in. beam splices were hand-tight and some were pretensioned, the bolts tested in tension splices were hand-tight and pretensioned, respectively. The pretensioned bolts tested for slip and shear were installed using the calibrated wrench method. The bolts were tightened to a preload of 32.9 kips which is 12 % larger than the $1.05 \times 28 = 29.4$ kips minimum preload specified by the AISC specifications for bolts installed using the calibrated wrench method. Table 3-5 shows the actual versus nominal diameters of the bolts tested. The actual diameters showed a 0.4 % to 0.6 % variation.

Table 3-5 Actual versus nominal diameters of web bolts

Bolt Lot #	Actual Diameter in.	Nominal Diameter in.	Variation %	Length in.
1	0.622	5/8	0.5	2.488
2	0.621	5/8	0.6	2.486
3	0.747	3/4	0.4	2.490

3.3.1 Test Set-Up

Figure 3-1 show the compression splice test set-up. The test fixture of the compression splice consists of two relatively rigid plates placed in two jaws. The bottom jaw is fixed to the testing machine, whereas, the top jaw can move downwards by moving the head of the testing machine downwards. When the top jaw moves downwards, it forces one of the two rigid plates to move downwards and shear the bolt. Since the plates in the compression splice are rigid, the measured joint deformation is the bearing deformation of the bolt only. Figure 3-2 show the tension splice test set-up. The tension splice plate were manufactured from the actual beam and splice plate material. For both test set-ups, linear potentiometers were used to measure the joint deformation. The measured joint deformation in the compression splices represent the bearing deformation of the bolt only. However, the joint deformation in the tension splices represent the slip, the bearing deformation of the bolt, the bearing deformation of the connected plates, and the axial deformation of the splice plates.

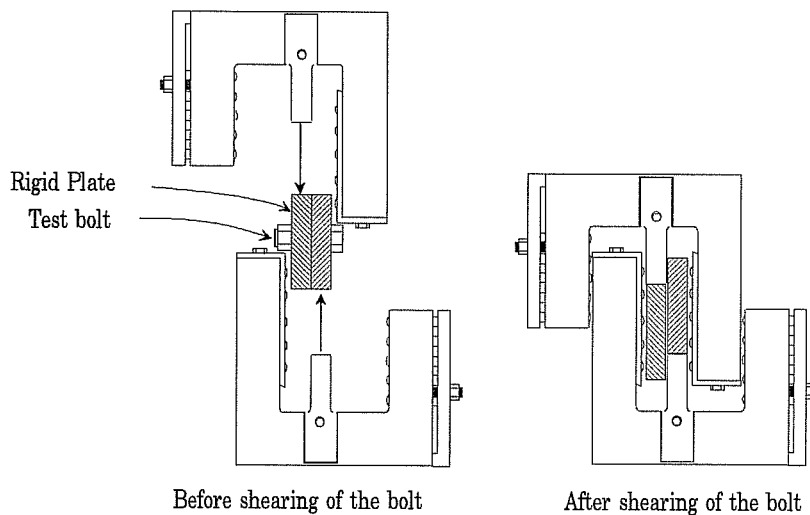


Figure 3-1 Test set-up for single bolt in compression single-shear splice

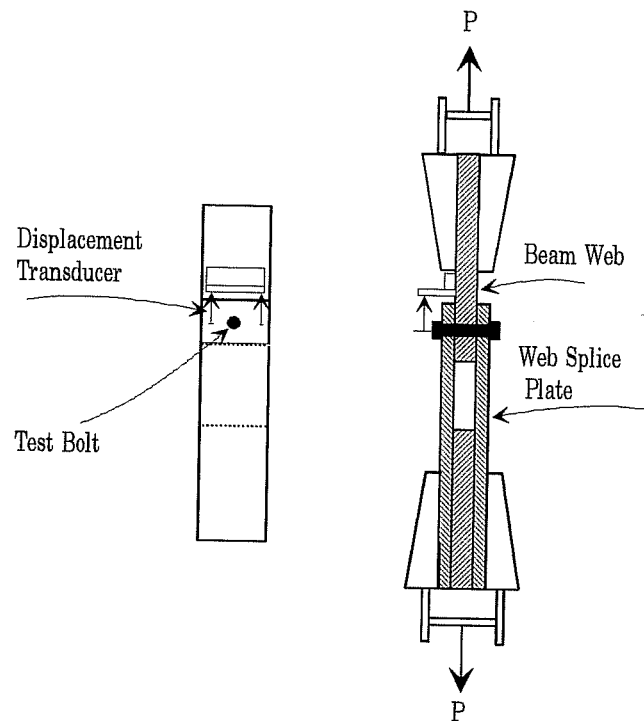


Figure 3-2 Test set-up for single bolt in tension double slip and shear splice

3.3.2 Single-shear tests for individual bolts in compression splices

The results of the single-shear tests on the bolts in compression splices and the estimated double shear capacity of the 5/8 in. bolts are shown in Table 3-6.

Table 3-6 The results of compression single-shear tests on A325 5/8" Bolts

Lot Number	Specimen Number	Shear Plane Location	Single-Shear Capacity kips	Test Spec.	Estimated Double-Shear Capacity
1	1	Shank	26.70	1.16	53.40
1	2	Shank	25.95	1.13	51.90
1	3	Shank	26.10	1.13	52.20
1	Average	Shank	26.25	1.14	52.50
2	1	Shank	27.10	1.18	54.20
2	2	Shank	28.20	1.23	56.40
2	3	Shank	27.00	1.17	54.00
2	4	Shank	26.55	1.15	53.10
2	5	Shank	27.85	1.21	55.70
2	6	Shank	26.85	1.17	53.70
2	Average	Shank	27.26	1.19	54.52

Where:

Spec. is the value given in the AISC (LRFD) specification after eliminating the strength reduction factor (0.75 for shear and 1 for slip) and the shear lag factor (0.80 for shear and 1.0 for slip)

The 26.25 and 27.26 kips tested shear strength of the 5/8 in. bolts were 14% to 19% larger than the 23 kips value specified in the AISC (LRFD) specification after eliminating the 0.75 strength reduction factor and the 0.8 shear lag effect factor.

The bearing deformation was not measured for the 5/8 in. bolts. However, since the bearing deformation for the 3/4 in. bolts was measured when tested in

tension splices, the bearing deformation for the 3/4 in. bolts in compression splices was measured to compare the contribution of bearing deformation of the bolt to the total joint deformation. The results of the single-shear compression tests and the estimated double shear capacity of the 3/4 in. bolts are shown Table 3-7 in and Table 3-8, respectively. Figure 3-3 shows the Load versus bearing deformation of an individual 3/4 in. A325 high strength bolt in a compression splice with rigid plates.

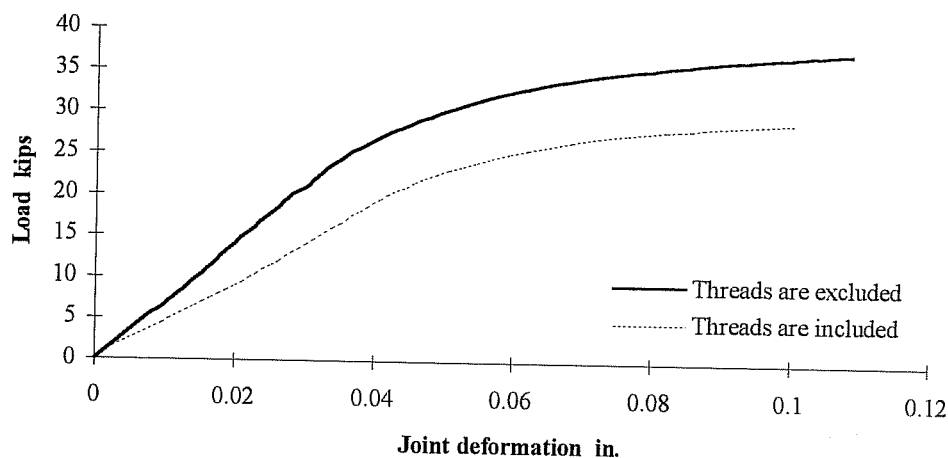


Figure 3-3 Load versus bearing deformation of an individual 3/4 in. A325 high strength bolt in a single shear compression splice with rigid plates

The ratio of shear strength of an individual bolt when the threads are included in the shear plane to the strength of the bolt when the threads are excluded from the shear plane was $29.06/37.94 = 0.77$. This 0.77 ratio agrees closely (4 % difference) with the 0.8 ratio used in the AISC specifications.

The 37.94 and 29.06 kips tested shear strength of the 3/4 in. bolts when the threads are excluded and included were 14 % and 9.7 % larger than the 33.2 and 26.5 kips values specified in the AISC (LRFD) specification after eliminating the 0.75 strength reduction factor and the 0.8 shear lag effect factor.

Table 3-7 The results of single-shear compression tests of A325 3/4" Bolts

Specimen Number	Location of Shear Plane	Joint Deformation in.	Single-Shear Capacity kips	Test Spec.
1	Shank	0.127	38.94	1.17
2	Shank	0.119	36.66	1.10
3	Shank	0.111	38.98	1.17
4	Shank	0.109	35.33	1.06
5	Shank	0.132	37.35	1.13
6	Shank	0.132	40.38	1.22
Average	Shank	0.122	37.94	1.14
1	Threads	0.109	28.80	1.09
2	Threads	0.114	28.26	1.07
3	Threads	0.124	30.18	1.14
4	Threads	0.115	29.96	1.13
5	Threads	0.091	28.11	1.06
Average	Threads	0.111	29.06	1.10

Table 3-8 The estimated double shear capacity of A325 3/4" bolts tested in compression splices

No. of Shear Planes	Location of First Shear Plane	Location of Second Shear Plane	Shear Capacity kips	Normalized Shear Capacity kips
1	Shank	-	37.94	1
1	Threads	-	29.06	0.77
2	Shank	Shank	75.88	2
2	Shank	Threads	67.00	1.77

3.3.3 Double slip and shear tests for individual bolts in tension splices

Double-shear tests for individual bolts in tension splices were performed on the web bolts used in the 40 in. beam tests only. Even though, the double shear capacity of the web bolts was approximated by adding the single shear capacities obtained from the compression splices, the actual load-deformation response of the web bolts with the actual girder and plate material was needed for the non-linear analysis which will be used later in Chapter 4 to determine the distribution of the forces within the web bolts, the distribution of forces between the flange and web splices, and finally the predicted capacity of the splice. Figure 3-4 and Figure 3-5 show a typical test bolt before and after failure, tested in a tension splice.

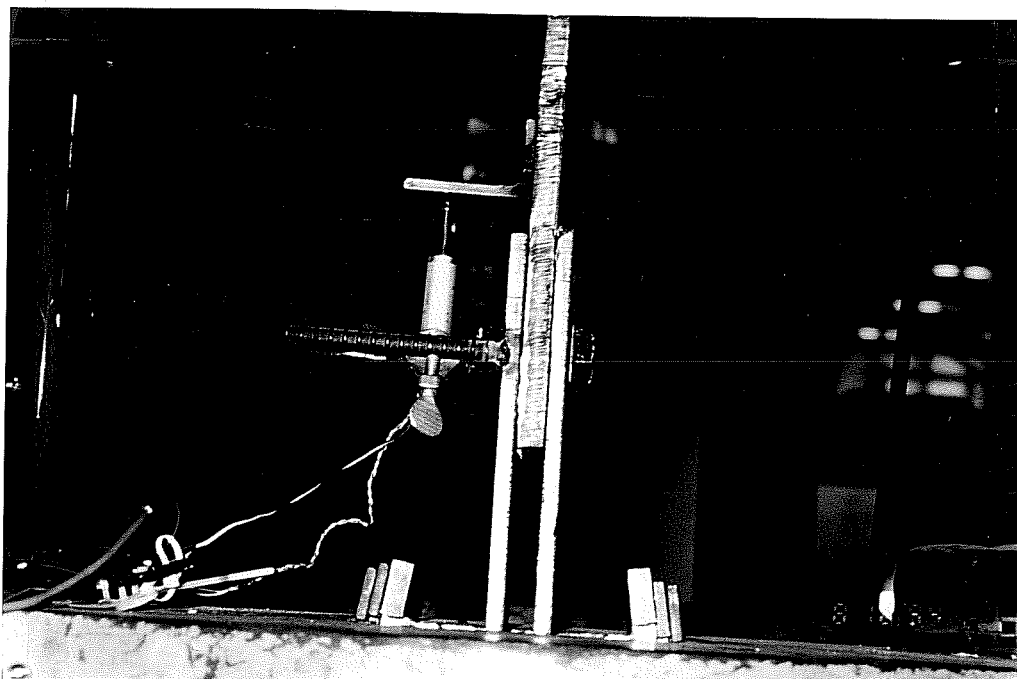


Figure 3-4 Typical test bolt before failure, tested in a tension splice

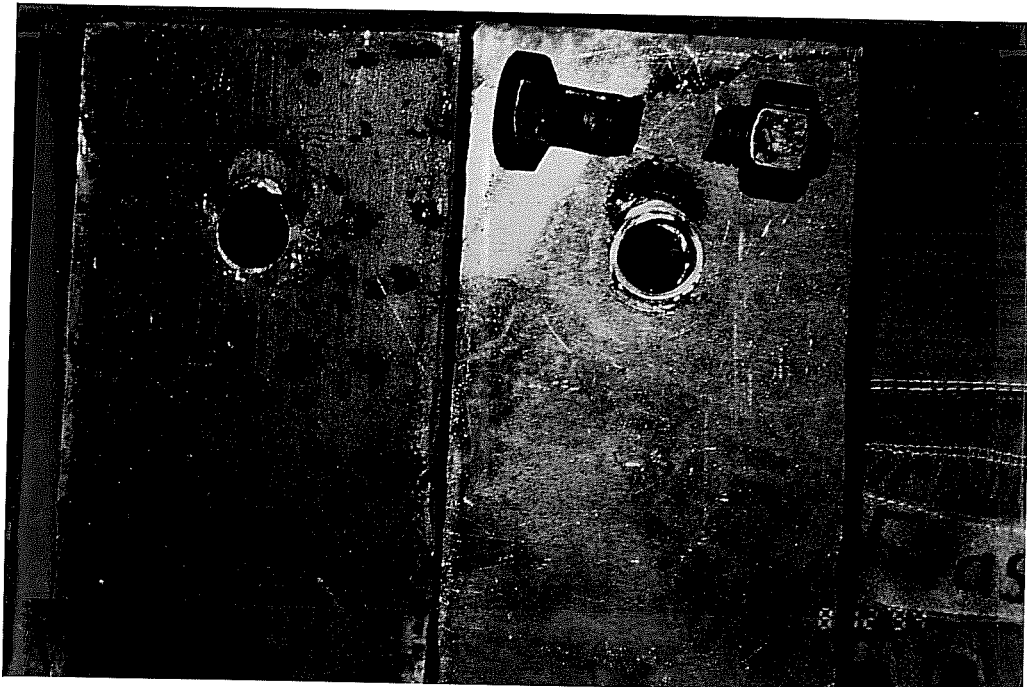


Figure 3-5 Typical test bolt after failure, tested in a tension splice

Since the load versus bearing deformation response of a pretensioned single bolt is different from that of a hand-tight bolt, and since both installation procedures of the web bolts were used in the testing program, the tension splice shear tests of the bolts were performed on both pretensioned and hand-tight bolts. The load versus joint deformation responses for the different tension shear splices are shown in Figure 3-6. For the tests done on the pretensioned bolts the slip load was determined using the test method adopted in Appendix A of the AISC (LRFD) specification for structural joints (the load that corresponds to 0.02 in. deformation, sudden decrease in stiffness, or sudden drop in load). For the tests performed, the slip load of the 3/4" bolts when connecting 3/8" plates with punched holes corresponded to 0.02 in. deformation. The slip load of the 3/4 " bolts when connecting 3/8" plates with drilled holes corresponded to a sudden drop in load. The slip loads of the bolts when connecting 3/16" plates corresponded to a single corner point where the stiffness decreased suddenly. The average results of the shear tests of individual hand-tight bolts in tension splices are shown in Table 3-9. The results of the slip and shear tests of individual pretensioned bolts in tension splices are shown in Table 3-10 and Table 3-11.

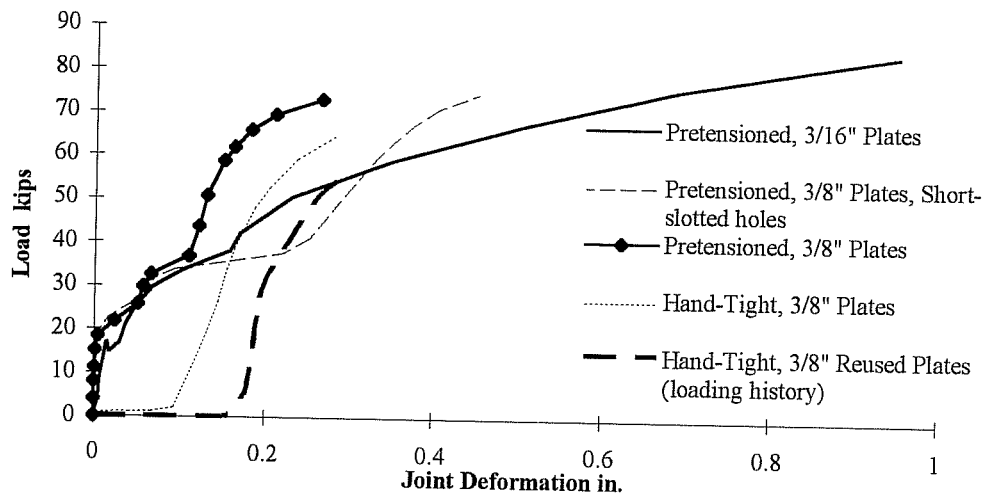


Figure 3-6 Load versus Joint Deformation for 3/4" A325 Bolts tested in double shear tension splices

For the hand-tight bolts with drilled inner plates tested, the 64.42 and 65.25 kips tested shear strength of the 3/4 in. bolts when the threads were included in one shear plane and excluded from the second shear plane was 8 % and 9 % larger than the $(15.9+19.9)/(0.75 \times 0.8) = 59.7$ kips value specified in the AISC (LRFD) specification after eliminating the 0.75 strength reduction factor and the 0.8 shear lag effect factor. On the other hand, for the hand-tight bolts with either punched inner plates or used plates tested, the 55.88 and 55.41 kips tested shear strength of the 3/4 in. bolts when the threads are included in one shear plane and excluded from the second shear plane was 6 % and 7 % smaller than the $(15.9+19.9)/(0.75 \times 0.8) = 59.7$ kips value specified in the AISC (LRFD) specification after eliminating the 0.75 strength reduction factor and the 0.8 shear lag effect factor.

Table 3-9 The results of tension double-shear tests on Hand-Tight 3/4" A325 Bolts with 3/8" outer plates (Threads are included in one shear plane)

Specimen Number	Plates	Outer Plates	Inner Plate	Joint Deformation in.	Double-Shear Capacity Kips	<u>Test Spec.</u>
1	New	Drilled	Drilled	0.259	67.33	1.13
2	New	Drilled	Drilled	0.303	64.26	1.08
3	New	Drilled	Drilled	0.284	61.66	1.03
Average	New	Drilled	Drilled	0.282	64.42	1.08
1	New	Punched	Drilled	0.331	67.33	1.13
2	New	Punched	Drilled	0.280	65.10	1.09
3	New	Punched	Drilled	0.275	63.15	1.06
4	New	Punched	Drilled	0.267	65.42	1.10
Average	New	Punched	Drilled	0.288	65.25	1.09
1	New	Punched	Punched	0.269	52.46	0.88
2	New	Punched	Punched	0.291	60.50	1.01
3	New	Punched	Punched	0.258	54.68	0.92
Average	New	Punched	Punched	0.273	55.88	0.94
1	Used	Drilled	Drilled	0.257	54.27	0.91
2	Used	Drilled	Drilled	0.337	56.56	0.95
Average	Used	Drilled	Drilled	0.297	55.41	0.93

Table 3-10 The results of tension double-shear tests on Pretensioned 3/4" A325 Bolts with 3/8" outer plates (Threads are included in one shear plane)

Specimen Number	Outer Plates	Inner Plate	Joint Deformation in.	Slip Load Kips	Test Spec.	Double-Shear Capacity Kips	Test Spec.
1	Punched	Punched	0.227	19.55	1.15	70.17	1.18
2	Punched	Punched	0.296	22.30	1.31	74.51	1.25
3	Punched	Punched	0.278	21.68	1.28	74.17	1.24
Average	Punched	Punched	0.267	21.18	1.25	72.95	1.22
1	Punched	Drilled	0.240	20.07	1.18	75.28	1.26
2	Punched	Drilled	0.342	17.35	1.02	69.77	1.17
3	Punched	Drilled	0.283	28.27	1.66	76.84	1.29
Average	Punched	Drilled	0.288	21.90	1.29	73.96	1.24
1	Punched Slotted	Drilled Standard	0.446	23.23	1.37	69.37	1.16
2	Punched Slotted	Drilled Standard	0.470	18.60	1.09	74.77	1.25
3	Punched Slotted	Drilled Standard	0.446	24.41	1.44	79.52	1.33
Average	Punched Slotted	Drilled Standard	0.454	22.08	1.30	74.55	1.25

For the pretensioned bolts with 3/8 in. outer plates, regardless of the hole making procedure and of the hole size, the 72.95, 73.96 and 74.55 kips tested shear strength of the 3/4 in. bolts when the threads are included in one shear plane and excluded from the second shear plane was 22, 24, and 25 % larger than the $(15.9+19.9)/(0.75 \times 0.8) = 59.7$ kips value specified in the AISC (LRFD) specification after eliminating the 0.75 strength reduction factor and the 0.8 shear lag effect factor. Also, for the pretensioned bolts regardless of the hole making

procedure and of the hole size, the 21.18, 21.9 and 22.08 kips tested double slip loads of the 3/4 in. bolts correspond to 0.32, 0.33, and 0.34 friction coefficient. The tested friction coefficients agree closely with the 0.33 friction coefficient used in the AISC specifications for class A faying surface; clean mill scale.

Table 3-11 The results of tension double slip and shear tests on Pretensioned 3/4 A325 Bolts with 3/16" outer plates (Threads are excluded from both shear planes)

Specimen Number	Outer Plates	Inner Plate	Slip Load Kips	$\frac{\text{Test}}{\text{Spec.}}$	Double-Shear Capacity Kips	$\frac{\text{Test}}{\text{Spec.}}$
1	Punched	Drilled	18.32	1.08	57.23 ^{BK}	-
2	Punched	Drilled	17.11	1.01	57.88 ^{BK}	-
3	Punched	Drilled	16.92	1.00	84.09	1.27
4	Punched	Drilled	16.32	0.96	69.08 ^{TR}	-
Average	Punched	Drilled	17.17	1.01	84.09	1.27

Where:

BK Plate buckled

TR Tear out failure

For the pretensioned bolts with the 3/16 in outer plates, the 84.09 kips tested shear strength of the 3/4 in. bolts when the threads were excluded from both of the shear planes was 27 % larger than the 66.3 kips value specified in the AISC (LRFD) specification after eliminating the 0.75 strength reduction factor and the 0.8 shear lag effect factor. Also, for the pretensioned bolts, the 17.17 kips tested double slip load of the 3/4 in. bolts corresponds to 0.26 friction coefficient which is

21 % smaller than the 0.33 friction coefficient used in the AISC specifications for class A faying surface; clean mill scale.

3.3.4 The effect of preload on the shear strength of an individual bolt

The results of tests performed on individual pretensioned and hand-tight bolts in double shear tension splices are shown in Table 3-12 and Figure 3-7. Table 3-12 and Figure 3-7 show that the preload in the bolt affects greatly the shear strength of high strength bolts. The absence of the bolt preload caused a 13.3 % decrease in the shear strength. The 13.3 % decrease in the shear strength due to the absence of the bolt preload does not agree with the previous test results done by Wallaert and Fisher¹⁵. However, Wallaert and Fisher's tests were done on both snug and fully tightened bolts, whereas, the tests done in this program were done on both hand-tight and fully tightened bolts. In Wallaert and Fisher's tests, the snug bolts had a preload of approximately 8 kips; whereas, the hand-tight bolts tested in this program had no preload. Further, in Wallaert and Fisher's tests both shearing planes passed through the shank, whereas, one of the shearing planes in this testing program passed through the threads. Also, in Wallaert and Fisher's tests the holes were drilled, whereas, the holes in this testing program were drilled and punched.

The absence of preload in the bolt allows the bolt to undergo more bending deformation than that of a pretensioned bolt. Therefore, a bolt with no preload will fail at a lower shear load than that of a pretensioned bolt. Further, the presence of the frictional resistance between the plates, due to the preload in the bolt, causes a pretensioned bolt to fail at a higher load than that of a hand-tight bolt.

The decrease in the shear strength of a high strength bolt due to the absence of the preload in the bolt was even larger for bolts placed in punched holes. However, the decrease in shear strength for bolts with no preload placed in punched holes is due not only to the absence of the preload but also to punching of the holes. The effect of punching of the plates on the shear strength of the bolts will be discussed further in detail in Section 3.3.5.

Table 3-12 The effect of preload on the shear strength of bolts

Hole in Outer Plates	Hole in Inner Plate	Hand-Tight Double-Shear Capacity Kips	Pretensioned Double-Shear Capacity Kips	Difference %
Punched	Drilled	65.25	73.96	13.3
Punched	Punched	55.88	72.95	30.5

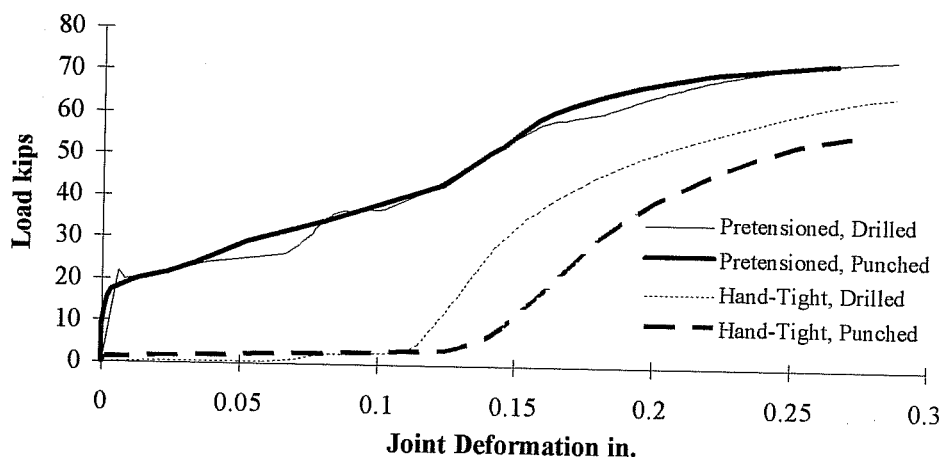


Figure 3-7 The load versus joint deformation for an individual 3/4 in. A325 pretensioned and hand-tight bolt in double shear tension splices

3.3.5 The effect of hole making procedure on the shear strength of an individual bolt

The results of tests performed on individual bolts in double shear tension splices are shown in Table 3-13 and Figure 3-7.

Table 3-13 The effect of the hole making procedure on the shear strength of bolts

Preload in bolt	Hole in Outer Plates	Hole in Inner Plates	Joint Deformation in.	Slip Load Kips	Double-Shear Capacity Kips
Yes	Punched	Punched	0.267	21.18	72.95
Yes	Punched	Drilled	0.288	21.90	73.96
Yes	Punched Slotted	Drilled Standard	0.454	22.08	74.55
No	Punched	Punched	0.273	-	55.88
No	Punched	Drilled	0.288	-	65.25
No	Drilled	Drilled	0.282	-	64.42

Table 3-13 and Figure 3-7 show that the hole making procedure and the hole size affects neither the slip load (the slip load was 21.18 kips for bolts placed in punched holes and 21.9 kips for bolts placed in drilled holes) nor the shear strength of an individual pretensioned high strength bolt (the shear load was 72.95 kips for bolts placed in punched holes and 73.96 kips for bolts placed in drilled holes). On the other hand, the hole making procedure affects greatly the shear strength of hand tight bolts. The shear strength of hand tight bolts placed in drilled holes was 64.42 kips; whereas, the shear strength of hand tight bolts placed in punched holes was 55.88 kips. Thus, due to punching of the inner plate, the shear capacity of hand tight bolts decreased by 13.3 %.

In an effort to explain the effect of hole making on the shear capacity of hand tight high strength bolts, the change in the hardness of the plate material in the vicinity of both punched and drilled holes was examined. Four specimens were cut across each hole, as shown in Figure 3-8, and a hardness test, Rockwell B, was performed at three different points across the width of the plate. The first three test points were at 1/16" away from the edge of the hole. Then, the spacing of the test points varied up to 2.5 times the diameter of the hole away from the hole edge. The results of the hardness tests are shown in Table 3-14, Table 3-15, and Figure 3-8.

Table 3-14 The hardness of web splice plate and girder material around Punched Holes

Plate	3/8"	5/8"
L/d in./in.	Hardness/Minimum Hardness number	Hardness/Minimum Hardness number
0.08	1.16	1.13
0.15	1.09	1.05
0.31	1.01	1.01
0.46	1.00	1.01
0.62	1.01	1.01
0.92	1.00	1.01
1.23	1.00	1.00
1.54	1.00	1.00
1.85	1.00	1.01
2.15	1.00	1.00
2.46	1.00	1.00

Where:

L the distance from the test point to the edge of the hole in inches

d the diameter of the hole

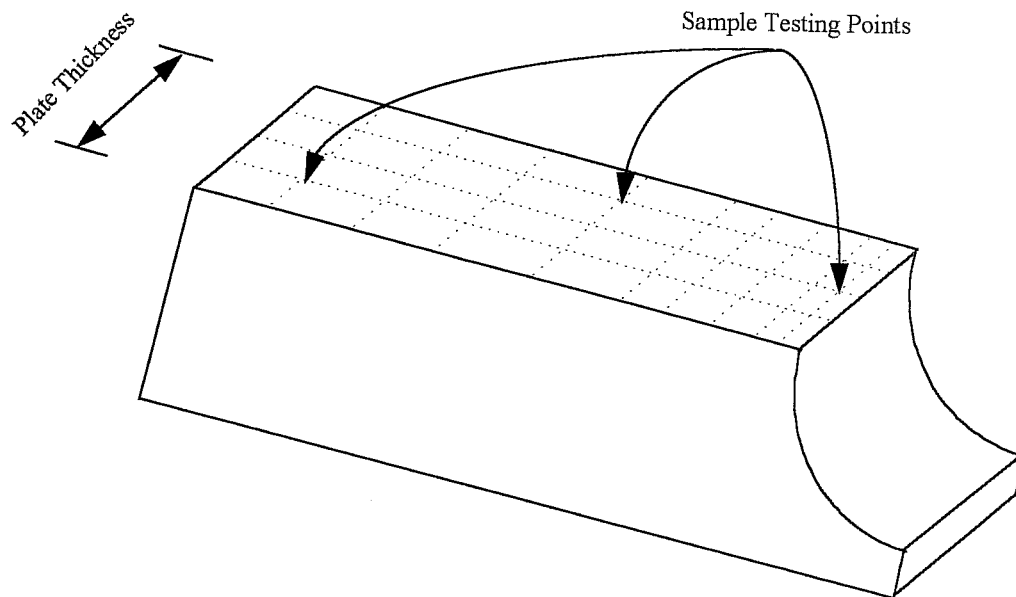


Figure 3-8 The hardness test specimen

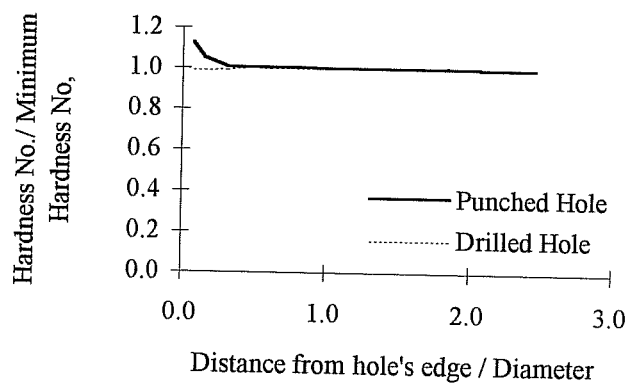


Figure 3-9 The effect of hole making procedure on the hardness of the plate

Table 3-15 The hardness of the web splice plate and girder material around Drilled Holes

Plate	3/8"	5/8"
L/d in./in.	Hardness/Minimum Hardness number	Hardness/Minimum Hardness number
0.15	0.98	0.99
0.31	1.00	1.00
0.46	1.00	1.00
0.62	1.00	1.00
0.92	1.00	1.00
1.23	1.00	1.00
1.54	1.00	1.00
1.85	1.00	1.00
2.15	1.00	1.00
2.46	1.00	1.00

Figure 3-9, Table 3-14, and Table 3-15 show that drilling of the holes does not affect the hardness of the plate, whereas, punching of the hole increases the hardness of the plate by 13-16 %. However, this increase in hardness is limited to the material in the vicinity of the hole. Further, the hardness of the punched plates remains unchanged after 30 % of the hole diameter away from the hole edge. The increase in hardness in the vicinity of the punched hole is due to strain hardening of the material caused by the plastic deformation while shearing the plate material.

After explaining the effect of the hole making procedure on the hardness of the plate material, the change in the shear strength of the bolt can be explained. Since the punched material underwent strain hardening, the plate when subjected to

bearing stresses undergoes less bearing deformation than that of a drilled hole (the drilled holes in the inner splice underwent 0.74/16 in. elongation; whereas, the punched holes in the inner splice underwent 0.32/16 in. elongation). Therefore, the bolt placed in a punched hole will undergo larger bending deformation which in turn produces a combination of bending and shearing stresses on the bolt. This combination of stresses will cause the bolt to fail earlier than the bolt placed in a drilled hole.

Further, when the bolts are pretensioned, drilled holes will not be free to deform as much as those with loose bolts. The clamped plates will prevent the plate material from piling up due to bearing stresses. Therefore, for pretensioned bolts, the hole making procedure does not affect the shear strength of the bolts.

3.3.6 The effect of material loading history on the shear strength of an individual bolt

Since some of the web splice specimens were performed using reused holes, it was necessary to evaluate the effect of the material loading history on the shear strength of individual bolts for the purpose of predicting the capacity of those splices. The results of tests performed on individual bolts in double shear new and reused tension splices is shown in Table 3-16 and Figure 3-10.

Table 3-16 The effect of material loading history on the shear strength of Hand-Tight bolts

Plate Material	Hole in Outer Plates	Hole in Inner Plates	Joint Deformation in.	Shear Capacity Kips	Normalized Shear Capacity
New	Drilled	Drilled	0.282	64.42	1
Used	Drilled	Drilled	0.297	55.41	0.86
New	Punched	Punched	0.273	55.88	0.87

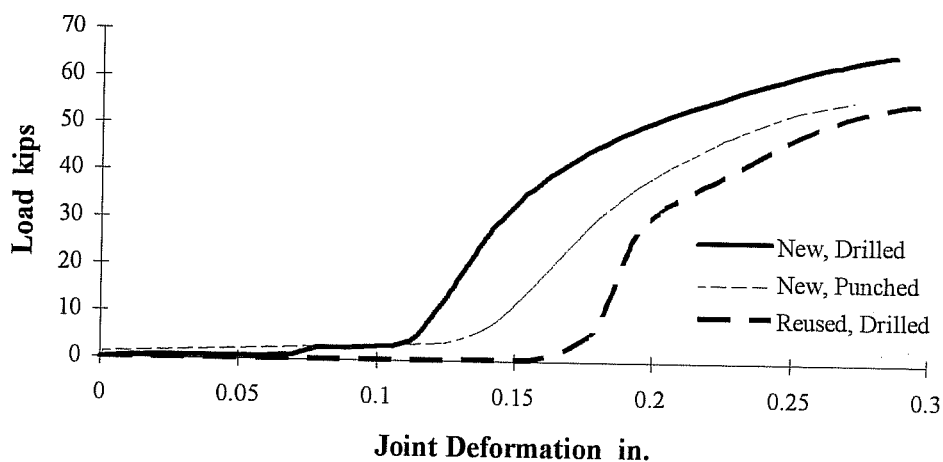


Figure 3-10 The load versus joint deformation for an individual 3/4 in. A325 bolt in double shear new and reused tension splices

Table 3-16 and Figure 3-10 show that the shear capacity of a high strength bolt decreased from 64.42 kips when placed in a new hole to 55.41 kips when placed in a reused hole, a difference of 14 %. Further, the shear capacity of an individual bolt placed in a reused drilled hole is equal to the shear strength of an individual bolt placed in a new punched hole. The reason for this equality in strength is that both the punched and reused material underwent strain hardening and henceforth will have the same amount of bearing deformation. Further, these bearing deformation will cause bending deformation and stresses, as explained earlier in Section 3.3.5, in the bolt which in turn cause an earlier shear failure of the bolt.

3.3.7 Comparison between the shear strength of 3/4 in. A325 bolts tested in compression and in tension splices

Table 3-17 shows that the shear strength of hand-tight bolts tested in compression splices with rigid plates is about 17 % larger than the shear strength of hand-tight bolts tested in tension splices with punched inner holes. On the other hand, the shear strength of hand-tight bolts tested in compression splices with rigid plates is equal (only 4 % difference) to the shear strength of hand-tight bolts tested in tension splices with drilled inner holes.

Table 3-17 The shear strength of hand-tight 3/4 in. A325 bolts tested in compression and in tension splices

Type of splice	Inner Plate	Shear Capacity kips	Normalized Shear Capacity kips
Compression	-	67	1
Tension	Punched	55.88	0.83
Tension	Drilled	64.42	0.96

Thus, since the web holes in the test beams were drilled, the estimated shear strength of the bolts tested in compression splice with rigid plates should be satisfactory.

3.3.8 Summary and conclusions of bolt shear tests

Based on the results of shear tests of the A325 bolts tested in this testing program, the following conclusions are made:

- The hole making procedure does not affect the shear strength of a fully tightened high strength bolt.
- Due to bending of the bolts, the shear capacity of hand-tight bolts placed in punched holes is approximately 13 % less than that of bolts placed in drilled holes. Further, the shear capacity of hand-tight bolts placed in punched holes is less than the value specified in the AISC specifications. Thus, it is recommended that a hole making procedure reduction factor of 0.85 be included in the specifications for snug bolts in punched holes.
- The shear strength of 3/4 in. A325 hand-tight bolts is 13 % less than that of pretensioned bolts.
- The shear strength of hand-tight bolts tested in compression splices with rigid plates is about 17 % larger than the shear strength of hand-tight bolts tested in tension splices with punched inner holes. On the other hand, the shear strength of hand-tight bolts tested in compression splices with rigid plates is equal (only 4 % difference) to the shear strength of hand-tight bolts tested in tension splices with drilled inner holes.

Chapter 4

4. Large-Scale Experimental Program for Steel Girder Bolted Splices

4.1. Introduction

The results of 32 large-scale steel girder bolted splice testing program are presented and discussed. These splices included seventeen web splices, eight symmetric web-flange splices, and seven unsymmetric web-flange splices.

The behavior of web splices before and after slip is introduced and the proper method of analysis of the bolts is determined. Also, the behavior of w-f splices before and after slip is introduced. The effect of the moment resistance of the flanges on the design forces for the web splice is determined at both the service level and at maximum load. The shear carried by the flanges of symmetric w-f splices with adequate flanges is determined. The theoretical distribution of forces between the web splice and flange splices is introduced and compared with test results. The effect of moment-shear interaction on the strength of the splice plates is examined. Finally, the effect of preload in the web bolts, and the effect of the size of the web holes on the strength of the splice is examined.

4.2. Test Set-Up

Two different testing beams were used; W24×55 and W40×167. The W24×55 and W40×167 beams will be referred to herein as the 24 in. and 40 in. beam, respectively.

For the 24 in. beam experimental program, a W24×55 A36 simply supported steel girder with a span of 16 feet was used. The girder was reinforced by two 8×1/2" A572 grade 50 cover plates to enable the girder to carry higher shear and moment. The 600 kip universal testing machine was used to apply a concentrated load at midspan to the specimen. The girder was spliced at the quarter points at each end. This helped in testing two splices simultaneously. Once a splice on one end of the beam had failed, by shearing the critical web bolt that is the farthest from the center of the rotation, the failed connection was reinforced to enable the failure of the splice on the other end of the beam. The web splice bolts were 5/8" A325 high strength bolts. The flange splice bolts for the first splice tested were 3/4" A325 high strength bolts. For the rest of the splices, the flanges were welded. The holes in the girder were drilled. The holes in the splice plates were punched to speed up the fabrication process. All holes were 1/16 in. larger than the nominal diameter of the bolts.

The test set-up for the 24 in. beam is shown in Figure 4-1. The flange splice plates were 8×1/2 " A572 grade 50 steel and were kept constant for splices 1, 2, 3, and 4. For splice #5, the flanges were cut to a width of 4 inches to reduce the moment carried by the flanges and to force the web to carry the additional moment not carried by the flanges. The thickness of each of the web splice plates was 1/2" for all the splices. All the web splice plates were A36 steel. All bolts were installed using a spud wrench; no calibration for the tension in the bolts was done.

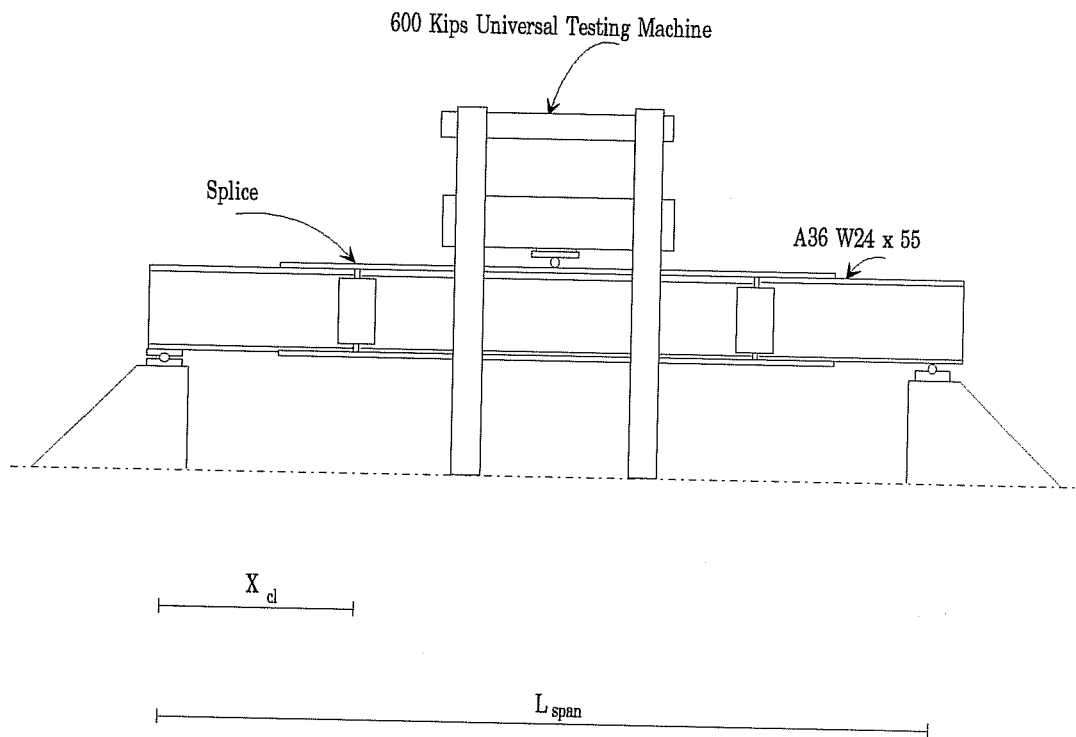


Figure 4-1 The 24 in. Beam Test Set-Up

For the 40 in. beam experimental program, a W40×167 A572 grade 50 simply supported steel girder with a span of 18 feet was used. The bottom flange of the girder was cut to a width of 7.5 inches for a different project. The 600 kip universal testing machine was used to apply a concentrated load at midspan to the specimen. The girder was spliced at a variable location from the end support to vary the moment/shear ratio at the centerline of the splice, as needed. The clearance of the splice, the gap between the two ends of the connected girders, was 1/2-3/4 inch for the web-flange splices and varied as needed for the web splices. Also, for web splices, the flange and web of the girder was coped on the compression side to ensure that the two girders do not butt against each other (due to excessive rotation) before the critical web bolt fractures.

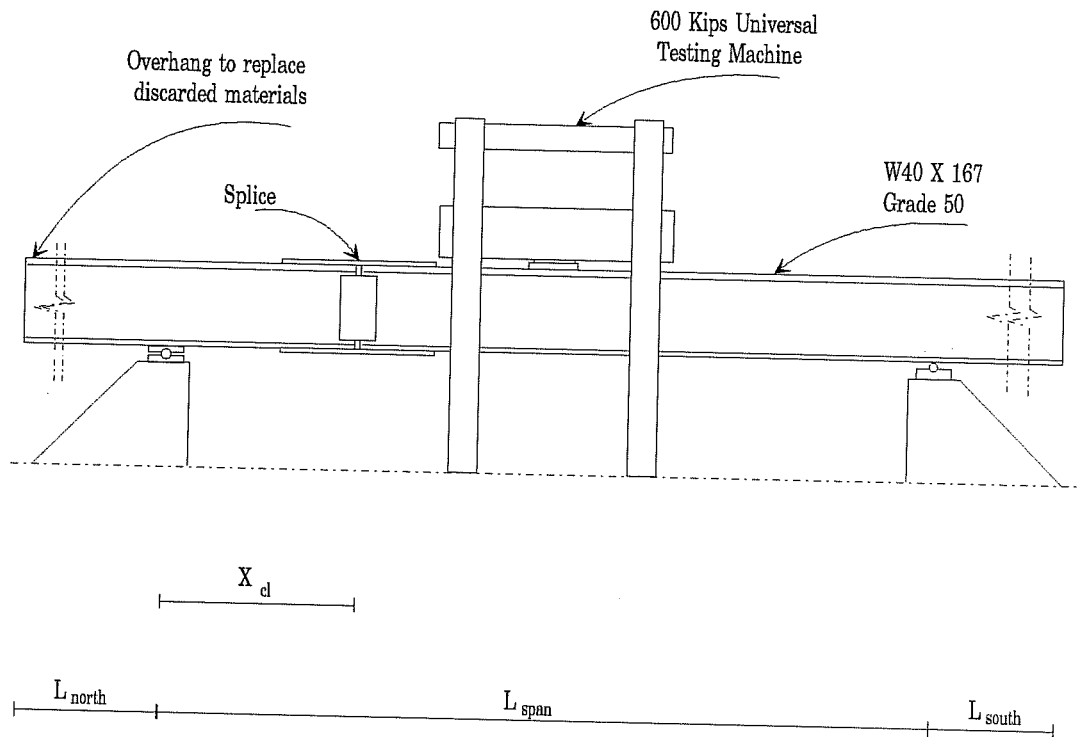


Figure 4-2 The 40 in. Beam Test Set-Up

The test set-up for the 40 in. beam is shown in Figure 4-2. Once a splice had failed, the length of the girder used for the splice was cut and replaced by bringing the two pieces of the girder together. The girder had two overhangs on each end to serve as a replacement to the discarded pieces. A325 3/4" high strength bolts with a length of 2.5 inches were used for both the web splice and the bottom flange splice of the unsymmetric web-flange splices. A325 3/4" high strength bolts with a length of 2.75 inches were used for both the flange splices of the symmetric web-flange splices and the larger flange splice of the unsymmetric web-flange splices. The larger flange splice plate was 10×1/2 " A36 steel and was kept constant for both the symmetric and unsymmetric splices. The small flange

plates were varied from $10 \times 1/2$ " A36 steel for the symmetric splices to $7.5 \times 1/4$ " A36 steel for the unsymmetric splices. The web splice plates were A36 steel. The thickness of each of the web splice plates was $3/8$ " and was kept constant for all splices except for splices 18 and 20 where the thickness was decreased to $3/16$ " to enable the web splice plates to reach their plastic moment and shear yield capacities simultaneously. All bolts were installed using the calibrated wrench method. The bolts were calibrated by an applied torque of 275 lb.ft. to ensure a full frictional resistance in the splice. The applied torque corresponded to a 32.9 kip pretension load in the bolt. However, the web bolts of splices 14, 19, 21, 22, 23, 24, and 25 were tightened by hand to determine the effect of pretension load in the web bolts on the strength of the splice. The holes in the girder web were drilled, whereas, the holes in the splice plates and in the girder flanges were punched to speed up the fabrication process. All holes were $1/16$ in. larger than the nominal diameter of the bolts. Figure 4-3 shows a photograph of the 40 in. beam test set-up.



Figure 4-3 A photograph of the 40 in. beam test-up

4.3. Details of the steel girder splice tests

Figure 4-4 shows the geometrical details and the distribution of bolts of the tested splices. The geometrical details and the distribution of bolts of the tested splices are presented in Table 4-1 through Table 4-6.

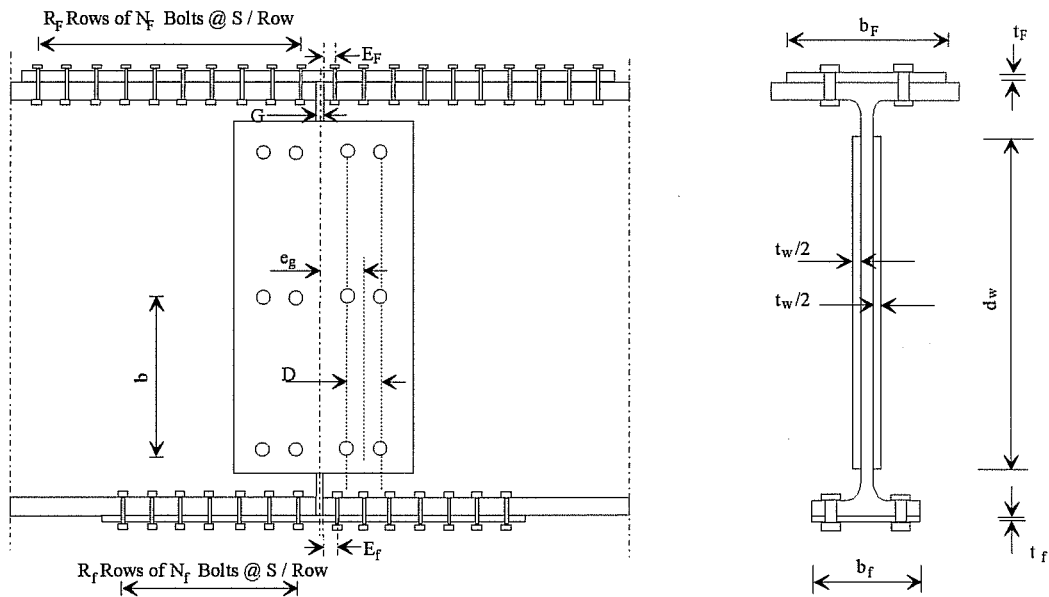


Figure 4-4 The geometrical details and the distribution of bolts of the tested splices

Table 4-1 Geometrical Details of the 24 in. Beam Splices

Splice	X_{cl} in.	$b_F \times t_F = b_f \times t_f$ in.	$d_w \times t_w/2$ in.	L_{span} in.
1s	48.0	8.072×0.495	12×0.489	192
2s	48.0	8.072×0.495	12×0.489	192
3s	48.0	8.072×0.495	12×0.489	192
4s	48.0	8.072×0.495	18×0.489	192
5s	48.0	4×0.495	18×0.489	192
6w	48.0	-	12×0.489	192

Table 4-2 Geometrical Details of the 40 in. Beam Web Splices

Splice	X_{cl} in.	$d_w \times t_w/2$ in.	L_{span} in.	L_{north} in.	L_{south} in.
11w	48.0	29×0.403	216	158.0	139.5
12w	48.0	29×0.403	216	145.2	134.5
13w	48.0	29×0.403	216	140.3	127.5
14w	48.0	29×0.403	216	140.3	127.5
21w	49.2	29×0.403	216	101.1	73.5
22w	49.2	29×0.403	216	101.1	73.5
23w	49.2	29×0.403	216	101.1	73.5
24w	49.2	29×0.403	216	93.7	65.6
25w	49.2	29×0.403	216	93.7	65.6
26w	49.2	29×0.403	216	86.1	58.3
27w	49.2	29×0.403	216	86.1	58.3
28w	49.2	29×0.403	216	78.7	52.1
29w	49.2	29×0.403	216	78.7	52.1
30w	48.0	29×0.403	216	72.4	43.9
31w	48.0	29×0.403	216	72.4	43.9
32w	48.0	29×0.403	216	67.8	36.5

Table 4-3 Geometrical Details of the 40 in. Beam Web-Flange Splices

Splice	X_{cl} in.	$b_F \times t_F$ in.	$b_f \times t_f$ in.	$d_w \times \frac{t_w}{2}$ in.	L_{span} in.	L_{north} in.	L_{south} in.
7u	48.0	10.03 × 0.503	-	28.94 × 0.403	216	198.0	164.5
8u	48.0	10.03 × 0.503	-	28.94 × 0.403	216	198.0	164.5
9u	48.0	10.03 × 0.503	7.51 × 0.246	28.94 × 0.403	216	183.0	149.5
10u	48.0	10.03 × 0.503	7.51 × 0.246	28.94 × 0.403	216	163.0	144.5
15u	48.0	10.03 × 0.503	7.51 × 0.246	28.94 × 0.403	216	120.0	94.1
16s	60.0	10.03 × 0.503	10.03 × 0.503	28.94 × 0.403	216	102.8	103.7
17u	48.0	10.03 × 0.503	7.51 × 0.246	8.94 × 0.403	216	114.8	91.7
18s	59.9	10.03 × 0.503	10.03 × 0.503	18.5 × 0.182	216	98.0	91.3
19u	48.0	10.03 × 0.503	7.51 × 0.246	28.94 × 0.403	216	107.4	77.2
20s	49.2	10.03 × 0.503	10.03 × 0.503	25 × 0.182	216	101.1	73.5

Table 4-4 Distribution of the Bolts for the 24 in. Beam Splices

Splice	$n \times m$	b in.	D in.	e_g in.	G in.	$N \times R_F$	E_F in.	$N \times R_f$	E_f in.	S in.
1s	2 × 1	6	0	4.5	3	5 × 2	3	5 × 2	3	2.5
2s	2 × 1	6	0	4.5	3	Welded	0	Welded	0	-
3s	2 × 1	2.5	0	5.5	3	Welded	1	Welded	0	-
4s	2 × 1	15	0	4.0	3	Welded	0	Welded	0	-
5s	3 × 1	5	0	4.0	3	Welded	0	Welded	0	-
6w	2 × 1	8	0	7.5	3	-	-	-	-	-

Table 4-5 Distribution of the Bolts for the 40 in. Beam Web Splices

Splice	$n \times m$	b in.	D in.	e_g in.	G in.
11w	7×2	4.1875	3	3.75	1/2
12w	4×1	4.1875	0	2.25	1/2
13w	6×1	4.25	0	2.5	1/2
14w	6×1	4.25	0	2.5	1/2
21w	5×2	4.75	3.5	4	3/4
22w	5×1	4.75	0	5.75	3/4
23w	3×2	4.75	3.5	4	3/4
24w	5×2	4.75	3.5	4	3/4
25w	5×2	4.75	3.5	4	3/4
26w	5×1	4.75	0	5.75	3/4
27w	5×1	4.75	0	5.75	3/4
28w	3×1	12.25	0	2.5	3/4
29w	3×2	4.75	3.5	4	3/4
30w	5×1	4.75	0	5.75	3/4
31w	6×1	4.25	0	2.5	3/4
32w	6×1	4.25	0	2.5	3/4

Table 4-6 Distribution of the Bolts for the 40 in. Beam Web-Flange Splices

Splice	n × m	b in.	D in.	e _g in.	G in.	N × R _F	E _F in.	N × R _f	E _f in.	S in.
7u	7 × 2	4.1875	3	3.75	1/2	10 × 2	1.5	-	-	2.5
8u	4 × 1	4.1875	0	2.25	1/2	10 × 2	1.5	-	-	2.5
9u	6 × 1	4.25	0	2.5	1/2	10 × 2	1.5	7 × 2	1.5	2.5
10u	6 × 1	4.25	0	2.5	1/2	10 × 2	1.5	6 × 2	4	2.5
15u	3 × 1	12.25	0	2.5	3/4	10 × 2	1.5	7 × 2	4	2.5
16s	2 × 1	24	0	2.25	3/4	10 × 2	1.5	10 × 2	4	2.5
17u	2 × 1	3	0	3	3/4	10 × 2	1.5/4	6 × 2	9	2.5
18s	4 × 1	4.5	0	2.25	3/4	10 × 2	1.5	10 × 2	4	2.5
19u	6 × 1	4.25	0	2.5	3/4	10 × 2	1.5	7 × 2	4	2.5
20s	5 × 2	4.75	3.5	4	3/4	10 × 2	1.5	10 × 2	4	2.5

Where:

n the number of web bolts in a vertical row

m the number of web bolts in a horizontal row

b the vertical spacing of the web bolts

D the horizontal spacing of the web bolts

e_g the geometrical eccentricity; the distance from centerline of splice to centroid of the web bolts

G the gap between the two girders

N × R_f the number of small flange bolts per row × the number of rows

N × R_F the number of big flange bolts per row × the number of rows

E_f, E_F the edge distance for the small and the big flange edge bolt at the south side of the splice, respectively

S the longitudinal spacing of the flange bolts

b_f, t_f the width and thickness of the small flange splice plate, respectively

b_F, t_F the width and thickness of the big flange splice plate, respectively

X_{cl} the location of splice with respect to the north support

L_{span} the span of the girder

L_{north} the length of the north overhang

L_{south} the length of the south overhang

Table 4-7 Slip and Shear Resistance of an individual web bolt of the tested splices

Splice	Web Bolt Preload	Loading History	Double Slip Load kips	Double Shear Capacity kips
1, 2, 3, 4	No	No	-	52.50
5, 6	No	No	-	54.52
7, 8, 9, 10, 11, 12, 13, 15, 16, 17	Yes	No	21.90	73.96
31	Yes	No	22.08	74.55
18, 20	Yes	No	17.17	84.09
19, 24, 26, 28, 29, 30	No	No	-	65.25
14, 21, 22, 23, 25, 27, 32	No	Yes	-	55.88

The span of the 40 in. beam girder was 18 feet. However, the original length of the girder of the girder was 50 feet; thus, the overhangs were 32 feet long. To eliminate the effect of the self weight of the overhangs on the splice strength, the self weight was included in the analysis. Table 4-8 shows the self weight shear and moment at the centerline of all the 40 in. beam splices.

Table 4-8 Self weight forces at the centerline of the 40 in. beam splices

Splice	Shear kip	Moment kip-in
7u	1.12	-180.1
8u	1.12	-180.1
9u	1.09	-145.3
10u	0.93	-109.2
11w	0.92	-99.3
12w	0.85	-78.2
13w	0.86	-68.7
14w	0.86	-68.7
15u	0.92	-32.3
16s	0.60	-8.0
17u	0.90	-25.7
18s	0.65	0.6
19u	0.92	-14.1
20s	0.89	-5.8
21w	0.89	-5.8
22w	0.89	-5.8
23w	0.89	-5.8
24w	0.88	2.8
25w	0.88	2.8
26w	0.86	10.8
27w	0.86	10.8
28w	0.85	17.8
29w	0.85	17.8
30w	0.86	22.6
31w	0.86	22.6
32w	0.86	26.6

4.4. Test procedures of girder splices

For the 24 in. beam testing program, a series of six splices were tested. All splices were loaded monotonically to failure with an increment that varied based on the observed load versus deflection plot. The static load was recorded at several loading stages before failure.

For the 40 in. beam testing program, a series of twenty-six splices were tested. All splices, except for the hand-tight web splices, were cycled at the service level, before a slip had occurred. After a major slip had occurred, the splice was loaded monotonically to failure with an increment that varied based on the observed load versus deflection plot. The static load was recorded at several loading stages before failure.

4.5. The fabrication, instrumentation, loading, and behavior of a typical unsymmetric splice with inadequate flanges

This section describes the fabrication, the instrumentation, the loading, and interprets the behavior of a typical specimen (specimen 10).

The splice plates of both the flanges and web were flame cut to the desired dimensions. The girder was also flame cut at the splice location. The holes in the girder web and web splice plates were drilled, whereas, the holes in the girder flanges and flange splice plates were punched. All holes were 1/16 in. larger than the nominal diameter of the bolts.

After cutting, drilling, and punching the splice components, the splice was ready for assembly. The longer girder was placed securely on two supports at its ends. The smaller girder was carried by the crane from its ends and was brought towards the longer girder. When both girders were separated by the 1/2 in desired gap, the crane was shut down and the short girder was free to swing for final alignment. The flange splice were assembled first to ensure that the girders are aligned in a straight line before the web splice was assembled. The flange bolts were placed in their respective holes and were not tightened. Then, the web splice was assembled. The web bolts were placed in their respective holes and were not tightened. After the assembly of all the splice components, the bolts were tightened by a spud wrench to a full man's strength. At this stage, the full tension in the bolts was not yet produced.

After the assembly process of the splice was completed, the beam was ready to be placed in the testing machine. A spreader beam was placed on top of the test beam and chained to the test beam. To ensure that the splice will not be overstressed (due to its self weight) during the transportation process, the spreader beam was chained to the test beam from three locations along the span. Then, the beam was transported by the crane to the testing machine. The beam was placed from one end on the south pedestal and was rolled inside the testing machine by both the crane from one end and the fork-lift from the other end. When the centerline of the splice was at the desired location, the beam was braced laterally by means of clip angles.

After bracing the beam, the bolts in both the flanges and the web were tightened using the calibrated wrench method to produce the clamping force. The

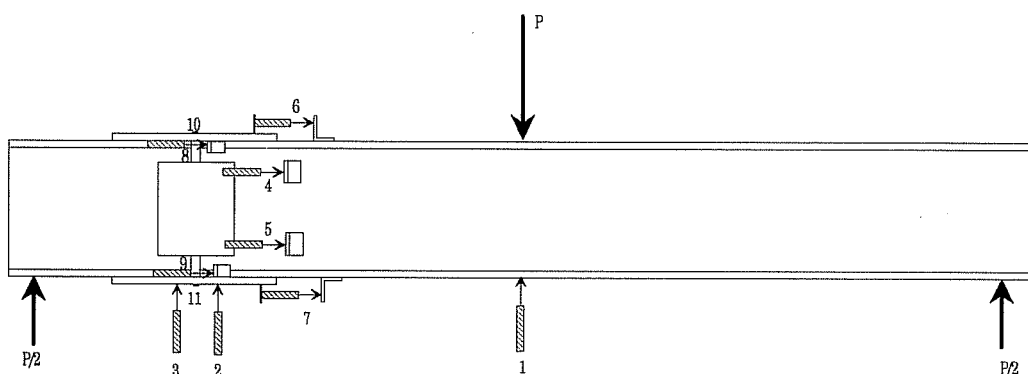


Figure 4-5 The instrumentation of a typical splice

beam was instrumented using strain gages in the flanges and displacement transducers as shown in Figure 4-5.

The load was applied to the specimen at a rate of 300 pounds per second. The specimen was cycled three times in the elastic range up to about 85 % of the theoretical web slip load. The slip of the web was calculated based on the total shear at an eccentricity $e = e_g + M_w / V$, where, M_w is the moment resisted by the web.

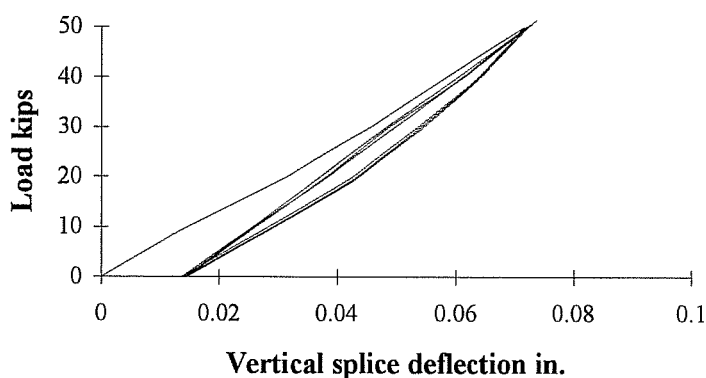


Figure 4-6 The permanent deformation of the girder at the end of the first cycle (channel 2)

During the first cycle, the beam did not return to its original position and had a 1/64 in. permanent vertical displacement as shown in Figure 4-6. However, the permanent displacement of the girder at the end of the first cycle was small and was probably caused by the settlement of the support. This support settlement was observed in all the splices tested. During the second and third cycle, the beam behaved elastically (no permanent deformation). After the end of the third cycle, the load was increased monotonically up to slipping of the web splice plates. When the load exceeded the theoretical slip load of the web based on the elastic analysis of the bolts, the stiffness of the web splice decreased and the load deformation response of the web splice became nonlinear as shown in Figure 4-7.

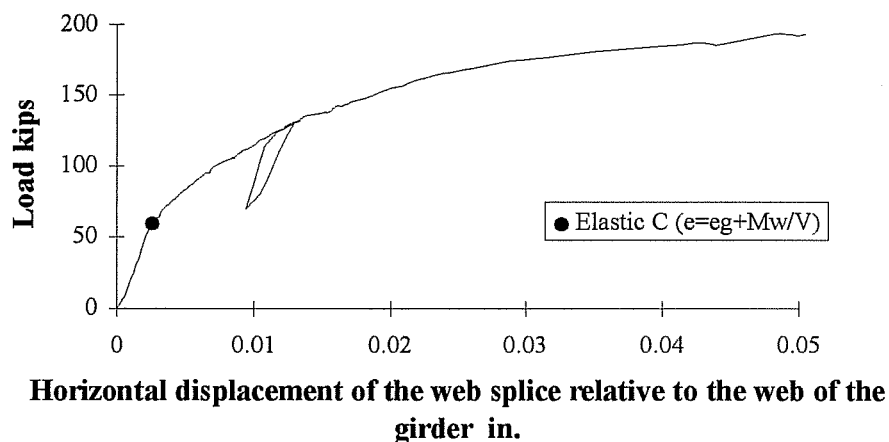


Figure 4-7 The theoretical versus actual slip load of the web splice of splice 10 (channel 5)

The decrease in stiffness combined with the nonlinear response of the web splice indicates that the web splice plates had slipped. However, looking at both the load versus horizontal and vertical splice displacement response, shown in

Figure 4-8 and Figure 4-9, indicated that the girder underwent neither additional rotation nor additional vertical displacement due to slipping of the web splice plates. Since the flanges of splice 10 did not slip nor yielded at this stage, they prevented the girder from undergoing any additional rotation. That the girder did not undergo any additional vertical deflection at the splice location means that the web splice maintained its shear capacity after slipping of the web due to moment. This shear capacity is based on an eccentricity e_g .

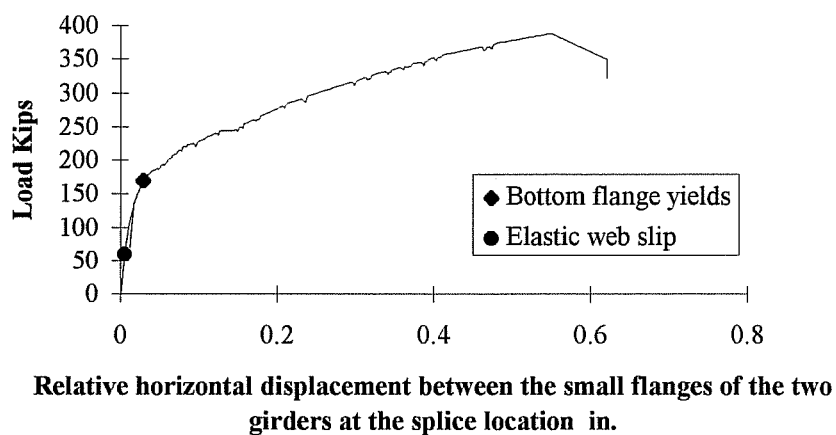


Figure 4-8 The load versus relative horizontal girder deflection at the splice location of splice 10 (channel 9)

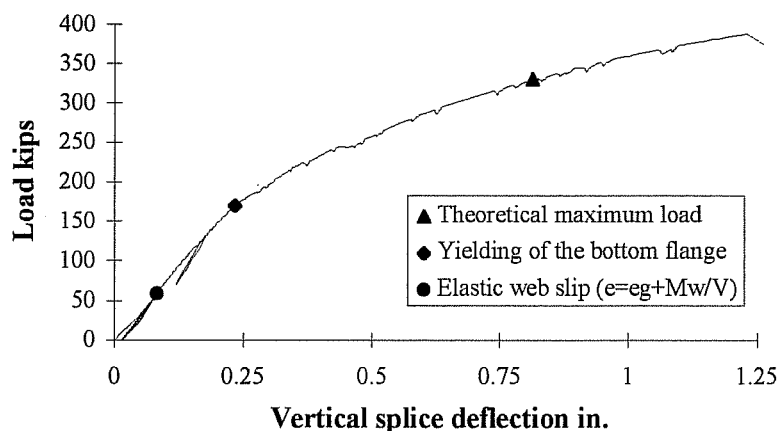


Figure 4-9 The load versus vertical deflection at the splice location of splice 10 (channel 2)

After slipping of the web splice plates, the flanges carried the moment not resisted by the web. When the small flange yielded at the gross section, the rotation and vertical stiffness of the girder decreased. This indicates that at service load the flanges should be limited to yielding on the gross section. Figure 4-8 and Figure 4-9 show the decrease in rotation and lateral stiffness due to yielding of the small flange. Also, after yielding of the small flange, the big flange underwent strain reversal which indicates the formation of a shear kink. The strain reversal in the big flange can be shown in Figure 4-10. During the test, it was observed that the formation of a shear kink was accompanied by the formation of a plastic hinge in the big flange at the location of first row of flange bolts.

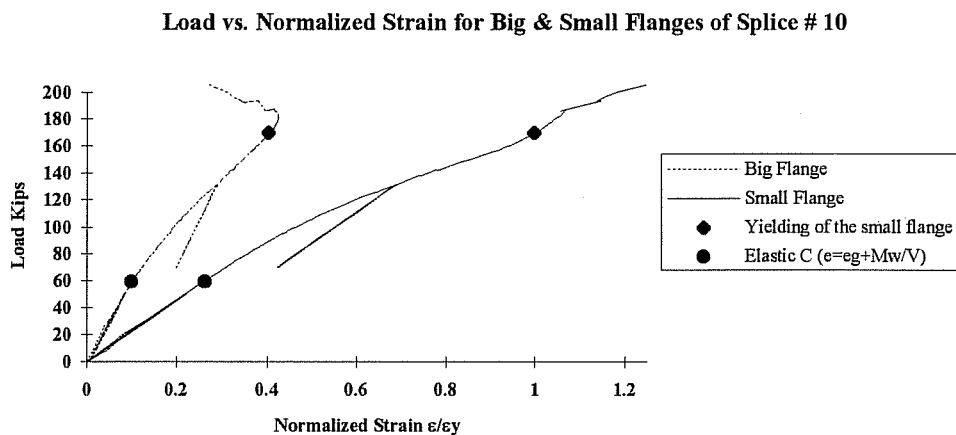


Figure 4-10 The load versus normalized strain in the small and big flange of splice 10 (channels 10 & 11)

As the load increased beyond yielding of the small flange, the splice underwent additional rotation and vertical shear kink. The additional applied moment not resisted by the small flange was resisted by the web and big flange splice plates. This was evident through the visual formation of yield lines around the web bolts closer to the small flange and in the big flange splice plate. When the applied load exceeded the theoretical shear capacity of the bolts (based on the nonlinear analysis of the bolt), necking of the small flange at the net section was visual. When the critical bolt (the bolt at the small of the web splice) reached its individual shear capacity, the connection failed by shearing of the critical bolt. Due to strain hardening of the small flange, the connection failed at a load 15.3 % larger than the theoretical maximum load.

Necking of the small flange at the net section occurred only in splices 9 and 10 where the applied moment in the splice was 2.42 times the small flange yield moment and 1.31 times the big flange yield moment. In a typical splice, the small flange is usually adequate to carry the total applied moment and necking of the flange does not occur.

Splices 9 and 10 (and all the unsymmetric splices) were able to achieve their flange moment capacities even though the ratio of the net to the gross section area of the small flange was 78%. Thus, there is no need to reduce the calculated gross area into an effective gross area, as required by AASHTO, when the net to gross section area is less than 85%.

4.6. Test results of girder splices

Table 4-9 through Table 4-11 show the applied midspan load at failure, the applied moment and shear at the center line of the splice at failure, and the failure mode of the web, symmetric web-flange, and unsymmetric web-flange splices, respectively.

Table 4-9 Test Results of Girder Web Splices

Splice	P_u kips	M_u kips-in.	V_u kips	Failure Mode
6w	15	360	7.2	Fracture of top critical web bolt
11w	245.3	5788	123.6	Fracture of top two web bolts
12w	52.9	1191	27.30	Fracture of top critical web bolt
13w	106.8	2494	54.26	Fracture of top critical web bolt
14w	81.5	1887	41.61	Fracture of top critical web bolt
21w	104.8	2572	53.29	Fracture of top two web bolts
22w	47.3	1158	24.54	Fracture of top critical web bolt
23w	64.4	1578	33.09	Butting at the top of the girder + Fracture of bottom critical web bolt
24w	118.3	2913	60.03	Fracture of bottom two web bolts
25w	75.1	1850	38.43	Fracture of bottom second critical web bolt
26w	44.7	1110	23.21	Fracture of bottom critical web bolt
27w	41.0	1019	21.36	Fracture of bottom critical web bolt
28w	57.8	1439	29.75	Fracture of bottom critical web bolt
29w	49.1	1225	25.40	Fracture of bottom critical web bolt
30w	48.8	1194	25.26	Fracture of bottom critical web bolt
31w ^{sh}	94.2	2283	47.96	Fracture of bottom critical web bolt
32w ^{sh}	67.5	1647	34.61	Fracture of bottom critical web bolt

In Table 4-9, the critical bolt is the bolt which has the largest force resultant and undergoes the largest amount of deformation.

Table 4-10 Test Results of Web-Flange Symmetric Splices

Splice	P_u kips	M_u kips-in	V_u kips	Failure Mode
1s	142	6408	71	Fracture of top critical web bolt
2s	142+	6408+	71+	Did not continue loading to failure
3s	90	2160	45	Fracture of top critical web bolt and the top weld
4s	190	4560	95	Fracture of top critical web bolt
5s	124	2976	62	Fracture of top critical web bolt and the top weld
16s	313.6	9400	157.4	Fracture of two critical web bolts
18s	333.2	9980	167.2	Buckling of the splice plates
20s	468.8	11527	235.3	Buckling of the splice plates

Table 4-11 Test Results of Web-Flange Unsymmetric Girder Splices

Splice	P_u kips	M_u kip-in	V_u kips	Failure Mode
7u	411.2	9689	206.7	Lateral torsional buckling of the girder
8u	208.1	4814	105.2	Fracture of bottom critical web bolt
9u	380.2	8979	191.2	Fracture of bottom four web bolts and of the bottom flange at the net section
10u	387.8	9198	194.8	Fracture of bottom critical web bolt
15u	300.6	7182	151.2	Fracture of bottom critical web bolt
17u	147.2	3507	74.50	Fracture of bottom critical web bolt
19u	340.3	8153	171.1	Fracture of bottom critical web bolt

4.7. Discussion of test results

4.7.1. Web Splices

4.7.1.1. The Behavior and analysis of web splices up to Slip

At the service level, slip load, the appropriate method of determining the slip resistance of eccentrically loaded group of bolts needs to be determined. For axially loaded connections, the behavior was depicted in Chapter 1 and the slip was defined as the load at which all bolts reach their individual slip load. For eccentrically loaded bolts, the problem is more complicated than the axially loaded case. For the latter, it is assumed² that a group of bolts rotates about its center of rotation and that the connection will not slip until all bolts reach their individual slip load. This assumption will be examined further herein and will be then compared with test results. The method of determining the slip resistance of eccentrically loaded group of bolts based on the assumption that the connection slips when all bolts reach their individual slip load will be referred to, herein, as the *plastic method* of analysis.

A typical behavior of an eccentrically loaded group of bolts at the service level as found in this testing program is shown in Figure 4-11. Initially, the connection behaves elastically. When the load in the critical bolt reaches its slip load, the stiffness of the connection starts to decrease. However, a major slip, large amount of deformation or drop in load, will not occur until all bolts reach their individual slip load. The range where the stiffness of the connection start to decrease and up to where all the bolts reach their slip capacities will be called herein the *transitional slip range*. The amount of additional deformation due to the decrease in stiffness in the transitional slip range is dependent on the size of the

holes and on the initial location of the bolts in their respective holes during fabrication. This range, as found herein, can be large for oversize holes and slotted holes, where the critical bolt will not be able to come into contact with the hole edge shortly after reaching its slip load. Figure 4-15 shows the load-deformation response of short-slotted web splice. Since the transitional slip range is concurrent with reaching the slip resistance of the critical bolt and since the transitional slip range might be extremely large and dependent on the location of the hole size and the initial location of the bolt, the load that corresponds to reaching the slip load of the critical bolt should be considered as the slip load. Consequently, the slip load should be calculated from a direct simple elastic analysis where the connection is considered to fail when the slip resistance of the critical bolt is reached. Table 4-12 shows the results of the theoretical slip loads using elastic and plastic analyses of the web bolts for the web splices tested in this program. Since the actual slip test load is difficult to define as a single value, the results of the theoretical elastic and plastic analyses are plotted on the actual load deformation plots for the specimens tested. Figure 4-12 through Figure 4-15 show the theoretical elastic and plastic slip loads vs. the actual on the actual load-deformation plots of the tested splices.

Table 4-12 The theoretical slip loads using both elastic and plastic analyses of the web bolts

Splice	P_u Elastic kips	P_u Plastic kips
11w	70.10	91.70
12w	15.15	17.57
13w	28.27	35.59
31w	24.91	32.29

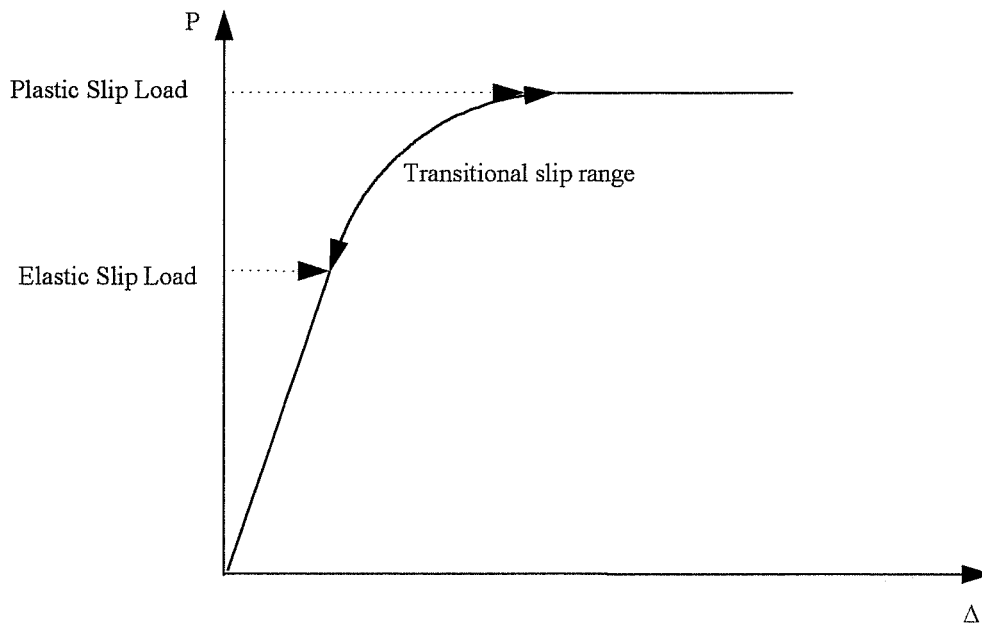


Figure 4-11 The slip behavior of eccentrically loaded group of bolts up to slip

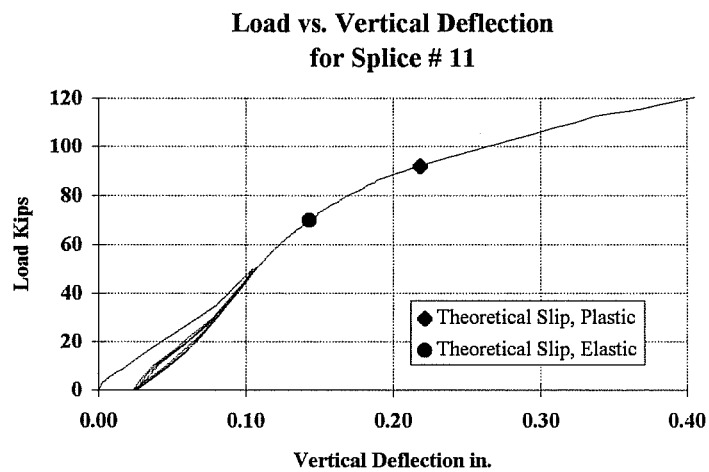


Figure 4-12 The load versus vertical deflection (channel 2) at the splice location up to slip for specimen 11

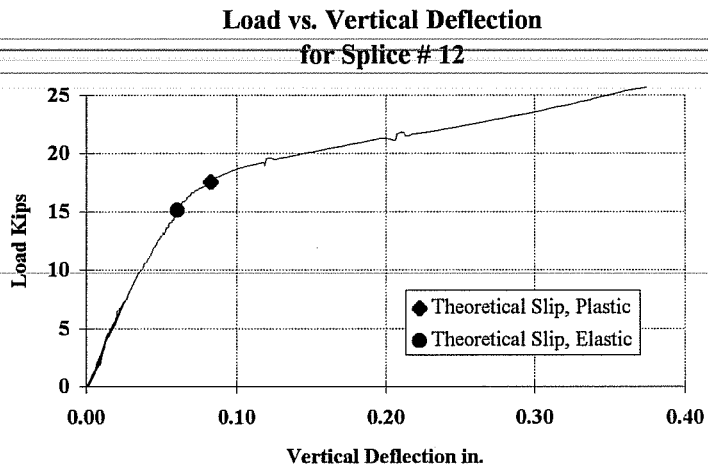


Figure 4-13 The load versus vertical deflection (channel 2) at the splice location up to slip for specimen 12

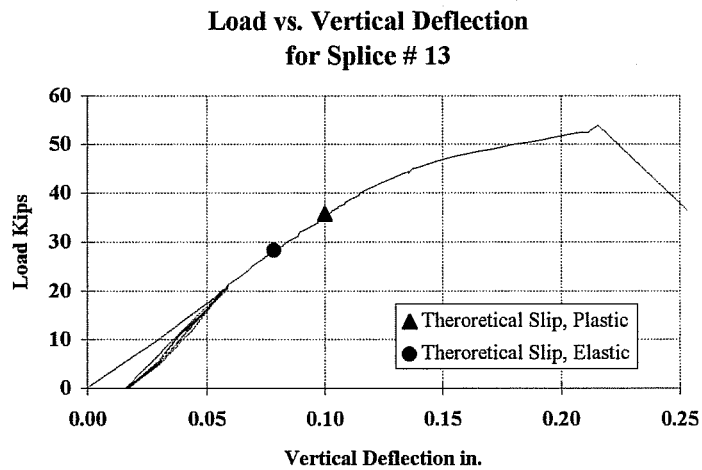


Figure 4-14 The load versus vertical deflection (channel 2) at the splice location up to slip for specimen 13

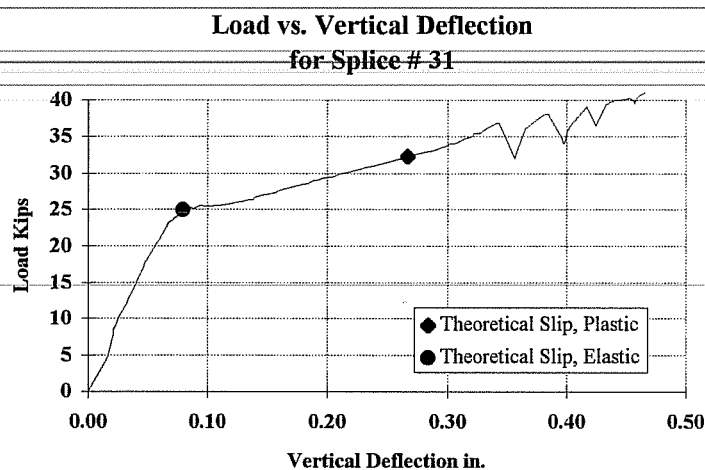


Figure 4-15 The load versus vertical deflection (channel 2) at the splice location up to slip for specimen 31 (short slotted holes)

Figure 4-12 through Figure 4-15 show that the theoretical slip loads predicted well the experimental slip values. Further, the elastic analysis agrees best with the initial slip of the splice. The additional slip resistance that can be gained from plastic analysis was accompanied by either large deformation or significant decrease in stiffness and therefore should not be counted upon to predict the slip load.

4.7.1.2. The Behavior and analysis of web splices after Slip

In Chapter 2, the elastic and the empirical non-linear analyses of eccentrically loaded group of bolts were reviewed and evaluated. It was shown that the elastic analysis is conservative yet adequate, whereas, the non-linear analysis is unconservative. The difference between the two analyses was explained by studying the contribution of each bolt to moment and shear. However, neither

analysis actually represents the actual behavior of the connection. An eccentrically loaded bolted connection behaves in neither the assumed linear nor the empirical nonlinear manner at all loading stages through failure by shearing of the critical bolt. The reason the empirical non-linear behavior does not represent the actual behavior is that the empirical load deformation of an individual bolt is assumed to be continuous. In fact, the opposite is true. The response is discontinuous due to slip. Figure 4-16 shows the empirical and the actual response of an individual bolt.

The holes in a bolted connection are usually made 1/16 in. larger than the nominal diameter of the bolts for ease of assembly. The value of the slip can be anywhere from zero to two hole clearances based upon the initial location of the bolt in its hole during fabrication. The slip can be of small value with respect to the joint deformation at failure if the bearing strength is large ($>3F_u$). However, typical connections are designed not to exceed a bearing stress of 2.4-3 times the tensile strength of the connected plates. Therefore, the value of slip is a significant portion of the total joint deformation. For the A325 3/4 in. bolts that had a bearing strength 2.0 F_u of the connected drilled plates, the total joint deformation were proportioned approximately as follows: 1/3 slip ($2 \times 1/16''$), 1/3 bearing deformation of the bolt ($1.9/16''$), and 1/3 bearing deformation of the connected plates ($2 \times 0.99/16''$).

Further, the maximum deformation, 0.34 in., assumed by the non-linear analysis was obtained from one sample of testing program that represents one type of bolt, diameter, strength, and specific connected plates. It is, therefore, expected that a randomly selected bolt and connected plates will not undergo the assumed bearing deformation of 0.34 inches. Figure 4-16 shows the empirical load response of an individual bolt versus the response of four bolts used in this testing program.

Three of the bolts had a bearing strength of 2 times F_u . Two of the three bolts were pretensioned and placed in a standard hole and short-slotted hole, respectively. The third bolt was placed in a standard hole but was hand-tight, with no preload. The fourth bolt was placed in a standard hole but had a shear strength of 4 times F_u .

Figure 4-16 shows that the empirical response can be drastically different from that of an actual bolt used in a typical connection. Therefore, in predicting the capacities of the web splices tested, the actual measured load-deformation response of the bolts is used in the non-linear analysis. Nevertheless, the results of the linear, empirical non-linear, and non-linear analysis will be examined in detail for a typical connection.

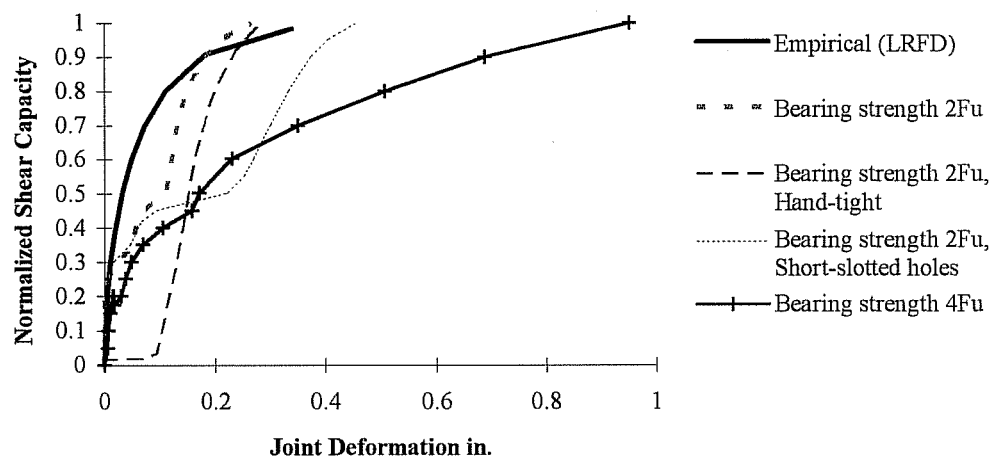


Figure 4-16 The load versus joint deformation for double shear tension splice with one bolt for different bearing to shear ratios

In the non-linear analysis, the same assumptions that were used in the empirical non-linear analysis are used. The only difference is that after determining

the deformation in each bolt, the corresponding load in a bolt is obtained from the actual measured response of the bolt. Since the measured response is a collection of data points, a linear interpolation between two data points is carried out for determining the force in a bolt. Figure 4-17 shows the behavior of a typical web splice versus the theoretical slip and maximum load.

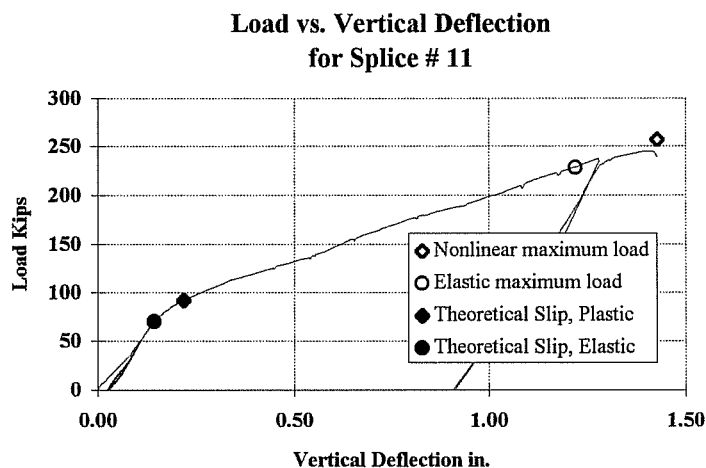


Figure 4-17 The load deflection behavior of typical web splice with pretensioned bolts (splice 11)

In Chapter 2 the difference between the elastic and the empirical nonlinear bolt forces was compared. However, the test force in each bolt is unknown since there is no experimental instrumentation that can measure the shear force in the bolt. Thus, splices 11 and 30, that had pretensioned and hand tight bolts respectively, were chosen for further comparison between the bolt forces obtained from the elastic, the empirical non-linear, and the non-linear analysis. The difference of the force level in each bolt of the empirical and the elastic analysis is compared with that of the nonlinear analysis since the nonlinear analysis using the measured load-deformation response on an individual bolt represents the estimate

closest to test values. Table 4-13 and Table 4-14 show the results of the elastic, empirical, and nonlinear analyses for specimens 11 and 30, respectively. Figure 4-18 and Figure 4-19 show the numbering of the web bolts for specimen 11 and 30 used in the comparison presented in Table 4-13 and Table 4-14, respectively.

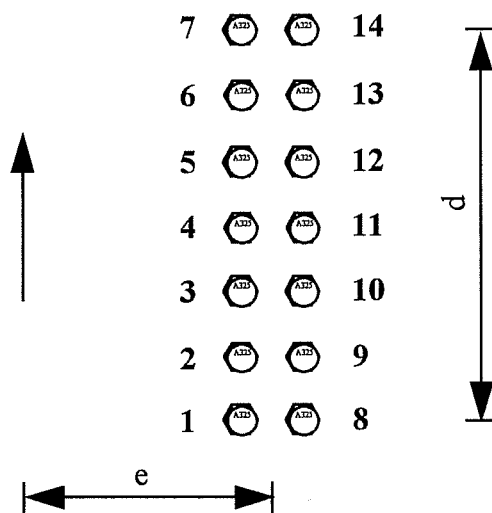


Figure 4-18 The numbering of the web bolts for specimen 11

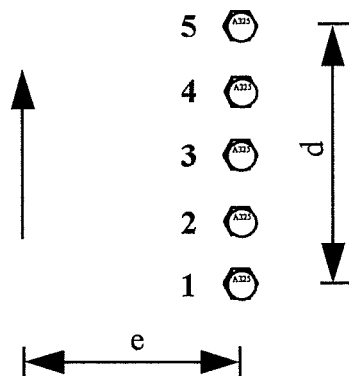


Figure 4-19 The numbering of the web bolts for specimen 30

Table 4-13 Comparison between the theoretical load level in each bolt using the elastic, nonlinear, and empirical nonlinear methods for specimen 11 (pretensioned web bolts)

Bolt	% Load Elastic	% Load Nonlinear	% Load Empirical	% Difference Elastic	% Difference Empirical
1	100	100	98.2	0.0	-1.9
2	68.8	87.0	94.5	-21.0	8.6
3	39.6	54.9	84.0	-27.7	53.2
4	22.7	35.2	68.0	-35.4	93.1
5	39.6	54.9	84.0	-27.7	53.2
6	68.8	87.0	94.5	-21.0	8.6
7	100	100	98.2	0.0	-1.9
8	97.4	99.7	98.0	-2.3	-1.7
9	64.9	83.8	93.9	-22.6	12.0
10	32.5	49.8	80.4	-34.8	61.4
11	0.5	15.3	28.8	-96.6	88.5
12	32.5	49.8	80.4	-34.8	61.4
13	64.9	83.8	93.9	-22.6	12.0
14	97.4	99.7	98.0	-2.3	-1.7
P	228.4	257 ($P_{test}=245$)	283.5	-6.8	15.7

Table 4-13 shows that, for connections with pretensioned bolts, the empirical analysis yields larger forces in all the interior bolts than the nonlinear analysis. On the other hand, the elastic analysis yields smaller forces in the interior bolts than the nonlinear analysis.

Table 4-14 Comparison between the theoretical load level in each bolt using the elastic, nonlinear, and empirical nonlinear methods for specimen 30 (hand-tight web bolts)

Bolt	% Load Elastic	% Load Nonlinear	% Load Empirical	% Difference Elastic	% Difference Empirical
1	100	100	98.2	0.0	-1.9
2	50.6	47.5	89.5	6.6	88.7
3	8.9	0.8	30.7	1027.8	3788.6
4	50.6	0.4746	89.5	6.6	88.7
5	100	100	98.2	0.0	-1.9
P	56.5	55.5 ($P_{test}=48.6$)	66.6	16.2	37

For connections with hand-tight bolts, Table 4-14 shows that both the elastic and empirical analyses yield larger forces in the interior bolts than the nonlinear analysis. Nevertheless, the elastic estimates of forces are closer to the nonlinear values. Further, both the elastic and empirical analyses yield unconservative prediction of strength. However, the elastic solution is closer to test results (26% error) than the empirical nonlinear analysis (37% error).

The reason both analyses overestimate the forces in the interior bolts for hand-tight bolts is that both methods assume that all bolt have initial stiffness, whereas for hand tight bolts, all bolts have zero initial stiffness due to the absence of the clamping force and bearing stresses, provided that the bolts are not in contact with the hole edge.

Table 4-15 shows the results of the linear, nonlinear, and test results. The nonlinear analysis predicted the ultimate load with an average error of $\pm 7.8\%$. The linear analysis predicted the ultimate load within an average error of $\pm 8.4\%$. Therefore, simple direct analysis appears to be adequate and there is no need to perform an iterative non-linear analysis.

Table 4-15 shows that the elastic analysis of eccentrically loaded group of pretensioned bolts yields conservative results in general. Specimen 6 had only two bolts, therefore, the elastic analysis was unconservative due to the excessive rotation of the connection as explained in Chapter 2. For the specimens with hand tight bolts (no preload) the elastic analysis yielded unconservative results. Figure 4-16 shows that, initially, hand-tight bolts have no stiffness and will undergo slip. Some of the interior bolts that are close to the center of rotation in hand-tight web splices will undergo a small amount of deformation and, therefore, will have zero load according to the measured response. These bolts, on the other hand, are assumed to carry an equal share of shear and a portion of the total moment according to the elastic analysis. Thus, the elastic analysis overestimates the forces in the hand-tight bolts that are close to the center of rotation and therefore yields unconservative results.

Table 4-15 The linear, nonlinear, and test results of web splices

Splice	Loading History	Clamping Force	e/d	P _u Test kips	P _u Linear kips	Error Linear %	P _u Nonlinear kips	Error Nonlinear %
6W	No	No	6.73	15	16.1	7.3	-	-
11W	No	Yes	2.02	245	228.4	-6.8	257.0	4.9
12W	No	Yes	3.6	52.9	44.0	-16.7	46.0	-13.0
13W	No	Yes	2.27	107	89.4	-16.5	98.6	-7.9
31W	No	Yes	2.36	94.1	86.3	-8.2	89.8	-4.5
24W	No	No	2.76	118	119.6	1.4	117.7	-0.2
26W	No	No	2.83	44.2	55.7	26.0	54.7	23.8
28W	No	No	3.51	57.7	60.3	4.6	59.5	3.1
29W	No	No	5.53	49	50.6	3.2	48.9	-0.3
30W	No	No	2.79	48.6	56.5	16.2	55.5	14.1
32W	Yes	No	2.36	67.5	63.9	-5.4	63.0	-6.6
14W	Yes	No	2.23	81.3	67.6	-16.8	66.7	-17.9
21W	Yes	No	2.75	105	101.9	-3.0	99.8	-4.9
22W	Yes	No	2.79	47.3	47.8	1.0	47.5	0.4
27W	Yes	No	2.82	44.2	47.2	6.8	46.9	6.0
Average	-	-	-	-	-	±8.4	-	±7.8

4.7.1.3. The effect of the hole size of the web bolts on the strength of web splices

To examine the effect of hole size of the web bolts, specimen 13 was replicated in specimen 31. However, the web holes in specimen 31 were horizontal short-slotted holes. Figure 4-20 shows the load deformation response of both specimens up to failure by shearing of the critical web bolt.

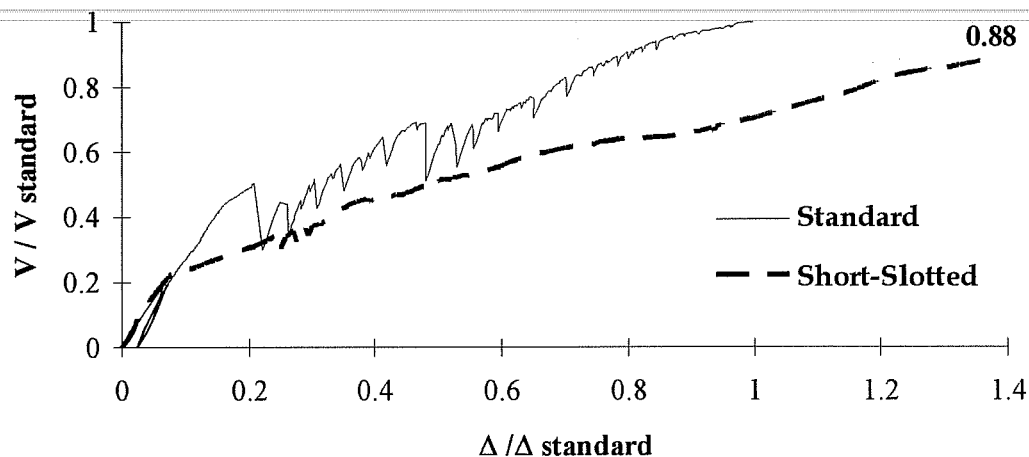


Figure 4-20 The effect of size of the web holes on the strength and deformation of web splices

Figure 4-20 shows that the size of the hole affects neither the initial stiffness of the girder nor the slip load of the splice. However, at failure, the splice with horizontal short-slotted holes underwent approximately 40% larger deformation than the splice with standard holes. Also, the splice with horizontal short-slotted holes failed earlier than the splice with standard holes. Splice 13 failed at a load of 106.7 kips, whereas, splice 31 failed at a load of 94.1; a 11.8% decrease in strength. However, the shear strength of an individual bolt is not affected by the hole size. The decrease in strength of the splice due to the use of short-slotted holes is due mainly to the inability of some of the interior bolts to bear against the edge hole and develop their bearing resistance. The ability of the interior bolts to develop their bearing resistance is dependent on the initial location of the bolts in their respective holes.

4.7.1.4. Summary and conclusions of web splice tests

Based on the results of the testing program of 17 large-scale web splices, the following conclusions are made:

I. At the service level:

- When the critical bolt reaches its slip load, the stiffness of the connection decreases. Thus, for predicting the slip load of web splices, elastic analysis of the bolts must be performed. The gain in the slip resistance when using plastic analysis of the bolts can be accompanied by significant decrease in stiffness and large deformation and, therefore, should not be counted upon for predicting the slip resistance of web splices.

II. At maximum load:

- The empirical nonlinear analysis of the web bolts does not represent the actual behavior of bolted web splices and is unconservative.
- The nonlinear analysis using the actual measured load deformation of the bolts agrees best with test results for both pretensioned and hand-tight bolts. However, the analysis is iterative. Moreover, the load-deformation response of randomly selected bolt and plate thickness and strength is not available and costly to obtain.
- In general, the elastic analysis is conservative for the pretensioned bolts and unconservative for the hand-tight bolts. However, simple direct elastic analysis of the web bolts appears to be adequate for both the pretensioned and hand-tight bolts.
- Web splices with short slotted horizontal web holes have less capacity than web splices with standard web holes

4.7.2. Web-Flange Splices

In the first few tests performed on the 24 in. beam specimens, the behavior of the web-flange splice was not yet clear. The distribution of forces between the flanges and the web splices was in question. However, since the behavior and force distribution among the web bolts in a web splice was understood, the main focus in all the tests was to fail the web bolts in shear. After failing the web bolts, the web forces were easily determined. The flange forces were determined from the equilibrium equations to provide equilibrium with the externally applied forces at the center line of the splice.

Before introducing the distribution of forces between the web and flange splices at both the service and maximum load, the observed behavior of the splice before and after slip will be introduced.

4.7.2.1. The Behavior of W-F splices up to Slip

At the service level, two major behaviors were observed for w-f splices. The type of behavior was found to be dependent on the moment resistance of the flanges. In the following discussion of the splice behavior at the service level, the two major behaviors are called herein the case of adequate moment resistance of the flanges, and the case of inadequate moment resistance of the flanges. As the name indicates, the case of adequate flanges means that the flanges can resist the total applied service moment. The case of inadequate flanges means that the flanges can not resist the total applied service moment and therefore the additional moment must be resisted by the web.

4.7.2.1.1. Adequate moment slip resistance of the flanges:

Figure 4-21 depicts the slip behavior of a web-flange splice for the case of adequate moment resistance of the flanges. When the flanges can carry the total applied moment, the splice behaves in the following manner:

1. The girder and the splice plates deform elastically under the applied moment and shear with no relative displacement between them. At this time, the web carries its elastic portion of the total moment and the applied shear.
2. When the moment in the web plates exceeds the slip moment of the web bolts based on a total eccentricity $e = e_g + M_w / V$, the web plates move with respect to the web of the girder and therefore release a portion of their elastic deformation and forces. This portion of the released forces is a function of the number of the bolts, the spacing of the bolts, and the initial location of the bolts in their individual holes. However, the girder does not undergo any additional rotation nor deflection provided that the flanges neither yield nor slip due to the total applied moment. The flanges, if adequate, prevent the girder from undergoing any relative rotation. Even though the web had slipped due to moment and shear based on an eccentricity $e = e_g + M_w / V$, the web maintains its shear capacity based on an eccentricity $e = e_g$. Thus, the web splice prevents the girder from undergoing any relative vertical deformation, shear kink.
3. When the applied shear exceeds the slip shear capacity of the web bolts, based on the geometrical eccentricity, e_g , a major slip occurs. The girder undergoes a relative vertical deflection at the location of the splice. The web plates bend in double curvature and an inflection point is formed at the center line of the splice.

At this time, the web plates are subjected, at the center line of the splice, to shear only.

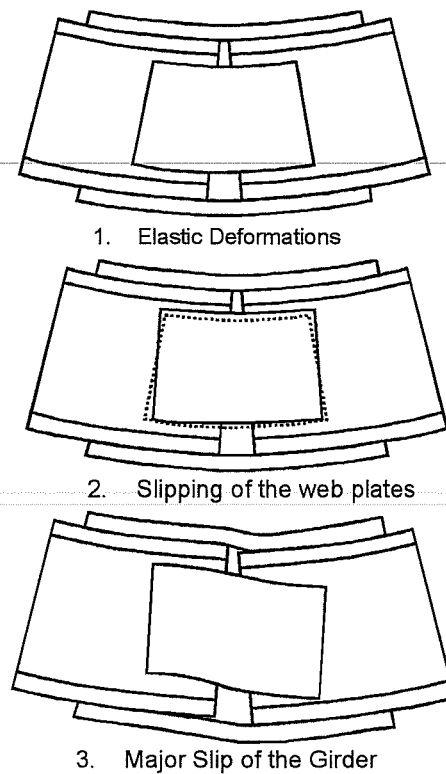


Figure 4-21. The slip behavior of a bolted splice with adequate slip moment resistance of the flanges

4.7.2.1.2. Inadequate moment slip resistance of the flanges:

Figure 4-21 depicts the slip behavior of a web-flange splice for the case of adequate moment resistance of the flanges. When the total applied moment is larger than the moment resistance of the flanges, the splice behaves in the following manner:

1. The girder and the splice plates deform elastically under the applied moment and shear with no relative displacement between them. At this time, the web carries its elastic portion of the total moment and the applied shear.
2. When the applied moment exceeds the summation of both the slip moment resistance of the web and flange plates, a major slip occurs; the girder undergoes a relative rotation at the location of the splice (flexural kink). At this time the web plates are subjected to their portion of the total moment and the total shear applied at the centerline of the splice. The flanges are subjected to the difference between the applied moment and the web moment.

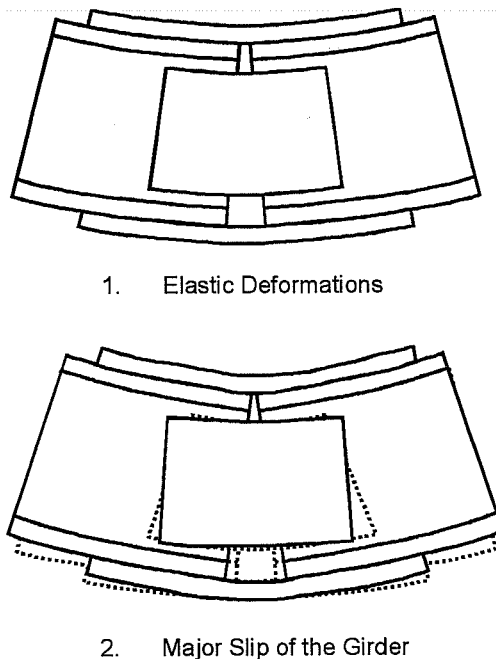


Figure 4-22. The slip behavior of a bolted splice with inadequate slip moment resistance of the flanges

4.7.2.2. The Behavior of W-F splices after Slip

In this section, the behavior of the general case of unsymmetric w-f splices is introduced. After a major slip occurs in the girder, three major behaviors were observed for unsymmetric w-f splices. The type of behavior was found to be dependent on the moment capacities of the flanges. In the following discussion of the splice behavior at the ultimate level, maximum load, the three major behaviors are called herein the case of adequate small flange, inadequate small flange and adequate big flange, and the case of inadequate flanges. As the name indicates, the case adequate small flange means that the small flange can resist the total applied moment. The case of inadequate small flange and adequate big flange means that the small flange can not resist the total applied moment and; therefore, the additional moment should be resisted by both the web and big flange. Finally, the case of inadequate flanges means that the both flanges can not resist the total applied moment and; therefore, the additional moment should be resisted by the web.

4.7.2.2.1. Adequate small flange:

For the case of adequate small flange, the girder forms a shear kink at failure. The web undergoes a double curvature and an inflection point is formed at the centerline of the splice. Thus, at failure, the web carries the total shear applied at an eccentricity calculated as the distance from the centerline of the splice to the center of gravity of the web bolts on one side of the joint. Also, the flanges if not fully yielded, carry not only the total moment but also a portion of the total shear due to the lateral stiffness of the flanges. This was visualized by seeing the formation of plastic hinges in the each flange at the location of the first bolt on each side of the joint. The shear carried by the flanges is a function of the applied

moment to the moment capacity of the flanges. The shear in the flanges will be derived in detail for symmetric girders using the plastic model. However, the flanges will carry zero shear if they yield axially at failure. Figure 4-23 and Figure 4-24 show the failed specimen and the failed web splice of a typical w-f splice with adequate small flange.

4.7.2.2.2. Inadequate small flange:

For the case of inadequate small flange and adequate big flange, the girder forms a combination of flexural and shear kink at failure. The web undergoes double curvature and an inflection point will be located at the centerline of the splice. Thus, due to the formation of the inflection point at the centerline of the splice, the web carries the total shear applied at an eccentricity calculated as the distance from the centerline of the splice to the center of gravity of the web bolts on one side of the joint. Also, due to the additional moment in excess of the small flange capacity, the web carries a horizontal force that is necessary to equilibrate the difference between the big and small flange axial loads. Figure 4-25, Figure 4-26, and Figure 4-27 show the failed specimen, the top flange, and the small flange of a typical w-f splice with inadequate small flange and adequate big flange.

4.7.2.2.3. Inadequate flanges:

For the case of inadequate flanges, the girder forms a flexural kink at failure. When the moment exceeds the big flange moment capacity, both flanges reached their axial yield load and can not provide any additional moment resistance. Thus, the web carries, in addition to the vertical shear and the horizontal force, the additional moment in excess of the flanges capacity. Figure 4-28, Figure 4-29, and

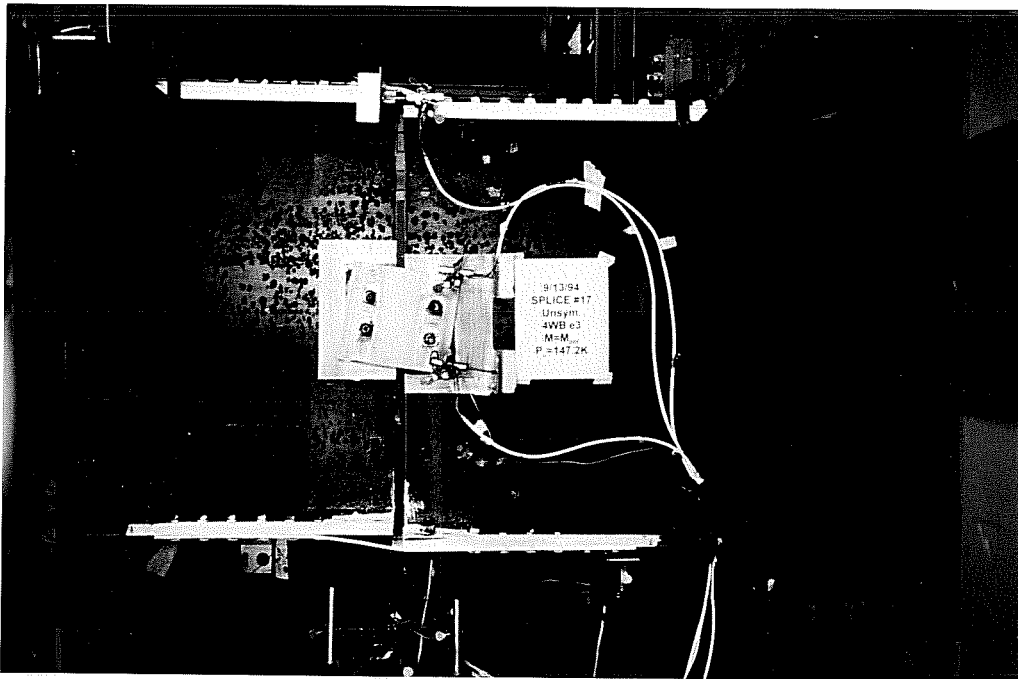


Figure 4-23 Typical failed unsymmetric w-f splice with adequate small flange

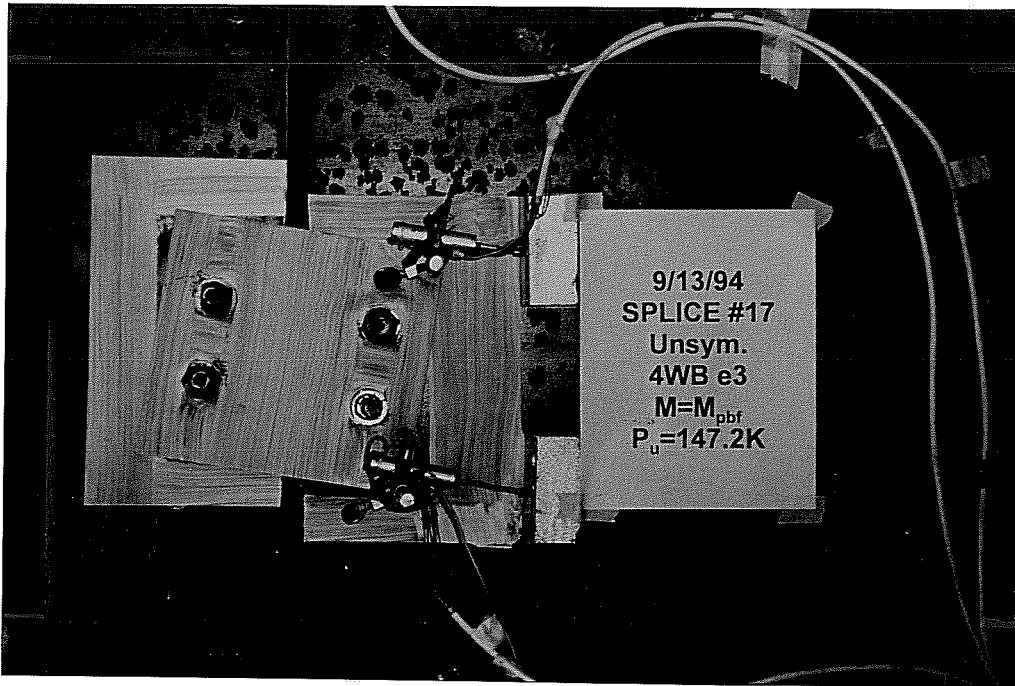


Figure 4-24 The failed web splice of a typical unsymmetric w-f splice with adequate small flange

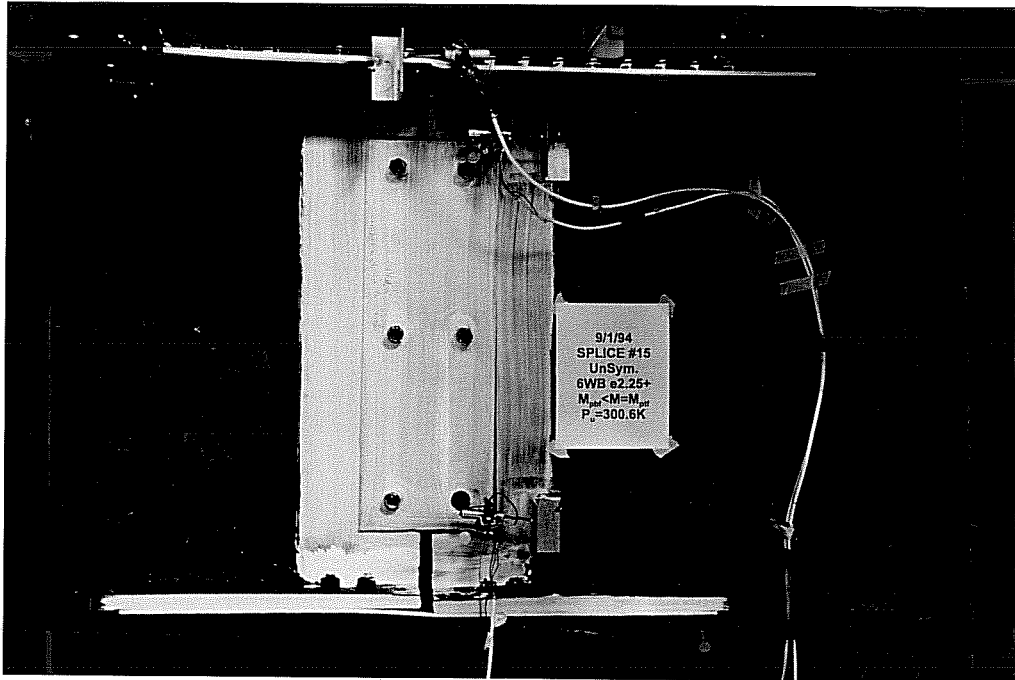


Figure 4-25 Typical failed unsymmetric w-f splice with inadequate small flange and adequate big flange

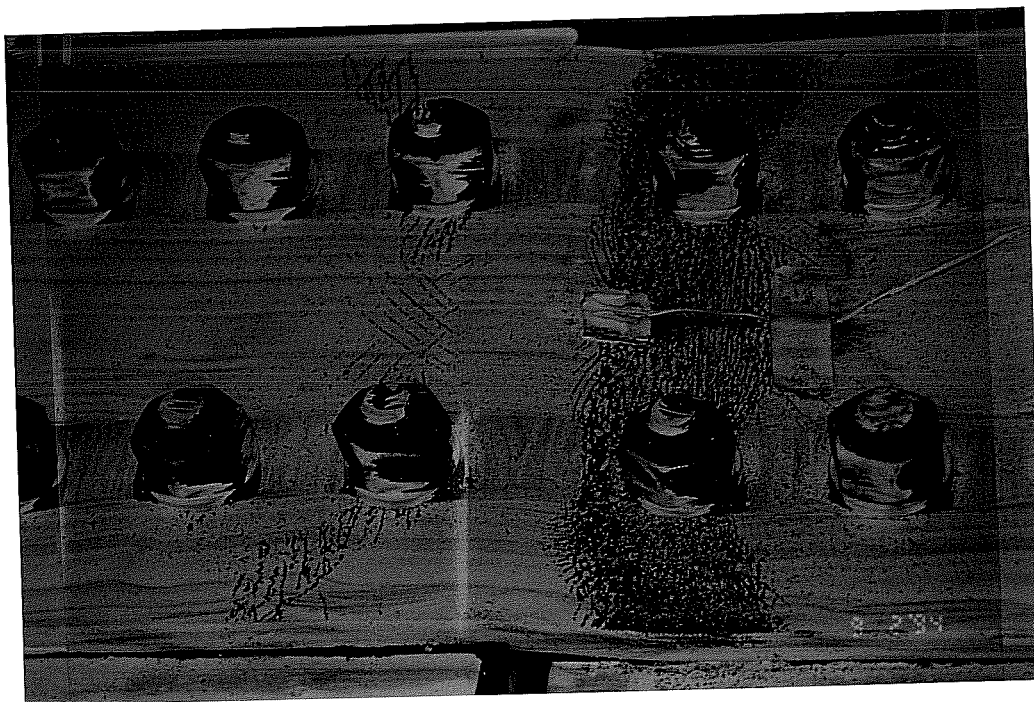


Figure 4-26 The big flange splice of a typical failed unsymmetric w-f splice with inadequate small flange and adequate big flange

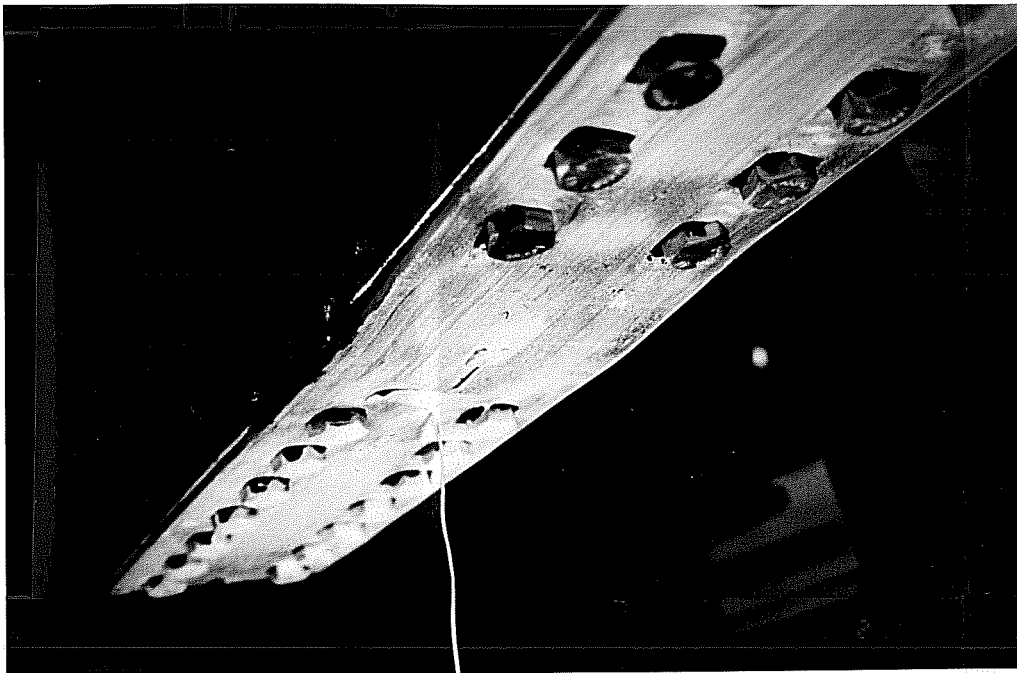


Figure 4-27 The small flange splice of a typical failed unsymmetric w-f splice with inadequate small flange and adequate big flange

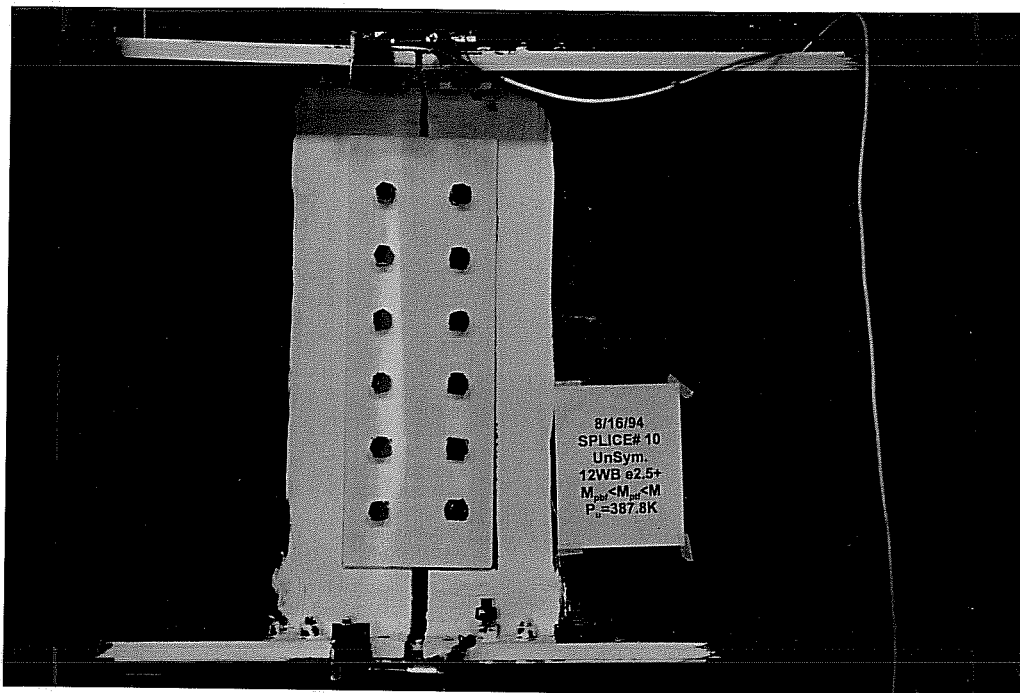


Figure 4-28 Typical failed unsymmetric w-f splice with inadequate flanges

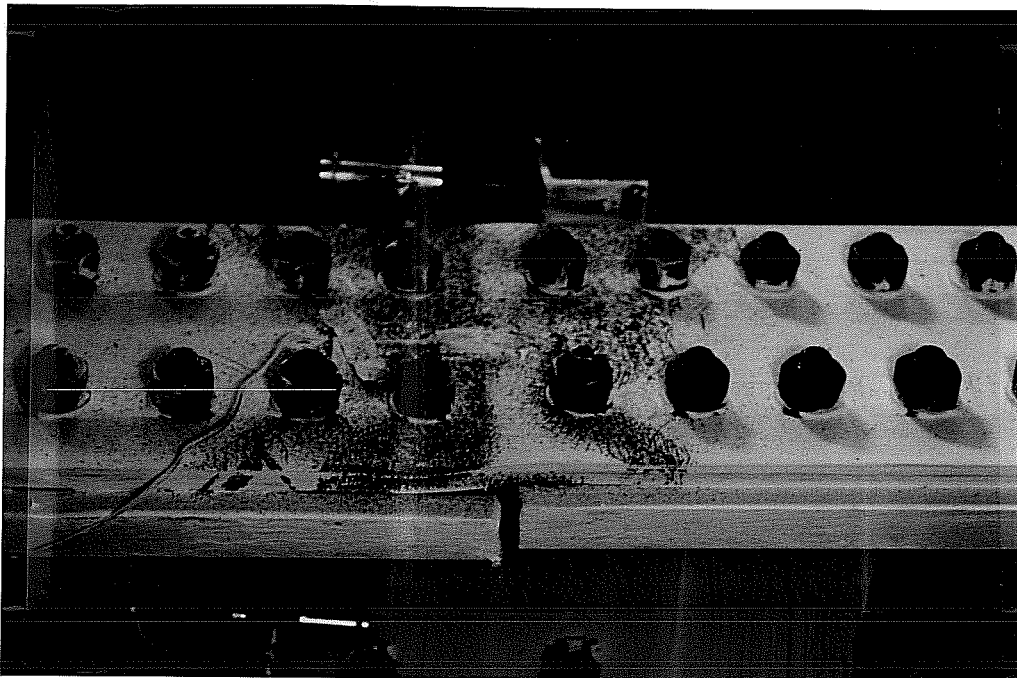


Figure 4-29 The big flange splice of a typical failed unsymmetric w-f splice with inadequate flanges

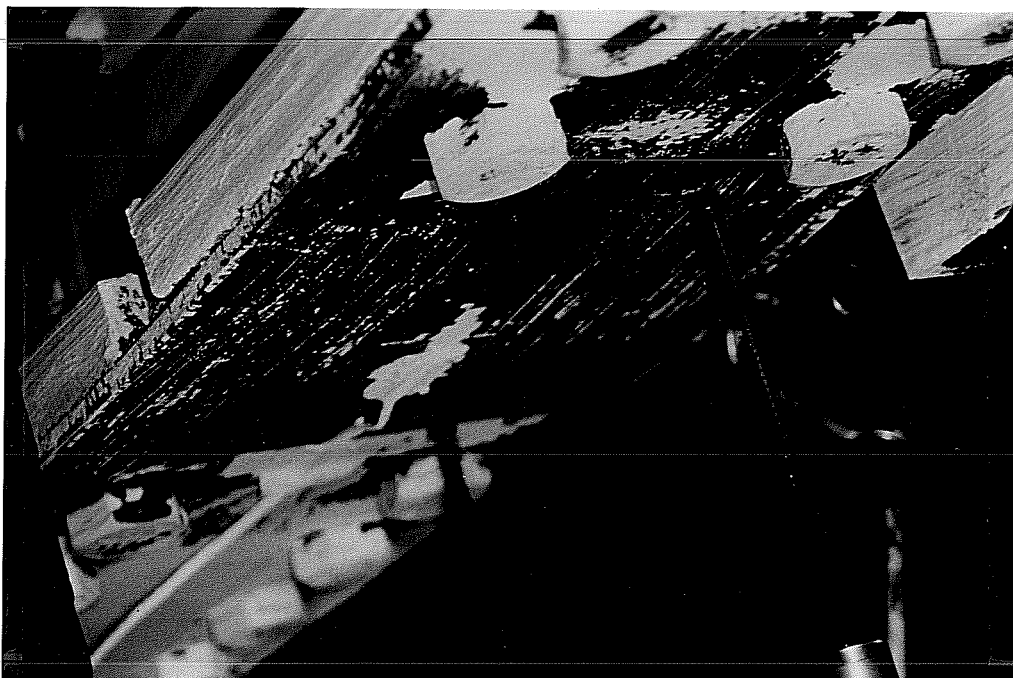


Figure 4-30 The small flange splice of a typical failed unsymmetric w-f splice with inadequate flanges

4.7.2.3. The effect of the shear in the flanges on the strength of w-f splices with adequate flanges

After performing the first test on w-f splices, it was noticed that the maximum applied shear exceeded the shear capacity of the web bolts (based on an eccentricity e_g) by 19%. Therefore, it was concluded that the flanges carried a portion of the total shear. However, the shear carried by the flanges needed to be predicted theoretically to validate the conclusion and to explain the behavior of the splice. Thus, the plastic model was developed.

4.7.2.3.1. The Plastic Model for predicting the flanges shear in symmetric w-f splices with adequate flanges, $M \leq M_f$

When the flanges are not fully yielded they provide shear stiffness to the splice. The contribution of the flanges shear to the total shear will be examined herein.

At maximum load, the splice plates of the web and the flanges should not be thought of as a continuous cross section since the plates had slipped. Therefore, elastic stress analysis for the cross section of the splice can not be used to determine the distribution of forces or stresses. Furthermore, the splice occupies a certain length of the beam and should not be thought of as a cross section at one point. Instead, it should be thought of as a structure of its own. This can be seen by looking at Figure 4-31 which shows the actual failure mechanism of the symmetric splice with adequate flanges.

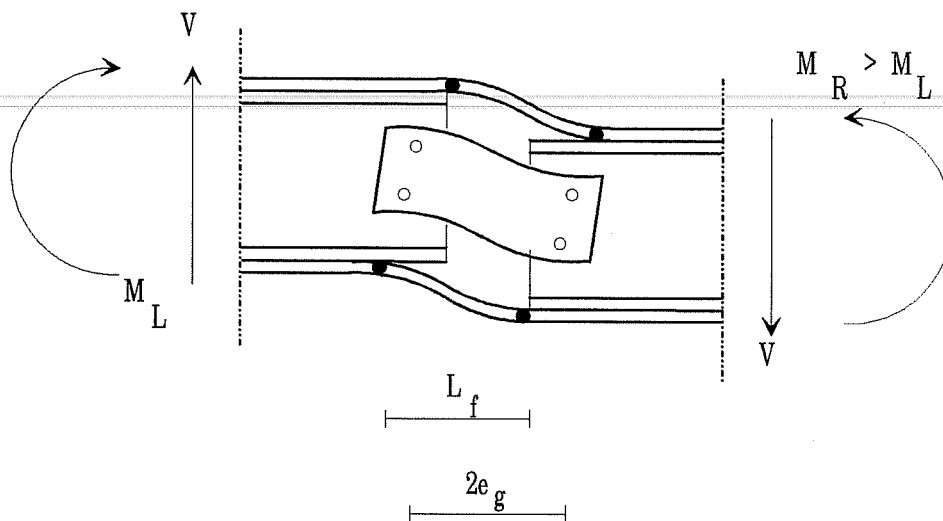


Figure 4-31 The failure mode for a w-f bolted splice with adequate flanges

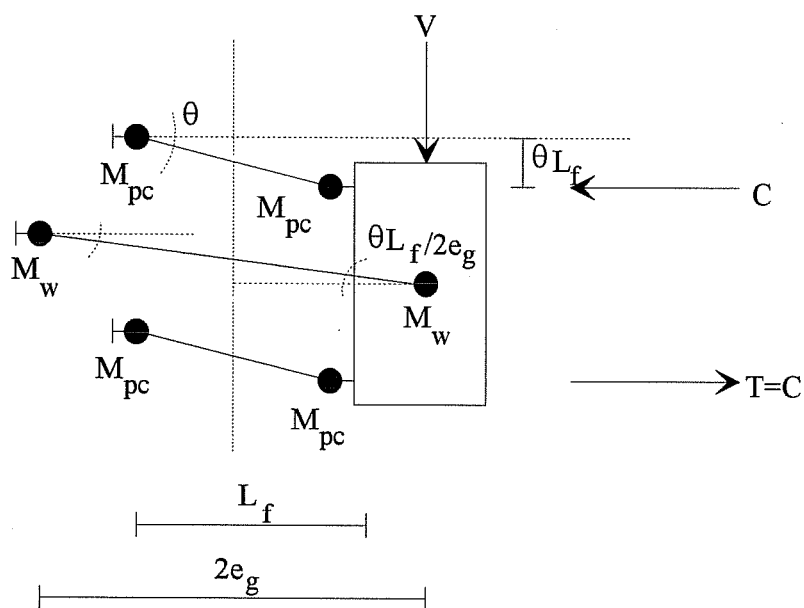


Figure 4-32 The plastic model for predicting the shear strength of w-f splices including the shear carried by the flanges with equal shear gaps

To determine the distribution of shear and moment between the flange and web plates, the plastic model is developed. The analytical plastic model is shown in Figure 4-32. The flange splices are depicted by the lines connecting M_{pc} and the web splice is depicted by the line connecting M_w .

The flanges act as beam columns that carry axial load, shear, and moment. The web plates act as a beam that carries both shear and moment. In this model, it is assumed that the flanges develop their modified plastic moment capacity in the presence of axial load. This axial load is simply the total applied moment divided by the depth of the beam plus the thickness of one flange. It is also assumed that both bolt groups on each side of the joint develop their eccentric shear capacity simultaneously. This means that an inflection point is present at the center line of the web splice and most importantly the eccentricity of the shear is constant and equal to one half the distance between the opposite bolt groups. This constant eccentricity is the geometrical eccentricity, e_g , which is the distance from the centerline of the splice to the centroid of the group of bolts at one side of the joint.

From virtual work principal, one can get:

$$L_f V = 4M_{pc} + \frac{2M_w L_f}{2e_g} \quad (4-1)$$

By rearranging equation (4-1):

$$V = \frac{4M_{pc}}{L_f} + \frac{2M_w}{2e_g} \quad (4-2)$$

Equation (4-2) can be rewritten as:

$$V = V_f + V_w \quad (4-3)$$

Equation (4-3) shows that the total shear carried by a w-f splice with adequate flanges is distributed between the flange and web plates.

Since Equation (4-3) is general, a more detailed relation between the total shear and the flanges and web plates shear will be developed herein.

Figure 4-33 shows the idealized stress distribution in both the bottom and top flange plates due to both axial load and bending moment of the flanges.

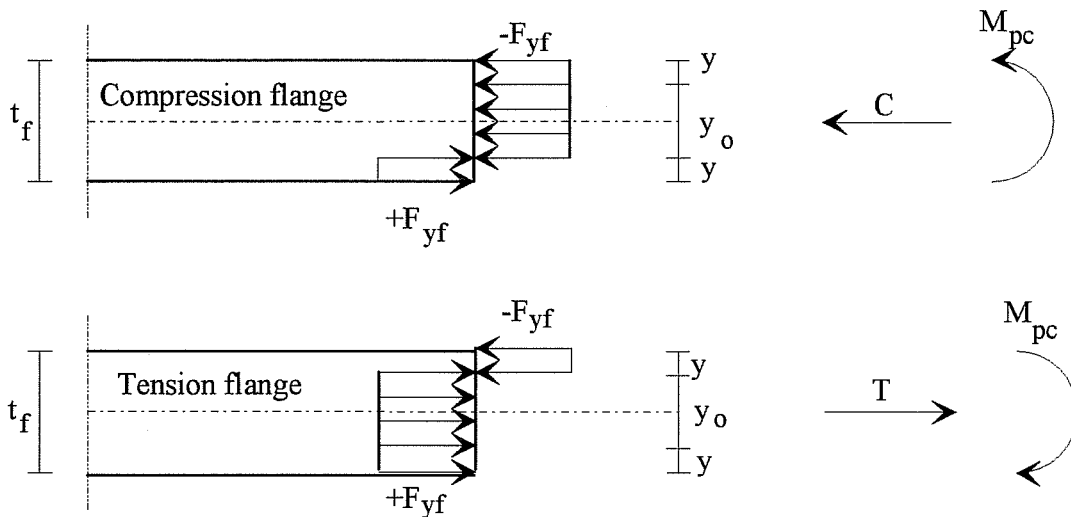


Figure 4-33 The idealized stress distribution in both the small and big flange plates due to both axial load and bending moment if the flanges

From the horizontal equilibrium of forces in both flanges, one gets:

$$y_o = \frac{C}{F_{yf} b_f} + \frac{T}{F_{yf} b_f} \quad (4-4)$$

However;

$$y = \frac{t_f - y_o}{2} \quad (4-5)$$

Therefore;

$$M_{pc} = F_{yf} b_f y (t_f - y) \quad (4-6)$$

Let us assume that the ratio of axial load in the flanges to the total shear is constant and equal to α , thus;

$$\alpha = \frac{C}{V} \quad (4-7)$$

Substitute Equations (4-4), (4-5), and (4-7) into Equation (4-6):

$$M_{pc} = F_{yf} b_f \left(\frac{t_f}{2} - \frac{\alpha V}{2F_{yf} b_f} \right) \left(t_f - \frac{t_f}{2} + \frac{\alpha V}{2F_{yf} b_f} \right) \quad (4-8)$$

Rearrange Equation (4-8);

$$M_{pc} = \frac{F_{yf} b_f}{4} \left[t_f^2 - \left(\frac{\alpha V}{F_{yf} b_f} \right)^2 \right] \quad (4-9)$$

Thus;

$$M_{pc} = \left(\frac{b_f t_f^2}{4} \right) F_{yf} - \frac{\alpha^2 V^2}{4 F_{yf} b_f} \quad (4-10)$$

Equation (4-10) can be rewritten as:

$$V = \frac{b_f t_f^2 F_{yf}}{L_f} - \frac{\alpha^2 V^2}{F_{yf} b_f L_f} + \frac{2M_w}{2e_g} \quad (4-11)$$

Substitute Equation (4-7) into Equation (4-11):

$$V = \frac{b_f t_f^2 F_{yf}}{L_f} - \frac{\left(\frac{M}{Vh} \right)^2 V^2}{F_{yf} b_f L_f} + \frac{V_w e_g}{e_g} \quad (4-12)$$

Define M_f as;

$$M_f = \left[(b_f t_f) F_{yf} \right] h \quad (4-13)$$

Define \overline{M}_f as;

$$\overline{M}_f = \left(\frac{b_f t_f^2}{4} \right) F_{yf} \quad (4-14)$$

Thus, Equation (4-14) can be rewritten as:

$$V = \frac{4\overline{M}_f}{L_f} \left[1 - \left(\frac{M}{\overline{M}_f} \right)^2 \right] + V_w \quad (4-15)$$

Equation (4-15) represents the moment-shear interaction for the w-f splice with adequate flanges. Equation (4-15) shows that the total shear is distributed between the flange plates and the web plates. The portion of the shear carried by the flanges ranges from zero if the flanges are fully yielded due to axial load up to a maximum value that can be calculated from equation (4-15) when the total applied moment at the center line of the splice is equal to zero. This maximum value corresponds to the case of a splice located at the inflection point since the axial force in the flange would be zero.

However, if M is known and is a function of V , then Equation (4-11) can be rewritten as:

$$\left(\frac{\alpha^2}{b_f F_{yf} L_f} \right) V^2 + V - \left(\frac{b_f t_f^2 F_{yf}}{L_f} + \frac{2M_w}{2e_g} \right) = 0 \quad (4-16)$$

Equation (4-16) is a second order equation of V that has a feasible solution as follows:

$$V = \frac{b_f F_{yf} L_f}{2\alpha^2} \left[-1 + \sqrt{1 + \left(\frac{4\alpha^2}{b_f F_{yf} L_f} \right) \left(\frac{b_f t_f^2 F_{yf}}{L_f} + V_w \right)} \right] \quad (4-17)$$

Where:

$$V_w = CR$$

C is the effective number of web bolts to carry the vertical shear based on the geometrical eccentricity only

R is the capacity of one web bolt

Equation (4-17) provides a direct solution for the total shear capacity of bolted web-flange splices. The limit on this equation is (adequate flanges):

$$\alpha \leq \frac{M_f}{Vh} \quad (4-18)$$

In the case of unequal length of the flanges as shown in Figure 4-34, it can be shown that the total shear capacity of the bolted web-flange splice becomes:

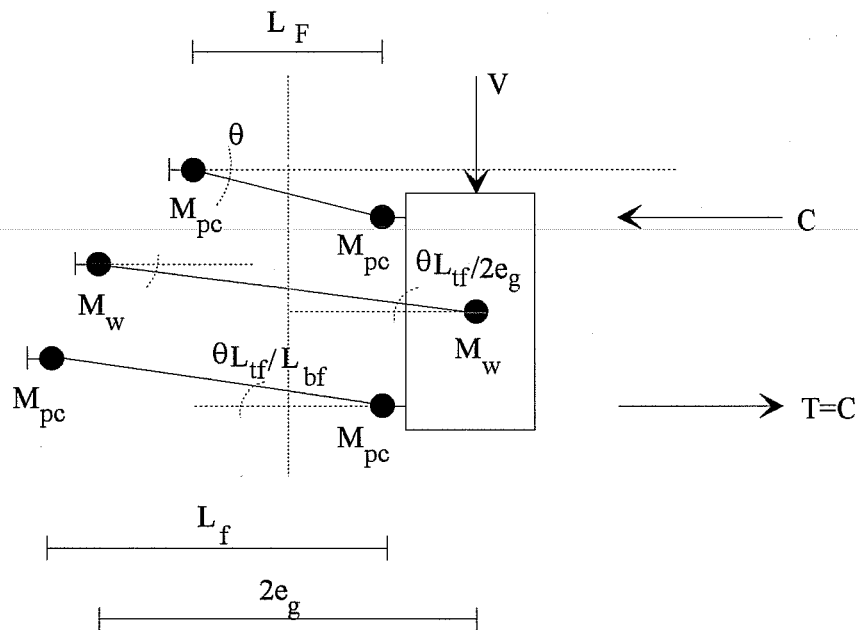


Figure 4-34 The plastic model for predicting the shear strength of w-f splices including the shear carried by the flanges with unequal shear gaps

$$V = \frac{\left[-1 + \sqrt{1 + \left(\frac{2\alpha^2}{b_f F_{yf}} \right) \left(\frac{1}{L_f} + \frac{1}{L_F} \right) \left[\frac{b_f t_f^2 F_{yf}}{2} \left(\frac{1}{L_f} + \frac{1}{L_F} \right) + V_w \right]} \right]}{\frac{\alpha^2}{b_f F_{yf}} \left(\frac{1}{L_f} + \frac{1}{L_F} \right)} \quad (4-19)$$

4.7.2.3.2. Comparison between the Plastic Model for predicting the flanges shear and test results

To validate the effect of the shear in the flanges on the strength of the connection, the capacity of splices 1 through 4 was calculated using the plastic model. In these splices, the axial load in the flanges ranged from 43% (for

specimen 3) to 91% (for specimen 4) of the axial yield load. It was found that the shear carried by the flanges ranged from 51% (for splice 3) to 5% (for splice 4). The plastic model prediction agreed well with test results. The average error of the plastic model prediction was +2.9%. Figure 4-39 through Figure 4-42 show the results of the plastic model plotted on the actual load-deflection response of splices 1, 2, 3, and 4.

Table 4-16 The theoretical plastic model versus test results for the 24 in. beam splices

SPLICE #	1	2	3	4
Flanges	Bolted	Welded	Welded	Welded
L_F "	3	3	4	3
L_f "	6	3	3	3
$2V_w$ Kips	116.5	116.5	46.4	184.7
$2V_f$ Kips	27.3	33.5	48.3	9.7
V_w/V	0.81	0.78	0.49	0.95
M/M_f	0.68	0.72	0.43	0.91
$P_{P.M.}$ Kips	143.8	150	94.7	194.4
P_{test} Kips	142	142 ⁺	90	190
Error %	1.3	-	5.2	2.3

⁺ Specimen 2 was not loaded to failure by fracturing of the critical web bolt.

Therefore, the flanges of w-f splices, if not fully yielded, carry a portion of the total shear. This shear is a function of the ratio of the applied moment to the moment capacity of the flanges. Equations (4-15) and (4-17) show that the shear carried by the flanges is a function of:

1. Gap clearance in the girder. The shear in the flanges decreases as the gap increases
2. Edge distance of the flange fasteners. The shear in the flanges decreases as the edge distance of the flange fasteners increases
3. Level of flange axial force required for moment; axial force / $(A_f F_{yf})$.
The shear in the flanges decreases as the Level of flange axial force increases

Nevertheless, assuming that the applied shear is resisted by the web of w-f splices with adequate flanges should yield conservative results.

4.7.2.4. The theoretical distribution of forces for unsymmetric w-f splices at the service level (Slip)

4.7.2.4.1. Adequate slip moment resistance of the flanges:

Since the flanges are adequate to carry all the moment, the web will only carry the following forces at the *center line of the splice*

$$M_w = 0 \quad (4-20)$$

$$e = e_g \quad (4-21)$$

$$V_w = V \quad (4-22)$$

4.7.2.4.2. Inadequate slip moment resistance of the flanges:

For the case of inadequate flanges, the moment in excess of the flanges capacity should be carried by the web. The forces on the web can be obtained from

the elastic flexural theory since the plates did not slip and form a continuation of the beam. At the center line of the splice:

$$\sigma = \frac{My}{I} \quad (4-23)$$

$$H = t_w \int_{d_w} \sigma dy \quad (4-24)$$

$$H = \frac{t_w d_w}{2} (\sigma_{tw} + \sigma_{bw}) = A_w \frac{(\sigma_{tw} + \sigma_{bw})}{2} \quad (4-25)$$

$$M_w = t_w \int_{d_w} \sigma \bar{y} dy \quad (4-26)$$

If the centroid of the web bolts coincides with the centroidal axis of the web/web splice, then M_w can be calculated as follows:

$$M_w = \frac{t_w d_w}{2} \left[(\sigma_{tw} + \sigma_{bw}) \left(\frac{d_w}{2} - \frac{d_w}{3} \right) \right] \quad (4-27)$$

or:

$$M_w = \frac{t_w d_w^2}{12} (\sigma_{tw} + \sigma_{bw}) = \frac{I_w}{d_w} (\sigma_{tw} + \sigma_{bw}) \quad (4-28)$$

$$e = e_g + M_w / V \quad (4-29)$$

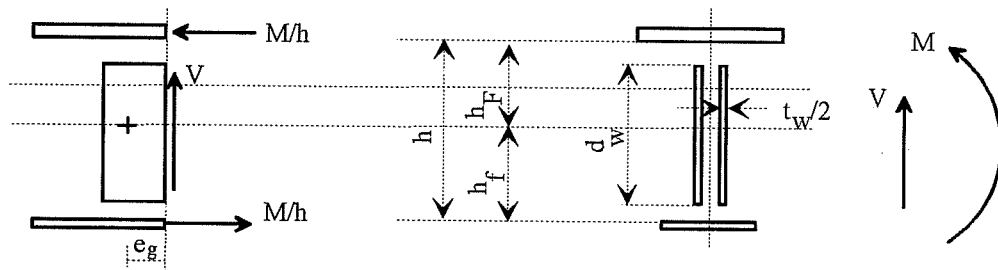
$$V_w = V \quad (4-30)$$

$$M_f = M - M_w \quad (4-31)$$

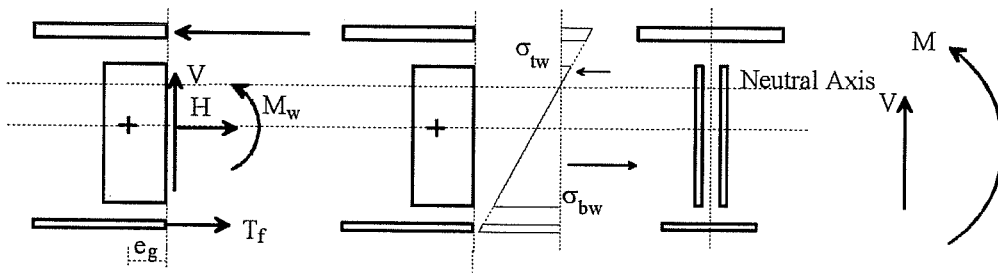
Where:

- A_w is the area of the web/web splice = $t_w d_w$
- C is the effective number of bolts to resist the shear; $C=V/R$. When determining the *slip capacity of the bolts, elastic analysis* must be performed.
- d_w is the depth of the web/web splice
- e is the total design eccentricity of the web bolts
- e_g is the geometrical eccentricity of the web bolts; half the distance between the opposite bolt groups across the centerline of the splice
- H is the horizontal design load of the web splice required for horizontal equilibrium
- I is the moment of inertia of either the girder or the splice plates, whichever is smaller
- I_w is the moment of inertia of the web/web splice about its centroidal axis = $t_w d_w^3/12$
- M is the total design moment at the center line of the splice
- M_f is the design moment of the flanges
- M_w is the design moment of the web
- R_s is the slip load of an individual bolt
- s is the bending stress in the web/web splice fiber under consideration to the neutral axis
- σ_{tw} is the bending stress in the top fiber of the web/web splice

- σ_{bw} is the bending stress in the bottom fiber of the web/web splice
- t_w is the thickness of the web/web splice
- V is the total vertical design shear at the center line of the splice
- V_w is the vertical design shear for the web
- y is the distance of the web/web splice fiber under consideration to the neutral axis
- \bar{y} is the distance of the web/web splice fiber under consideration to the centroid of the web bolts



1. The moment slip resistance of the small flange > M



2. The moment slip resistance of the small flange < M

Figure 4-35. The slip design forces for an unsymmetric bolted splice

4.7.2.5. The theoretical distribution of forces for unsymmetric w-f splices at the ultimate level (maximum load)

For all the following cases, a direct *elastic analysis of the bolts* can be performed.

4.7.2.5.1. Adequate small flange, $M < M_f$

Since the flanges are adequate to carry all the moment, the web can be designed to carry only the applied shear at the center line of the splice. The axial load in the flanges can be calculated as the forces required to resist the applied moment. Thus, the distribution of forces at the center line of the splice can be calculated as follows:

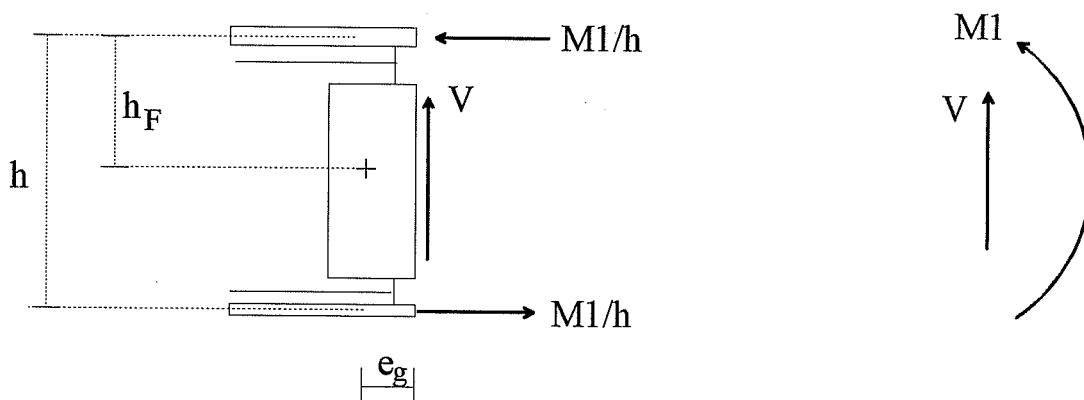


Figure 4-36 The force distribution between the web and flange splices for the case of adequate flanges

$$V_w = V \quad (4-32)$$

$$M_w = 0 \quad (4-33)$$

$$M_f = A_f F_{yf} h \geq M/h \quad (4-34)$$

Where:

M_f is the moment resistance of the small flange as defined in Equation (4-34)

A_f is the area of the small flange

F_{yf} is the yield stress of the small flange

h is the depth of the beam plus half the thickness of each of the big and small flanges

4.7.2.5.2. Adequate big flange and inadequate small flange, $M_f < M < M_F$

When the small flange yields due to the flange forces required to resist the applied moment, the web and the adequate big flange will provide the forces required to resist the moment in excess of the small flange capacity. Therefore, in addition to the shear carried by the web, the web has to carry the addition horizontal force.

Thus, the distribution of forces at the center line of the splice can be calculated as follows:

$$V_w = V \quad (4-35)$$

$$H_w = [M - (A_f F_{yf})h] / h_F \leq A_F F_{yF} - A_f F_{yf} \quad (4-36)$$

$$M_w = 0 \quad (4-37)$$

$$M_F = A_F F_{yF} h \geq M_f + H_w h_F \quad (4-38)$$

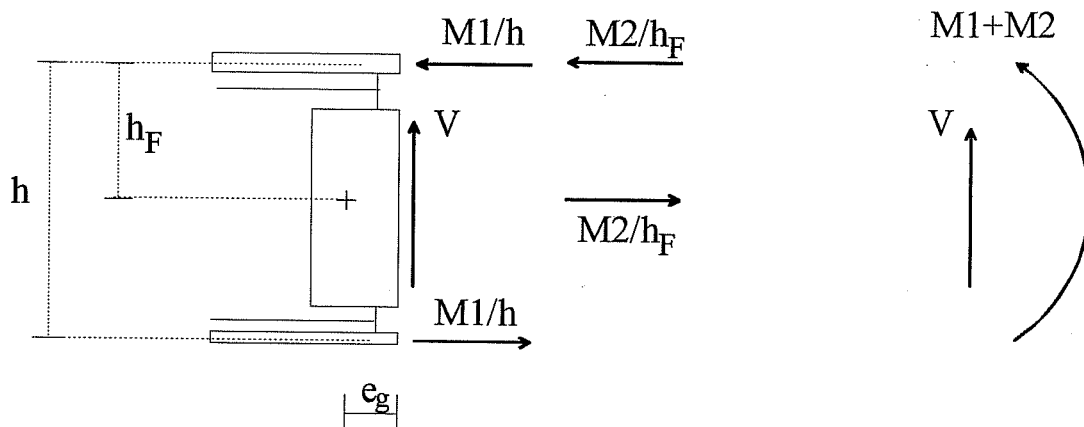


Figure 4-37 The force distribution between the web and flange splices for the case of inadequate small flange and adequate big flange

Where:

- M_F is the plastic moment of the big flange as defined in the previous equation
- H_w is the horizontal shear resisted by the web; the difference between the axial yield load of the big flange and the axial yield load of the small flange
- A_F is the area of the big flange
- F_{yF} is the yield stress of the big flange
- h_F is the vertical distance between the midthickness of the big flange plate and the center of gravity of the bolts
- h_f is the vertical distance between the midthickness of the small flange plate and the center of gravity of the bolts

4.7.2.5.3. Inadequate flanges, $M > M_F$

After yielding of both the flanges, the web needs to carry the moment in excess of the big flange capacity in addition to the shear and horizontal force which equals to the difference in the flanges axial yield loads. Thus, the distribution of forces at the *center line* of the splice can be calculated as follows:

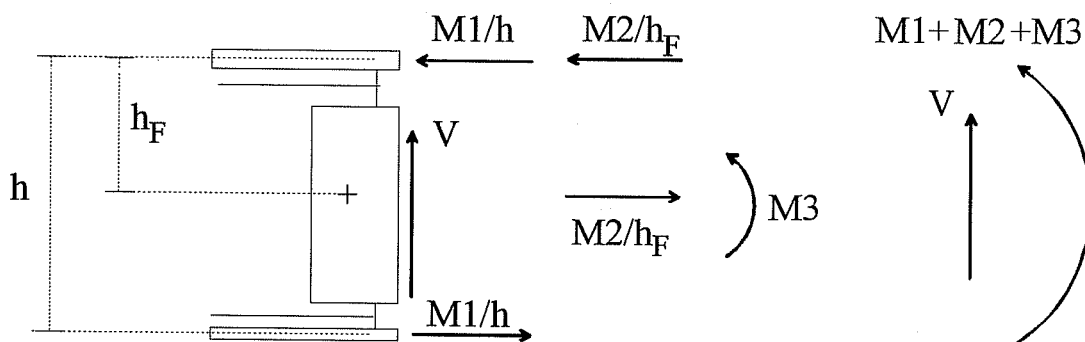


Figure 4-38 The force distribution between the web and flange splices for the case of inadequate flanges

$$V_w = V \quad (4-39)$$

$$H_w = A_F F_{yF} - A_f F_{yf} \quad (4-40)$$

$$M_w = M - M_F \quad (4-41)$$

4.7.2.6. Comparison between the theoretical and experimental loads at both the service (slip) and the ultimate level (maximum load)

From the tests of web splices at the service level, it was established that the slip load should be based on elastic, and not on plastic, analysis of the bolts. Therefore, elastic analysis was used for the prediction of the slip load. Table 4-17 and Table 4-18 show the theoretical slip loads for symmetric and unsymmetric web-flange splices, respectively. The experimental slip load is defined herein as the end of the linear elastic region of the load deformation response of the splice. However, the end of the linear region can not be easily determined. Therefore, the theoretical slip load was plotted on the load deformation response of the splice for the purpose of evaluating the analysis. Figure 4-44 through Figure 4-52 show the theoretical web and girder slip loads plotted on the load-deflection response of the specimens tested for slip.

At maximum load, the theoretical maximum loads were calculated twice. First, the elastic analysis of the web bolts was used. Then, the nonlinear analysis of the web bolts using the measured nonlinear response of the web bolts was used. The nonlinear analysis was used to validate the theoretical distribution of the forces between the flanges and the web splices. Then, the elastic analysis was used to examine its adequacy in evaluating the maximum load of the splice.

Table 4-19 and Table 4-20 show the results of the theoretical maximum loads and the theoretical error associated with both the nonlinear and elastic analyses. Figure 4-39 through Figure 4-53 show the theoretical maximum load plotted on the measured load-deflection response of all the w-f splices tested.

For specimens 1 through 4, the plastic model for predicting the shear capacity of the w-f splice that takes into account the shear carried by the flanges was used. Figure 4-39 through Figure 4-42 show the predicted plastic model maximum load plotted on the measured load-deflection response of the splice.

Table 4-17 Test Results of Symmetric W-F Splices at Service Load

Splice	$P_{\text{slip web}}$ kips	P_{service} kips	At slip, the applied forces exceeded
16 _{AF}	45.9	84.89	Slip shear resistance of web splice
18 _{AF}	79.5	116.4	Slip shear resistance of web splice
20 _{AF}	102.0	178.1	Slip shear resistance of web splice

Table 4-18 Test Results of Unsymmetric W-F Splices at Service Load

Splice	$P_{\text{slip web}}$ kips	P_{service} kips	At slip, the applied forces exceeded
7 _{IF}	104.7	104.7	Slip moment resistance of web splice
8 _{IF}	28.4	28.4	Slip moment resistance of web splice
9 _{IF}	59.1	139.1	yielding of bottom flange
10 _{IF}	57.8	137.6	yielding of bottom flange
15 _{AF}	41.1	123.8	Slip shear resistance of web splice
17 _{AF}	25.2	37.38	Slip shear resistance of web splice

Table 4-19 Test Results of Symmetric W-F Girder Splices at Maximum Load

Splice	P_u Test kips	P_u Elastic kips	Error Elastic %	P_u Nonlinear kips	Error Nonlinear %	Failure Mode
1 _{AF}	142	145.80	0.1	-	-	Fracture of top critical web bolt
2 _{AF}	142+	145.80	-	-	-	Did not continue loading to failure
3 _{AF}	90	96.10	5.8	-	-	Fracture of top critical web bolt and the top weld
4 _{AF}	190	198.00	2.4	-	-	Fracture of top critical web bolt
5 _{IF}	124	120.10	-6.0	-	-	Fracture of top critical web bolt and the top weld
16 _{AF}	313.6	288.68	-7.9	288.68	-7.9	Fracture of two critical web bolts
18 _{IF}	325	307.71	-5.3	310.75	-4.4	Buckling of the splice plates ($M=1.02M_p$ & $V=1.05V_p$)
20 _{IF}	457	448.8	-1.8	465.8	1.9	Buckling of the splice plates ($M=1.11M_p$ & $V=1.10V_p$)
Avg.	-	-	+2.8 -5.3	-	+1.9 -6.2	

Where:

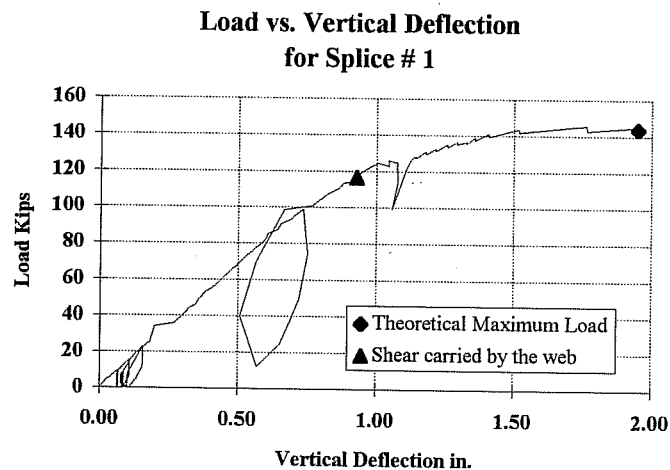
AF Means adequate flanges

IF Means inadequate flanges

In Table 4-17 and Table 4-18, the slip moment resistance of the web is the resistance that corresponds to an eccentricity $e = e_g + M_w/V$. On the other hand, the slip shear resistance of the web is the resistance that corresponds to an eccentricity $e = e_g$.

Table 4-20 Test Results of Unsymmetric W-F Girder Splices at Maximum Load

Splice	P_u Test kips	P_u Elastic kips	Error Elastic %	P_u Nonlinear kips	Error Nonlinear %	Failure Mode
7 _{AF}	411.2	347.2	-15.6	427.9	4.1	Lateral torsional buckling of the girder
8 _{AF}	208.1	199.7	-3.7	217.2	4.7	Fracture of bottom critical web bolt
9 _{IF}	380.2	294.6	-22.5	329.6	-13.3	Fracture of bottom four web bolt and of the bottom flange at the net section
10 _{IF}	387.8	293.3	-24.3	328.3	-15.3	Fracture of bottom critical web bolt
15 _{AF}	300.6	249.6	-16.7	269.0	-10.2	Fracture of bottom critical web bolt
17 _{AF}	147.2	130.5	-11.3	130.5	-11.3	Fracture of bottom critical web bolt
19 _{IF}	340.3	279.1	-18.0	308.8	-9.2	Fracture of bottom critical web bolt
Avg.	-	-	-16	-	+4.4 -11.9	

**Figure 4-39 The load versus vertical deflection (channel 2) at the splice for splice 1 (symmetric adequate flanges)**

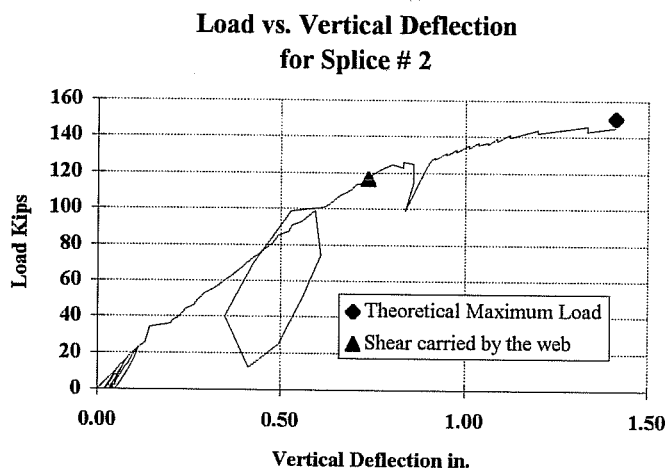


Figure 4-40 The load versus vertical deflection (channel 2) at the splice for splice 2 (symmetric adequate flanges)

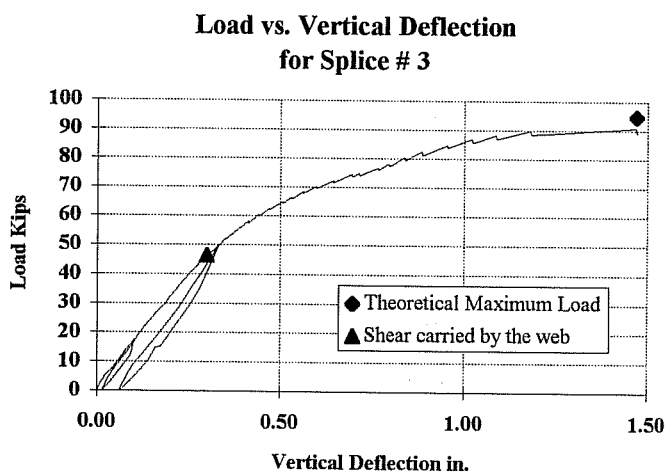


Figure 4-41 The load versus vertical deflection (channel 2) at the splice for splice 3 (symmetric adequate flanges)

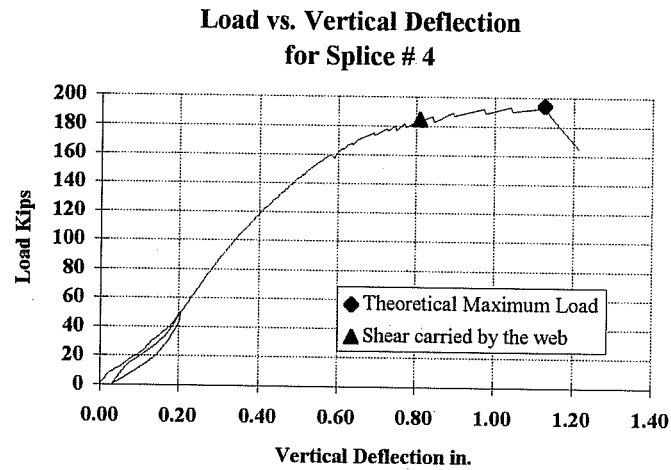


Figure 4-42 The load versus vertical deflection (channel 2) at the splice for splice 4 (symmetric adequate flanges)

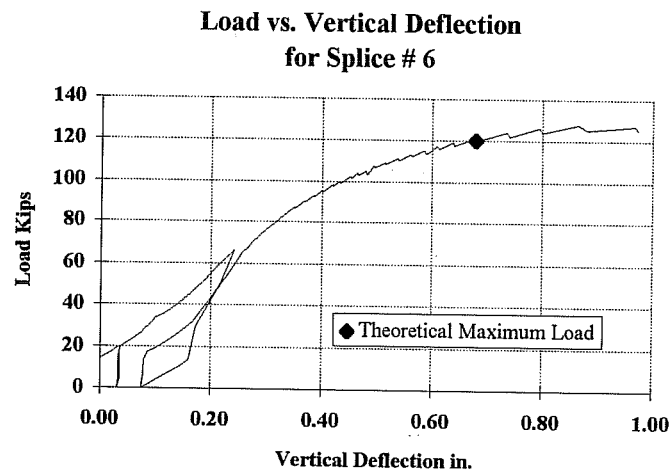


Figure 4-43 The load versus vertical deflection (channel 2) at the splice for splice 6 (symmetric inadequate flanges)

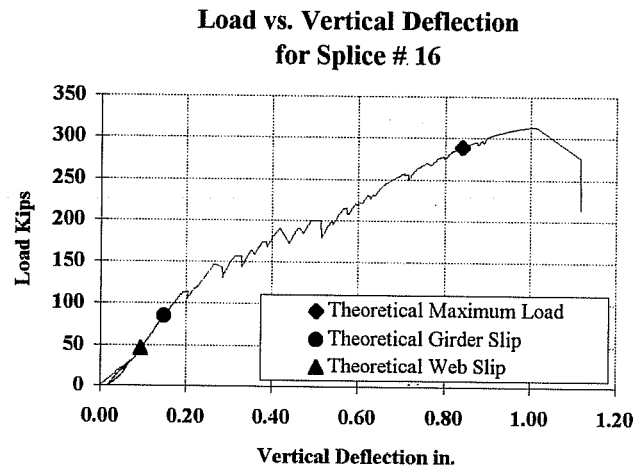


Figure 4-44 The load versus vertical deflection (channel 2) at the splice for splice 16 (symmetric adequate flanges)

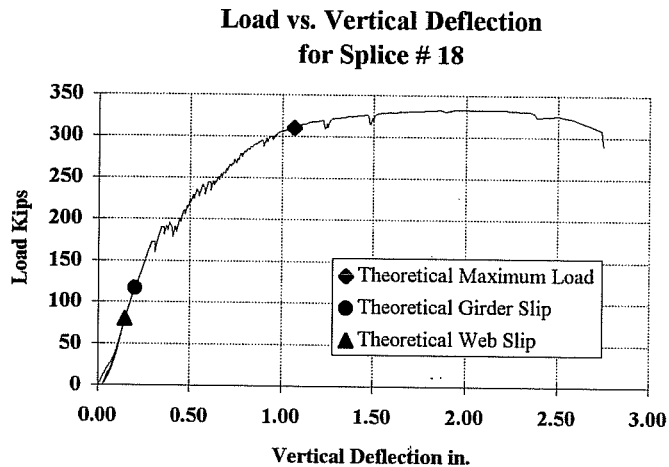


Figure 4-45 The load versus vertical deflection (channel 2) at the splice for splice 18 (symmetric adequate flanges at service load & inadequate flanges at maximum load; $M=M_p$, $V=V_p$)

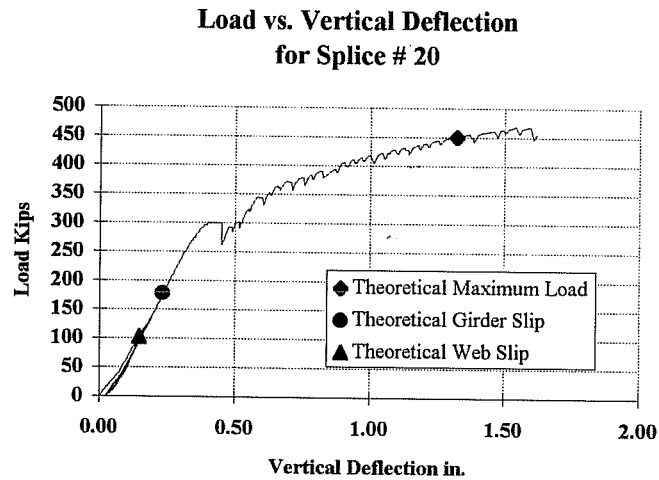


Figure 4-46 The load versus vertical deflection (channel 2) at the splice for splice 18 (symmetric adequate flanges at service load & inadequate flanges at maximum load; $M=M_p$, $V=V_p$)

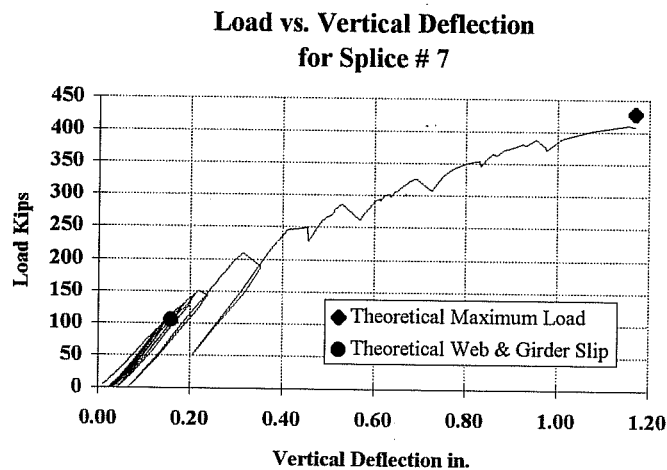


Figure 4-47 The load versus vertical deflection (channel 2) at the splice for splice 7 (unsymmetric inadequate small flange)

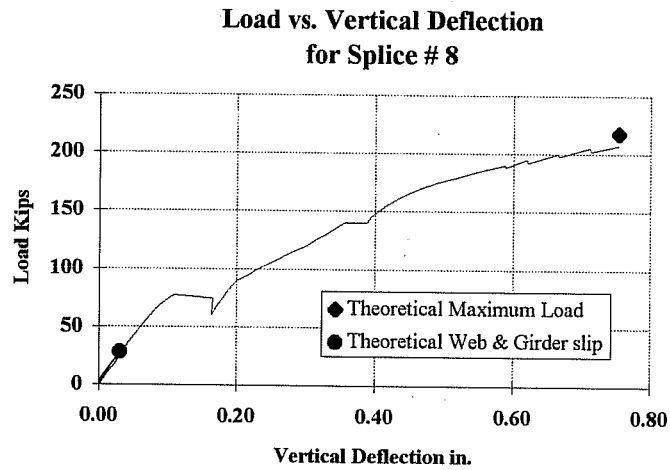


Figure 4-48 The load versus vertical deflection (channel 2) at the splice for splice 8 (unsymmetric inadequate small flange)

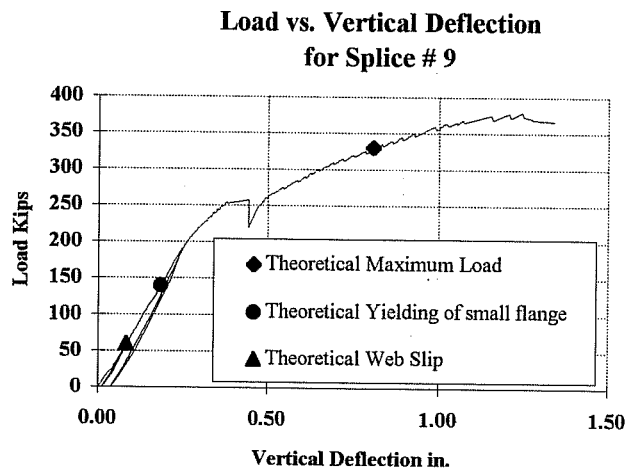


Figure 4-49 The load versus vertical deflection (channel 2) at the splice for splice 9 (unsymmetric inadequate flanges)

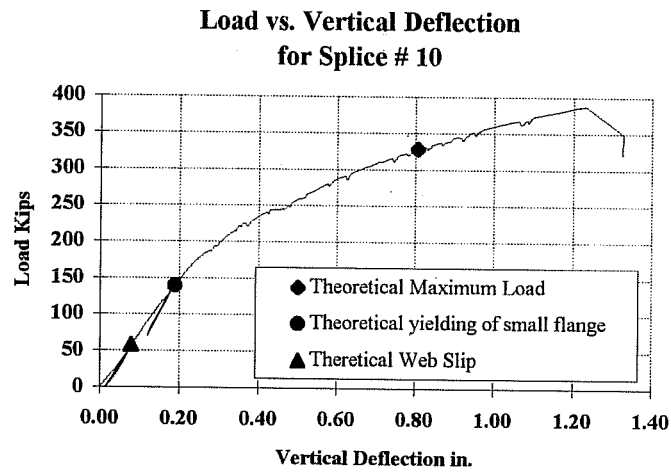


Figure 4-50 The load versus vertical deflection (channel 2) at the splice for splice 10 (unsymmetric inadequate flanges)

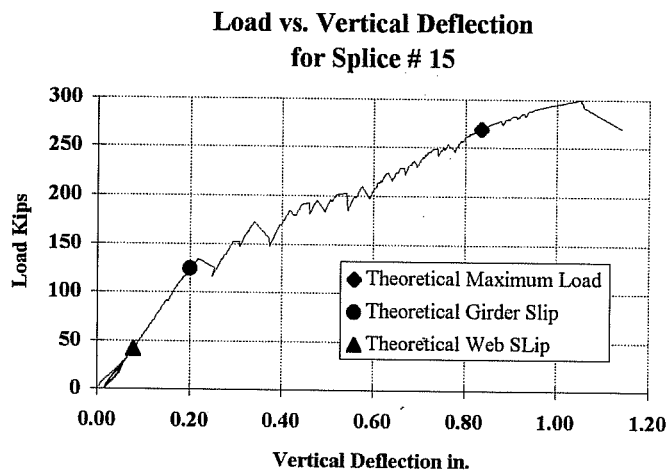


Figure 4-51 The load versus vertical deflection (channel 2) at the splice for splice 15 (unsymmetric adequate flanges at service load & inadequate small flange at maximum load)

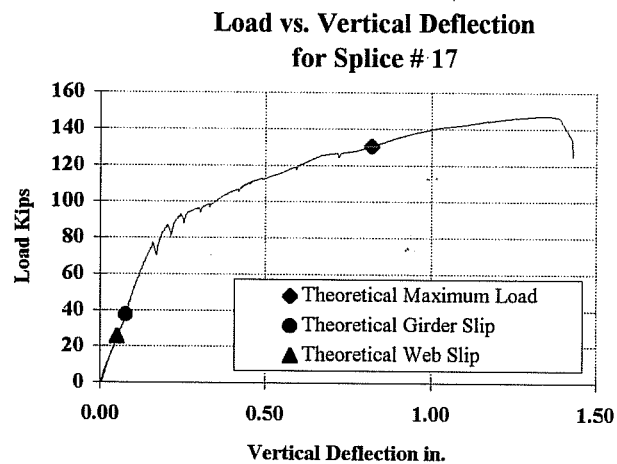


Figure 4-52 The load versus vertical deflection (channel 2) at the splice for splice 17 (unsymmetric adequate flanges)

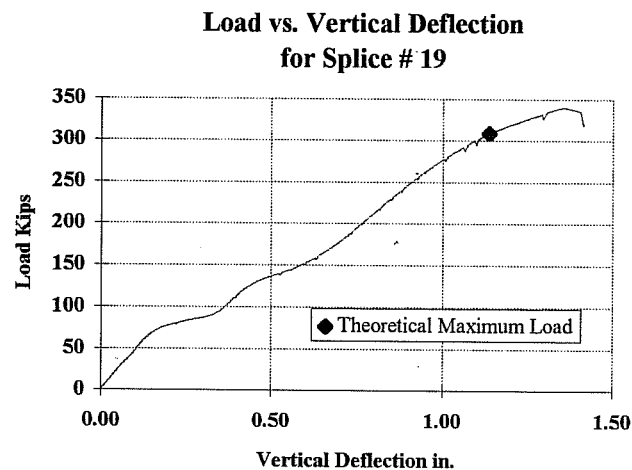


Figure 4-53 The load versus vertical deflection (channel 2) at the splice for splice 19 (unsymmetric inadequate flanges with hand-tight web bolts)

Figure 4-44 through Figure 4-52 show that the theoretical slip loads were reasonably conservative and agreed with the girder slip behavior. The theoretical web slip predicted well the girder slip for splices with inadequate flanges. However, the theoretical web slip can be very unconservative in predicting the slip of the girder when the flanges are adequate to resist the total service moment. Thus, for the latter case, the theoretical slip must be based on the girder slip and not on the web slip. The girder slip load is the load that corresponds to exceeding the shear capacity of the web bolts based on the geometrical eccentricity e_g .

At maximum load, the tests covered a wide range of the applied moment to the flange moment ratios. The applied moment to the small moment flange ratio ranged from 0.43 to 2.43. Also, the applied moment to big flange moment ratio ranged from 0.43 to 2.34. Table 4-21 and Table 4-22 show the tested ratios of moment to moment capacity of the flanges.

Table 4-21 The tested moment to flanges moment capacity for the 24 in. beam splices

Splice	M / M_f
1s	0.68
2s	0.72
3s	0.43
4s	0.91
5s	1.11

Table 4-22 The tested moment to flanges moment capacity for the 40 in. beam splices

Splice	$M_{\text{nonlinear}} / M_f$	$M_{\text{nonlinear}} / M_F$
7u	∞	2.34
8u	∞	1.05
9u	2.42	1.31
10u	2.42	1.31
15u	2.00	1.09
16s	1.00	1.00
17u	0.97	0.53
18s	1.08	1.08
19u	2.31	1.25
20s	1.33	1.33

The maximum theoretical error associated with the elastic analysis of the web bolts was -7.9% for the symmetric splices and -13.3% for the unsymmetric splice #9 and 15.3% for the unsymmetric splice #10. The increase in error for splices 9 and 10 was due to strain hardening of the small flange where the ratio of the applied moment to the small flange moment was 2.42. The strain hardening of the small flange for splices 9 and 10 was evident experimentally. At failure the small flange of splices # 9 and # 10 fractured and necked down at the net section, respectively. However, strain hardening of the flange should help decrease the forces applied on the web splice. For the case of symmetric splices, strain hardening of the flanges will decrease the applied moment to web splice. For unsymmetric splices, strain hardening of the small flange should decrease both the applied moment and horizontal force on the web splice. The decrease in web forces due to strain hardening of the flanges was evident through the conservative error

produced in the analysis. For the unsymmetric splices 7 and 8, the error decreased to 4.1% and 4.7% since the bottom flanges were not connected and therefore the effect of strain hardening was eliminated. However, in the latter splices the error was unconservative due to the unconservative nature of the nonlinear analysis of the pretensioned web bolts which was discussed in Chapter 2.

For symmetric w-f splices, Table 4-19 shows that the theoretical force distribution combined with the theoretical nonlinear analysis of the web bolts predicted the ultimate load with an average error of +1.9% to -6.2%. On the other hand, the theoretical force distribution combined with the theoretical elastic analysis of the web bolts predicted the ultimate load with an average error of +2.8 to -5.3%.

For unsymmetric w-f splices, Table 4-20 shows that the theoretical force distribution combined with the theoretical nonlinear analysis of the web bolts predicted the ultimate load with an average error of +4.4% to -11.9%. On the other hand, the theoretical force distribution combined with the theoretical the elastic analysis predicted the ultimate load with an average error of -16%.

Therefore, the theoretical force distribution combined with nonlinear analysis agrees best with the test results. Unfortunately, the nonlinear load deformation responses for all commonly used bolts and plates are not available. Fortunately, the theoretical force distribution combined with a simple elastic analysis appears to be adequate and there is no need to perform an iterative nonlinear analysis.

4.7.2.7. The effect of the moment shear interaction on the strength of w-f splice plates

Splices 18 and 20 were designed to simultaneously fail the web bolts and the flange and web splice plates. Further, the splice plates were designed to reach their plastic moment capacity; whereas, the web plates were designed to reach their full shear yield and their plastic moment capacity simultaneously. Table 4-19 shows that both splices achieved their full plastic moment capacities and shear yield capacities. The plates of splice 18 reached 1.02 of its plastic moment capacity and 1.05 of its plastic shear capacity. The plates of splice 20 reached 1.11 of its plastic moment capacity and 1.1 of its plastic shear capacity. Therefore, practically, the splice plates can be designed ignoring any shear-moment interaction.

Further, the splice plates of specimens 18 and 20 were able to develop their plastic moment and plastic shear capacities regardless of the number of rows of web bolts. Thus, there is no need to require the web splice to have a minimum of two rows of bolts as required by AASHTO. Figure 4-54 and Figure 4-55 show splices 18 and 20 at failure. Also, Figure 4-56 and Figure 4-57 show the top and bottom flange of splice 18 at failure.

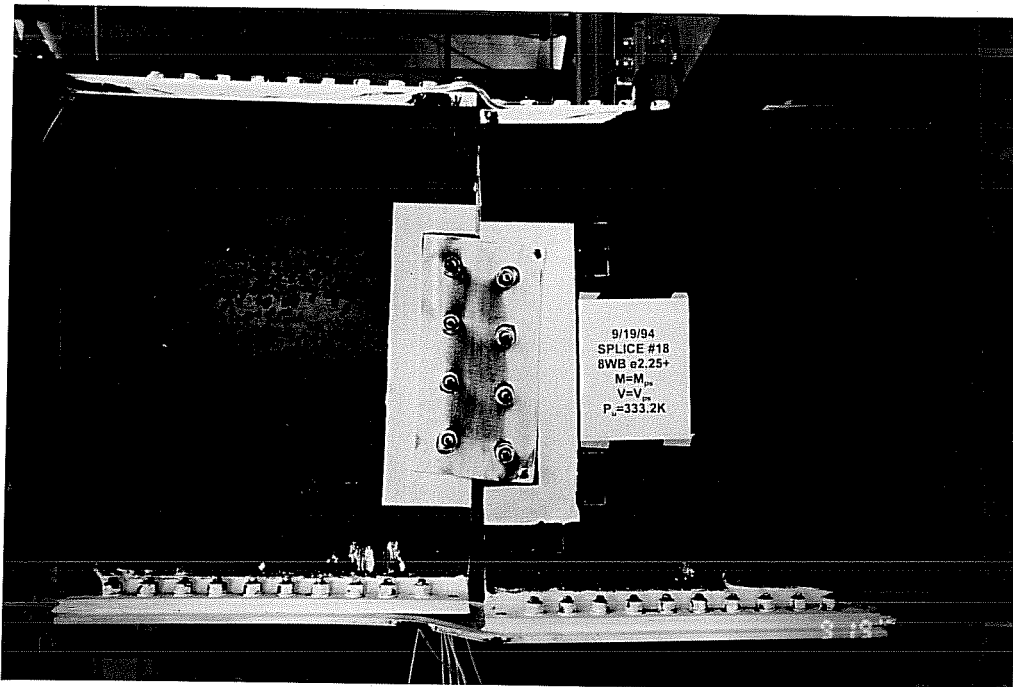


Figure 4-54 Typical failed symmetric w-f splice with inadequate flanges, $M=M_p$, $V=V_p$, splice 18.

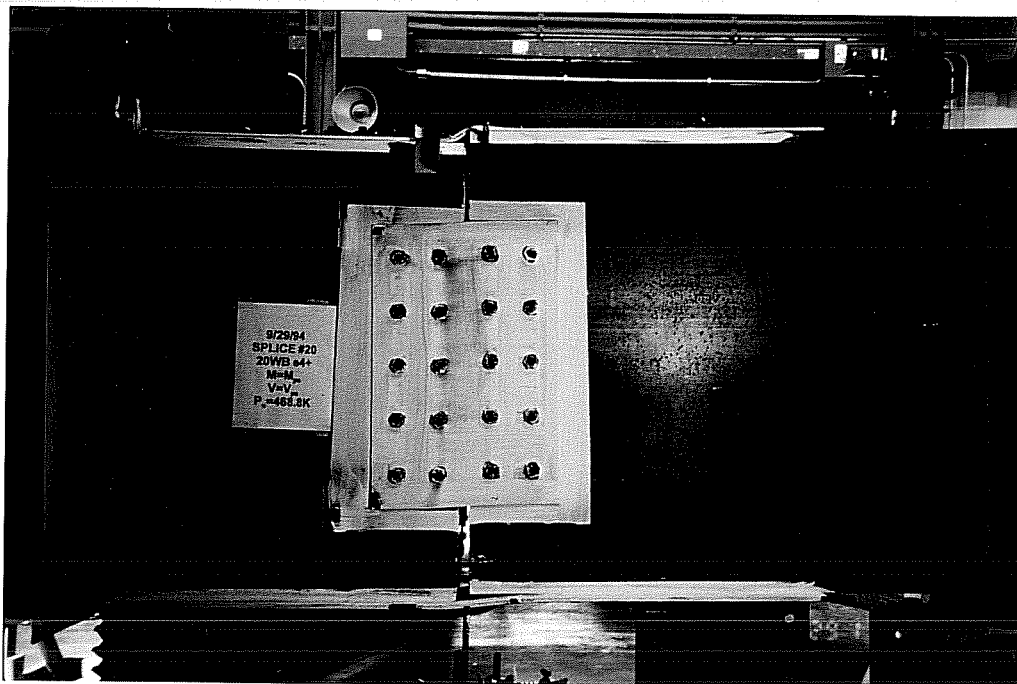


Figure 4-55 Typical failed symmetric w-f splice with inadequate flanges, $M=M_p$, $V=V_p$, splice 20.

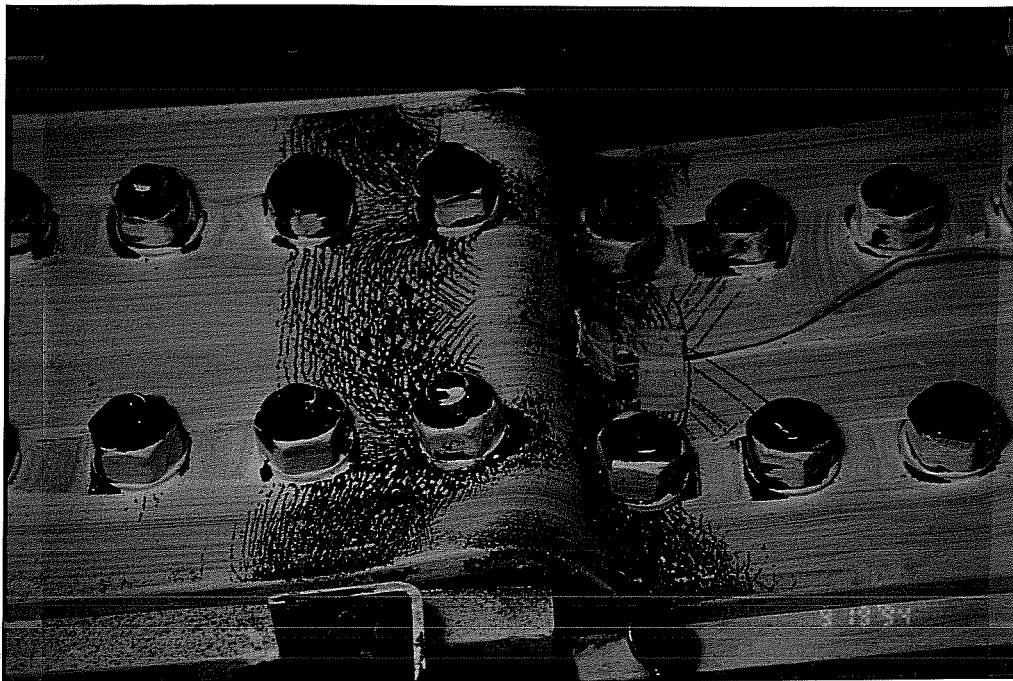


Figure 4-56 The top flange of a typical failed symmetric w-f splice with inadequate flanges, $M=M_p$, $V=V_p$, splice 18.

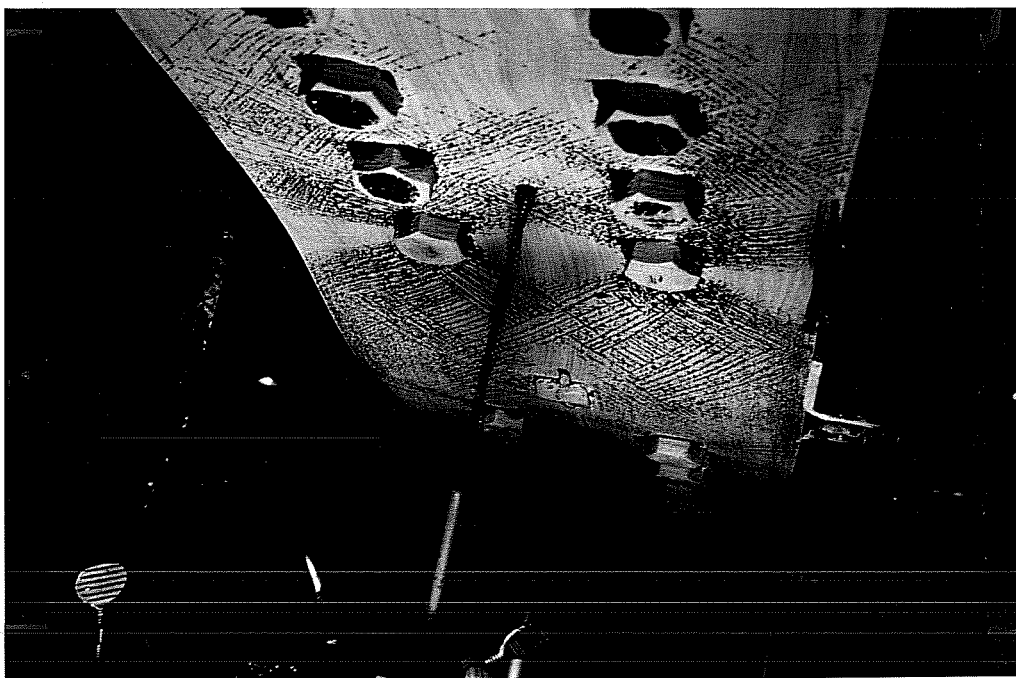


Figure 4-57 The bottom flange of a typical failed symmetric w-f splice with inadequate flanges, $M=M_p$, $V=V_p$, splice 18.

4.7.2.8. The effect of the web bolts preload on the strength of w-f splices

To examine the effect of preload in the web bolts, specimen 10 was replicated in specimen 19. However, the web bolts in specimen 19 were hand-tight bolts; no preload. Figure 4-58 shows the load deformation response of both specimens up to failure by shearing of the critical web bolt.

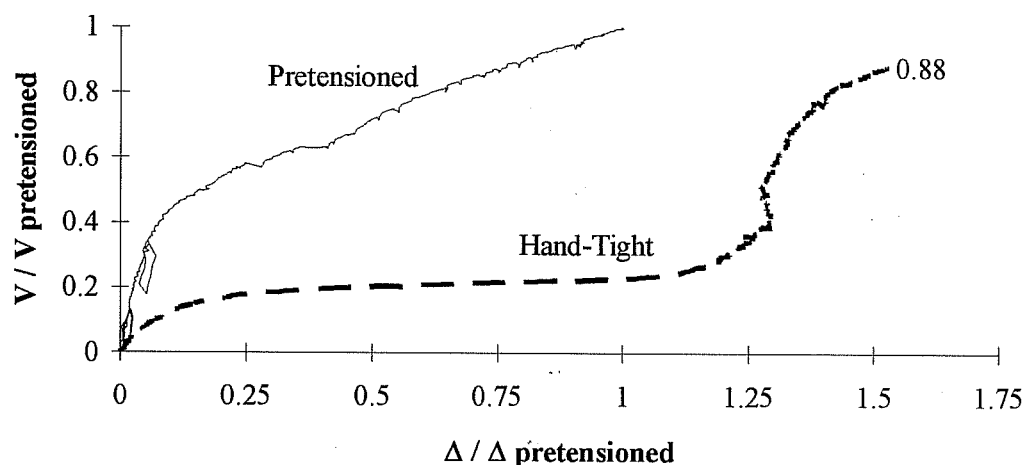


Figure 4-58 The effect of preload in the web bolts on the strength and deformation of web-flange splices

Figure 4-58 shows that the splice with hand-tight web bolts underwent approximately 55% larger deformation than the splice with pretensioned web bolts. Also, the splice with hand-tight web bolts failed earlier than the splice with pretensioned web bolts. Splice 10 failed at a load of 387.8 kips, whereas, splice 19 failed at a load of 340.3; a 12.2% decrease in strength. However, the shear strength of an individual hand-tight bolt was 11.8% less than that of a pretensioned bolt. Therefore, the decrease in strength of w-f splices due to the absence of the

full pretension force in the bolts is due mainly to the lower shear capacity of an individual hand-tight bolt.

4.7.2.9. Summary and conclusions of web-flange splice tests

Based on the results of the testing program of 15 large-scale web-flange bolted splices, the following conclusions are made:

I. At the service level:

- To limit the permanent deformation at service load, the flanges should be limited to their yield stress at the gross area.
- When predicting the web slip, elastic analysis of the web bolts must be performed.
- When the flanges are adequate to carry the service load moment, the web needs to be designed for shear only. This shear is applied at the centerline of the splice with an eccentricity calculated as the distance from the centerline of the splice to the centroid of the web bolts at one side of the splice.
- When the small flange of an unsymmetric girder is not adequate to carry the service load moment, the web needs to be designed for the total shear, the moment resisted by the web, and the horizontal force required from equilibrium of forces.

II. At maximum load:

- When the small flange of an unsymmetric girder is adequate to carry the maximum design moment, the web needs to be designed for shear only. This shear is applied at the centerline of the splice with an eccentricity calculated as the distance from the centerline of the splice to the centroid of the web bolts at one side of the splice.

- When the design moment exceeds the moment resistance of the small flange but is less than the moment resistance of the big flange, the web needs to be designed for the design shear along with the horizontal force which represents the difference in the flanges axial forces
 - When the design moment exceeds the moment resistance of the big flange, the web needs to be designed for the design shear, the horizontal force which represents the difference in the flanges axial forces, and the moment in excess of the big flange moment capacity.
 - Elastic analysis of the web bolts appears to be adequate and there is no need to perform nonlinear analysis of the bolts.
 - The flanges of w-f splices, if not fully yielded, carry a portion of the total shear. This shear is a function of the ratio of the applied moment to the moment capacity of the flanges. In general, the shear carried by the flanges is a function of:
 1. Gap clearance in the girder. The shear in the flanges decreases as the gap increases
 2. Edge distance of the flange fasteners. The shear in the flanges decreases as the edge distance of the flange fasteners increases
 3. Level of flange axial force required for moment; axial force / $(A_f F_{yf})$.
The shear in the flanges decreases as the Level of flange axial force increases
- Thus, assuming that the applied shear is resisted by the web of w-f splices with adequate flanges should yield conservative results.
- The w-f splice plates can develop their plastic moment and plastic shear capacities simultaneously. Thus, there should not be a reduction in the capacity of w-f splice plates due to moment shear interaction.

- The flanges of w-f splices can develop their moment capacity at the gross section, provided that it does not exceed the fracture capacity at the net section, even though the net to gross area is less than 85%. Thus, there should not be a reduction to the gross area to obtain an effective area when the net to gross area is less than 85%, as required by AASHTO.
- The w-f splice plates can develop their plastic moment and plastic shear capacities regardless of the number of rows of web bolts, provided that the web bolts are adequate to resist the shear and moment applied to the web splice. Thus, there is no need to require the web splice to have a minimum of two rows of bolts as required by AASHTO.
- W-F splices with hand tight (no preload) web bolts have less capacity than w-f splices with pretensioned bolts

Chapter 5

5. Design Procedures for Steel Girder Bolted Splices

5.1. Introduction

The following design procedures are based on the results of the testing program performed at the University of Texas on 32 large-scale steel girder bolted splices. The design procedures include the interpretation of AASHTO's minimum strength requirements for bolted splices. Based on the results of the experimental program, the procedures ignore three of AASHTO's rules that were found unnecessary. These rules are:

1. The assignment of moment to the web
2. The minimum two rows of web bolts
3. The reduction in the gross area for holes in excess of 15% of the gross area

The procedures are applicable to symmetric, unsymmetric, and composite steel girders.

The design procedures include two major steps:

1. The determination of the distribution of design forces between the flanges and the web.
2. The design of the web and flange splice plates and bolts

The following limits are the limit states for a web-flange steel girder bolted splice:

I. At overload:

1. Slip of the splice plates
2. Yielding of the gross section of either the web in shear or the flanges in axial load

II. At maximum load:

1. Yielding of the gross section of either the web in shear or the flanges in axial
2. Fracturing of the net section of either the web in shear or the tension flange in axial tension
3. Block shear failure of either the web due to shear or the flanges due to axial tension
4. Bending limit state of the web splice plates
5. Bearing failure of either the web or the flanges
6. Shearing of the bolts of either the web or the flanges

5.2. Design Procedures

5.2.1. The distribution of design forces between the flange and web splices

It was shown in Chapter 4 that the web needs to be designed for shear only if the flanges are adequate to carry the applied moment. This shear acts at the centerline of the splice. It was also shown that the web needs to be designed for shear and for the additional moment in excess of the flanges' capacity if the flanges

are not adequate to carry the total moment. For unsymmetric girder, the web needs to be designed (in addition to the shear and moment, if any) for the difference of the axial loads in the big and small flanges required for equilibrium of forces.

5.2.1.1. The distribution of forces at the service level (Slip)

5.2.1.1.1. Adequate moment resistance of the flanges:

This is the case where:

$$M \leq M_f = \Omega F_{yf} A_{gf} \times h \quad (5-1)$$

The service design axial force in the flanges is:

$$T_f = T_F = \frac{M}{h} \quad (5-2)$$

Since the flanges are adequate to carry the applied service moment, the web needs to be designed to carry the following forces at the center line of the splice:

$$M_w = 0 \quad (5-3)$$

$$H_w = 0 \quad (5-4)$$

$$V_w = V \quad (5-5)$$

Where:

A_{gf} The gross sectional area of the small flange

F_{yf}	The Yield stress of the small flange
h	The distance from the centroid of the small flange to the centroid of the big flange
H_w	The design horizontal axial load of the web at service load
M	The applied moment at service load
M_f	The moment resistance of the small flange
M_w	The service design moment of the web
T_f	The design axial load of the small flange at service load
T_F	The design axial load of the big flange at service load
V	The applied shear at service load
V_w	The design shear of the web at service load
Ω	Factor to limit the permanent deformations due to residual stresses. $\Omega = 0.95$ for non-composite steel girder and for composite girder in a positive moment region. $\Omega = 0.8$ for composite girder in a negative moment region

5.2.1.1.2. Inadequate moment resistance of the flanges:

This is the case where:

$$M_f = \Omega F_{yf} A_{gf} \times h < M \leq M_y \quad (5-6)$$

The design axial loads in each flange can be calculated as:

$$T_f = \sigma_f A_{gf} \quad (5-7)$$

$$T_F = \sigma_F A_{gF} \quad (5-8)$$

The normal bending stress can be calculated from the elastic flexural formula, $\sigma = M \times y / I$.

If the centroid of the web bolts coincides with the centroidal axis of the web/web splice (the case of a typical splice), then M_w can be calculated as follows:

$$M_w = \frac{t_w d_w^2}{12} (\sigma_{tw} + \sigma_{bw}) = \frac{I_w}{d_w} (\sigma_{tw} + \sigma_{bw}) \quad (5-9)$$

For the case of inadequate flanges, the moment in excess of the flanges capacity must be carried by the web. The forces on the web can be obtained from stress calculations. At the center line of the splice:

$$H_w = \frac{t_w d_w}{2} (\sigma_{tw} + \sigma_{bw}) = A_w \frac{(\sigma_{tw} + \sigma_{bw})}{2} \quad (5-10)$$

$$V_w = V \quad (5-11)$$

Where:

A_{gf} The gross sectional area of the big flange

A_{gw} The gross area of the web splice plates = $t_w d_w$

d_w The depth of the web splice plates

I_w The moment of inertia of the web splice plates about its centroidal axis = $t_w d_w^3 / 12$

I The moment of inertia of the splice

M_y The first yield moment of the girder

σ_{tw}	The normal bending stress at the top of the web splice plates at service load. The sign of the bending stress is (+) if in tension and (-) if in compression
σ_{bw}	The normal bending stress at the bottom of the web splice plates at service. The sign of the bending stress is (+) if in tension and (-) if in compression load
σ_f	The normal bending stress at the outer fiber of the small flange splice plate at service load
σ_F	The normal bending stress at the outer fiber of the big flange splice plate at service load
t_w	The thickness of the web splice plates
y	The distance from fiber under consideration to the elastic neutral axis

5.2.1.2. The distribution of forces at the ultimate level (maximum load)

Calculate the moment capacity of the big and small flanges as follows:

$$\phi T_{nf} = \phi(\text{minimum of } F_{yf}A_{gf} \text{ or } F_{uf}A_{nf}) \quad (5-12)$$

$$\phi T_{nF} = \phi(\text{minimum of } F_{yF}A_{gF} \text{ or } F_{uF}A_{nF}) \quad (5-13)$$

$$\phi M_{nf} = \phi T_{nf} \times h \quad (5-14)$$

$$\phi M_{nF} = \phi T_{nf} \times h_f + \phi T_{nF} \times h_F \quad (5-15)$$

Where:

A_{nf} The net sectional area of the small flange

A_{gF} The gross sectional area of the big flange

A_{nF}	The net sectional area of the big flange
F_{uf}	The ultimate stress of the small flange
F_{uF}	The ultimate stress of the big flange
ϕ	Strength reduction factor $\phi = 1$, for yielding limit state $\phi = 0.8$, for fracture limit state
ϕM_{nf}	The moment capacity of the girder's small flange
ϕM_{nF}	The moment capacity of the girder's big flange
ϕM_n	The moment capacity of the girder
ϕT_{nf}	The axial load capacity of the girder's small flange
ϕT_{nF}	The axial load capacity of the girder's big flange
h_f	The distance between the centroid of the small flange splice plates and the centroid of the web bolts
h_F	The distance between the centroid of the big flange splice plates and the centroid of the web bolts
M_u	The maximum design moment

5.2.1.2.1. Adequate small flange:

This is the case where:

$$M_u \leq \phi M_{nf} \quad (5-16)$$

Since the flanges are adequate to carry the maximum design moment, the web can be designed to carry only the applied shear at the center line of the splice. The axial load in the flange can be calculated as the forces required to resist the

applied moment. Thus, the distribution of forces at the center line of the splice can be calculated as follows:

$$T_{uf} = \frac{M_u}{h} \geq \text{minimum of} \left[0.75\phi T_{nf} \quad \text{or} \quad \frac{(\phi T_{nf} + M_u / h)}{2} \right] \quad (5-17)$$

$$T_{uF} = \frac{M_u}{h} \geq \text{minimum of} \left[0.75\phi T_{nF} \quad \text{or} \quad \frac{(\phi T_{nF} + M_u / h)}{2} \right] \quad (5-18)$$

$$M_{uw} = 0 \quad (5-19)$$

$$H_{uw} = 0 \quad (5-20)$$

$$V_{uw} = V_u \geq \text{minimum of} \left[0.75\phi V_n, \frac{(\phi V_n + V_u)}{2} \right] \quad (5-21)$$

- ϕV_n The shear strength of the girder's web
- H_{uw} The maximum design horizontal axial load of the web splice plates
- M_{uw} The maximum design moment of the web splice plates
- T_{uf} The maximum design axial load of the small flange splice plate
- T_{uF} The maximum design axial load of the big flange splice plate
- V_u The maximum applied shear
- V_{uw} The maximum design shear of the web splice plates

5.2.1.2.2. Adequate big flange and inadequate small flange

This is the case where:

$$\phi M_{nf} \leq M_u \leq \phi M_{nF} \leq \phi M_n \quad (5-22)$$

When the small flange yields due to the flange forces required to resist the applied moment, the web and the adequate big flange will provide the forces required to resist the moment in excess of the small flange capacity. Therefore, in addition to the shear carried by the web, the web must carry the addition horizontal force.

Thus, the distribution of forces at the center line of the splice can be calculated as follows:

$$T_{uf} = \phi T_{nf} \quad (5-23)$$

$$T_{uF} = H_{uw} + T_{uf} \geq \text{minimum of} \left[0.75\phi T_{nF}, \frac{\phi T_{nF} + (H_{uw} + T_{uf})}{2} \right] \quad (5-24)$$

$$M_{uw} = 0 \quad (5-25)$$

$$H_{uw} = \frac{M_u - \phi M_{nf}}{h_F} \quad (5-26)$$

$$V_{uw} = V_u \geq \text{minimum of} \left[0.75\phi V_n, \frac{(\phi V_n + V_u)}{2} \right] \quad (5-27)$$

5.2.1.2.3. Inadequate flanges:

This is the case where:

$$\phi M_{nF} \leq M_u \leq \phi M_n \quad (5-28)$$

After yielding of both the flanges, the web needs to carry the moment in excess of the big flange capacity in addition to the shear and horizontal force which equals to the difference in the flanges axial yield loads. Thus, the distribution of forces at the center line of the splice can be calculated as follows:

$$T_{uf} = \phi T_{nf} \quad (5-29)$$

$$T_{uF} = \phi T_{nF} \quad (5-30)$$

$$M_{uw} = M_u - \phi M_{nF} \geq \text{minimum of} \left[0.75\phi M_{nw}, \frac{\phi M_{nw} + (M_u - \phi M_{nF})}{2} \right] \quad (5-31)$$

$$H_{uw} = \phi T_{nF} - \phi T_{nf} \quad (5-32)$$

$$V_{uw} = V_u \geq \text{minimum of} \left[0.75\phi V_n, \frac{(\phi V_n + V_u)}{2} \right] \quad (5-33)$$

5.2.2. Splice Design

5.2.2.1. The design of flange splice plates

1. Serviceability limit state

$$\text{Required } A_{gf} = T_f / \Omega F_{yf} \quad (5-34)$$

$$\text{Required } A_{gF} = T_F / \Omega F_{yF} \quad (5-35)$$

2. Yielding of the gross section limit state

$$\text{Required } A_{gf} = T_{uf} / \phi F_{yf} \quad (5-36)$$

$$\text{Required } A_{gF} = T_{uF} / \phi F_{yF} \quad (5-37)$$

3. Fracturing of the net section limit state

$$\text{Required } A_{nf} = T_{uf} / (\phi F_{uf}) \quad (5-38)$$

$$\text{Required } A_{nF} = T_{uF} / (\phi F_{uF}) \quad (5-39)$$

For the assumption of a uniform ultimate stress at the net section to be acceptable, the net area used in the calculations must be limited to 85% of the gross area.

4. block shear limit state:

a) If $0.58F_u A_{nv} > F_u A_{nt}$:

$$\phi T_n = \phi (0.58F_u A_{nv} + F_y A_{gt}) \geq T_u \quad (5-40)$$

b) If $0.58F_u A_{nv} < F_u A_{nt}$, then:

$$\phi T_n = \phi (0.58F_u A_{nt} + F_y A_{gv}) \geq T_u \quad (5-41)$$

Where:

A_{gt} The gross area in tension corresponding to the rupture mode of the flange under consideration

A_{nt} The net area in tension corresponding to the rupture mode of the flange under consideration

A_{gv} The gross area in shear corresponding to the rupture mode of the flange under consideration

A_{nv} The net area in shear corresponding to the rupture mode of the flange under consideration

F_y The yield strength of the flange under consideration

F_u The ultimate strength of the flange under consideration

ϕT_n The axial load block shear rupture capacity of the flange under consideration

T_u The design axial maximum load of the flange splice plate under consideration

5.2.2.2. The design of web splice plates

1. Serviceability limit state

$$\text{Required } A_{gw} = V / (\Omega \times 0.58 F_{yw}) \quad (5-42)$$

$$\text{Required } A_{gw} = H / (\Omega \times F_{yw}) \quad (5-43)$$

2. Yielding of the gross section limit state

$$\text{Required } A_{gw} = V_{uw} / (\phi \ 0.58 F_{yw}) \quad (5-44)$$

$$\text{Required } A_{gw} = H_{uw} / \phi \ F_{yw} \quad (5-45)$$

3. Fracturing of the net section limit state

$$\text{Required } A_{nw} = V_u / (\phi \ 0.58 F_{uw}) \quad (5-46)$$

$$\text{Required } A_{nw} = H_{uw} / \phi \ F_{uw} \quad (5-47)$$

4. Bending limit state

$$\text{Required } Z_{xw} = M_{uw} / \phi \ F_{yw} \quad (5-48)$$

Where:

Z_{xw} The plastic section modulus of the web splice plates

5. block shear limit state:

a) If $0.58F_{uw}A_{nv} > F_{uw}A_{nt}$, then:

$$\phi V_n = \phi (0.58F_{uw}A_{nv} + F_{yw}A_{gt}) \geq V_u \quad (5-49)$$

b) If $0.58F_{uw}A_{nv} < F_{uw}A_{nt}$, then:

$$\phi V_n = \phi (0.58F_{uw}A_{nt} + F_{yw}A_{gv}) \geq V_u \quad (5-50)$$

A_{gt} The gross area in tension corresponding to the rupture mode of the web splice plates

A_{nt} The net area in tension corresponding to the rupture mode of the web splice plates

A_{gv} The gross area in shear corresponding to the rupture mode of the web splice plates

A_{nv} The net area in shear corresponding to the rupture mode of the web splice plates

F_{yw} The yield strength of the web splice plates

F_{uw} The ultimate strength of the web splice plates

ϕV_n The block shear rupture capacity of the web splice plates

V_u The design shear of the web splice plates

5.2.2.3. The design of flange bolts

1. Slip limit state:

$$N_b A_b = T / \phi R_s N_s \quad (5-51)$$

2. Bolt shear limit state:

$$N_b A_b = T_u / \phi R_u N_s \quad (5-52)$$

3. Plate bearing limit state:

$$N_b = T_u / \phi R_b \quad (5-53)$$

Where:

- N_b The total number of bolts
- A_b The area of one bolt
- T The axial design load at the service level in the flange splice plates under consideration
- T_u The axial design load at maximum load in the flange splice plates under consideration
- ϕR_s The design slip resistance per unit area of one bolt
- ϕR_u The design shear strength per unit area of one bolt
- ϕR_b The design bearing strength per unit area of the connected materials
- N_s The number of shear planes

5.2.2.4. The design of web bolts

1. Slip limit state:

$$\text{Required } C = V / (\phi R_s N_s N_b A_b) \quad (5-54)$$

2. Bolt shear limit state:

$$\text{Required } C = V_u / (\phi R_u N_s A_b) \quad (5-55)$$

3. Plate bearing limit state:

$$\text{Required } C = V_u / \phi R_b \quad (5-56)$$

Where:

C The normalized design capacity of one web bolt; the eccentric shear capacity of the group of bolts calculated from elastic analysis/ the design capacity of one bolt. When performing elastic analysis of the web bolts, the horizontal force should be included for the case of unsymmetric splice with inadequate small flange. The design eccentricity used in the elastic analysis of the web bolts can be calculated as follows:

I. At the slip level

$$e = e_g + M_w / V \quad (5-57)$$

II. At maximum load

$$e = e_g + M_{uw} / V_u \quad (5-58)$$

Where:

e_g The geometrical eccentricity; the distance from the centerline of the splice to the centroid of the web bolts at one side of the splice

e The design eccentricity

Chapter 6

6. Composite Girder Bolted Splice Design Examples

The examples presented herein are actual girders and loads taken from the Texas Department of Transportation and from the American Institute of Steel Construction Marketing splice design project studied by the HDR consulting firm. However, the design of the splices done herein is based on the design procedures presented in Chapter 5.

6.1. Design Example 1, splice in a negative moment region

Design a bolted splice for the steel girder shown in Figure 6-1 to be located next to the pier of a bridge.

Given:

$$M_{DL} = -8,853 \text{ kip-ft.}$$

$$M_{LL+I} = -3,729 \text{ kip-ft.}$$

$$V_{DL} = 219 \text{ kip}$$

$$V_{LL+I} = 108 \text{ kip-ft.}$$

$$F_{yf} = F_{yw} = 50 \text{ ksi}$$

$$b_F = b_f = 24 \text{ in.}$$

$$t_F = t_f = 3 \text{ in.}$$

$$d_w = 72 \text{ in.}$$

$t_w = 11/16$ in.

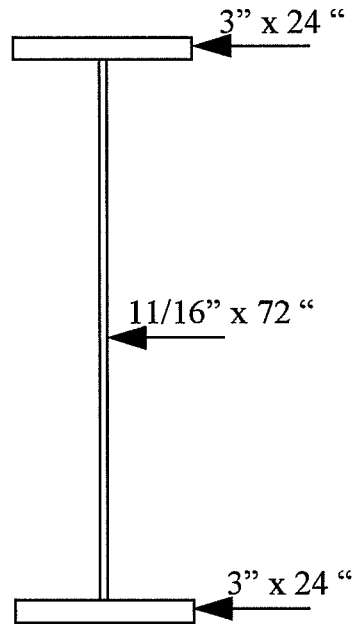


Figure 6-1 The steel girder of Example 1

Solution:

Since the splice is located in a negative moment region, the concrete slab will not contribute to the strength of the member and the girder is non-composite.

6.1.1. Design Forces

6.1.1.1. Required Slip Resistance

$$M_{\text{overload}} = M_{\text{DL}} + 1.667M_{\text{LL+I}} = 8,853 + 1.667(3,729) = \underline{\underline{15,068 \text{ K-ft.}}}$$

$$V_{\text{overload}} = V_{\text{DL}} + 1.667V_{\text{LL+I}} = 219 + 1.667(108) = \underline{\underline{399 \text{ k}}}$$

6.1.1.2. Required strength of the member

$$M_u = 1.3M_{DL} + 2.17M_{LL+I} = 1.3(8,853) + 2.17(3,729) = \underline{\underline{19,601 \text{ K-ft.}}}$$

$$V_u = 1.3V_{DL} + 2.17V_{LL+I} = 1.3(219) + 2.17(108) = \underline{\underline{519.1 \text{ k}}}$$

6.1.1.3. AASHTO Design Forces

Check the adequacy of the flanges to carry the overload and maximum moment alone.

$$A_{gf} = 3 \times 24 = 72 \text{ in.}^2$$

Assume using four rows of 1" bolts in each flange:

$$A_{nf} = 3 \times (24 - 4(1 + 1/8)) = 58.5 \text{ in.}^2$$

$$A_{nf}/A_{gf} = 58.5/72 = 0.81 < 0.85$$

$$h = 1.5 + 72 + 1.5 = 75 \text{ in.}$$

$$\phi M_{nf} = \phi (A_{gf} F_{yf}) h = 1.0 \times (72 \times 50) \times 75 / 12 = 22,500 \text{ kip-ft.}$$

$$\phi M_{nf} = \phi (A_{nf} F_{uf}) h = 0.80 \times (58.5 \times 65) \times 75 / 12 = 19,013 \text{ k-ft.} < 22,500 \text{ controls}$$

$$\phi M_{nf} = 19,013 \text{ K-ft.} \approx M_u = 19,601 \text{ K-ft.} \text{ (3\% less than } M_u)$$

$$0.8\phi M_{nf} = 0.8 \times 22,500 = 18,000 \text{ K-ft.} > M_{\text{overload}} = 15,068 \text{ K-ft.}$$

Therefore, the flanges are adequate to carry both the total overload and maximum moments.

Shear Strength of the web:

From AASHTO 10.48.4.1, the shear capacity is calculated as follows:

$$V_u = CV_p; \quad V_p = 0.58F_{yw}Dt_w$$

For unstiffened girders, $k = 5$

$$\frac{D}{t_w} = \frac{72}{0.6875} = 104.7 > \frac{7,500\sqrt{k=5}}{\sqrt{F_{yf} = 50,000}} = 75$$

$$\Rightarrow C = \frac{4.5 \times 10^7 k}{\left(\frac{D}{t_w}\right)^2 F_y} = \frac{4.5 \times 10^7 \times 5}{(104.7)^2 \times 50,000} = 0.4103$$

$$V_u = CV_p = 0.4103 \times 0.58 \times 50 \times 72 \times 0.6875 = 0.4103 \times 1,435.5 = 589 \text{ Kips}$$

Average of the Required Strength and the Member Strength:

There is no need to perform this calculation for moment since the applied moment equals the moment strength of the flanges.

$$V_u = \frac{519.1 + 589}{2} = 554.1 \text{ K. } \underline{\text{Controls}} \text{ (1.07 of the required strength)}$$

75% of the Member Strength:

There is no need to perform this calculation for moment since the applied moment equals the moment strength of the flanges.

$$V_u = 0.75 \times 589 = 441.8 \text{ kips}$$

Therefore, AASHTO design forces are:

$$M_u = 19,601 \text{ kip-ft.}$$

$$V_u = 554.1 \text{ kips}$$

6.1.2. Splice Design

6.1.2.1. The design of flange bolts

Slip requirement: Assuming **class B** contact surface,

$$N_b A_b = M_{\text{overload}} / (\phi R_s N_s h) = 15,068 \times 12 / \{32.5 \times 2 \times 75\} = 37.1 \text{ in.}^2$$

Bolt shear requirement: use bolts with threads excluded from shear planes

$$N_b A_b = M_u / (\phi R_u N_s h) = 19,601 \times 12 / \{36 \times 1.25_{\text{excluded}} \times 2 \times 75\} = \underline{34.8 \text{ in.}^2}$$

Thus, overload controls.

$$A_b = \pi (1)^2 / 4 = 0.785 \text{ in.}^2$$

$$N_b = 37.1 / (0.785) \cong \underline{\underline{48 \text{ bolts}}}$$

Bearing on the plates:

$$N_b = M_u / (1.8d t_f F_{uf} h) = 19,601 \times 12 / \{1.8 \times 1 \times 3 \times 65 \times 75\} \cong 9$$

Thus, bolts bearing does not control.

Use 12 A325 1" bolts / row @ 3 1/2" spacing in 4 rows (Joint length = 42")

6.1.2.2. The design of web bolts

Since the flanges are adequate to carry both the overload and maximum design moments, the web should be designed for the total design shear applied at the center line of the splice. Assume that the clearance gap = 1/2", and the horizontal edge distance for the bolts = 1 3/4". Thus, the geometrical eccentricity, distance between the center line of the splice and the centroid of the bolts, $e_g = 1/4 + 1.75 = 2"$.

Slip requirement: Assuming **class B** contact surface,

$$\text{Required } C = V_{\text{overload}} / (\phi R_s N_s N_b A_b) = 399 / (32.5 \times 2 \times 0.785) = 7.8$$

Bolt shear requirement: use bolts with threads included in the shear planes

$$\text{Required } C = V_u / (\phi R_u N_s A_b) = 554.1 / (36 \times 2 \times 0.785) = \mathbf{9.8}$$

Bearing on the plates:

$$\text{Required } C = V_u / (1.8d t_w F_{uw}) = 554.1 / (1.8 \times 1 \times 10 / 16 \times 65) = 7.6$$

Thus, bolt shear controls the design of the web bolts.

Try one vertical row of 10 1" bolts @ 5 1/4" vertical pitch;

$$C = \frac{n}{\sqrt{\left[\frac{6 \times e}{(n+1) \times b}\right]^2 + 1}} = \frac{10}{\sqrt{\left[\frac{6 \times 2}{(10+1) \times 5.25}\right]^2 + 1}} = 9.8 = C_{\text{required}} = 9.8 \text{ OK}$$

Use one vertical row of 10 1" bolts @ 5 1/4" vertical pitch

Note that $9.8 / 10 = 0.98$ (lost only 2% of shear capacity due to eccentricity effect).

6.1.2.3. The design of flange splice plates

$$\text{Required } A_{gf} = M_{\text{overload}} / (0.8F_{yf} h) = 15,068 \times 12 / (0.8 \times 50 \times 75) = 60.3 \text{ in.}^2$$

$$\text{Required } A_{gf} = M_u / (F_{yf} h) = 19,601 \times 12 / (50 \times 75) = 62.7 \text{ in.}^2$$

$$\text{Required } A_{nf} = M_u / (0.8 F_{uf} h) = 19,601 \times 12 / (0.8 \times 65 \times 75) = 60.3 \text{ in.}^2$$

Use double flange splice plates:

$$\mathbf{1 \text{ Plate } (24 \times 1 \frac{5}{8}) \text{ and } 2 \text{ Plates } (11 \times 1 \frac{3}{4}); A_{gf} = 77.5 \text{ in.}^2, A_{nf} = 62.3 \text{ in.}^2}$$

$$A_{nf} / A_{gf} = 62.3 / 77.5 = 0.8 < 0.85 \text{ OK}$$

Check block shear:

Tensile load per flange:

$$T_u = M_u / h = 19,601 \times 12 / 75 = 3,136 \text{ kips}$$

Tensile load per flange plate:

$$T_{u1} = 3,136 / 2 = 1,568 \text{ kips}$$

Check block shear for the 24" plate:

The length of the bolted connection from the edge of the plate to the last bolt is:

$$(12_{\text{bolts}} - 1) \times 3.5 + 1.75_{\text{edge distance}} = 40.25$$

$$A_{nv} = 2_{\text{shear planes}} \times (40.25 - 11.5(1 + 1/8)) \times 1.625 = 88.8 \text{ in.}^2$$

$$A_{nt} = 2 \times (8.25 - 1.5(1 + 1/8)) \times 1.625 = 21.3 \text{ in.}^2$$

$$A_{gv} = 2(40.25) \times 1.625 = 130.8 \text{ in.}^2$$

$$A_{gt} = 2 \times 8.25 \times 1.625 = 26.8 \text{ in.}^2$$

$$0.58F_u A_{nv} = 0.58 \times 65 \times 88.8 = 3,346$$

$$F_u A_{nt} = 65 \times 21.3 = 1,385$$

Since $0.58F_u A_{nv} > F_u A_{nt}$:

$$T = 0.8 \times (0.58F_u A_{nv} + F_y A_{gt}) = 0.8 \times (3,346 + 50 \times 26.8) = 3,749 > T_{u1} = 1,568 \text{ kips}$$

Check block shear for the 11" plates:

$$A_{nv} = 2 \times 2(40.25 - 11.5(1 + 1/8)) \times 1.75 = 191.2 \text{ in.}^2$$

$$A_{nt} = 2(5.5 - (1 + 1/8)) \times 1.75 = 15.3 \text{ in.}^2$$

$$A_{gv} = 2(2 \times 40.25) \times 1.75 = 281.8 \text{ in.}^2$$

$$A_{gt} = 2 \times 5.5 \times 1.75 = 19.25 \text{ in.}^2$$

$$0.58F_u A_{nv} = 0.58 \times 65 \times 191.2 = 7,208$$

$$F_u A_{nt} = 65 \times 15.3 = 995$$

Since $0.58F_u A_{nv} > F_u A_{nt}$:

$$T_2 = 0.8 \times (0.58F_u A_{nv} + F_y A_{gt}) = 0.8 \times (7,208 + 50 \times 19.25) = 6,536 > T_{u2} = 1,568 \text{ kips}$$

Check block shear for the flange of the girder:

$$A_{nv} = 2(40.25 - 11.5(1 + 1/8)) \times 3 = 163.9 \text{ in.}^2$$

$$A_{nt} = 2(8.25 - 1.5(1 + 1/8)) \times 3 = 39.4 \text{ in.}^2$$

$$A_{gv} = 2(40.25) \times 3 = 241.5 \text{ in.}^2$$

$$A_{gt} = 2 \times 8.25 \times 3 = 49.5 \text{ in.}^2$$

$$0.58F_u A_n = 0.58 \times 65 \times 163.9 = 6,178$$

$$F_u A_{nt} = 65 \times 39.4 = 2,561$$

Since $0.58F_u A_{nv} > F_u A_{nt}$:

$$T = 0.8 \times (0.58F_u A_{nv} + F_y A_{gt}) = 0.8 \times (6,178 + 50 \times 49.5) = 6,922 > T_u = 3,136 \text{ kips}$$

6.1.2.4. The design of web splice plates

Since the flanges are adequate to carry both the overload and maximum design moments, the web needs to be designed for shear only.

$$\text{Required } A_{gw} = V_{\text{overload}} / (0.8 \times 0.58 F_{yw}) = 399 / (0.8 \times 0.58 \times 50) = 17.2 \text{ in.}^2$$

$$\text{Required } A_{gw} = V_u / (0.58 F_{yw}) = 554.1 / (0.58 \times 50) = 19.1 \text{ in.}^2$$

$$\text{Required } A_{nw} = V_u / (0.8 \times 0.58 F_{uw}) = 554.1 / (0.58 \times 65) = 18.4 \text{ in.}^2$$

Use double web splice plates with one vertical row of 10 1" bolts @ 5 3/4" vertical pitch with 2 1/8" horizontal and vertical edge distance:

Use 2 Plates (56×5/16); $A_{gw} = 35 \text{ in.}^2$, $A_{nw} = 28 \text{ in.}^2$

Check block shear:

$$A_{nv} = (56 - 2.125 - 9.5(1 + 1/8)) \times 0.625 = 27 \text{ in.}^2$$

$$A_{nt} = (2.125 - 0.5(1 + 1/8)) \times 0.625 = 0.99 \text{ in.}^2$$

$$A_{gv} = (56 - 2.125) \times 0.625 = 33.7 \text{ in.}^2$$

$$A_{gt} = 2.125 \times 0.625 = 1.33 \text{ in.}^2$$

$$0.58 F_u A_{nv} = 0.58 \times 65 \times 27 = 1,018$$

$$F_{uw}A_{nt} = 65 \times 0.99 = 64.4$$

Since $0.58F_{uw}A_{nv} > F_{uw}A_{nt}$:

$$V = 0.8 \times (0.58F_{uw}A_{nv} + F_{yw}A_{gt}) = 0.8 \times (1,018 + 50 \times 1.33) = 867.3 > V_u = 554.1 \text{ kips}$$

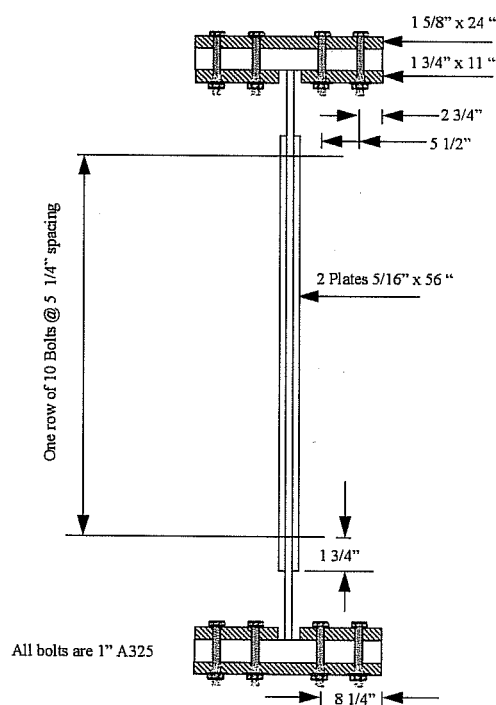


Figure 6-2 Splice details of Example 1

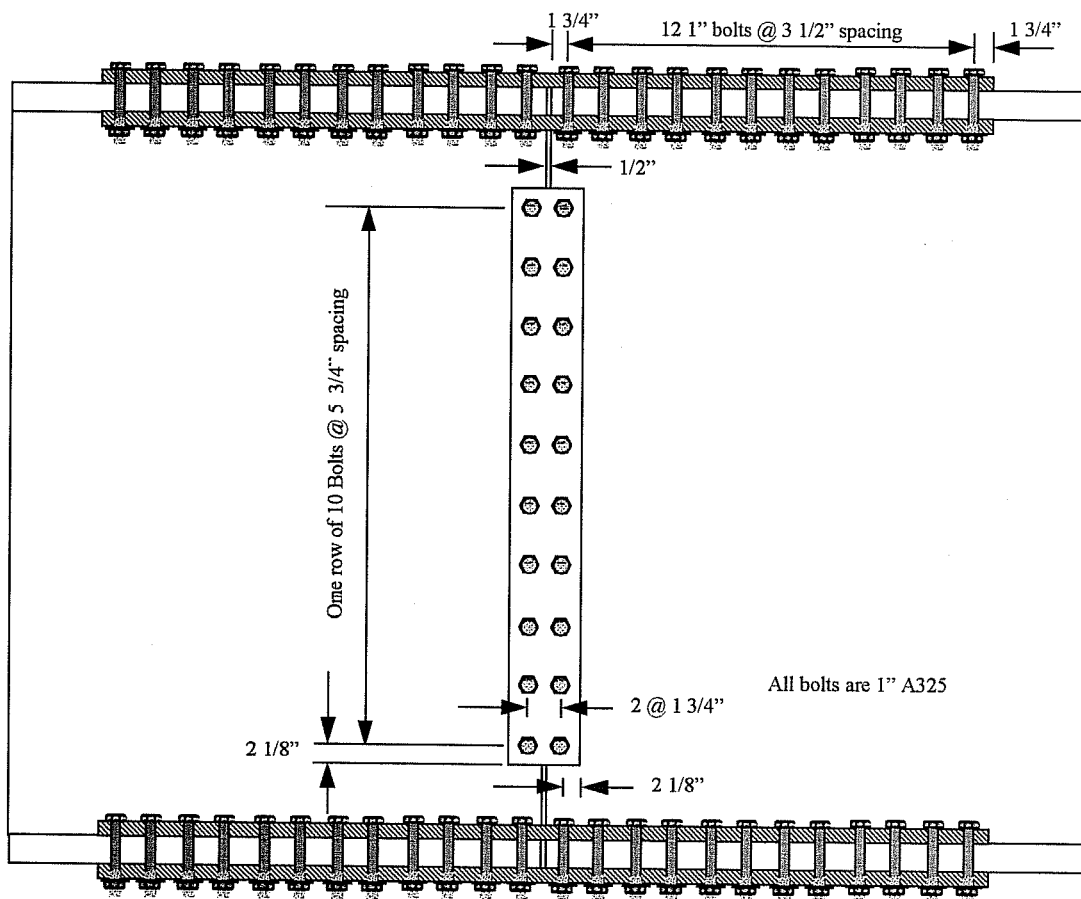


Figure 6-3 Longitudinal view of the splice of Example 1

6.2. Design Example 2, splice in a positive moment region

Design a bolted splice for the composite girder shown in Figure 6-4 to be located in a positive moment region.

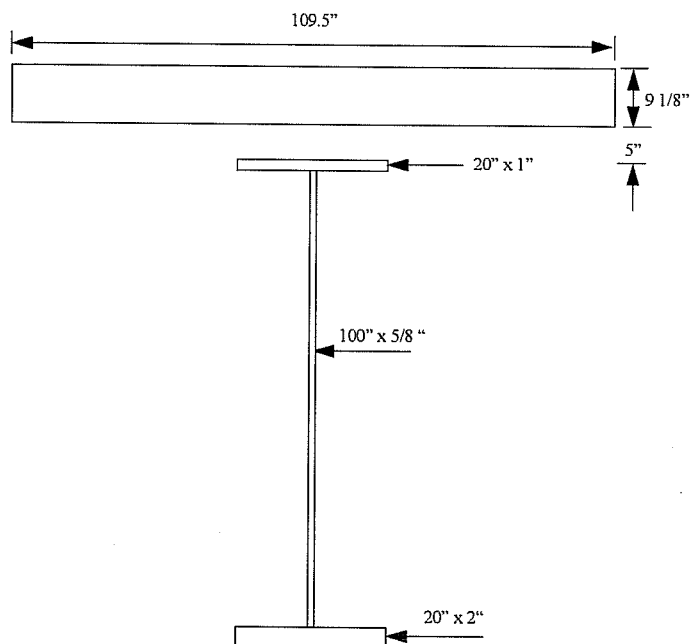


Figure 6-4 The composite girder of Example 2

Given:

$$M_{DL} = 5,147 \text{ kip-ft.}$$

$$M_{LL+I} = 3,034 \text{ kip-ft.}$$

$$V_{DL} = 101.4 \text{ kip}$$

$$V_{LL+I} = 79.4 \text{ kip}$$

$$F_{yf} = F_{yw} = 50 \text{ ksi}$$

$$b_{\text{slab}} = 109.5 \text{ in.}$$

$$t_{\text{slab}} = 9 \frac{1}{8} \text{ in.}$$

$$f'_c = 3.3 \text{ ksi}$$

$$G = 5 \text{ in.}$$

$$b_F = b_f = 20 \text{ in.}$$

$$t_F = 2 \text{ in.}$$

$$t_f = 1 \text{ in.}$$

$$d_w = 100 \text{ in.}$$

$$t_w = 5/8 \text{ in.}$$

Solution:

The splice is located in a positive moment region. Therefore, the concrete slab will contribute to the strength of the member and the girder is composite.

6.2.1. Design Forces

6.2.1.1. Required Slip Resistance

$$M_{\text{overload}} = M_{\text{DL}} + 1.667M_{\text{LL+I}} = 5,147 + 1.667(3,034) = \underline{\underline{10,204 \text{ K-ft.}}}$$

$$V_{\text{overload}} = V_{\text{DL}} + 1.667V_{\text{LL+I}} = 101.4 + 1.667(79.4) = \underline{\underline{233.7 \text{ k}}}$$

6.2.1.2. Required strength of the member

$$M_u = 1.3M_{\text{DL}} + 2.17M_{\text{LL+I}} = 1.3(5,147) + 2.17(3,034) = \underline{\underline{13,265 \text{ K-ft.}}}$$

$$V_u = 1.3V_{DL} + 2.17V_{LL+I} = 1.3(101.4) + 2.17(79.4) = \underline{\underline{303.9 \text{ k}}}$$

6.2.1.3. AASHTO Design Forces

To examine the ability of ignoring the concrete slab in the design of the slab, the adequacy of the top flange moment capacity needs to be determined.

The axial force in the top flange:

$$13,265 \times 12 / (1 + 100 + 0.5) = 1,568 \text{ kips}$$

The stress on the gross area of the top flange:

$$1,568 / (20 \times 1) = 78 \text{ ksi} > F_{yf} = 50 \text{ ksi}$$

Therefore, the top flange is not adequate to carry the design moment and the concrete slab needs to be included in the design of the slab.

Check the adequacy of the tension flange and the concrete slab to carry the overload and maximum moment alone as follows:

Calculate the moment capacity of the girder's bottom flange with holes, assume using six rows of 7/8" bolts:

$$A_{gf} = 2 \times 20 = 40 \text{ in.}^2$$

$$A_{nf} = 2 \times (20 - 6(7/8 + 1/8)) = 28 \text{ in.}^2$$

$$A_{nf}/A_{gf} = 28/40 = 0.7 < 0.85$$

Calculate the maximum compressive force for the slab:

$$C_c = 0.85 \times 3.3 \times 109.5 \times 9.125 = 2,803 \text{ kips}$$

Calculate the maximum tensile force for the bottom flange:

$$\phi T_n = \text{minimum of } (1 \times 40 \times 50, 0.80 \times 28 \times 65)$$

Thus:

$$\phi T_n = \text{minimum of } (2,000, 1,456) = 1,456 \text{ kips} < C_c = 2,803 \text{ kips}$$

Therefore, the neutral axis lies in the concrete slab and the top flange will not be in compression.

Calculate the approximate lever arm for the tensile force in the bottom flange and the compressive force in the concrete slab conservatively as follows:

$$h = 1 + 100 + 1 + 5 + 9.125/2 = 111.6 \text{ in}$$

$$\phi M_{nf} = \phi T_n h = 1,456 \times 111.6 / 12 = 13,541 \text{ k-ft.}$$

$$\phi M_{nf} = 13,541 \text{ K-ft.} > M_u = 13,265 \text{ K-ft.}$$

At overload:

$$M_f = 0.95 \times 2,000 \times 111.6 / 12 = 17,670 \text{ k-ft.}$$

$$\mathbf{M_f = 17,670 \text{ K-ft.} > M_{\text{overload}} = 10,204 \text{ K-ft.}}$$

Therefore, the tension flange and the concrete slab are adequate to carry both the total overload and maximum moments.

Shear Strength of the web:

From AASHTO 10.48.4.1, the shear capacity is calculated as follows:

$$V_u = CV_p; \quad V_p = 0.58F_{yw}Dt_w$$

For unstiffened girders, $k = 5$

$$\frac{D}{t_w} = \frac{100}{5/8} = 160 > \frac{7,500\sqrt{k=5}}{\sqrt{F_{yf} = 50,000}} = 75$$

$$\Rightarrow C = \frac{4.5 \times 10^7 \text{ k}}{\left(\frac{D}{t_w}\right)^2 F_y} = \frac{4.5 \times 10^7 \times 5}{(160)^2 \times 50,000} = 0.176$$

$$V_u = CV_p = 0.176 \times 0.58 \times 50 \times 100 \times 5/8 = 319 \text{ kips}$$

Average of the Required Strength and the Member Strength:

$$M_u = \frac{13,265 + 13,541}{2} = 13,403 \text{ K-ft. Controls (1.01 of the required strength)}$$

$$V_u = \frac{303.9 + 319}{2} = 311 \text{ K. Controls (1.02 of the required strength)}$$

75% of the Member Strength

$$M_u = 0.75 \times 13,541 = 10,156 \text{ kip-ft.}$$

$$V_u = 0.75 \times 319 = 239.3 \text{ kips}$$

Therefore, AASHTO design forces are:

$$M_u = 13,403 \text{ kip-ft.}$$

$$V_u = 311 \text{ kips}$$

6.2.2. Splice Design

6.2.2.1. The design of flange bolts

Slip requirement: Assuming class A contact surface,

$$N_b A_b = M_{\text{overload}} / (\phi R_s N_s h) = 10,204 \times 12 / \{21 \times 2 \times 111.6\} = \underline{\underline{26.1 \text{ in.}^2}}$$

Bolt shear requirement: use bolts with threads excluded from shear planes

$$N_b A_b = M_u / (\phi R_u N_s h) = 13,403 \times 12 / \{36 \times 1.25_{\text{excluded}} \times 2 \times 111.6\} = 16.01 \text{ in.}^2 < 26.1$$

Thus, overload controls the design of the web bolts.

$$A_b = \pi (7/8)^2 / 4 = 0.601 \text{ in.}^2$$

$$N_b = 26.1 / (0.601) \cong \underline{\underline{44 \text{ bolts}}}$$

Bearing on the plates:

$$N_b = M_u / (1.8 d t_f F_{uf} h) = 13,403 \times 12 / \{1.8 \times 7/8 \times 1/2 \times 65 \times 111.6\} \cong 28 \text{ bolts}$$

Therefore, for the tension flange splice plates, use:

Use 8 A325 7/8" bolts / row @ 3" spacing in 6 rows (Joint length = 24")

For the compression flange splice plate, use conservatively:

Use 8 A325 7/8" bolts / row @ 3" spacing in 4 rows (Joint length = 24")

6.2.2.2. The design of web bolts

Since the flanges are adequate to carry both the overload and maximum moment, the web should be designed for the total design shear applied at the center line of the splice. Assume that the clearance gap = 1/2", and the horizontal edge distance for the bolts = 1 1/2". Thus, the geometrical eccentricity, distance

between the center line of the splice and the centroid of the bolts,
 $e_g = 1/4 + 1.5 = 1.75''$.

Slip requirement: Assuming **class A** contact surface,

$$\text{Required } C = V_{\text{overload}} / (\phi R_s N_s N_b A_b) = 233.7 / (21 \times 2 \times 0.601) = \mathbf{9.3}$$

Bolt shear requirement: use bolts with threads included in the shear planes

$$\text{Required } C = V_u / (\phi R_u N_s A_b) = 311 / (36 \times 2 \times 0.601) = 7.2 < 9.3$$

Bearing on the plates:

$$\text{Required } C = V_u / (1.8d t_w F_{uw}) = 311 / (1.8 \times 7/8 \times 10/16 \times 65) = 4.9 < 9.3$$

Thus, overload controls the design of the web bolts. Try one vertical row of 10 7/8" bolts @ 7" vertical pitch:

$$C = \frac{n}{\sqrt{\left[\frac{6 \times e}{(n+1) \times b}\right]^2 + 1}} = \frac{10}{\sqrt{\left[\frac{6 \times 1.75}{(10+1) \times 7}\right]^2 + 1}} = 9.9 > 9.3 \text{ OK}$$

Note that $9.9/10 = 0.99$ (lost only 1% of the shear capacity due to eccentricity effect).

Thus;

Use one vertical row of 10 7/8" bolts @7" vertical pitch

6.2.2.3. The design of flange splice plates:

$$\text{Required } A_{gf} = M_{\text{overload}} / (0.95F_{yf}h) = 10,204 \times 12 / (0.95 \times 50 \times 111.6) = 23.1 \text{ in.}^2$$

$$\text{Required } A_{gf} = M_u / (F_{yf} h) = 13,403 \times 12 / (50 \times 111.6) = 28.8 \text{ in.}^2$$

$$\text{Required } A_{nf} = M_u / (0.8 \times F_{uf} h) = 13,403 \times 12 / (0.8 \times 65 \times 111.6) = 27.7 \text{ in.}^2$$

For the tension flange, use double flange splice plates:

1 Plate (20" × 1") and 2 Plates (9" × 1 1/8"); $A_{gf} = 40.25 \text{ in.}^2$, $A_{nf} = 27.5 \text{ in.}^2$

$$A_{nf} / A_{gf} = 0.68 < 0.85 \text{ OK}$$

Check block shear:

$$T_u = M_u / h = 13,403 \times 12 / 111.6 = 1,441 \text{ kips}$$

Tensile load per flange plate:

$$T_{u1} = 1,441 / 2 = 721 \text{ kips}$$

Check block shear for the 20" plate:

The length of the bolted connection from the edge of the plate to the last bolt is:

$$(8_{\text{bolts}} - 1) \times 3 + 1.5_{\text{edge distance}} = 22.5$$

$$A_{nv} = 2_{\text{shear planes}} \times (22.5 - 7.5(7/8 + 1/8)) \times 1 = 30 \text{ in.}^2$$

$$A_{nt} = 2 \times (7.5 - 2.5(7/8 + 1/8)) \times 1 = 10 \text{ in.}^2$$

$$A_{gv} = 2(22.5) \times 1 = 45 \text{ in.}^2$$

$$A_{gt} = 2 \times 7.5 \times 1 = 15 \text{ in.}^2$$

$$0.58F_u A_{nv} = 0.58 \times 65 \times 30 = 1,131$$

$$F_u A_{nt} = 65 \times 10 = 650$$

Since $0.58F_u A_{nv} > F_u A_{nt}$:

$$T = 0.80 \times (0.58F_u A_{nv} + F_y A_{gt}) = 0.80 \times (1,131 + 50 \times 15) = 1,505 \text{ kips} > T_{u1} = 721 \text{ kips}$$

Check block shear for the 9" plates:

$$A_{nv} = 2 \times 2(22.5 - 7.5(7/8 + 1/8)) \times 1.125 = 67.5 \text{ in.}^2$$

$$A_{nt} = 2 \times 2 (1.5 - 0.5(7/8 + 1/8)) \times 1.125 = 4.5 \text{ in.}^2$$

$$A_{gv} = 2(2 \times 22.5) \times 1.125 = 101.25 \text{ in.}^2$$

$$A_{gt} = 2 \times 2 \times 1.5 \times 1.125 = 6.75 \text{ in.}^2$$

$$0.58F_u A_{nv} = 0.58 \times 65 \times 67.5 = 2,545$$

$$F_u A_{nt} = 65 \times 4.5 = 292.5$$

Since $0.58F_u A_{nv} > F_u A_{nt}$:

$$T_2 = 0.80 \times (0.58F_u A_{nv} + F_y A_{gt}) = 0.80 \times (2,545 + 50 \times 6.75) = 2,306 > T_{u2} = 721 \text{ kips}$$

Check block shear for the flange of the girder:

Since the area of the girder flange is exactly half of the area of the 20" plate the block shear capacity of the girder flange is $2 \times 1,131 = 2,262 > T_u = 1,441$ kips

Design the top flange splice plates:

Since the area of the compression flange is one half of the area of the tension flange and since the concrete slab will carry all of the compressive force, it should be safe to use double flange splice plates that are equal in area to one half of the bottom flange splice plates area:

1 Plate (20" × 1/2") and 2 Plates (9" × 9/16")

6.2.2.4. The design of web splice plates

Since the flanges are adequate to carry both the overload and maximum design moments, the web needs to be designed for shear only.

$$\text{Required } A_{gw} = V_{\text{overload}} / (0.95 \times 0.58 F_{yw}) = 233.7 / (0.95 \times 0.58 \times 50) = 8.5 \text{ in.}^2$$

$$\text{Required } A_{gw} = V_u / (0.58 F_{yw}) = 311 / (0.58 \times 50) = 10.7 \text{ in.}^2$$

$$\text{Required } A_{nw} = V_u / (0.8 \times 0.58 F_{uw}) = 311 / (0.58 \times 65) = 10.3 \text{ in.}^2$$

Use double web splice plates with one row of 10 $7/8''$ @ $7''$ spacing with 1.5'' horizontal and vertical edge distance:

2 Plates (66'' \times 5/16''); $A_{gw} = 41.3 \text{ in.}^2$, $A_{nw} = 35 \text{ in.}^2$
--

Check block shear:

$$A_{nv} = 2 \times ((66 - 1.5 - 9.5(7/8 + 1/8)) \times 5/16) = 34.4 \text{ in.}^2$$

$$A_{nt} = 2 \times (1.5 - 0.5(7/8 + 1/8)) \times 5/16 = 0.625 \text{ in.}^2$$

$$A_{gv} = 2 \times (66 - 1.5) \times 5/16 = 40.3 \text{ in.}^2$$

$$A_{gt} = 2 \times 1.5 \times 5/16 = 0.94 \text{ in.}^2$$

$$0.58 F_u A_{nv} = 0.58 \times 65 \times 34.7 = 1,296$$

$$F_{uw}A_{nt} = 65 \times 0.625 = 40.6$$

Since $0.58F_{uw}A_{nv} > F_{uw}A_{nt}$:

$$V = 0.8 \times (0.58F_{uw}A_{nv} + F_{yw}A_{gt}) = 0.8 \times (1,296 + 50 \times 0.94) = 1,074 \text{ kips} > V_u = 311 \text{ kips}$$

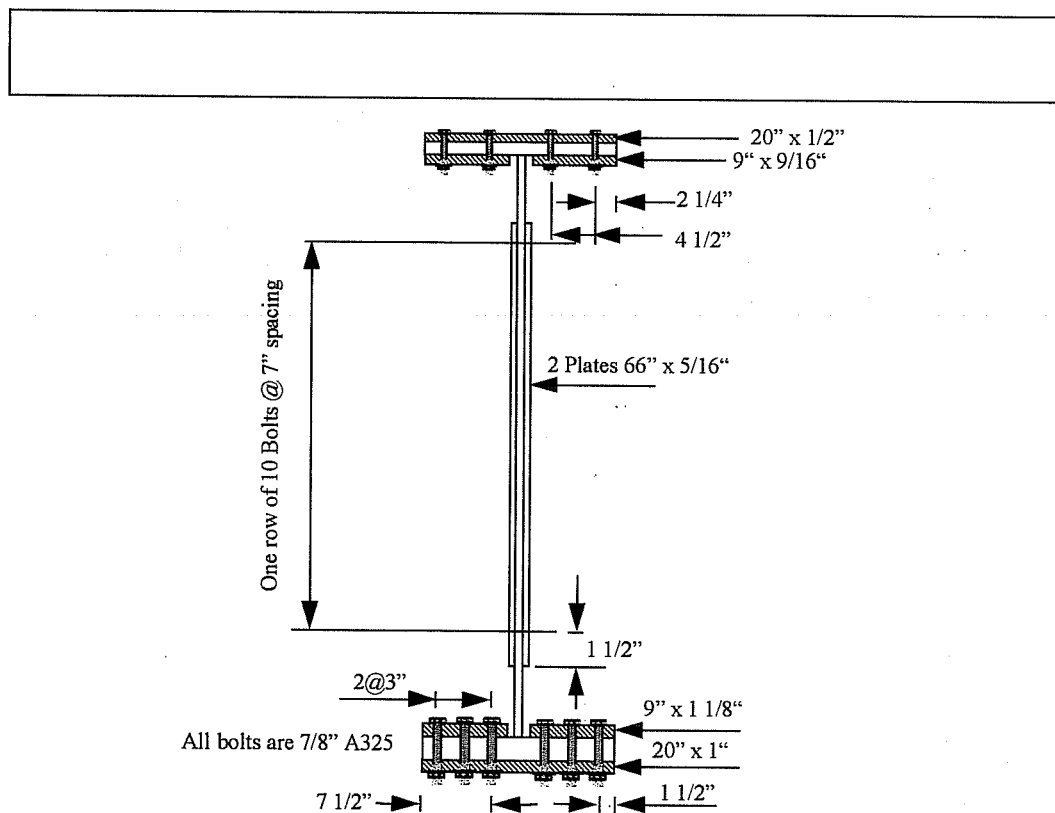


Figure 6-5 Splice details of Example 2

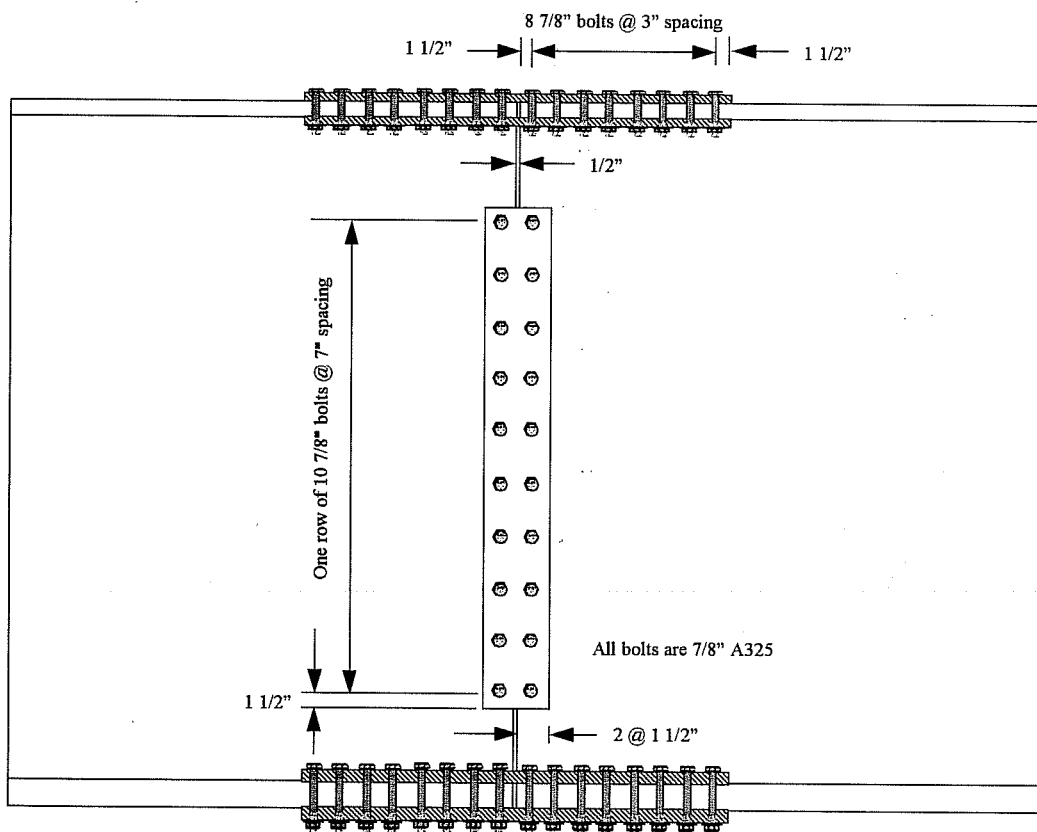


Figure 6-6 Longitudinal view of the splice of Example 2

6.3. Design Example 3, splice in a positive moment region

Design a bolted splice for the composite girder shown in Figure 6-7 to be located in a positive moment region.

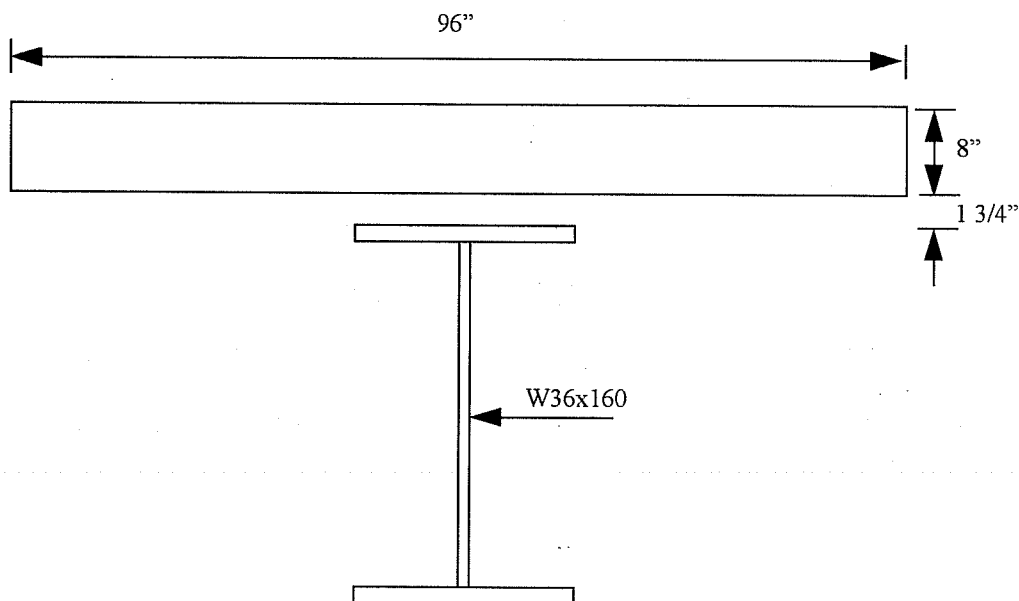


Figure 6-7 The composite girder of Example 3

Given:

$$M_{DL} = 19 \text{ kip-ft.}$$

$$M_{LL+I} = 320 \text{ kip-ft.}$$

$$V_{DL} = 35.7 \text{ kip}$$

$$V_{LL+I} = 48.4 \text{ kip}$$

$$b_{slab} = 96 \text{ in.}$$

$$t_{\text{slab}} = 8 \text{ in.}$$

$$f'_c = 3 \text{ ksi}$$

$$G = 1 \frac{3}{4} \text{ in.}$$

$$W36 \times 160$$

$$F_y = 36 \text{ ksi}$$

$$b_F = b_f = 12 \text{ in.}$$

$$t_F = t_f = 1 \text{ in.}$$

$$d_w = 34 \text{ in.}$$

$$t_w = 5/8 \text{ in.}$$

$$k = 1 \frac{15}{16} \text{ in.}$$

$$k_1 = 1 \frac{1}{8} \text{ in.}$$

Solution:

The splice is located in a positive moment region. Therefore, the concrete slab will contribute to the strength of the member and the girder is composite.

6.3.1. Design Forces

6.3.1.1. Required Slip Resistance

$$M_{\text{overload}} = M_{\text{DL}} + 1.667M_{\text{LL+I}} = 19 + 1.667(320) = \underline{\underline{552.3 \text{ K-ft.}}}$$

$$V_{\text{overload}} = V_{\text{DL}} + 1.667V_{\text{LL+I}} = 35.7 + 1.667(48.4) = \underline{\underline{116.4 \text{ k}}}$$

6.3.1.2. Required strength of the member

$$M_u = 1.3M_{\text{DL}} + 2.17M_{\text{LL+I}} = 1.3(19) + 2.17(320) = \underline{\underline{718 \text{ K-ft.}}}$$

$$V_u = 1.3V_{DL} + 2.17V_{LL+I} = 1.3(35.7) + 2.17(48.4) = \underline{\underline{151.3 \text{ k}}}$$

6.3.1.3. AASHTO Design Forces

Check the adequacy of the flanges to carry the overload and maximum moment alone. Calculate the capacity of the girder's flanges, assume using two rows of 7/8" bolts:

$$A_{gf} = 1 \times 12 = 12 \text{ in.}^2$$

$$A_{nf} = 1 \times (12 - 2(7/8 + 1/8)) = 10 \text{ in.}^2$$

$$A_{nf}/A_{gf} = 10/12 = 0.83 < 0.85$$

$$h = 36 - 1 = 35 \text{ in.}^2$$

$$M_r = (A_{gf}F_{yf})h = (11.8 \times 36) \times 35 / 12 = \mathbf{1,239 \text{ k-ft.}}$$

$$M_r = 0.8(A_{nf}F_{uf})h = 0.8(10 \times 58) \times 35 / 12 = 1,353 \text{ k-ft.}$$

$$\phi M_{nf} = \mathbf{1,239 \text{ K-ft.}} > M_u = \mathbf{718 \text{ K-ft.}}$$

$$M_r = 0.95 \times 1,239 = \mathbf{1,177 \text{ K-ft.}} > M_{\text{overload}} = \mathbf{552.3 \text{ K-ft.}}$$

Therefore, the flanges are adequate to carry both the total overload and maximum moments. The concrete slab can be conservatively ignored.

Shear Strength of the web:

From AASHTO 10.48.4.1, the shear capacity is calculated as follows:

$$V_u = CV_p; \quad V_p = 0.58F_{yw}Dt_w$$

For unstiffened girders, $k = 5$

$$\frac{D}{t_w} = 50 < \frac{6,000\sqrt{k=5}}{\sqrt{F_{yf} = 36,000}} = 70.7$$

$$\Rightarrow C = 1$$

$$V_u = CV_p = 1 \times 0.58 \times 36 \times 34 \times 5 / 8 = 0.4103 \times 1,435.5 = 443.7 \text{ Kips}$$

Average of the Required Strength and the Member Strength:

$$M_u = \frac{718 + 1,260}{2} = 989 \text{ K-ft. Controls (1.4 of the required strength)}$$

$$V_u = \frac{1513 + 443.7}{2} = 297.5 \text{ K.}$$

75% of the Member Strength:

$$M_u = 0.75 \times 1,260 = 945 \text{ kip-ft.}$$

$$V_u = 0.75 \times 443.7 = 332.8 \text{ kips} \quad \text{Controls (2.2 of the required strength)}$$

Therefore, AASHTO design forces are:

$$M_u = 989 \text{ kip-ft.}$$

$$V_u = 332.8 \text{ kips}$$

6.3.2. Splice Design

6.3.2.1. The design of flange bolts

Slip requirement: Assuming **class A** contact surface,

$$N_b A_b = M_{\text{overload}} / (\phi R_s N_s h) = 552.3 \times 12 / \{21 \times 2 \times 35\} = \underline{4.5 \text{ in.}^2}$$

Bolt shear requirement: use bolts with threads excluded from shear planes

$$N_b A_b = M_u / (\phi R_u N_s h) = 989 \times 12 / \{36 \times 1.25_{\text{excluded}} \times 2 \times 35\} = 3.8 \text{ in.}^2$$

$$A_b = \pi (7/8)^2 / 4 = 0.601 \text{ in.}^2$$

$$N_b = 4.5 / (0.601) \cong \underline{8 \text{ bolts}}$$

Bearing on the plates:

$$N_b = M_u / (1.8 d_t F_{uf} h) = 989 \times 12 / \{1.8 \times 7/8 \times 1 \times 58 \times 35\} \cong 4 \text{ bolts}$$

Use 4 A325 7/8" bolts / row @ 3" spacing in 2 rows (Joint length = 12")

6.3.2.2. The design of web bolts

Since the flanges are adequate to carry both the overload and maximum moment, the web should be designed for the total design shear applied at the center line of the splice. Assume that the clearance gap = 1/2", and the horizontal edge distance for the bolts = 1 1/2". Thus, the geometrical eccentricity, distance between the center line of the splice and the centroid of the bolts, $e_g = 1/4 + 1.5 = 1.75"$.

Slip requirement: Assuming **class A** contact surface,

$$\text{Required } C = V_{\text{overload}} / (\phi R_s N_s N_b A_b) = 116.4 / (21 \times 2 \times 0.601) = 4.6$$

Bolt shear requirement: use bolts with threads included in the shear planes

$$\text{Required } C = V_u / (\phi R_u N_s A_b) = 332.8 / (36 \times 2 \times 0.601) = 7.7 \text{ controls}$$

Bearing on the plates:

$$\text{Required } C = V_u / (1.8 d t_w F_{uw}) = 332.8 / (1.8 \times 7/8 \times 5/8 \times 58) = 5.8$$

Try one vertical row of 8 7/8" bolts @ 4" vertical pitch:

$$C = \frac{n}{\sqrt{\left[\frac{6 \times e}{(n+1) \times b}\right]^2 + 1}} = \frac{8}{\sqrt{\left[\frac{6 \times 1.75}{(8+1) \times 4}\right]^2 + 1}} = 7.7 = \text{required } C = 7.7$$

Use one vertical row of 8 7/8" bolts @ 4" vertical pitch

Note that $7.7/8=0.96$ (lost only 4% due to eccentricity effect).

6.3.2.3. The design of flange splice plates

$$\text{Required } A_{gf} = M_{\text{overload}} / (0.95F_{yf} h) = 552.3 \times 12 / (0.95 \times 36 \times 35) = 5.5 \text{ in.}^2$$

$$\text{Required } A_{gf} = M_u / (F_{yf} h) = 989 \times 12 / (36 \times 35) = 9.4 \text{ in.}^2$$

$$\text{Required } A_{nf} = M_u / (0.8F_{uf} h) = 989 \times 12 / (0.8 \times 58 \times 35) = 7.3 \text{ in.}^2$$

Use double flange splice plates:

1 Plate (12 × 7/16) and 2 Plates (4 3/4 × 9/16); $A_{gf} = 10.6 \text{ in.}^2$, $A_{nf} = 8.6 \text{ in.}^2$

$$A_{nf} / A_{gf} = 8.6/10.6 = 0.81 < 0.85 \quad \text{OK}$$

Check block shear:

$$T_u = M_u / h = 989 \times 12 / 35 = 339 \text{ kips}$$

Tensile load per flange splice:

$$T_{u1} = 339 / 2 = 169.5 \text{ kips}$$

Check block shear for the 12" plate:

The length of the bolted connection from the edge of the plate to the last bolt is:

$$(4_{\text{bolts}} - 1) \times 3 + 1.5_{\text{edge distance}} = 10.5$$

$$A_{nv} = 2(10.5 - 3.5(7/8 + 1/8)) \times 7/16 = 6.1 \text{ in.}^2$$

$$A_{nt} = 2 \times (2.375 - 0.5(7/8 + 1/8)) \times 7/16 = 1.6 \text{ in.}^2$$

$$A_{gv} = 2(10.5) \times 7/16 = 9.2 \text{ in.}^2$$

$$A_{gt} = 2 \times 2.375 \times 7/16 = 2.1 \text{ in.}^2$$

$$0.58F_u A_{nv} = 0.58 \times 58 \times 6.1 = 206$$

$$F_u A_{nt} = 58 \times 1.6 = 87$$

Since $0.58F_u A_{nv} > F_u A_{nt}$:

$$T = 0.8 \times (0.58F_u A_{nv} + F_{yw} A_{gt}) = 0.8 \times (206 + 36 \times 2.1) = 225 \text{ kips} > T_{u1} = 169.5 \text{ kips}$$

Check block shear for the flange of the girder:

The block shear capacity of the flanges can be obtained by multiplying the block shear capacity of the 12" splice plate with the flange/flange splice plate ratio as follows:

$$(225 \times 1) / (7/16) = 515 \text{ kips} > T_u = 339 \text{ kips}$$

6.3.2.4. The design of web splice plates

Since the flanges are adequate to carry both the overload and maximum design moments, the web needs to be designed for shear only.

$$\text{Required } A_{gw} = V_{\text{overload}} / (0.95 \times 0.58 F_{yw}) = 116.4 / (0.95 \times 0.58 \times 36) = 5.9 \text{ in.}^2$$

$$\text{Required } A_{gw} = V_u / (0.58 F_{yw}) = 332.8 / (0.58 \times 36) = 15.9 \text{ in.}^2$$

$$\text{Required } A_{nw} = V_u / (0.8 \times 0.58 F_{uw}) = 332.8 / (0.8 \times 0.58 \times 58) = 12.4 \text{ in.}^2$$

Use double web splice plates with one row of 8 7/8" @ 4" spacing with 1.5" horizontal and vertical edge distance:

2 Plates (31" × 5/16"); $A_{gw} = 19.4 \text{ in.}^2$, $A_{nw} = 14 \text{ in.}^2$

Check block shear:

$$A_{nv} = 2 \times ((31 - 1.5 - 7.5(7/8 + 1/8)) \times 5/16) = 13.8 \text{ in.}^2$$

$$A_{nt} = 2 \times (1.5 - 0.5(7/8 + 1/8)) \times 5/16 = 0.63 \text{ in.}^2$$

$$A_{gv} = 2 \times (31 - 1.5) \times 5/16 = 18.4 \text{ in.}^2$$

$$A_{gt} = 2 \times 1.5 \times 5/16 = 0.94 \text{ in.}^2$$

$$0.58F_u A_{nv} = 0.58 \times 58 \times 13.8 = 471$$

$$F_u A_{nt} = 58 \times 0.63 = 36.5$$

Since $0.58F_u A_{nv} > F_u A_{nt}$:

$$V = 0.8 \times (0.58F_u A_{nv} + F_y A_{gt}) = 0.8 \times (463 + 36 \times 0.94) = 397 \text{ kips} > V_u = 332.8 \text{ kips}$$

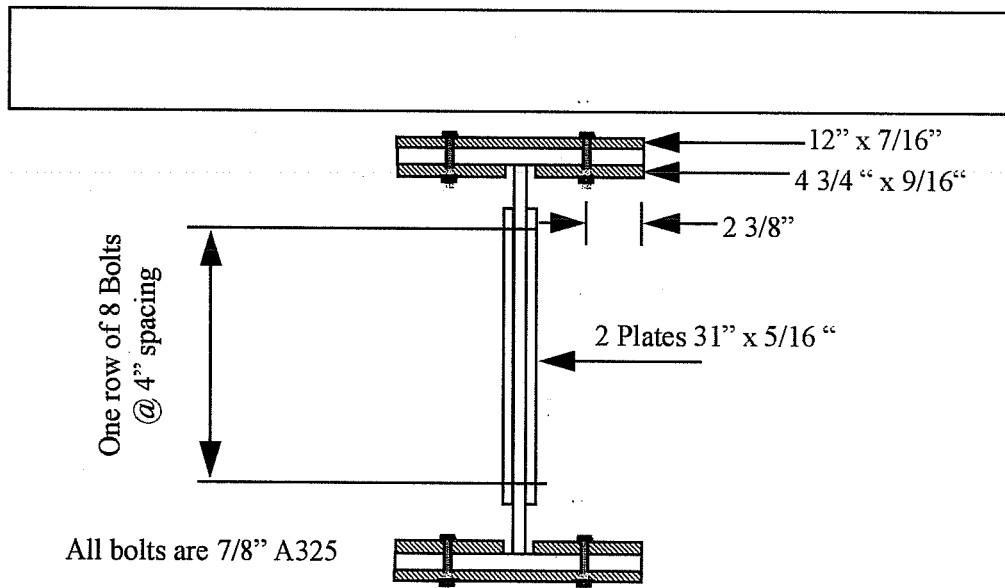


Figure 6-8 Splice details of Example 3

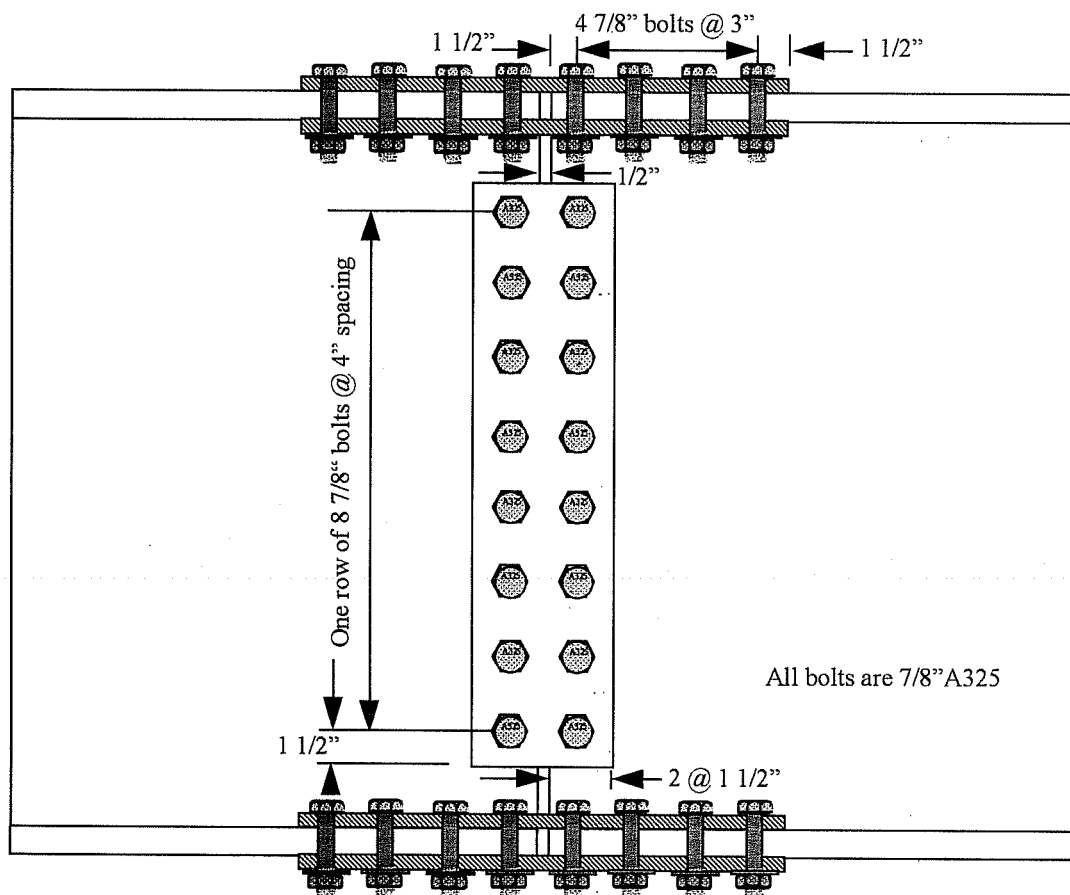


Figure 6-9 Longitudinal view of the splice of Example 3

Chapter 7

7. Summary and Conclusions

The available analyses of eccentrically loaded bolted connections are reviewed and the proper method of analysis is recommended. The effect of hole making, preload in the bolts, and material loading history on the shear strength of high strength bolts is determined. The results of 32 full-scale tests of steel girder bolted splices are presented and discussed. The distribution of moment and shear between the web and flange splices is determined and compared with test results. Simple design procedures for the splices of symmetric, unsymmetric, and composite girders are developed. Three design examples of composite girders using actual bridge forces are presented to demonstrate the application of the design procedures.

Based on the results of the testing of 3/4 in. A325 high strength bolts, the following conclusions are made:

- The hole making procedure does not affect the shear strength of a properly tightened high strength bolt.
- Due to bending of the bolts, the shear capacity of hand-tight bolts placed in punched holes is approximately 13 % less than that of bolts placed in drilled holes. Further, the shear capacity of hand-tight bolts placed in punched holes is less than the value specified in the AISC specifications. Thus, it is recommended that a hole making procedure reduction factor of 0.85 be included in the specifications for snug bolts placed in punched holes.

- The shear strength of 3/4 in. A325 hand-tight bolts is 13 % less than that of pretensioned bolts.
- The shear strength of hand-tight bolts tested in compression splices with rigid plates is about 17 % larger than the shear strength of hand-tight bolts tested in tension splices with punched inner holes. On the other hand, the shear strength of hand-tight bolts tested in compression splices with rigid plates is practically equal (only 4 % difference) to the shear strength of hand-tight bolts tested in tension splices with drilled inner holes.

Based on the results of the testing program of 17 large-scale web splices, the following conclusions are made:

I. At the service level:

- When the critical bolt reaches its slip load, the stiffness of the connection decreases. Thus, for predicting the slip load of web splices, elastic analysis of the bolts must be performed. The gain in the slip resistance when using plastic analysis of the bolts can be accompanied by a significant decrease in stiffness and large deformation and, therefore, should not be counted upon for predicting the slip resistance of web splices.

II. At maximum load:

- The empirical nonlinear analysis of the web bolts does not represent the actual behavior of bolted web splices and is always unconservative.
- The nonlinear analysis using the actual measured load deformation of the bolts agrees best with test results for both pretensioned and hand-tight bolts. Unfortunately, the load-deformation response of a randomly selected bolt and plate thickness and strength is not available.

- In general, the elastic analysis is conservative for pretensioned bolts and unconservative for hand-tight bolts. Nevertheless, simple direct elastic analysis of the web bolts appears to be adequate for pretensioned bolts.
- Web splices with short slotted horizontal web holes have less capacity than web splices with standard web holes.

Based on the results of the testing program of 15 large-scale web-flange bolted splices, the following conclusions are made:

I. At the service level:

- To limit the permanent deformation at service load, the flanges should be limited to their yield stress at the gross sectional area.
- When predicting the web slip, elastic analysis of the web bolts must be performed.
- When the flanges are adequate to carry the service load moment, the web needs to be designed for shear only. This shear is applied at the centerline of the splice with an eccentricity calculated as the distance from the centerline of the splice to the centroid of the web bolts at one side of the splice.
- When the small flange of an unsymmetric girder is not adequate to carry the service load moment, the web needs to be designed for the total shear, the moment resisted by the web, and the horizontal force required from equilibrium of forces.

II. At maximum load:

- When the small flange of an unsymmetric girder is adequate to carry the maximum design moment, the web needs to be designed for shear only. This shear is applied at the centerline of the splice with an eccentricity calculated as

the distance from the centerline of the splice to the centroid of the web bolts at one side of the splice.

- When the design moment exceeds the moment resistance of the small flange but is less than the moment resistance of the big flange, the web needs to be designed for the design shear along with the horizontal force which represents the difference in the flanges axial forces
- When the design moment exceeds the moment resistance of the big flange, the web needs to be designed for the design shear, the horizontal force which represents the difference in the flanges axial forces, and the moment in excess of the big flange moment capacity.
- Elastic analysis of the web bolts appears to be adequate and there is no need to perform nonlinear analysis of the bolts.
- The flanges of w-f splices, if not fully yielded, carry a portion of the total shear. This shear is a function of the ratio of the applied moment to the moment capacity of the flanges. In general, the shear carried by the flanges is a function of:
 1. Gap clearance in the girder. The shear in the flanges decreases as the gap increases
 2. Edge distance of the flange fasteners. The shear in the flanges decreases as the edge distance of the flange fasteners increases
 3. Level of flange axial force required for moment; axial force / $(A_f F_{yf})$.
The shear in the flanges decreases as the Level of flange axial force increases

Thus, assuming that the applied shear is resisted by the web of w-f splices with adequate flanges should yield conservative results.

- The w-f splice plates can develop their plastic moment and plastic shear capacities simultaneously. Thus, there should not be a reduction in the capacity of w-f splice plates due to moment shear interaction.
- The flanges of w-f splices can develop their moment capacity at the gross section, provided that it does not exceed the fracture capacity at the net section, even though the net to gross area is less than 85%. Thus, there should not be a reduction to the gross area to obtain an effective area when the net to gross area is less than 85%, as required by AASHTO.
- The w-f splice plates can develop their plastic moment and plastic shear capacities regardless of the number of rows of web bolts, provided that the web bolts are adequate to resist the shear and moment applied to the web splice. Thus, there is no need to require the web splice to have a minimum of two rows of bolts as required by AASHTO.
- W-F splices with hand tight (no preload) web bolts have less capacity than w-f splices with pretensioned bolts.

REFERENCES

1. Research Council on Structural Connections. *Load and Factor Design, Specifications for Structural Joints Using ASTM A325 or A490 Bolts*, Chicago, Illinois: American Institute of Steel Construction, Inc., June, 1988.
2. Kulak, L. G., Fisher, J. W., and Struik, J. H. A., *Guide to Design Criteria for Bolted and Riveted Joints, 2nd. ed.*, John Wiley and Sons, 1987.
3. AISC. "*Load & Resistance Factor Design.*", 2nd. ed., Vol. II, Chicago, IL: American Institute of Steel Construction, 1994.
4. AASHTO. *Standard Specifications for Highway Bridges*, 14th. ed. Washington, DC: The American Association of State Highway and Transportation Officials (444 North Capitol Street, N.W., Suite 225, Washington, DC 20001), 1989.
5. Salmon C., and J. Johnson, "*Steel Structures : Design and Behavior.*", third edition, New York: Harper and Row, 1990.
6. G. L., Kulak, and D. L. Green, "Design of Connectors in Web-Flange Beam or Girder Splices", *AISC Engineering Journal*, second quarter, 1990, pp. 41-48.
7. Gaylord, Jr., Gaylord, and Stallmeyer, "*Design of Steel Structures*", third edition, McGraw-Hill, Inc., 1992.
8. R. T. Douty, and W. McGuire, "High Strength Bolted Moment Connections, " *Journal of the Structural Division, ASCE*, Vol. 91, ST2, April 1965.
9. Sherwood, F., Crawford, S. F., and G. L. Kulak, "Eccentrically Loaded Bolted Connections", *ASCE journal of the structural division* 97: NO. ST3, March 1971. Page 765 - 782.

10. Higgins, T. R., "New Formulas for Fasteners Loaded Off Center", *Engineering News-Record*, May 21, 1964. Page 102-104.
11. A. L. Abolitz, " Plastic Behavior of Eccentrically-Loaded Fasteners," *Engineering Journal, AISC*, Vol. 3, No. 3, July 1966. Page 122-132.
12. J. W. Fisher, and G. L. Kulak, " Plastic Behavior of Eccentrically-Loaded Fasteners, Discussion" *Engineering Journal, AISC*, April 1967. Page 88-89.
13. C. L. Shermer, " Plastic Design of Eccentrically Loaded Connections," *Engineering Journal, AISC*, Vol. 8, No. 2, April 1971. Page 48-51.
14. G. L. Kulak, " Plastic Behavior of Eccentrically-Loaded Fasteners, Discussion" *Engineering Journal, AISC, October 1971*. Page 144-145.
15. Wallaert, J. J., and Fisher J. W., "Shear Strength of High-Strength Bolts", *ASCE journal of the structural division: NO. ST3* , June 1965. Page 99 - 125.
16. Brandt, G. D., "Rapid Determination of Ultimate Strength of Eccentrically Loaded Bolt Groups" *AISC Engineering Journal*, Second Quarter, 1982. Page 94-100.
17. Marsh, C., "Rapid Determination of Ultimate Strength of Eccentrically Loaded Bolt Groups, Discussion" *AISC Engineering Journal*, Fourth Quarter, 1982. Page 214-215.
18. Iwankiw, N., "Rapid Determination of Ultimate Strength of Eccentrically Loaded Bolt Groups, Discussion" *AISC Engineering Journal*, First Quarter, 1983. Page 46.
19. Rutenberg A., "Nonlinear Analysis of Eccentric Bolted Connections" *AISC Engineering Journal*, Fourth Quarter, 1984. Page 227-236.

Vita

Firas Sheikh Ibrahim, the son of Ibrahim and Amal, was born in Lattakia, Syria, on May 31, 1966. After receiving the Bachelor degree of Civil Engineering from Damascus University, Damascus, Syria, in August 1989, he was employed by the city of Damascus. In January, 1991, he entered the Graduate School at South Dakota State University. He married his wife Kim in July, 1991. After receiving the degree of Master of Science of Civil Engineering School from South Dakota State University, Brookings, South Dakota, in May, 1992, he entered the Graduate School at the University of Texas at Austin in August, 1992, to pursue the degree of Doctor of Philosophy of Civil Engineering.

Permanent address: Department of Civil and Environmental Engineering
Clarkson University
139 CAMP Building
P.O. Box 5710
Potsdam, New York 13699-5710

This dissertation was typed by the author.

